NASA CR-166,246

NASA CONTRACTOR REPORT 166246

NASA-CR-166246
19820009278

A Preliminary Design Study of a
Hybrid Airship for Flight Research

Ronald G.E. Browning

CONTRACT NAS2–10777
July 1981

NASA

NF02482

N83-17152#

A Preliminary Design Study of a Hybrid Airship for Flight Research

Ronald G.E. Browning
Goodyear Aerospace Corporation
1210 Massillon Road
Akron, Ohio 44315

NASA

ABSTRACT

The feasibility of using components from four small helicopters and
an airship envelope as the basis for a quad-rotor research aircraft
was studied.

Preliminary investigations included a review of candidate hardware
and various combinations of rotor craft/airship configurations. A
selected vehicle was analyzed to assess its structural and perform-
ance characteristics.

FOREWORD

The Preliminary Design Study of a Hybrid Airship for Flight Research
has been performed by Goodyear Aerospace Corporation, Akron, Ohio
under NASA-Ames Contract No. NAS2-10777.

Mr. Peter D. Talbot, Hybrid Airship Technology Program Manager at
NASA-Ames, served as the Technical Monitor. The Goodyear Aerospace
Project Engineer was Mr. Donald B. Block, and the principal
investigator was Mr. Ronald G. E. Browning.

TABLE OF CONTENTS

LIST OF ILLUSTRATIONS

LIST OF TABLES

SECTION I - INTRODUCTION

Recent studies have indicated military and civil needs for vertical lift of payloads exceeding the payload capacity of existing and anticipated heavy lift helicopters. Military needs include lifting heavy battlefield equipment and off-loading container ships over undeveloped shores. Examples of civil applications include logging and transport and enplacement of heavy equipment for large construction projects.

Use of multiple rotor vehicles appears to be a cost effective way to lift these heavy payloads since such vehicles can use existing helicopter propulsion and rotor systems. Hybrid aircraft employing rotor systems and a buoyant lifting hull appear to be particularly attractive, especially for extremely heavy lift, due to the relatively lower cost of buoyant lift.

The development of hybrid lifting devices is not without precedent. Fifty years ago, Oehmichen, a Frenchman, flew a rotor-equipped airship (Figure 1-1). More recent attempts have been made with twin lift helicopter arrangements where two helicopters work in tandem to lift a single load.

The first available reference made to a twin lift was in an experiment conducted by Boeing vertol in the late 1950's. Two H-21C helicopters were used to explore the operational suitability of the concept, but the experiment did not prove to be successful.

A decade later, Sikorsky Aircraft performed a feasibility test of twin lift for the Army. The demonstration utilized two CH-54B helicopters joined by a "twin lift kit" (ref. 1) which provided a lift capability almost double that of a single CH-54B.

The conclusions generated from this demonstration as postulated by ref. 1 were:

1. The hover and low speed regimes of the twin lift mission were demonstrated to be feasible.

2. The success of this test must to some degree be attributed to the visibility available from the aft facing pilot's station of the lead aircraft. Precision placement and gentle touchdown depend upon some means of observing the load.

3. The pilot effort required to fly the No. 2 or following aircraft is high.

4. Altitude and vertical velocity cues are inadequate when load shadows are not visible. (A radar altimeter or a load sighting device is recommended for the hovering phase.)

5. Cable angle displays for the forward facing pilot of the No. 2 aircraft are of little value unless they can be located in the field of view he uses for formation flying.

6. Centering the spreader bar directly over the load is a difficult task. Some thought should be given to developing a device or system to assist the pilots in pilots in this task.
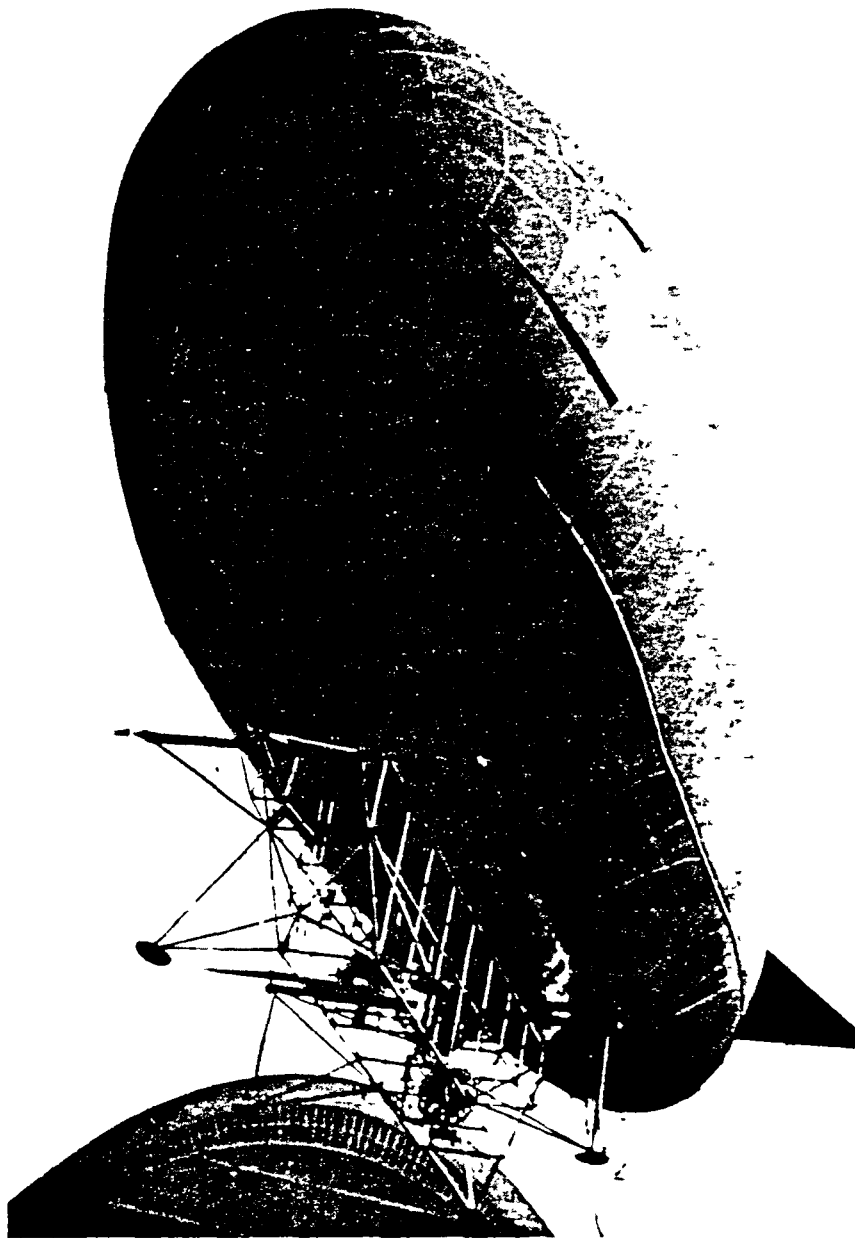
Figure 1-1 - Oehmichen's Hybrid Airship (1931)

7. The only aircraft limit approached during these tests was the dual engine torque limit. This occurred when coming to a stop with the 40,000 pound load and was due to the following aircraft assuming the major portion of the task to decelerate the load.

8. Any swaying of the bar and load exhibited was in a simple pendulum mode. Any edgewise oscillations of the bar dampened out rapidly.

9. With master/slave couplings and load stabilization systems installed much higher speeds should be possible.

The quad-rotor configuration is a vehicle that has the potential to alleviate some of the problems noted above with respect to speed and pilot workload. It employs a single centralized fly-by-wire (FBW) control system. Figure 1-2 illustrates a proposed buoyant heavy-lift production vehicle.

Because the quad rotor configuration is unlike any vehicle ever produced, a small scale flight research vehicle for ground and flight test, a "quad rotor research aircraft", is needed.

Building a research aircraft which can be tested both as a nonbuoyant quad-rotor (QRRA) configuration and as a buoyant quad-rotor (BQRRA) configuration is proposed. The research vehicle will serve to:

1. Prove the feasibility of the concept

2. Investigate systems integration aspects

3. Verify analysis and test results

4. Investigate operational characteristics

5. Develop handling qualities criteria

6. Enable investigation of configuration refinements
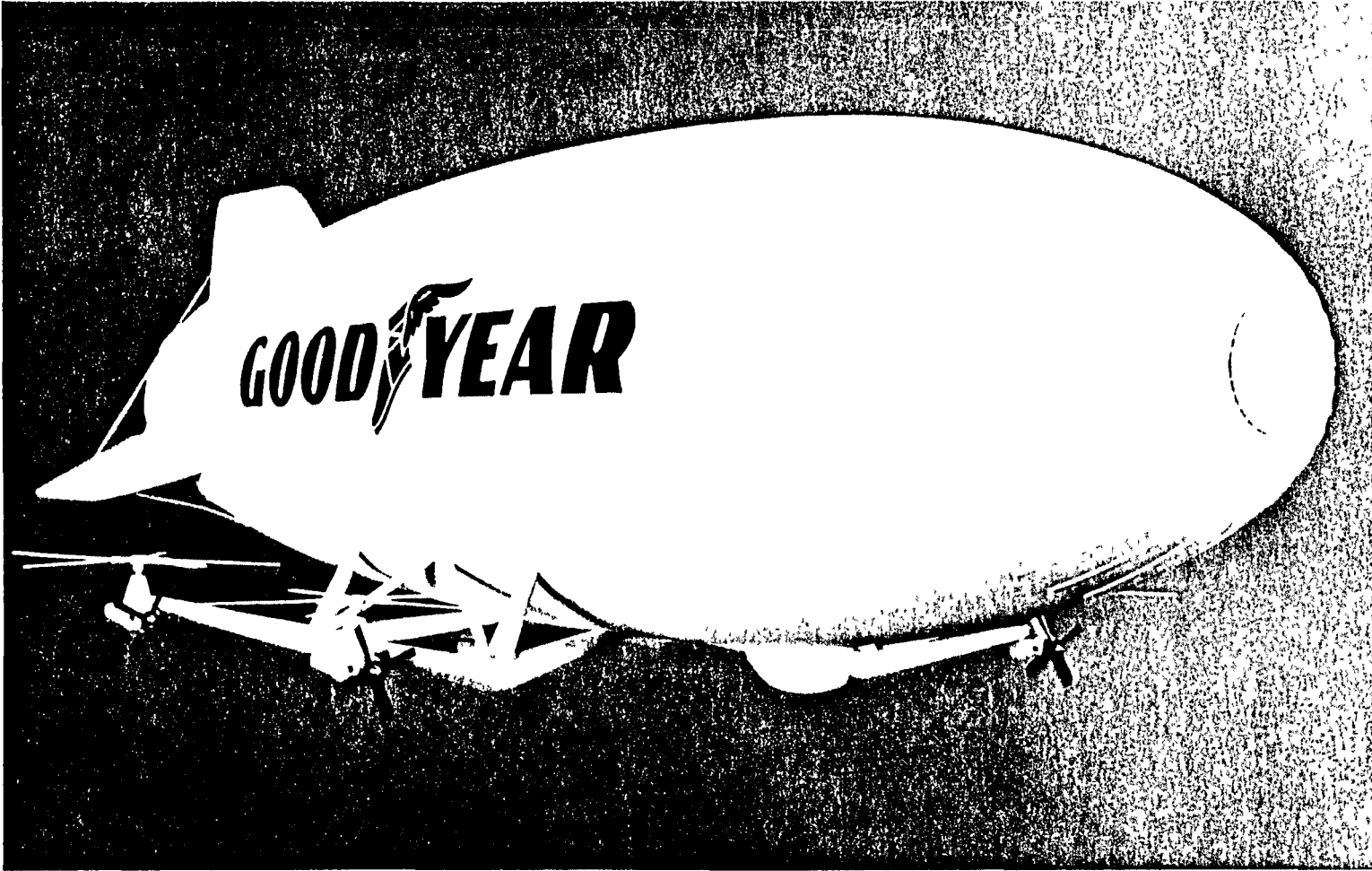
Figure 1-2 – Goodyear Quad-Rotor Heavy Lift Airship Concept

SECTION II - STUDY METHODOLOGY

1. APPROACH

A systematic approach to the development of a preliminary design of a hybrid airship for flight research was undertaken in accordance with the overall program plan identified in Figure 2-1. The major tasks in the study are:

1. To determine the best configuration that combines four modified small helicopters and an appropriate aerostat into a research aircraft suitable for ground and piloted flight test

2. To perform a preliminary stress and structural dynamics analysis and generate a group weight statement

3. To define a suitable flight control concept

4. To predict the performance of the aircraft and evaluate its controllability and safety

5. To estimate acquisition cost and a development schedule

Note that the baseline design was continually iterated, based on outputs from the analytical tasks in order to arrive at an optimal solution.

Once the Hughes OH-6A helicopter was selected as the preferred rotor system, a subcontract to Hughes was issued. All helicopter data were thus provided by the manufacturer.

2. METHODS

Due to the comprehensive nature of a total vehicle design, several analytical tools were utilized to address specific problem areas. These are identified in Table 2-1. Additional detail is contained in the section indicated in the table.

3. SPECIAL CONSIDERATIONS

a. Wind Tunnel Testing

Consideration was given to testing the full scale FRV in the 80-by-120-foot wind tunnel at NASA-Ames. Figure 2-2 shows a proposed FRV that utilized a GZ20 envelope in the tunnel test section.

The ratio of vehicle span to model span is 0.85. Wind tunnel literature suggests that the upper limit for the ratio of rotor span to tunnel width be between 0.6 and 0.7 (ref. 2,3). The frontal area blockage of the FRV, as shown in Figure 2-2, is approximately 20 percent. The upper limit on this type of blockage is generally considered to be 10 percent (ref 2,3). With these limitations, any data collected would require large corrections and therefore be of questionable reliability.
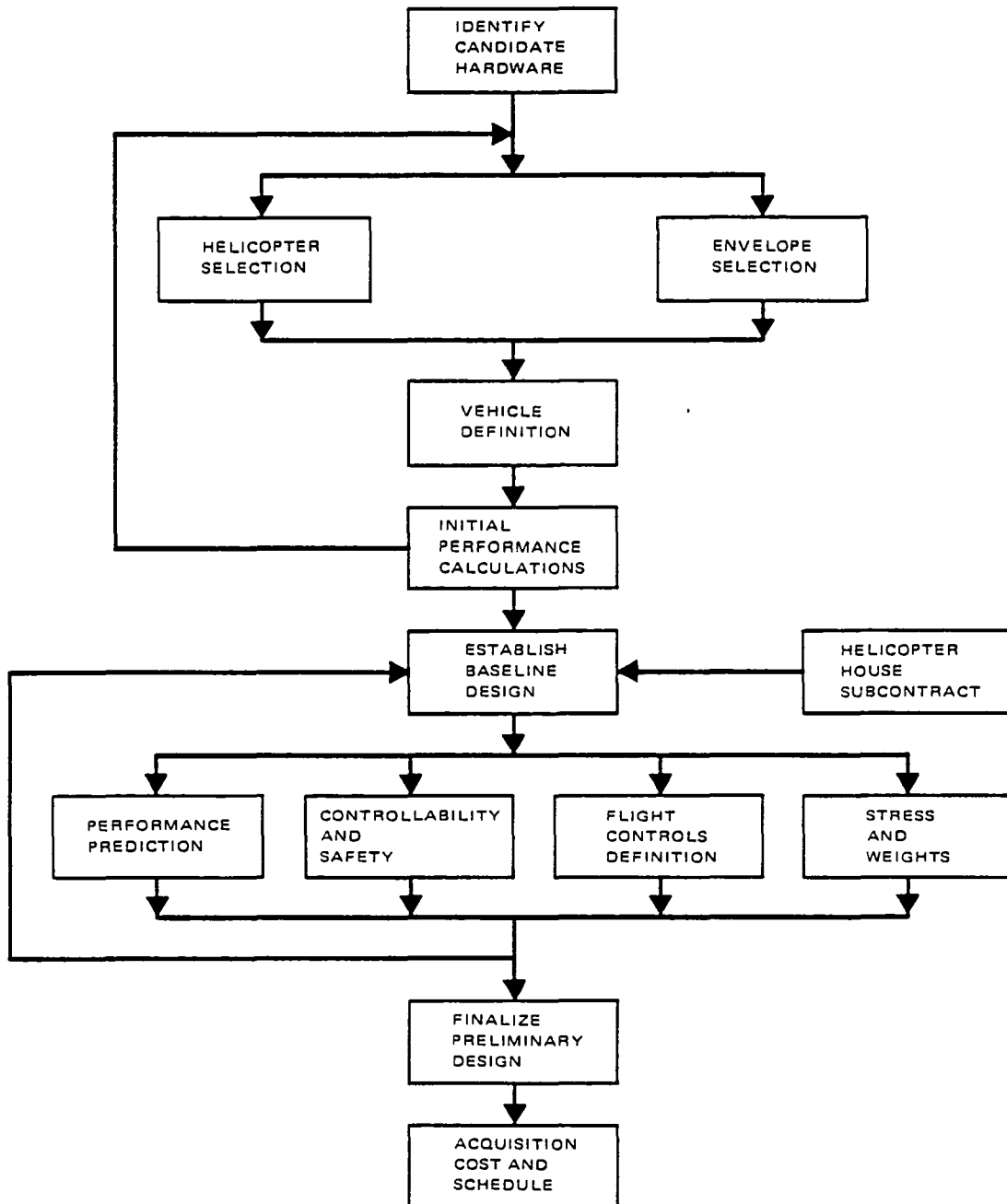
Figure 2-1 - FRV Program Plan

Figure 2-2 – FRV Installed in Test Section of NASA-Ames Wind Tunnel

45 92 FT DIAM

59 54 FT

100 FT 4 IN
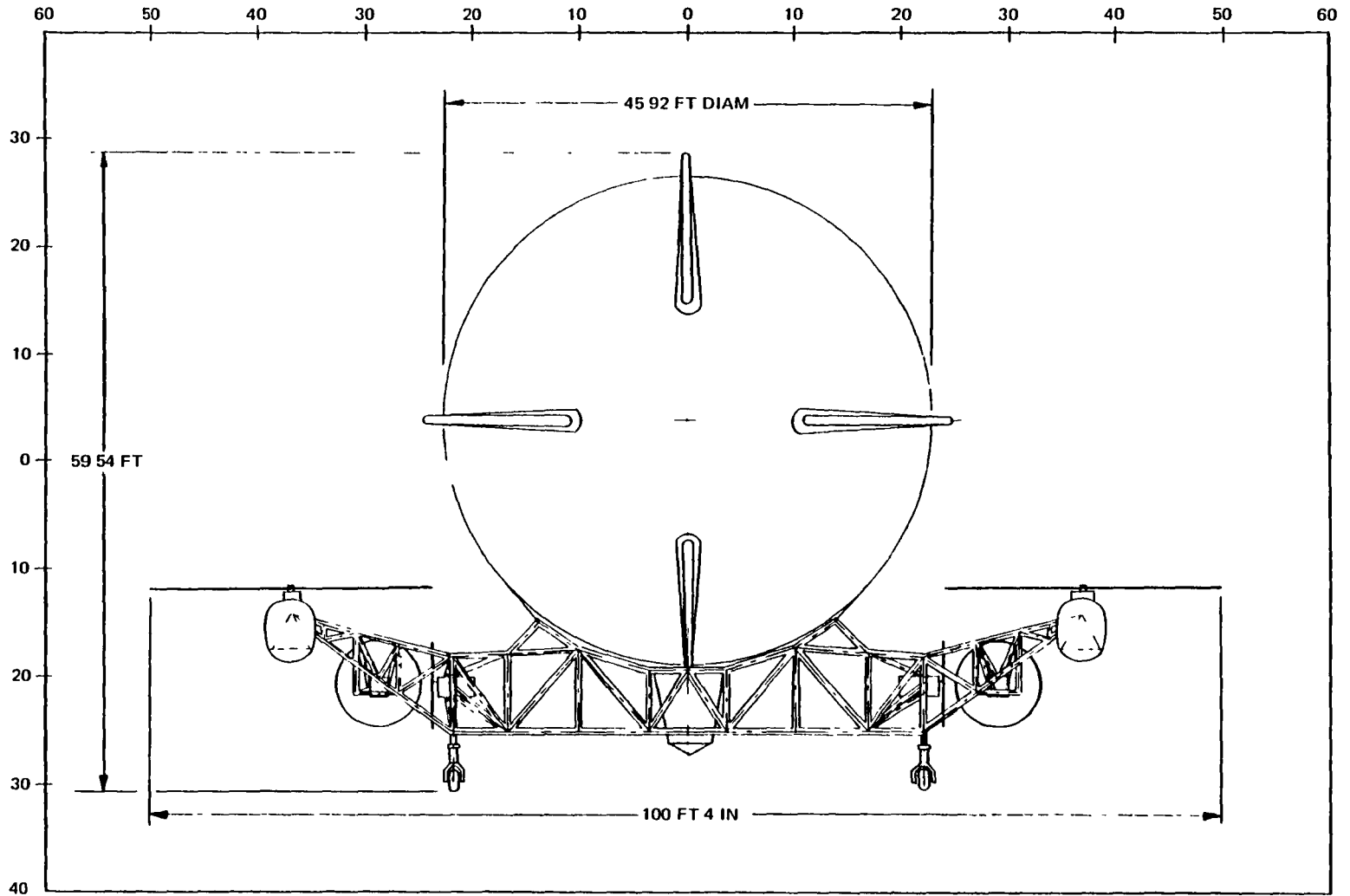
TABLE 2-1 - COMPUTERIZED ANALYSES

Item	Output	Section
Component drag prediction	First-order drag contribution of the interconnecting structure	III
Tail rotor analysis	Power and thrust requirements for specific tail rotors used as auxiliary propulsors	III
Computer aided design	Sectional displays of interconnecting structure	V
Mass properties	Vehicle mass property data by element	V
Structural analysis (STRUDL-11)	Axial load and bending moment of interconnecting structure members and prediction of joint deflections	V
Flight simulation	Six degree-of-freedom real-time hybrid piloted simulation	VII, VIII
Trim program	Six degree-of-freedom calculation of hover flight envelope	IX

A more severe limitation is that the FRV tests would be restricted to a very small range of yaw and pitch angles. Since there are very little available test data for airship envelopes at yaw angles greater than 20 degrees, the tunnel testing of a full-scale FRV would be of questionable value due to physical constraints that would exclude data in the 20 deg $\leq \psi \leq 180$ deg. range. Hence, testing of the full-scale FRV in the 80-by-120 foot wind tunnel does not appear to be feasible.

b. Static Test Stand

As an alternative to wind tunnel testing, consideration was given to mounting the FRV on an external test stand at NASA-Ames.

However, since the mean extreme daily peak gust at Moffett Field (based on data collected from 1945-1977) is 40 knots (ref. 4), the FRV envelope would experience significant loads that could not be diminished by rotation in a static installation. Thus, there would be a high probability of envelope deflation.

Hence, testing of the FRV in the static test stand does not appear feasible.

SECTION III - CONFIGURATION ANALYSIS

1. APPROACH

Figure 3-1 identifies the major elements of the tradeoff study that ensured the optimal overall flight vehicle research configuration.

The first step in the configuration analysis was to select a baseline combination, generate typical hardware elements, and then iterate the design based on the varying inputs as defined by the particular helicopter attributes. In this study, the OH-6A/GZ20 grouping represented the baseline case. The initial conceptual layout is shown in Figure 3-2.

Having established the basic geometry of the vehicle, several different configurations were generated using various envelope sizes and helicopter types. Preliminary stress and weight investigations were performed for each of the vehicles to provide adequate data for continued analysis.

Rudimentary performance analyses were undertaken using a lateral plane hover trim program and an airship simulation program. The preliminary trim program (Figure 3-3) inputs various vehicle characteristics and wind data. It generates: predicted maximum hover wind speed at various angles of sideslip; control forces and moment; control stick deflections, and cyclic deflections.

A block diagram of the advanced airship simulation is provided in Figure 3-4. A discussion of this model is provided in Section VIII. In essence, results of the simulation yield comparative data for vehicle control capabilities.

It was necessary at this point to identify some reference criteria for the evaluation of each vehicle's performance data. Several approaches to the specification of control power requirements can be postulated by:

1. Reference to MIL-SPEC requirements, such as MIL-F-83300, for VTOLs in similar roles.

2. Piloted simulation, through varying parameters important to hover maneuvering characteristics, while performing a specific task.

3. Analysis, based on some performance criterion such as hover precision control power to trim, power failure, or response.

Though developments have been made by both NASA and GAC with respect to Item 2, above, this was not an available option at the time.

Item 1 is a useful reference, but hybrid vehicles fall outside the familiar range of VTOLs and may require separate handling qualities criteria.

Figure 3-1 – Tradeoff Study Approach
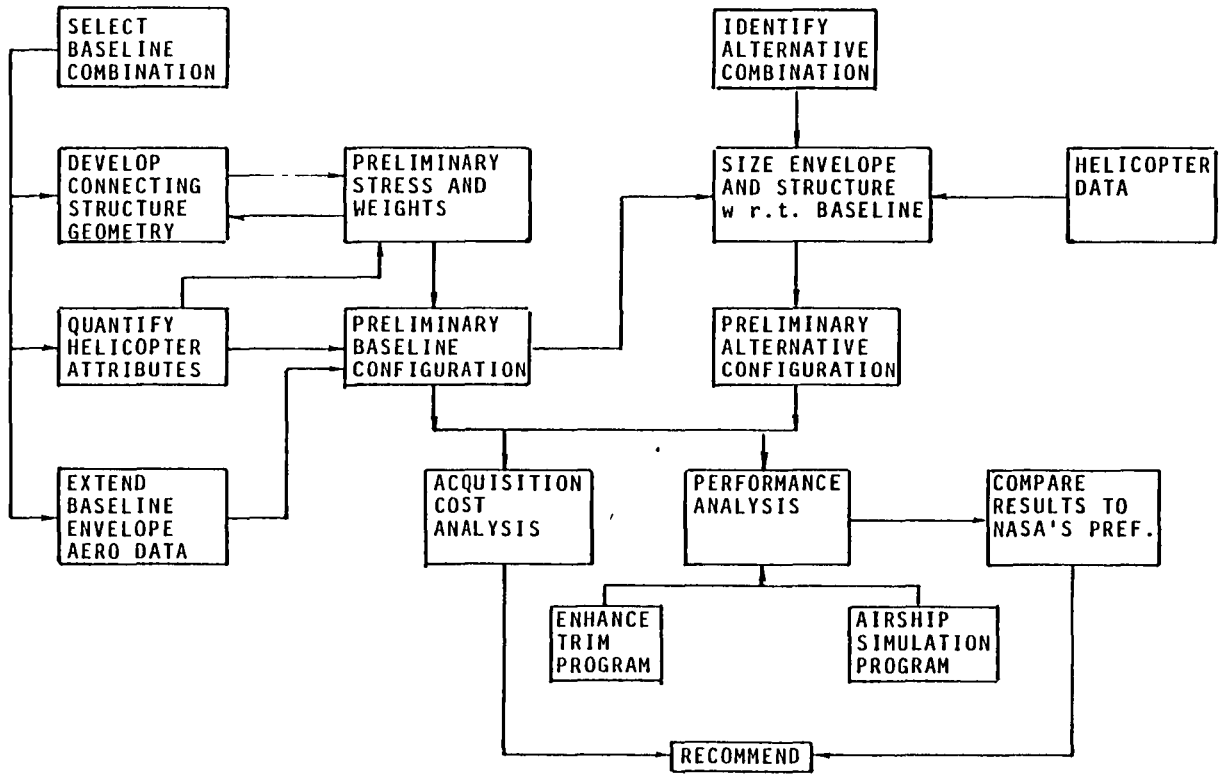
Figure 3-2 — Hughes OH-6A Helicopter and GZ20 Envelope

FRAME

26 FT 4 IN DIA

78 8 FT

19 5 FT

45 FT

86 95 FT

190 3 FT (THEORETICAL ENVELOPE)

2 2 FT

C B

59 54 FT

34 54 FT

17 FT

GROUND LINE (REF)
(RELATIVE LOCATION OF
CAR ON GZ 20 AIRSHIP)

70 0 FT

45 9 FT DIA

45 DEG

5 FT

6 5 FT DIA   6 31 FT (REF)

14 1/2 DEG (TIRE FLAT &
STRUT COLLAPSED –
RELATIVE LOCATION OF
CAR ON GZ 20 AIRSHIP)
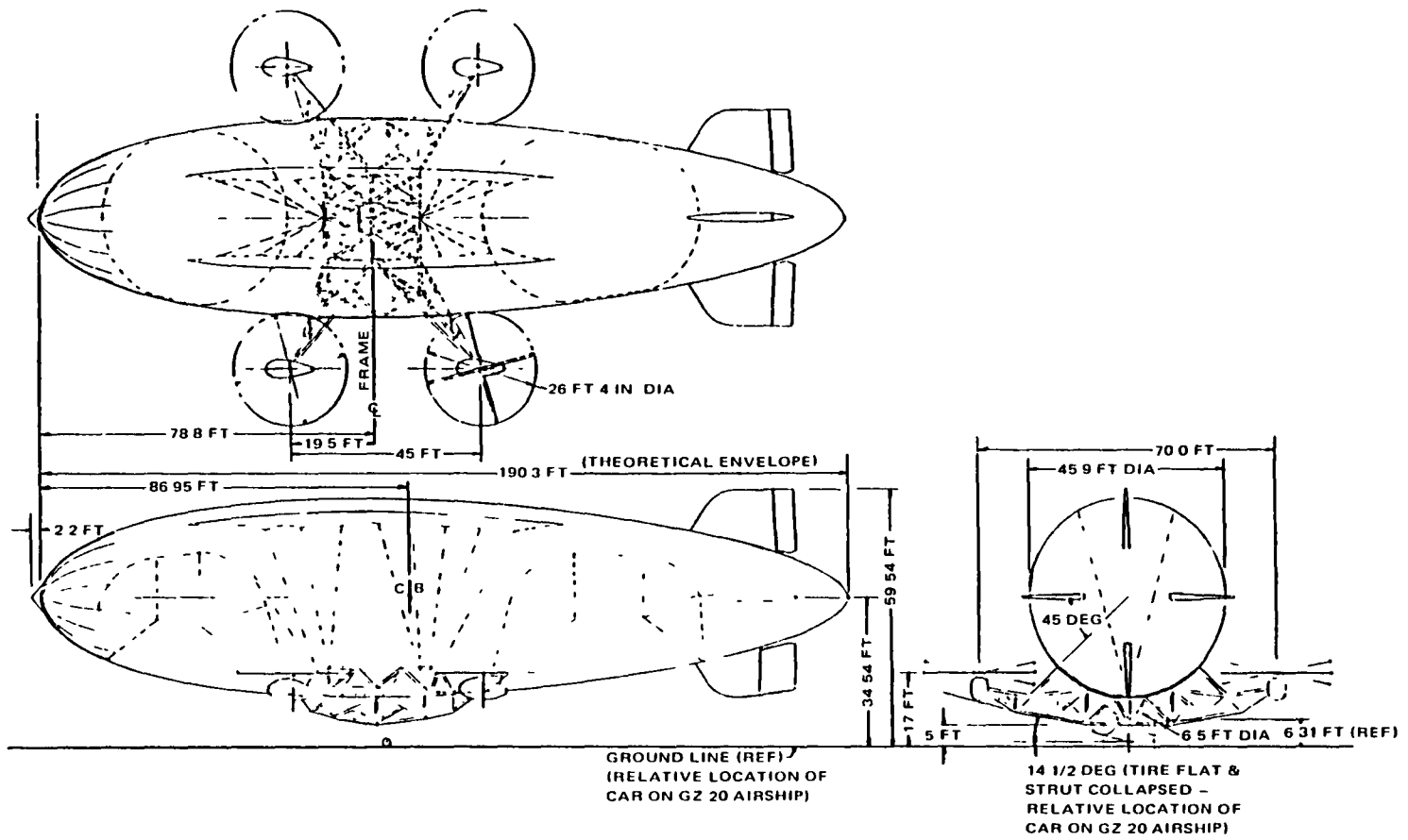
Figure 3-3 – Lateral Plane Hover Trim Program

DEFINE VEHICLE CHARACTERISTICS
- ROTOR THRUST
- MAX ENV DIAM
- ROTOR SPACING
- CYCLIC LIMITS
- AERO COEFF

SELECT SIDESLIP ANGLE

SELECT WIND SPEED

COMPUTE F_x, F_y, F_z

COMPUTE LATERAL CYCLIC

LIMIT ? — NO / YES

DECREMENT BY 1

COMPUTE YAW MOMENT & TOTAL CYCLIC

LIMIT ? — NO / YES

DECREMENT BY 1

COMPUTE LONG FORCE & TOTAL CYCLIC

LIMIT ? — NO / YES

DECREMENT BY 1

PREVIOUS DECREMENT ? — NO / YES

INCREMENT V BY 5 FT/SEC

OUTPUT

Figure 3-4 – Advanced Airship Simulation Block Diagram
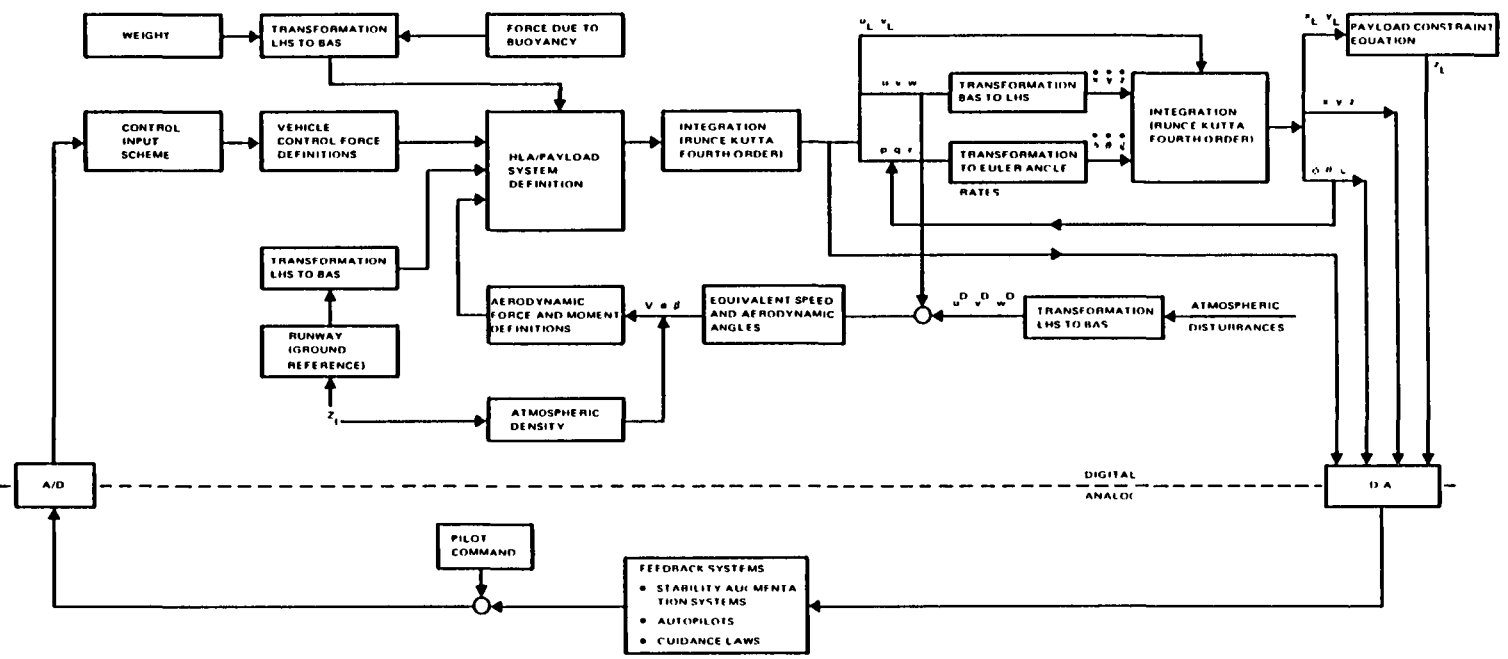
Item 3 appears to be the most plausible approach although it requires an analytical model of the FRV. Using this method, some of the design conditions are:

- Wind and turbulence
- Sideslip angle
- Buoyancy ratio
- Single propulsion unit failure
- Hover precision

As a way of beginning the analysis, the following arbitrarily chosen NASA guidelines were considered:

1. The design wind condition for stationkeeping is 20 knots steady wind at sea level on a standard day.

2. The airship shall be capable of stationkeeping in a steady wind up to sideslip angles of ± 30 degrees.

3. For a step change in wind sideslip angle of 10 degrees, the airship shall hold position over the ground within 10 feet.

4. For a step change in wind speed of 10 knots, the airship shall hold position within 5 feet.

5. For a single engine failure under the most adverse trim conditions, the airship shall lose less than 50 feet of altitude and change hover position over the ground less than 100 feet before control is recovered by the pilot. The airship shall be controllable with one engine out so that the pilot can make a safe landing. Load jettison can be assumed.

6. Airship pilot command response at the most extreme trim conditions in a steady wind (within 5 seconds) shall exhibit the following:

   - Longitudinal change of velocity over the ground of 10 feet per second
   - Lateral velocity over the ground of five feet per second
   - Rate of Climb of 400 feet per minute
   - Yaw or pitch rate of six degrees per second and a roll rate of 10 degrees per second

7. The requirements must apply to buoyancy ratios corresponding to maximum and zero useful loads.

2. HELICOPTERS

a. Requirements

Several qualities were initially established as being highly desirable for the chosen helicopter:

1. The helicopter should be lightweight to keep the overall vehicle smaller and less costly.

2. For safety considerations, a twin-engine helicopter system is desirable.

3. Since the helicopter would be restrained in some manner by its support frame, an articulated rotor system would handle the adverse moments being placed on the system better than a rigid rotor system. An articulated rotor system would also be the type of rotor system most likely to be incorporated into a future heavy lift airship design.

Consideration was also given as to the candidate helicopter's availability as GFE. A helicopter model furnished by the government would be highly desirable for this program from a cost standpoint.

Two goals were identified for on the selection of an envelope for the FRV. The most critical is to minimize cost which in essence mandates the use of an existing envelope. Choosing a new envelope design could double the cost. The envelope should also if possible, permit the FRV to attain a range of buoyancy ratios between 0.5 and 1.0.

b. Candidate Equipment

A list of potential helicopter candidates is presented in Table 3-1. Note that the equipment is grouped by rotor diameter; i.e., less than 25 feet, 25-30 feet, 30-35 feet, and greater than 35 feet. Although there are several helicopters available of the class called for in this study, two models stand out as particularly attractive - the Hughes 500 and the Messerschmitt-Bolkow-Blohm BO-105.

The Hughes 500 has a small rotor diameter (26.33 ft) and a very light airframe (1088 pounds). It can develop 2550 pounds of thrust and has an articulated rotor system. The most attractive feature of the Hughes 500, however, is that it is owned in quantity by the government in the form of the OH-6A. Since the design of the FRV requires four helicopter systems, helicopters supplied as government-furnished equipment represent a significant cost savings for this program.

The Messerschmitt-Bolkow-Blohm BO-105 is attractive primarily because of its twin-engine system which provides a significant safety advantage, especially in a research or experimental type vehicle. The BO-105 also provides more available thrust (5070 pounds). Obvious disadvantages of the BO-105 are its rigid rotor system (refer to Section 3.2.a) and acquisition cost.

Table 3-2 shows the approximate base price of five of the preferred candidate helicopters. As the table indicates, selection of a helicopter that is not GFE represents a substantial cost penalty to the program.

3. CANDIDATE VEHICLES

Several of the candidate helicopters were combined with various envelope sizes. The resulting preliminary configurations are listed in Table 3-3. The envelope sizes shown are those that would provide the desired range of buoyancy ratios (β), $0.5 \leq \beta \leq 1.0$. As Table 3-3 indicates, the OH-6A is the only helicopter that can be combined with an existing envelope and yield the desired range of β. The GZ20 is the designation of the airship envelope currently in use with the Goodyear Tire & Rubber Company's fleet of public relations airships.

TABLE 3-1 – CANDIDATE HELICOPTERS

Rotor diameter	Helicopter manufacturer	Country	Model	Engine Make	Engine Model	H P	No	Rotor system Type	blades	Diam (ft)	Disc area (ft²)	Empty (lb)	Max T O (lb)	Max disc (psf)	Max pwr (psf)
Less than 25 ft	Cicar'e	Argentina	C K 1		4C-27	190-200	1	Rigid	4	24 94	471 43	1034	1794	3 74	9 28
	Brantly-Hynes	U S A	B-2B	Lycoming	IVO-360 A1A	180	1	Articulated	3	23 75	442 0	1020	1670	3 77	9 27
	Berger	Switzerland	BX-110	Wankel		180	1	Semi-rigid	3	24 27	462 85	1014	1587	N/A	N/A
25 to 30 ft	Hughes	U S A	300C	Lycoming	410-360 -dia	190	1	Articulated	3	26 84	565 5	1050	2050	3 62	N/A
	Hughes	U S A	500	Allison	250-C18A	317	1	Articulated	4	26 33	544 63	1088	2550	N/A	N/A
	Hughes	U S A	500D	Allison	250-C20B	420	1	Articulated	5	26 5	547 81	1320	3000	5 48	7 14
	Robinson	U S A	R-22	Lycoming	0-320 -A28	150	1	Tri-hinged	2	25 17	197 4	764	1300	2 61	10 48
	Brantly-Hynes	U S A	305	Lycoming	IVO-540 -A1A	350	1	Articulated	2	28 67	N/A	1800	2700	4 65	9 84
	Berger	Switzerland	BX-50A	Continental	C90	90	1	Rigid	2	26 25	N/A	639	904	N/A	N/A
30 to 35 ft	Enstrom	U S A	F-28C/ 280C	Lycoming	M10-360 -E1AD	205	1	Articulated	3	32 0	804 0	1495	2200	2 74	10 73
	Enstrom	U S A	280L	Lycoming	H10-360 -11AD	225	1	Articulated	3	34 0	908 0	1560	2600	2 86	11 56
	Spitfire	U S A	Mark 1	Allison	250-C20B	420	1	Ariculated	3	32 0	804	1250	2300	2 86	9 58
	MBB	Germany	BO-105L	Allison	250-C28C	550	2	Rigid	4	32 28	N/A	2622	5070	5 43	6 25
	Helicop Jet	France		Turbomeca	LS TA LO11	500	1	--	4	30 83	747	992	2336	3 13	N/A
	Bell	U S A	206B	Allison	250-C20B	420	1	Semi-rigid	2	33 33	873	1615	3200	N/A	N/A
More than 35 ft	Aerospatiale	France	3A 316B	Turbomeca	111B	870	1	Articulated	3	36 15	N/A	2520	4850	N/A	N/A
	Aerospatiale	France	AS350D	Lycoming	LTS101 -600AZ	616	1	Articulated	3	35 02	N/A	2304	4300	N/A	N/A
	Aerospatiale	France	AS355E	Allison	250-C20F	425	2		3	35 02	N/A	2712	4630	N/A	N/A

TABLE 3-2 - PREFERRED HELICOPTERS

Manufacturer	Designation	Rotor diam/blades	Power plant	Max thrust (lb)	Empty weight (lb)	Approx base price (1980)
Brantly/-Hynes	B-2B	23.75 ft/3	Lycoming 180 HP	1670	840	$ 60,000
Hughes	OH-6A	26.33 ft/5	Allison 317 HP	3000	950	$257,500*
Enstrom	280C-Shark	32.0 ft/3	Lycoming 205 HP	2200	1295	$117,300
MBB	BO-105	32.28 ft/4	Allison 790 HP (2)	5070	2172	$680,000
Aerospatiale	Twinstar	35.06 ft/3	Allison 850 HP (2)	4630	2427	$510,000

*Price for Hughes 500 D
OH-6A may be available GFE

When the BO-105 helicopter is matched with the GZ20 envelope, the buoyancy ratios available become much less than those desired for the FRV. This is primarily due to the heavier weight of the twin-engine helicopter.

The various configurations are shown in Figure 3-2 and Figures 3-5 to 3-9. Highlights of each configuration are as follows:

1. Figure 3-2 - Hughes 500 (OH-6A) helicopter and GZ20 envelope. This arrangement shows a GZ20 envelope with the car removed and replaced with a support frame for four Hughes 500 helicopters. The tail boom and tail rotor have been removed from each helicopter.

2. Figure 3-5 - BO-105 helicopter and GZ20 envelope. This arrangement shows the dimensions involved in designing a support frame to accommodate four BO-105 helicopters and the GZ20 envelope. The tail boom and tail rotor have been removed from each helicopter.

3. Figure 3-6 - BO-105 helicopter and a dedicated envelope. This arrangement reflects the effect of incorporating a larger envelope into the design. The envelope volume is 370,000 cubic feet.

4. Figure 3-7 - Aerospatiale helicopter and dedicated envelope. This figure indicates the dimensions associated with combining Aerospatiale twinstar helicopters and an envelope with a volume of 370,000 cubic feet.

TABLE 3-3 - FRV CONFIGURATIONS STUDIED

HELICOPTER	ENVELOPE SIZE (FT³)	LIFT (LBS)				BUOYANCY RATIO	
		STATIC	ROTOR	TOTAL	NET	MAX PAYLOAD	EMPTY
B-2B	187,233	11,174	6,680	17,854	6,680	0 62	1 00
OH-6A	205,270*	12,292	12,016	24,308	12,177	0 51	1 01**
280C	240,115	14,452	8,800	23,252	8,800	0 58	1 00
BO-105	205,270*	12,292	20,460	32,752	13,232	0 38	0 63
BO-105	370,000	22,156	20,460	42,616	20,460	0 53	1 00
Twinstar	370,000	22,156	18,520	40,676	17,900	0 55	0 97

*GZ-20 ENVELOPE   ** BETA = 0.85 FOR CONFIGURATION WITH AUXILIARY PROPS

5. Figure 3-8 - Brantly-Hynes helicopter and dedicated envelope. This figure gives the principal dimensions for a configuration composed of Brantly-Hynes B-2B helicopters and an envelope with a volume of 187,233 cubic feet.

6. Figure 3-9 - Enstrom helicopter and dedicated envelope. This figure gives the principal dimensions for a configuration composed of Enstrom 280C helicopters and an envelope with a volume of 240,115 cubic feet.

4. PERFORMANCE PREDICTION

For the configurations listed in Table 3-3, preliminary performance calculations were conducted. Results are presented in Figure 3-10. Inherent in these plots are four key features:

1. Total allowable continuous cyclic was assumed to be four degrees. This is consistent with recommendations from Sikorsky Aircraft relative to predicted shaft fatigue life.

2. The cross-hatched area represents the predicted operating realm of the Goodyear 75-ton heavy lift airship (HLA) design. The lower curve represents the HLA operating empty, but with 60 percent reverse thrust acting on diagonally opposed rotors. The middle curve is the HLA fully loaded at 10 degrees cyclic. The upper curve is again the HLA fully loaded but with a total cyclic of 20 degrees.This is the predicted cyclic transient limit. At 10 degrees cyclic the main rotor shaft fatigue life is long. The 20 degree cyclic transient limit should be used for only short periods to react gusts as the fatigue life of the main rotor shaft is greatly reduced. The area between the 20 and 10 degree curve shown in Figure 3-10 is only for transient conditions.

C B

86 95 FT

78 8 FT

EXTERNAL SUSPENSION ATTACHMENT

INTERNAL SUSPENSION ATTACHMENT

78 FT

32 3 FT

20 FT

50 FT

45 92 FT

16 75 FT

14 5 FT

19 5 FT

GROUND LINE (REF)

13 DEG (REF)

Figure 3-5 – MBB BO-105 Helicopter and GZ20 Envelope

3-11
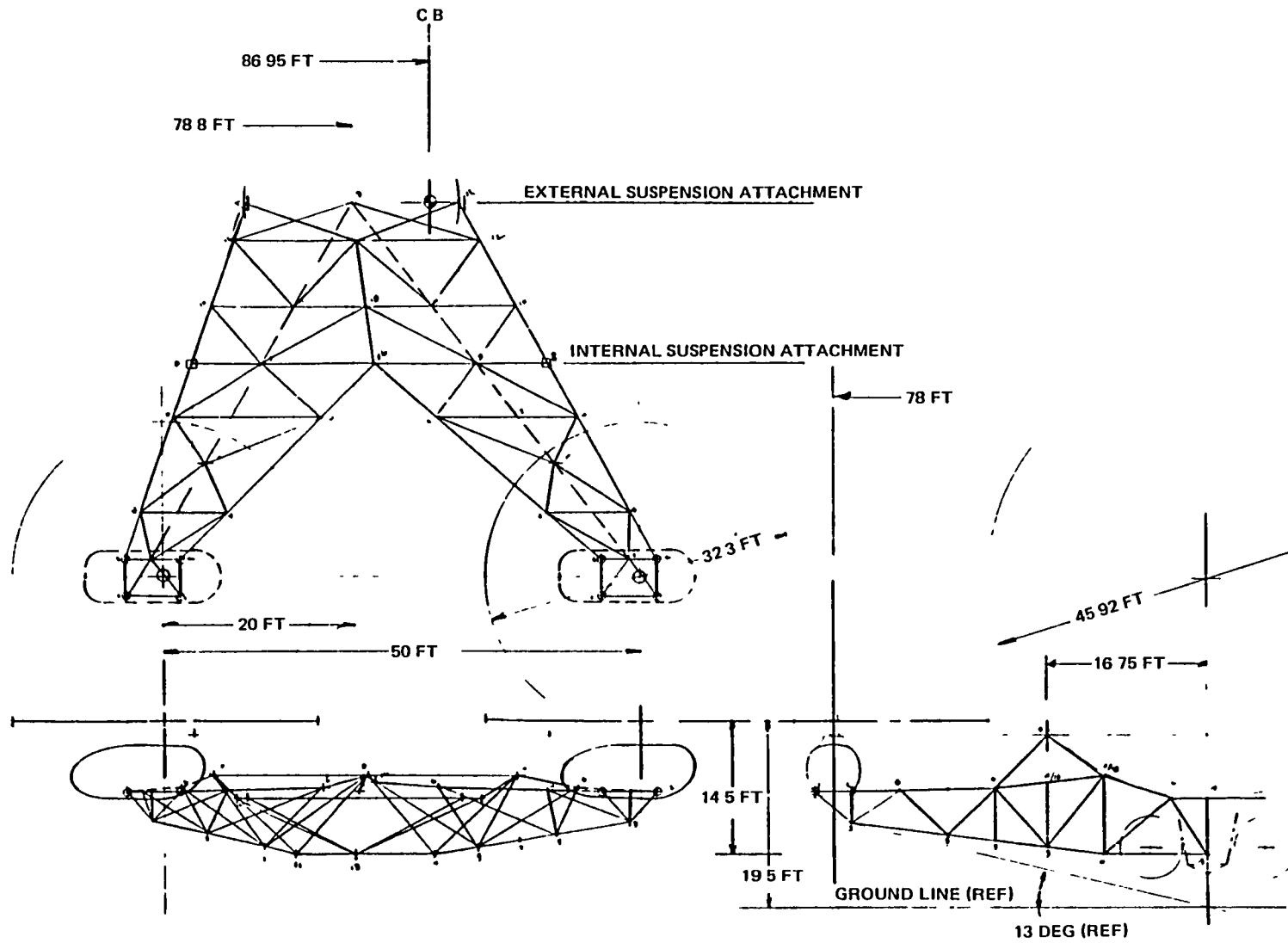
Figure 3-6 – MBB BO-105 Helicopter and a Dedicated Envelope
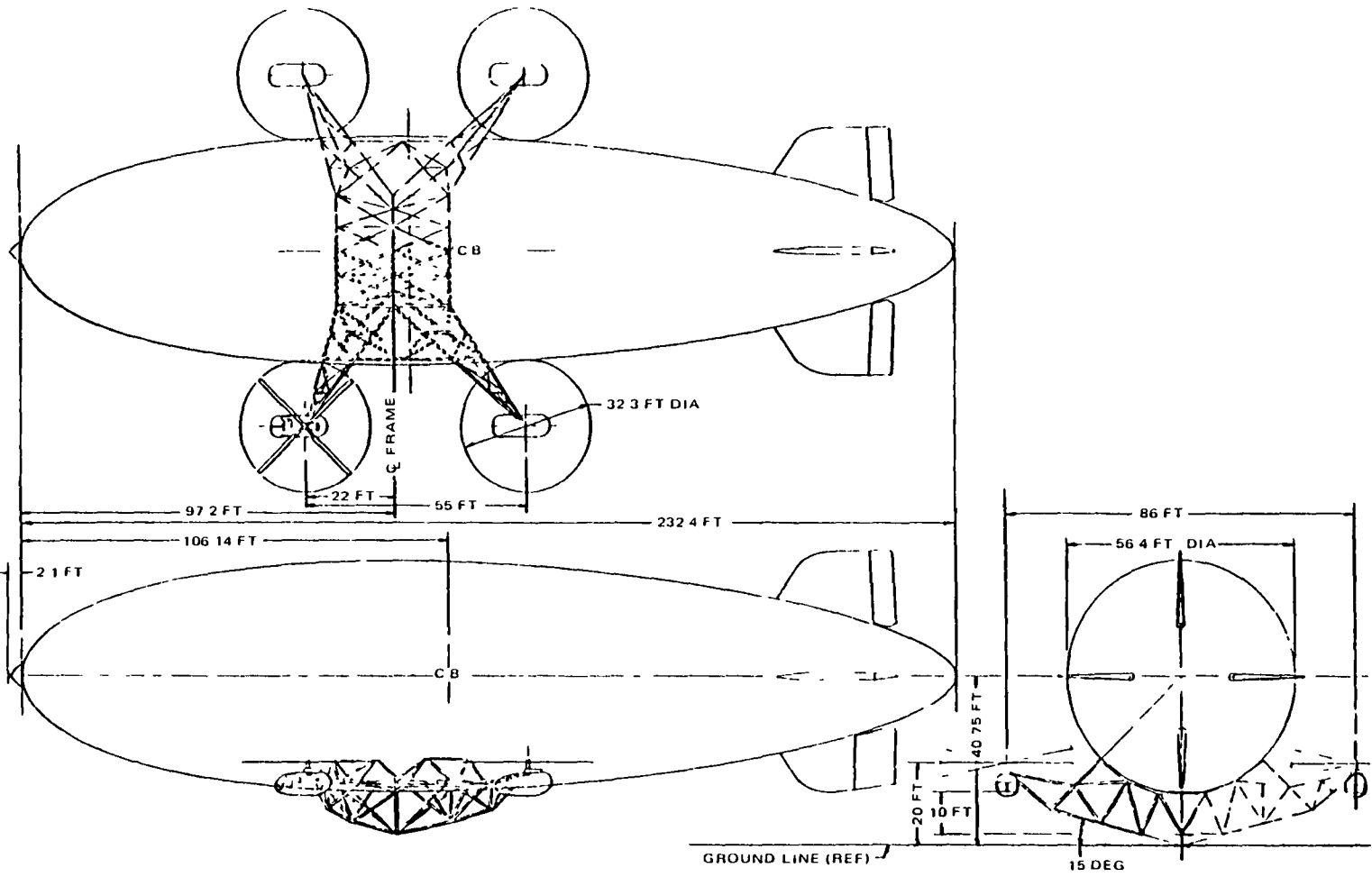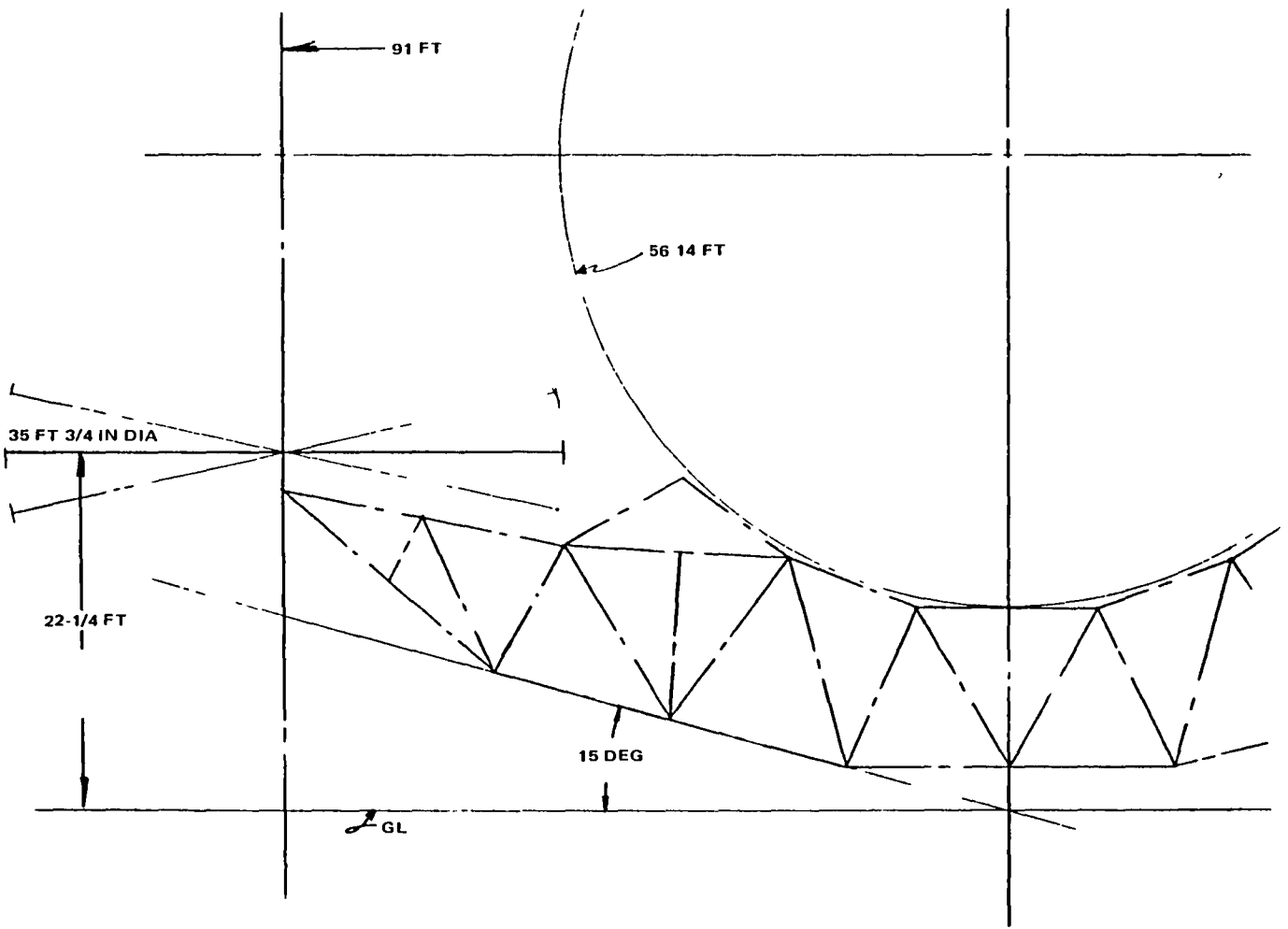
Figure 3-7 – Aerospatiale Helicopter and a Dedicated Envelope

91 FT

56 14 FT

35 FT 3/4 IN DIA

22-1/4 FT

15 DEG

GL

66 FT

44 5 FT

23 FT 9 IN DIAM

17 FT

15 DEG

α G L
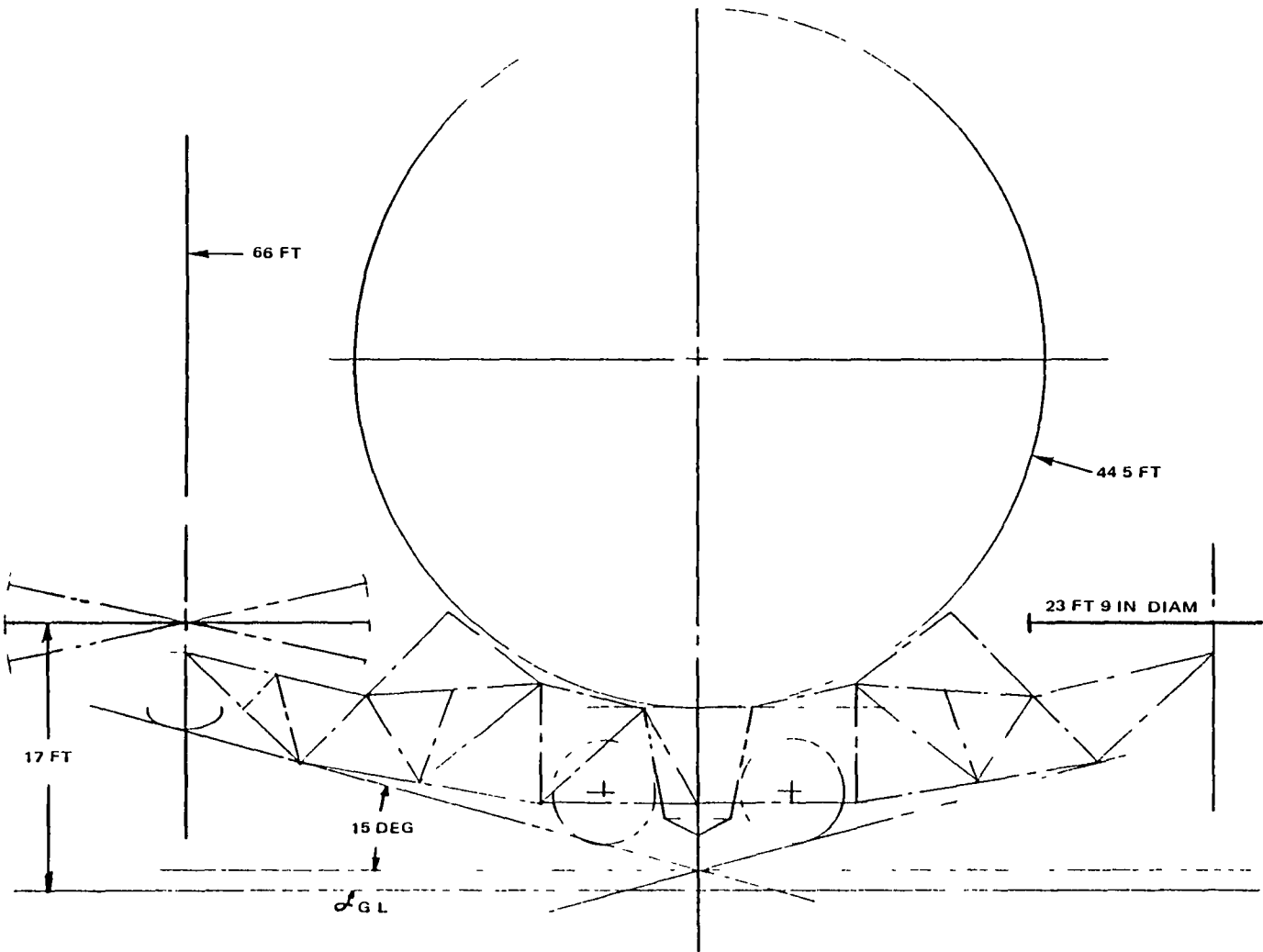
Figure 3-8 – Brantly-Hynes Helicopter and Dedicated Envelope

Figure 3-9 – Enstrom Helicopter and Dedicated Envelope

83 FT

48 38 FT

21 1/2 FT

15 DEG

3-15
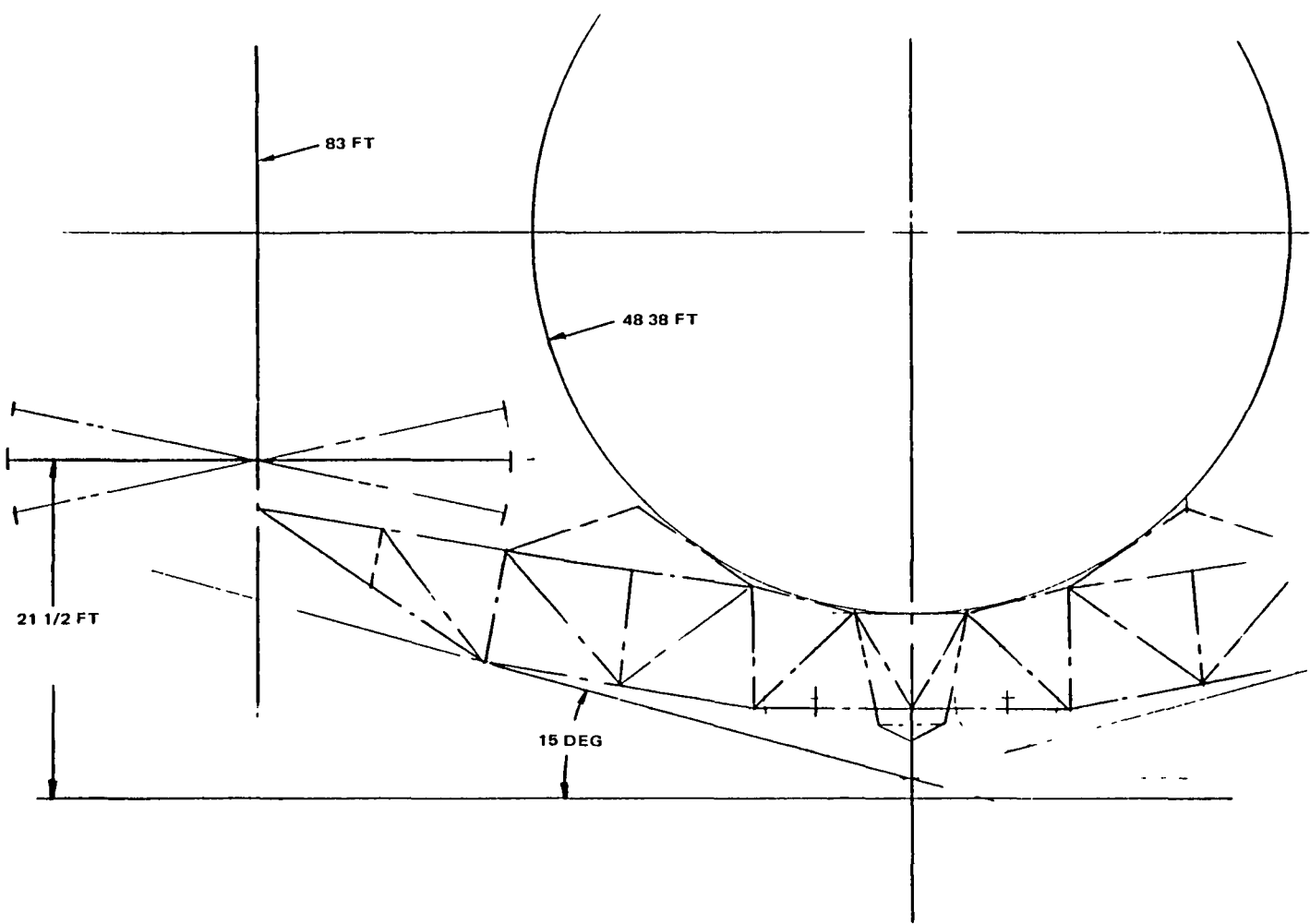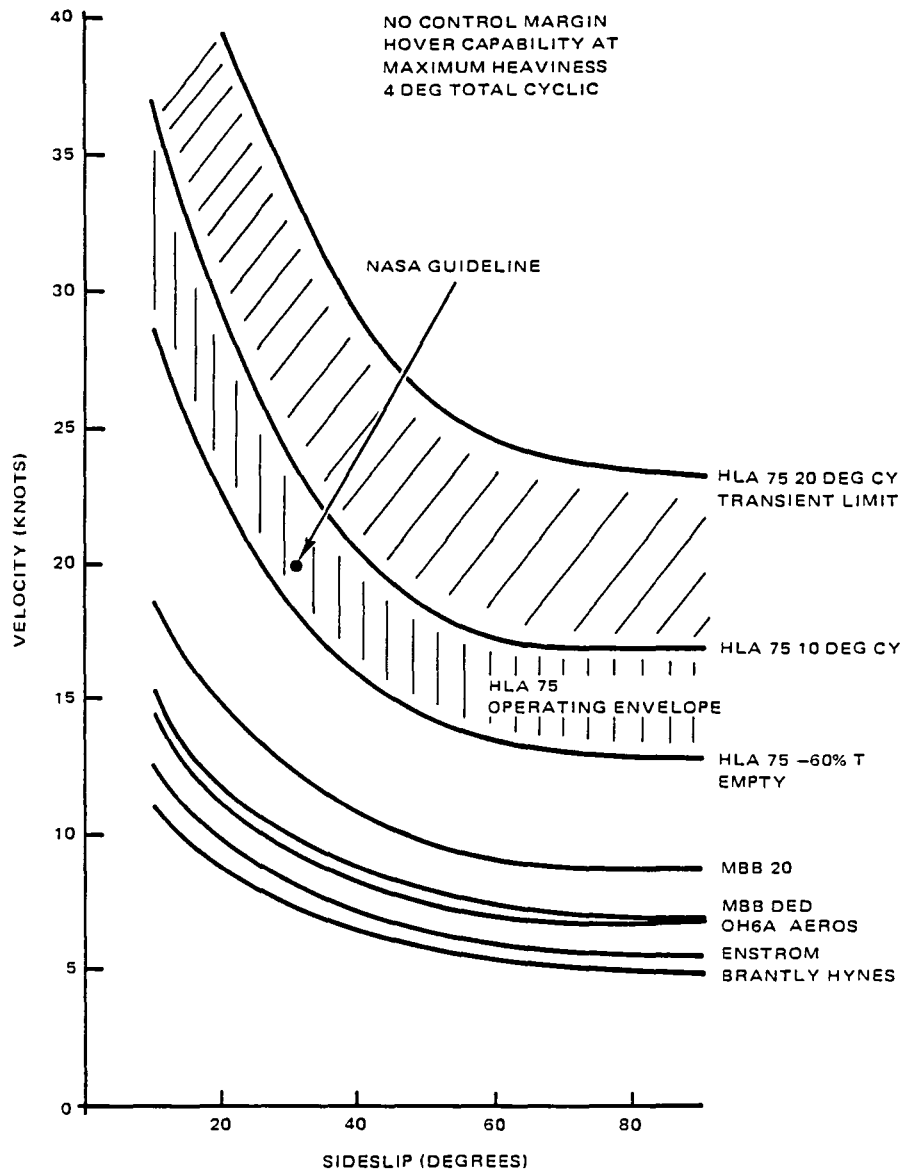
Figure 3-10 – Preliminary Performance Characteristics with Four Degrees Total Cyclic

3.   The design guideline of sustaining a 20 knot wind at a sideslip angle of 30 degrees is within the predicted operating envelope for the HLA.

4.   All plots for the new configurations are for a maximum heaviness condition.

Note that all curves representing FRV configurations are well below what might be considered acceptable. Therefore, to improve crosswind hover capabilities, the rotors were placed on a lateral hinge with an allowable travel of 12 degrees. The longitudinal cyclic of 4 degrees was retained.

Results of this change are shown in Figure 3-11. Even with this improvement, the MBB helicopter with the GZ20 envelope is the only configuration to fall within the HLA range. This can be attributed to this vehicle's large thrust availability and low buoyancy ratio. Of those vehicles capable of demonstrating a larger range of buoyancy ratios, the MBB with the dedicated envelope and the Hughes OH-6A with the GZ20 envelope perform best. Since the Hughes combination is inherently less expensive due to GFE considerations, it would be preferred.

The MBB/GZ20 and Hughes/GZ20 combination were further examined in a flight simulation using the design criteria described earlier. Results are shown in Table 3-4. While the position errors are small as a result of the idealized autopilot, their relative values are indicative of the differences between the two vehicles. The percent of lateral stick i.e., percent of available lateral force utilized for each condition indicates even more clearly that the MBB/GZ20 combination is preferable from a control point of view.

5. AUXILIARY PROPULSION

In assessing the Hughes/GZ20 versus the MBB/GZ20 vehicles the former has a decided cost advantage, while the latter has a marginal predicted performance advantage. Since the cost factors cannot be altered, consideration was given to enhancing the controlability of the Hughes/GZ20 combination.

The amount of lateral or forward thrust available from the rotor systems of a vehicle like the FRV is a direct function of the vehicle's heaviness. Since lateral or forward thrust is a component of the total thrust vector generated by the helicopter, the rotor system has to be operated in a heavily-loaded condition to generate large amounts of lateral or forward thrust. When the FRV is lightly loaded, lateral and forward thrust capability are decreased accordingly. This constraint represents a limit to vehicle cruise speed and crosswind hovering capability.

To overcome this constraint, a system of auxiliary propulsion units (APU) was proposed. The APU set would consist of four aircraft engines with reversible pitch propellers. Two engines would be mounted in the fore and aft direction and two engines would be mounted in the lateral direction. The forward facing APU's would be used together either to generate cruising thrust or differentially create low speed yawing moments. The lateral facing APU's would be used together to generate side force. Figure 3-12 shows the crosswind hover performance gains which can be realized by employing this auxiliary propulsion.
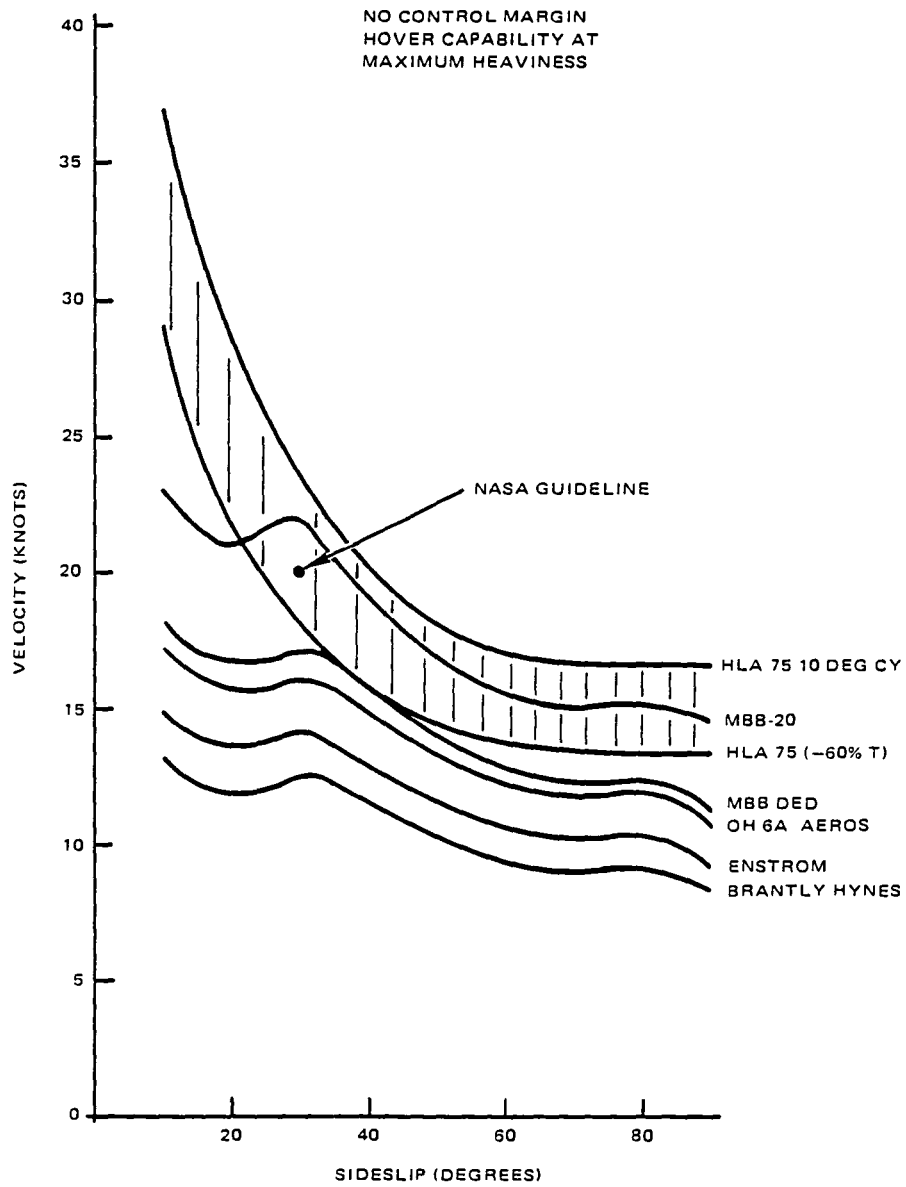
Figure 3-11 – Preliminary Performance Characteristics with 4 Degrees Longitudinal and 12 Degrees Lateral Cyclic

TABLE 3-4 - CLOSED LOOP RESPONSE TO WIND DISTURBANCES
(PAYLOAD = 12,000 POUNDS)

Hover Trim	Step Input	GZ-20/OH-6A				GZ-20/MBB-105			
		Maximum Position Error		Control Input		Maximum Position Error		Control Input	
		X (ft)	Y (Ft)	LONSTK (%)	LATSTK (%)	X (ft)	Y (ft)	LONSTK (%)	LATSTK (%)
V_w = 5 kts. ψ_w = 30°	$\Delta\psi$ = 10°	0.05	-0.10	0.5	12	0	-0.05	0	5
V_w = 0	ΔV_w =10 kts $\Delta\psi_w$ = 30°	0.05	0.35	4	35	0	-0.2	0.1	20
V_w = 10 kts ψ_w = 30°	$\Delta\psi_w$ = 10°	0.05	0.45	-2	45	0	0 25	-2.5	30
V_w = 5 kts ψ_w = 30°	ΔV_w =10 kts	-0.1	-0.75	9	75	-0.05	-0.45	5	45
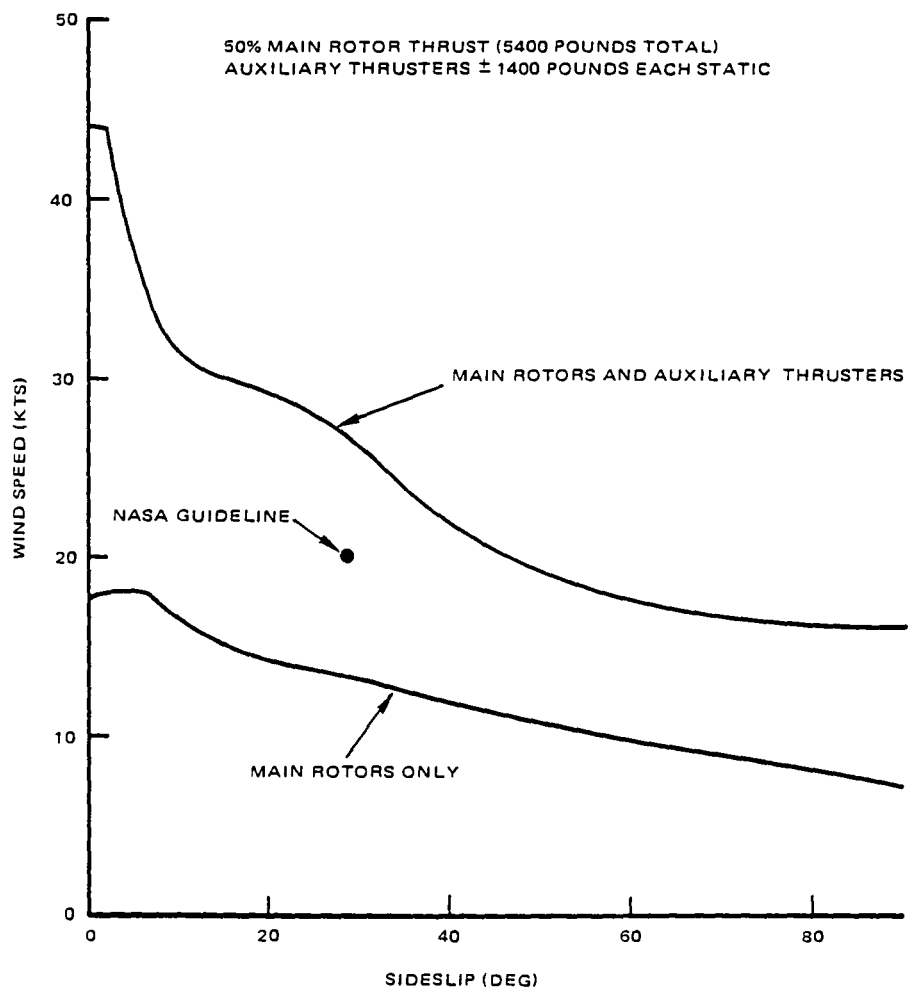
Figure 3-12 - Effect of APU's on Predicted Crosswind Hover Capability

a. Rotors and Power Plants

The key requirement of the proposed APU system is that it be capable of providing equal, or nearly equal, amounts of thrust in opposite directions. Since virtually all production aircraft propellers today incorporate some twist distribution, there is a fairly large penalty in fore and aft thrust symmetry associated with using a conventional aircraft propeller. One propeller that appears to be suitable for this application is the tail rotor from a helicopter designed to develop thrust in two directions. The possibility of using helicopter tail rotors for this application was investigated.

To address the question of whether it is possible to use helicopter tail rotors as auxiliary thrust devices, a survey of existing tail rotors and power plants was conducted. Several criteria were established. The only tail rotors and power plants considered were those installed on aircraft already in the military inventory. This decision was based on cost and availability considerations. It was also desired that the rotor be untwisted and have very little or no camber. A list of potential tail rotor systems is shown in Table 3-5. A list of potential power plants is shown in Table 3-6.

A computer program was used to predict the thrust available and power required for the various tail rotors. Thrust versus power curves for the different tail rotors are presented in Figure 3-13. The upper limit of each curve (tail rotor) represents the point at which the rotor is stalled and is unable to generate more thrust.

Also shown in Figure 3-13 are various power plants. The horsepower depicted for each engine represents the maximum rated horsepower minus 10 percent to account for installation losses. For a given tail rotor to generate a certain amount of thrust, the required horsepower is read from the abscissa of Figure 3-13. Any engine shown on the figure rated at a higher horsepower could presumably be used with that tail rotor.

Preliminary calculations indicate that a minimum of 1200 static pounds of thrust each from two engine propeller combinations is desired for adequate lateral controlability. Under these criteria, three rotors appear to be suitable: CH-3E, SH-3, and AH-1T. Since the CH-3E and SH-3 have five-bladed rotors, the AH-1T system (two blades) appears to be the best choice based on design simplicity.

The AH-1T tail rotor is untwisted and incorporates a small amount of camber. The rotor is capable of providing greater thrust in the "cambered" direction. The practical limit of the rotor for this application is therefore dictated by the amount of thrust it can provide in the "uncambered" direction. Analysis indicates that 1500 pounds can be generated in the "uncambered" direction (Figure 3-13). This value represents the upper limit of fully reversible thrust available with the AH-1T tail rotor.

Since the desired thrust level is 1200 pounds, any of the engines depicted in Figure 3-13 should be capable of delivering the required power. The two Continental engines are reciprocating and as such have good fuel consumption qualities. They are, however, quite heavy (dry weight is approximately 450 pounds).

TABLE 3-5 - POTENTIAL TAIL ROTORS

Helicopter	Disk area (sq/ft)	Diameter (ft)	Chord (ft)	Blade area (sq ft)	No. blades
Hughes 500M-D (OH-6)	14.19	4.25	0.4424	0.94 (each)	2
Bell Jetranger (OH-58)	23.0	5.41	0.4381	2.37 (total)	2
Kaman SH-2F	52.42	8.17	0.775	3.17 (each)	4
Bell UH-1H	56.7	8.5	0.70	2.98 (each)	2
Bell AH-1T	74.03	9.71	1.0	4.86 (each)	2
Sikorsky CH-3E	83.9	10.33	0.455	2.35 (each)	5
Sikorsky SH-3	88.3	10.58	0.4499	2.38 (each)	5
Sikorsky UH-60	95.0	11.0	0.8091	4.45 (each)	4
Sikorsky CH-54	201.0	16.0	1.283	8.28 (each)	4
Sikorsky CH-53E	314.16	20.0	not avail.	not avail.	4

TABLE 3-6 - AUXILIARY PROPULSION UNITS

Model (Mil Design)	Type	T.O. SHP (10% for Losses)	Weight (lb.)	SFC (lb/Hr/hp) T.O.; Cruise	Military (GFE)
Allison					
250-C18 (T63-A-5A)	Turboshaft	317 (285)	139	.697; .725	OH-6A, OH-58A
250-C20B (T63-A-720)	Turboshaft	420 (378)	158	.650; .709	OH-58
GMA 500	Turboshaft	≈ 800 (700)	300	≈ .55	Under development for U S Army
AVCO Lycoming					
T53-L-11	Turboshaft	1,100 (990)	496	.68	UH-1B, D, F
T53-L-13B	Turboshaft	1,400 (1,260)	540	.58	Adv. UH-1's and AH-1G
YT702-LD-700	Turboshaft	615 (554)	241	.567	Developing for U. S. Government (Bell 222)
GE					
T58-GE-3	Turboshaft	1,325 (1,193)	309	.61	UH-1F

TABLE 3-6 - Continued.

Model (Mil Design)	Type	T.O. SHP (10% for Losses)	Weight (lb.)	SFC (lb/hr/hp) T.O.; Cruise	Military (GFE)
Pratt & Whitney of Canada					
PT 6A-25	Turboprop (3 BL HARTZEL V Ptch D = 7.5 F)	580 (522)	321	.63; .63	Beech T-34C (Navy Trainer)
PT 6A-34B	Turboprop (3 BL HTZL V Pitch D = 7.75 F)	783 (705)	311	.595; .604	Beech T-44A (Navy Trainer)
PT 6A-41	Turboprop (3 BL VP Prop D = 8.2 F)	903 (813)	380	.590; .591	Beech C12C (Army & Navy Util Trans.)
PT 6A-21	Turboprop (HTZ 3BL VP D = 7.75 F)	580 (522)	300	.630; .649	Beech VC-6B (AF Trans)
PT 6A-28	Turboprop (HTZL 4BL VP D = 7.5 F)	715 (644)	300	.602; .612	Beech U21-F (Army Txp)
Continental					
IO-520-D	Recip (2 BL McCauly VP or 3 BL McCauly Opt. D = 6.67 F D = 6.8 F)	300 (270)	459	N/A	U-17 (Cessna 185) (AF Trainer)
IO-470-L	Recip (2 BL HTZL VPT D = 6.51)	260 (234)	446	N/A	T-42A Beech (Army Trainer)

TABLE 3-6 – Concluded.

Model (Mil Design)	Type	T.O. SHP (10% for Losses)	Weight (lb.)	SFC (lb/hr/hp) T.O.; Cruise	Military (GFE)
Garrett T76-G-416/417	Turboprop (3 BL Ham-Std D = 8.5 F)	715 (644)	341	.60	OV-10 (Rockwell; Marines, AF)
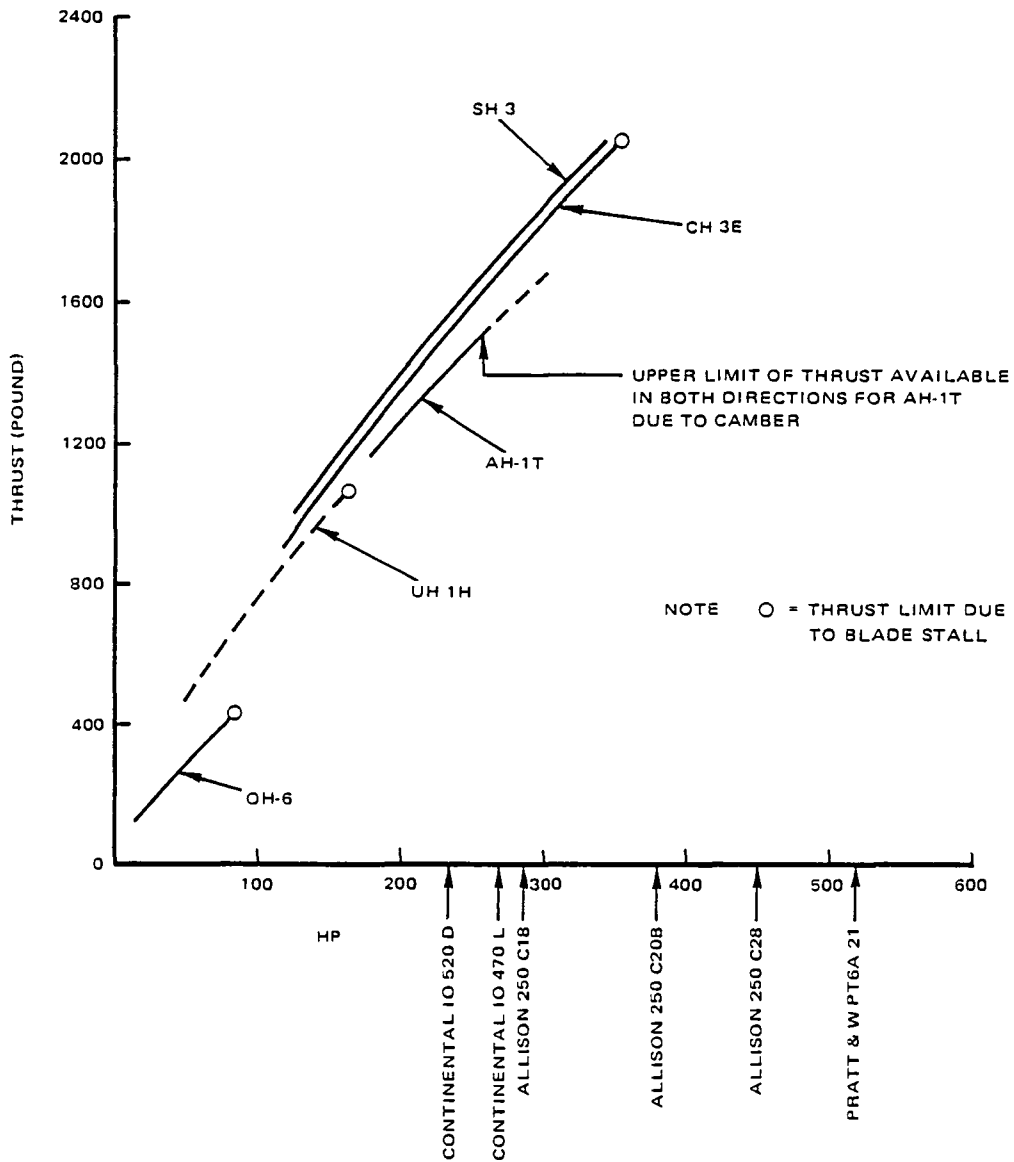
Figure 3-13 - Thrust Vs Required Horsepower for Various Tail
Rotor Engine Combinations

The Allison engines are turboshafts and despite higher fuel consumption, have good power-to-weight ratios. The Allison 250-C18 powers the OH-6 helicopter. The Allison 250-C20B is an uprated version of this engine and is installed on the OH-58 helicopter. Since the OH-6 is the proposed rotor system for the flight research vehicle, selecting the 250-C20B engine for the auxiliary propulsion units would provide a degree of commonality for the FRV's propulsion system.

b. Auxiliary Propulsion Unit Modifications

The 1500 pounds of thrust developed by the AH-1T tail rotor assumes that the engine can provide a shaft output of approximately 1480 rpm. The output shaft rpm of the 250-C20B engine is 6016. In order to use the AH-1T tail rotor, some type of gear reduction assembly would be required. The cost of independently developing a gear reduction assembly to accommodate the AH-1T tail rotor would be substantial.

There appears to be two alternatives that can enable the AH-1T tail rotor to be combined with the 250-C20B engine.

The first makes use of hardware used in a turboprop version of a 250-series engine developed by the Detroit Diesel Allison company. The 250-B17 engine is essentially the 250-C20B engine except for the addition of a modified accessory gearbox section and a propeller reduction gear assembly. Since the 250-series engines are of modular design, it is possible that government-furnished 250-C20B engines (installed on OH-58 helicopters) could be modified by an Allison distributor and converted into the 250-B17 version.

Figure 3-14 shows the two versions of the engine. The compressor, turbine, and combustor modules of a C20B version would be fitted to a B17 version accessory gearbox. A propeller gearbox would also be added. Discussions with Allison representatives suggest this modification would be less expensive than procuring a complete 250-B17 engine.

The output of the propeller reduction gearbox of the B17 engine is constant at 2030 rpm. This limitation required a re-evaluation of the AH-1T's tail rotor performance. Since the tail rotor diameter of the AH-1T is 9.7 feet, attaching it to a shaft with an output of 2030 rpm would result in a propeller tip speed of 1031 feet per second. Discussions with propeller manufacturers indicate that tip speeds of approximately 750 feet per second are usual design practice. The dominant consideration in limiting tip speed is noise generation. For the AH-1T tail rotor operating at 2030 rpm, tip speed can potentially be reduced by cutting a portion of the blade from each tip. The performance of the AH-1T tail rotor was re-evaluated using this criteria and results are shown in Figure 3-15. This shows the increase in thrust available with an increasing blade radius (and corresponding tip speed) at a constant 2030 rpm. The power required to generate the indicated thrust is also shown. If the B17 engine is selected with its fixed 2030 rpm output, a reasonable compromise between thrust required, power available, and noise considerations would be to remove 0.83 feet from each blade tip of the AH-1T tail rotor. The resulting rotor would then operate at a tip speed of 850 feet per second; generate approximately 1400 pounds of static thrust and absorb approximately 300 shaft horsepower. This alternative appears to be both mechanically and economically feasible.

The only potentially significant problem with this arrangement is the possibility that the coordinator on the 250-series engine might require modification. The coordinator is a device that simultaneously controls propeller and power turbine governors, input power, the condition lever, fuel cutoff, propeller reversal, and gas producer fuel. It is not presently

EXHAUST
19 0 IN
LH SIDE MOUNT
C/L
23 2 IN
2 7 IN
7 4 IN
RH SIDE MOUNT
FRONT (AND REAR) POWER TAKE OFF
COMPRESSOR INLET DIA 5 5 IN
TACHOMETER PADS

5 1 IN
TOP MOUNT
12 8 IN
TURBINE
COMPRESSOR
ACCESSORY GEARBOX
COMBUSTOR
GOVERNOR
LH SIDE MOUNT
FUEL FILTER
BOTTOM MOUNT
38 8 IN

C20B VERSION

PROP GEARBOX
PROP FLANGE
TACHOMETER PADS
LH SIDE MOUNT
PROP FLANGE
RH SIDE MOUNT
7 4 IN
22 5 IN
2 7 IN
C/L
EXHAUST
COMPRESSOR INLET DIA
19 0 IN
5 3 IN

5 1 IN
TOP MOUNT
12 8 IN
ACCESSORY GEARBOX
FUEL FILTER
GOVERNOR
COMPRESSOR
LH SIDE MOUNT
BOTTOM MOUNT
EXHAUST
COMBUSTOR
45 0 IN

B-17 VERSION

Figure 3-14 - Comparison of C20B and B-17 Versions of the Allison 250-Series Engines
(Source: Detroit Diesel Allison)
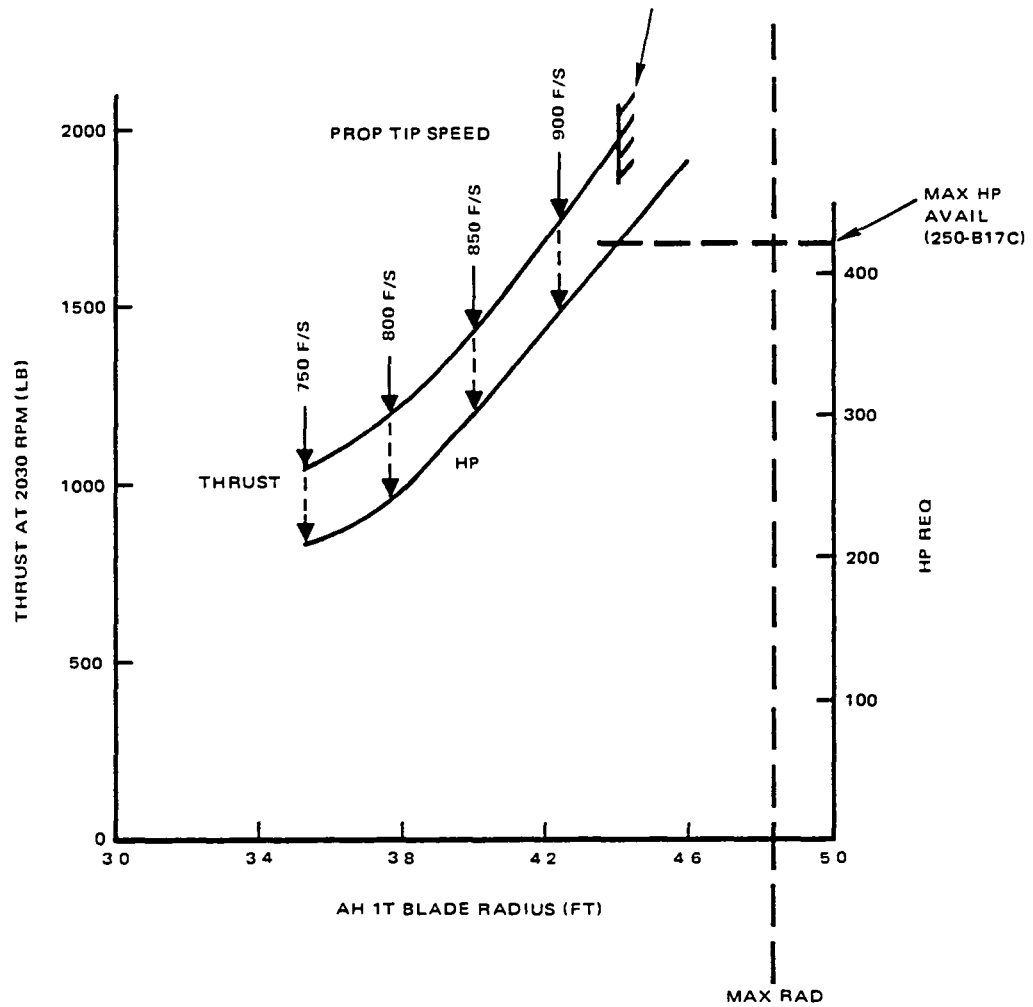
Figure 3-15 – AH-1T Tail Rotor Thrust-Power Relationships

DETROIT DIESEL ALLISON
GAS TURBINE

PROP GOVERNOR

PROP REDUCTION
GEARBOX

BATTERY

OIL TANK

OIL COOLER

PARTICLE
SEPARATOR

OUTPUT SHAFT FROM
ENGINE TO PROP
REDUCTION GEARBOX
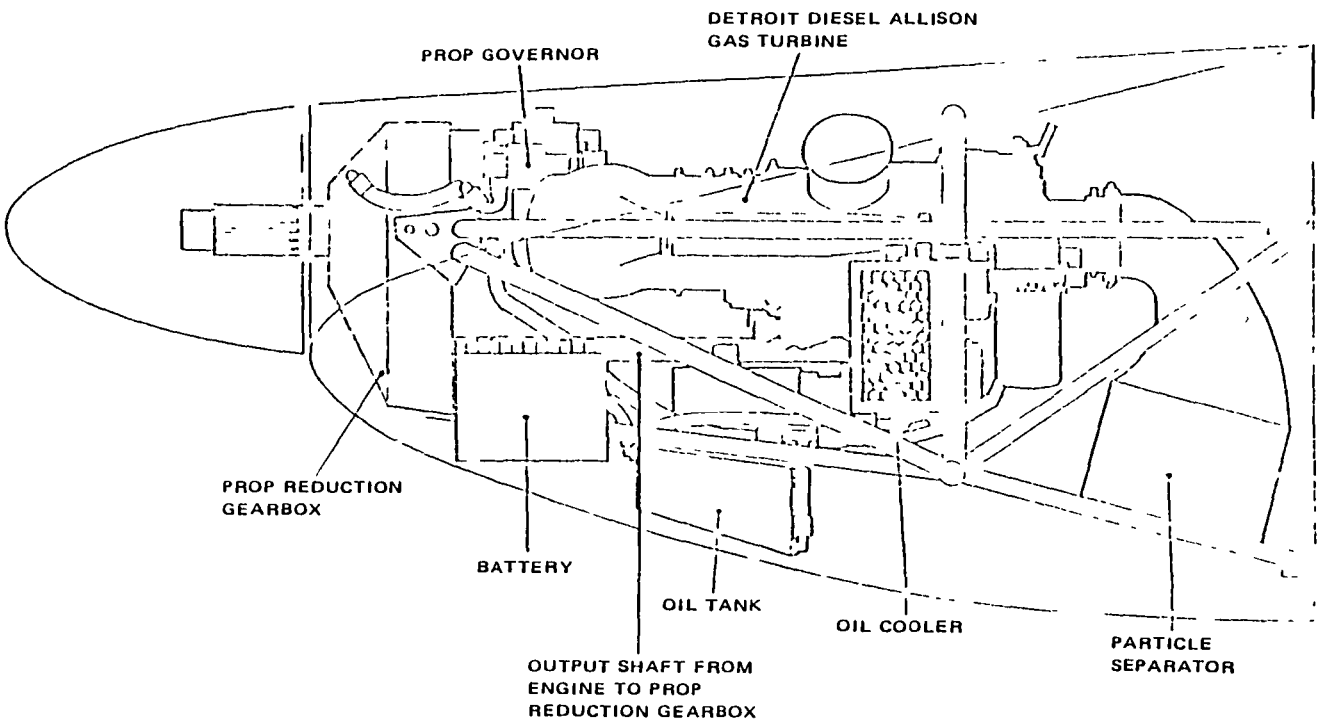
Figure 3-16 – Proposed Modification to Allison 250 Series Engine
(Source: Soloy Conversions Ltd., Chehalis, Washington)

designed to handle rapid thrust reversals of the type possible with the FRV operating in hover. If this APU configuration were selected, further study in this area would be necessary.

The second alternative concerns a recent technical development by Soloy Conversions, Limited of Chehalis, Washington. Soloy Conversions is presently developing a propeller reduction gearbox for use as an add-on to the 250-series Allison engine. The gear box is designed to adapt the 250-series engine to an agricultural type aircraft. Figure 3-16 shows a layout of this proposed engine modification. There are two advantages to this system. The output shaft and propeller reduction gearbox can be added to a 250-C20B engine (which has been removed from an OH-58 helicopter) without extensive modification to the engine. Also, the Soloy gearbox is designed to operate at an output of 1800 rpms. This would allow the 850 feet per second tip speed to be achieved by removing only slightly more than four inches from each blade tip of the tail rotor. Another feature that makes the Soloy gearbox attractive is that the Allison engine can be operated at less than 100 percent N_2 rpm. N_2 is the power turbine output rpm. The Allison 250-series engines can be operated at 90 percent and 75 percent of normal cruise power. By operating the engine at a reduced power setting (and output rpm) it might be possible, with the Soloy gearbox, to achieve the 1480 rpm required of an unclipped AH-1T tail rotor.

The Soloy conversion is presently under development with ground tests expected to begin in September 1981. The Soloy gearbox is designed to accommodate a variable pitch propeller. The potential problem of modifying the coordinator on the Allison engine, as outlined above, exists with the APU concept also.

6. CROSS-SHAFTING

The decision to employ the four APU's makes the FRV a significantly more complex system. Since the FRV as proposed incorporates eight engines, particular attention must be applied to the effect of engine failures. One solution to the engine failure problem is cross-shafting of drive trains to the various rotor systems. Figure 3-17 shows a design layout for a cross-shafting system for the FRV. The complexity of the system, the weight penalty, and the cost of developing a system like that shown are prohibitive. Further, analysis of engine out performance (discussed in Section IX) indicates that the effects of a power plant failure may not be severe enough to accept the penalties associated with a cross-shaft design.

7. SUMMARY

The selection of a particular combination of helicopter and envelope as the basis of a hybrid flight research vehicle has been predicated on several technical issues.

The primary consideration is the overall cost of acquiring the necessary helicopter components. At present, the only helicopter potentially available as GFE is the Hughes OH-6A from Army inventory. This alone makes it the most desirable helicopter if other criteria can be met.

Adaptability of these helicopters to the design is the next priority. The BO-105 has two disadvantages here stemming from a single source: its high hub moments. One is a shaft fatigue life problem which requires an operating limitation on the B-105 helicopter. This

Figure 3-17 – Schematic of Cross-Shafting Layout

3-32
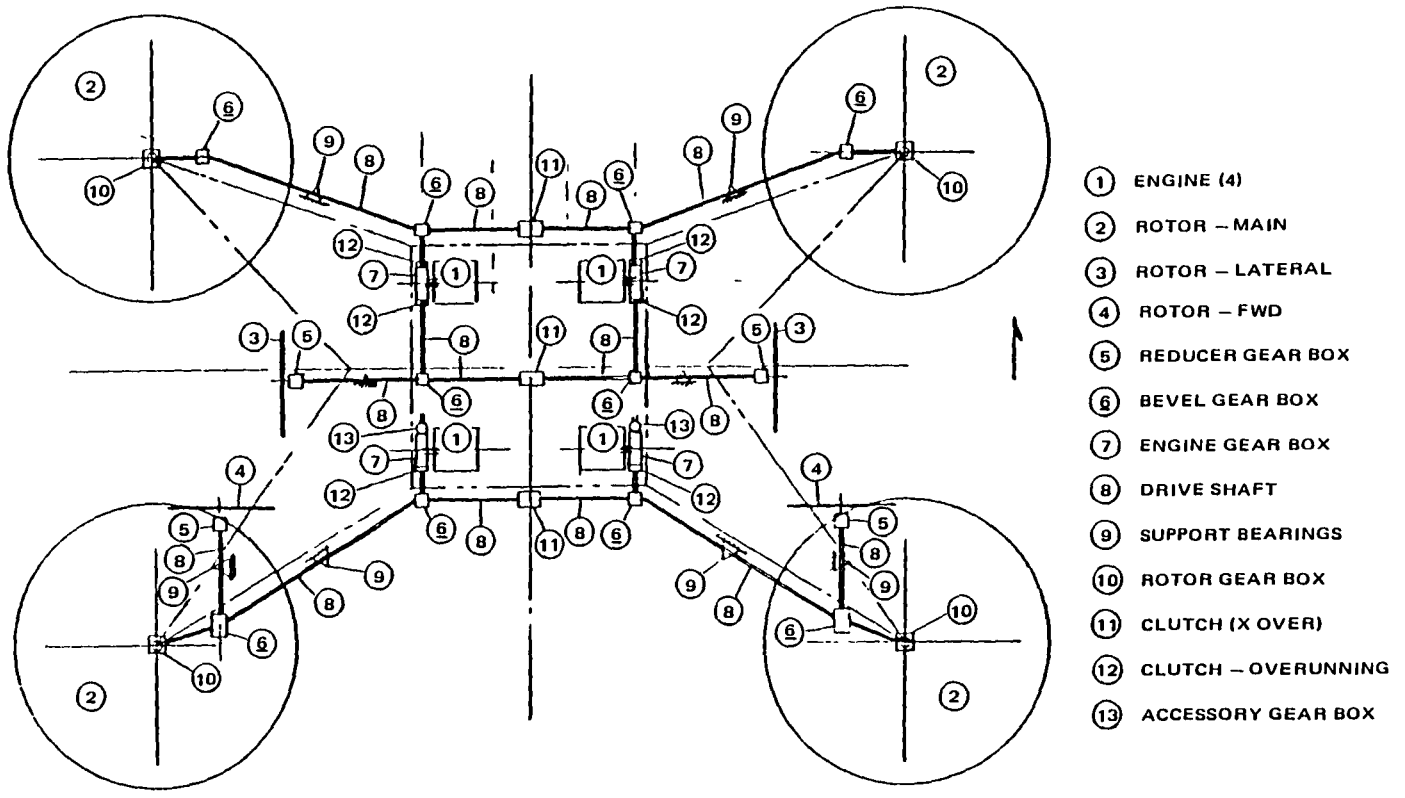
1. ENGINE (4)
2. ROTOR – MAIN
3. ROTOR – LATERAL
4. ROTOR – FWD
5. REDUCER GEAR BOX
6. BEVEL GEAR BOX
7. ENGINE GEAR BOX
8. DRIVE SHAFT
9. SUPPORT BEARINGS
10. ROTOR GEAR BOX
11. CLUTCH (X OVER)
12. CLUTCH – OVERUNNING
13. ACCESSORY GEAR BOX

LAYOUT NO 1 (4) ENGINE CROSS-SHAFTING
SCHEMATIC FLIGHT RESEARCH HYBRID AIRSHIP

constraint is seen as being even more limiting in the airship application due to lack of maneuver relief which is inherent in a helicopter (reduction of hub moments due to reorientation of the helicopter fuselage attitude). Another is the inability to make use of the hub moments for airship maneuvering.

The requirement for a dedicated envelope for the BO-105, enabling it to simulate the full β range, also represents a rather large cost consideration.

A third technical issue is safety, a prime reason for considering the twin-engined BO-105. This issue can be addressed by assuming that the payload can be jettisoned and that a safe landing can be made with two diagonally opposed operating rotors. Therefore, the use of the BO-105 appears not to be essential to the safety of this design.

A fourth and key issue is control power; that is, the maximum available axis maneuvering acceleration under the most severe trim conditions. None of the configurations appear to meet even modest trim conditions. None of the configurations appear to meet even modest maneuvering and trim requirements without the use of auxiliary horizontal propulsion. Specifically, the prototype cannot match the predicted 75-ton full-scale trim and maneuvering characteristics. The use of auxiliary propulsion, while undesirably increasing cost and decreasing reliability, appears mandatory. It also obviates the need for gimballing the rotors, and allows operation at high β. It is possible that a β ratio up to 1.00 can be simulated with an actual $\beta = 0.85$ by using a hybrid research control system. The need for reversing propellers could be met by using existing helicopter tail rotors.

In summary, the best compromise vehicle has the following characteristics:

1. Four OH-6A rotors

2. Four auxiliary propulsion units

3. GZ20 envelope

4. Tail rotors for the reversing propellers

A detailed description of the integration of these major components into a point design of a hybrid flight research vehicle is provided in Section IV.

SECTION IV - VEHICLE DESCRIPTION

1. GENERAL

The FRV concept consists of a non-rigid, buoyant hull that is attached to a structural frame supporting the propulsion components. The advantage of such an arrangement is that the empty weight of the vehicle is largely supported by the buoyancy force while the propulsive forces are available for lifting the payload and controlling the vehicle.

The proposed FRV configuration, shown in Figure 4-1, has a conventional airship envelope with an empennage. Propulsive forces are generated by lifting rotors and auxiliary propellers.

Overall dimensions of the vehicle are as follows: a maximum length of 192.2 feet, an overall height of 59.5 feet, and a width of 96.3 feet. Maximum diameter of the envelope is 45.9 feet and length is 190.3 feet.

2. ENVELOPE AND ACCESSORIES

General arrangement of the vehicle, as shown in Figure 4-1, consists of an envelope with the conventional airship contours. At the stern, four fins, together with movable control surfaces, are mounted in a cruciform configuration. The bow stiffening is typical, consisting of a nose cone, mooring spindle, and battens that extend to 10 percent of the envelope length.

The basic envelope structure is in the shape of a streamlined body of revolution consisting of 12 gores and 67 panels. The fabric is a high strength-to-weight ratio laminate consisting of aluminized Hypalon-neoprene coated, two-ply, Dacron (one bias ply, one straight ply). The design volume is 202,700 cubic feet.

Envelope pressure is regulated for various altitudes by two ballonets, one forward and one aft. They are fabricated of two-ply nylon. The total design volume of the ballonets is approximately 28 percent of the envelope volume. Two five-inch diameter windows are installed in each ballonet to permit a visual inspection of the envelope from inside the ballonet.

The forward ballonet has a volume of 27,400 cubic feet; the aft a volume of 31,300 cubic feet. The ballonet configuration limits the ceiling height in a standard atmosphere with no superheat to 10,500 feet.

A control car, similar to a foreshortened GZ20 car is located at the forward section of the support frame. Separate internal and external suspension systems provide support. Catenaries, support frame, and outrigger struts are positioned near the airship's center of buoyancy.

Three suspension systems (Figure 4-2) are employed in the support concept: an internal system and two external systems.

The internal suspension catenaries are assumed to carry 67 percent of the structure weight. They are made integral with the envelope and attached 30 degrees from the top centerline of the envelope. The two external catenaries around the structure are expected

Figure 4-1 – Proposed FRV Configuration

GZ20 INTERNAL SUSPENSION

GZ20 EXTERNAL SUSPENSION

ADDITIONAL EXTERNAL SUSPENSION

ADDITIONAL EXTERNAL SUSPENSION

INTERNAL SUSPENSION

EXISTING GZ20 EXTERNAL SUSPENSION
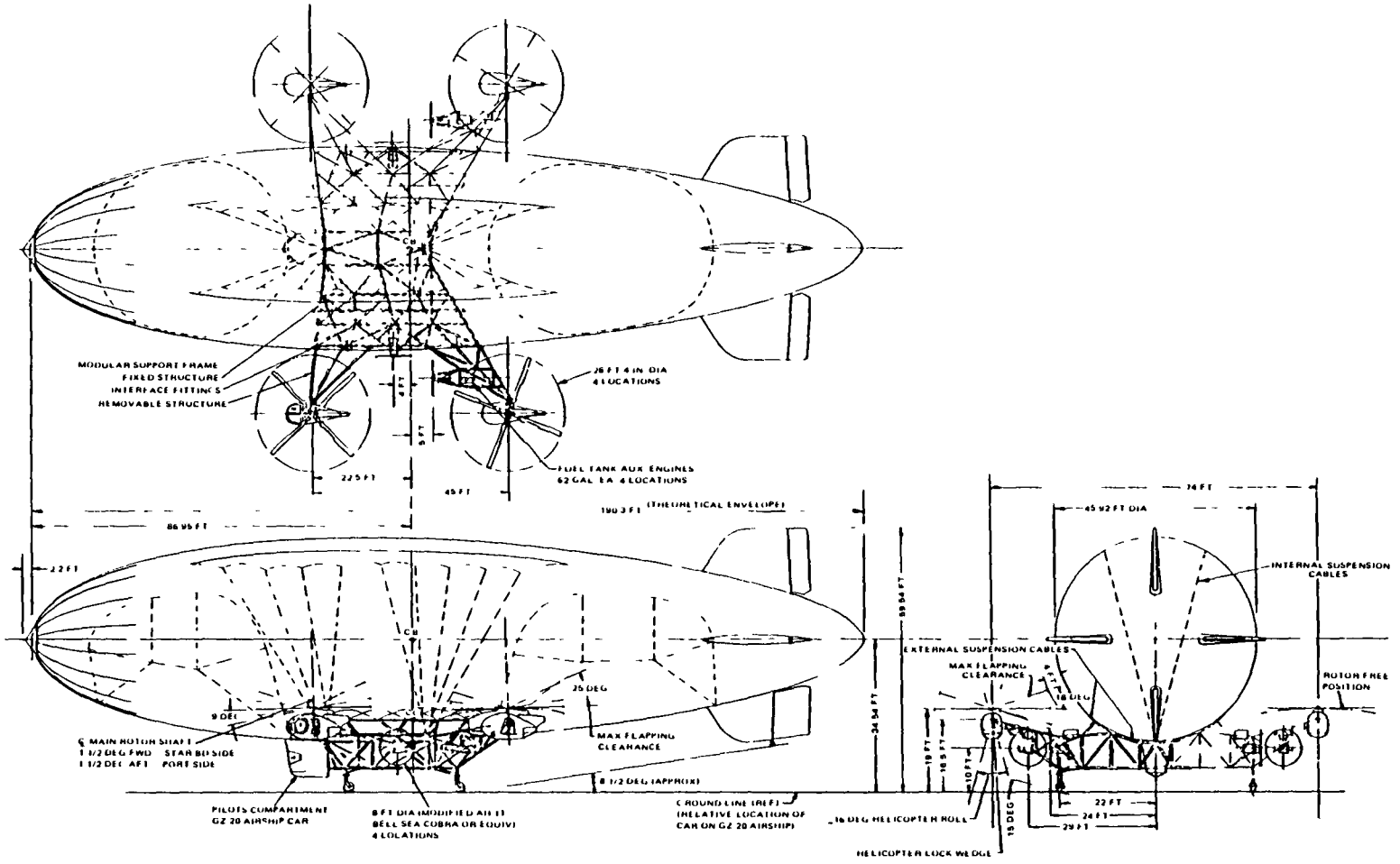
Figure 4-2 – FRV Suspension System
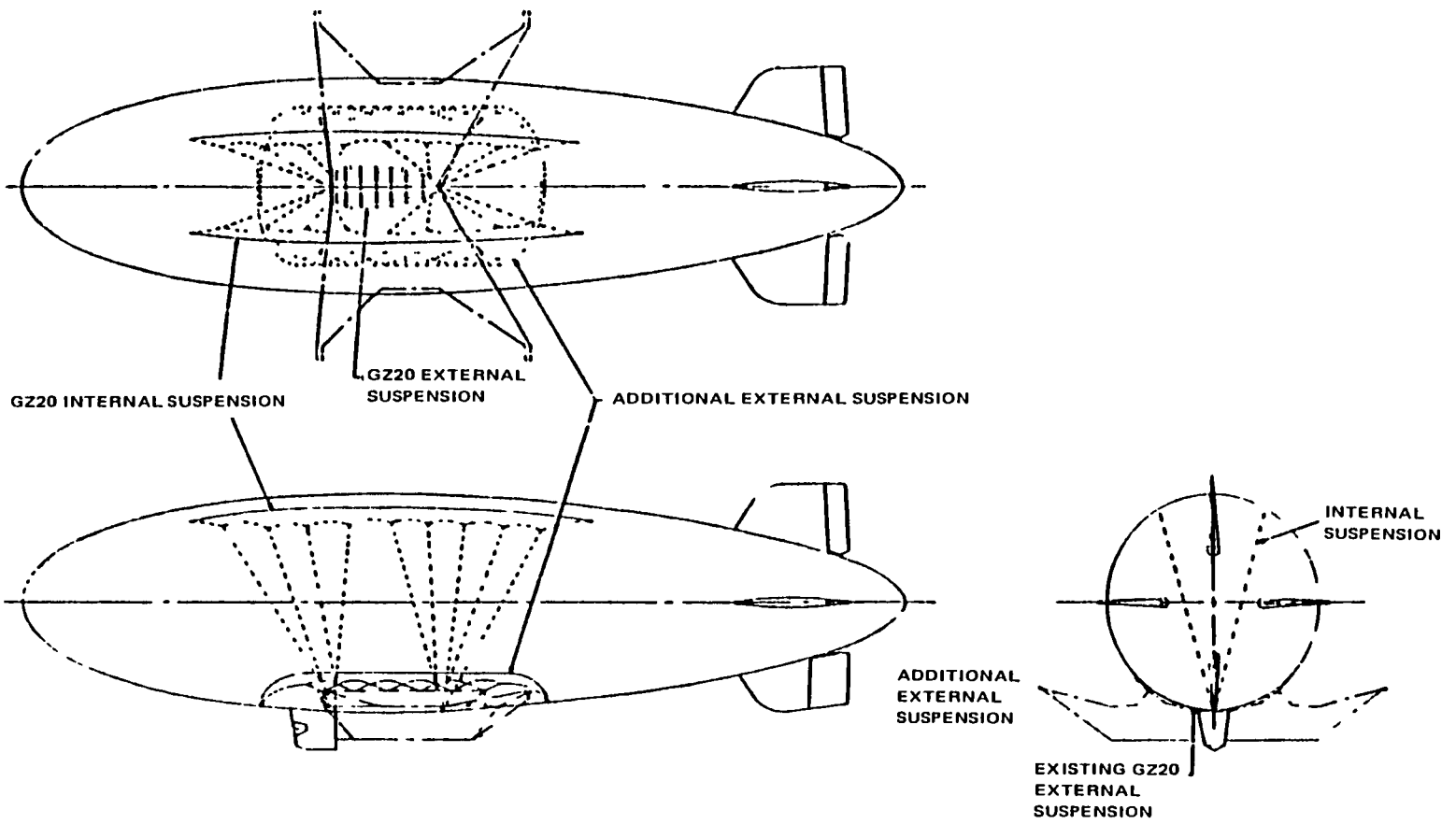
to carry the remaining 33 percent. The existing external catenary is retained and a second external catenary system is added to provide a wider base to react to rolling moments acting on the envelope.

The tail group consists of four fixed fins, four movable surfaces (elevators and rudders), and bracing. Total empennage area is 1005 square feet. The fins are positioned on the vertical and horizontal airship centerline planes in a standard cruciform configuration. A servo-spring tab is incorporated on the trailing edge of the lower rudder. The elevators include a spring system for static balance.

The fins are constructed of aluminum alloy covered with heat shrinkable dacron. Provisions are included for surface support to facilitate installation or removal.

The fins are braced to the envelope by wire rope cables. All wire rope brace cables and fittings are corrosion-resistant steel or suitably treated to resist corrosion.

The movable fin surfaces are aluminum alloy construction covered with heat-shrinkable dacron. Movable surfaces are designed so that there will be no mechanical interference between the movable surfaces and the envelope within the range of control surface movement during normal operation.

A nose stiffening and bow mooring assembly is provided to distribute the mooring forces and prevent collapse of the bow due to dynamic air pressure incurred in flight. The assembly consists of a nose cone approximately seven feet in diameter, with 16 radial truss frames and 16 battens which attach to the radial frames and are contoured to match the envelope. The nose stiffening and bow mooring assembly can withstand the loads imposed by a 70-knot (80.6 mph) wind, acting at an 11.7 degree longitudinal angle to the airship axis, without causing deformation or structural damage.

3. INTERCONNECTING STRUCTURE

The support structure includes four removable outrigger sections that support the OH-6A helicopters (Figure 4-3), and the interconnecting space frame that ties the outriggers together, and mates the resulting structure to the envelope suspension points. This space frame also provides attachment points for the landing gear, control car, fuel tanks, and auxiliary power plants.

To arrive at a reasonable balance between weight, cost, and development time schedule, welded 4130 steel tubing was chosen for the construction material. Since the size of the interconnecting structure, when assembled, even without the outriggers, is approximately 12 by 40 by 44 feet, shippable size components are recommended. Field welding at the assembly site will be required.

The alternative of providing sufficient bolted assembly splices incurs a considerable weight penalty. Manufacturing at the assembly site incurs added costs due to increased requirements for space, personnel, travel, and time scheduled for erection of the vehicle.
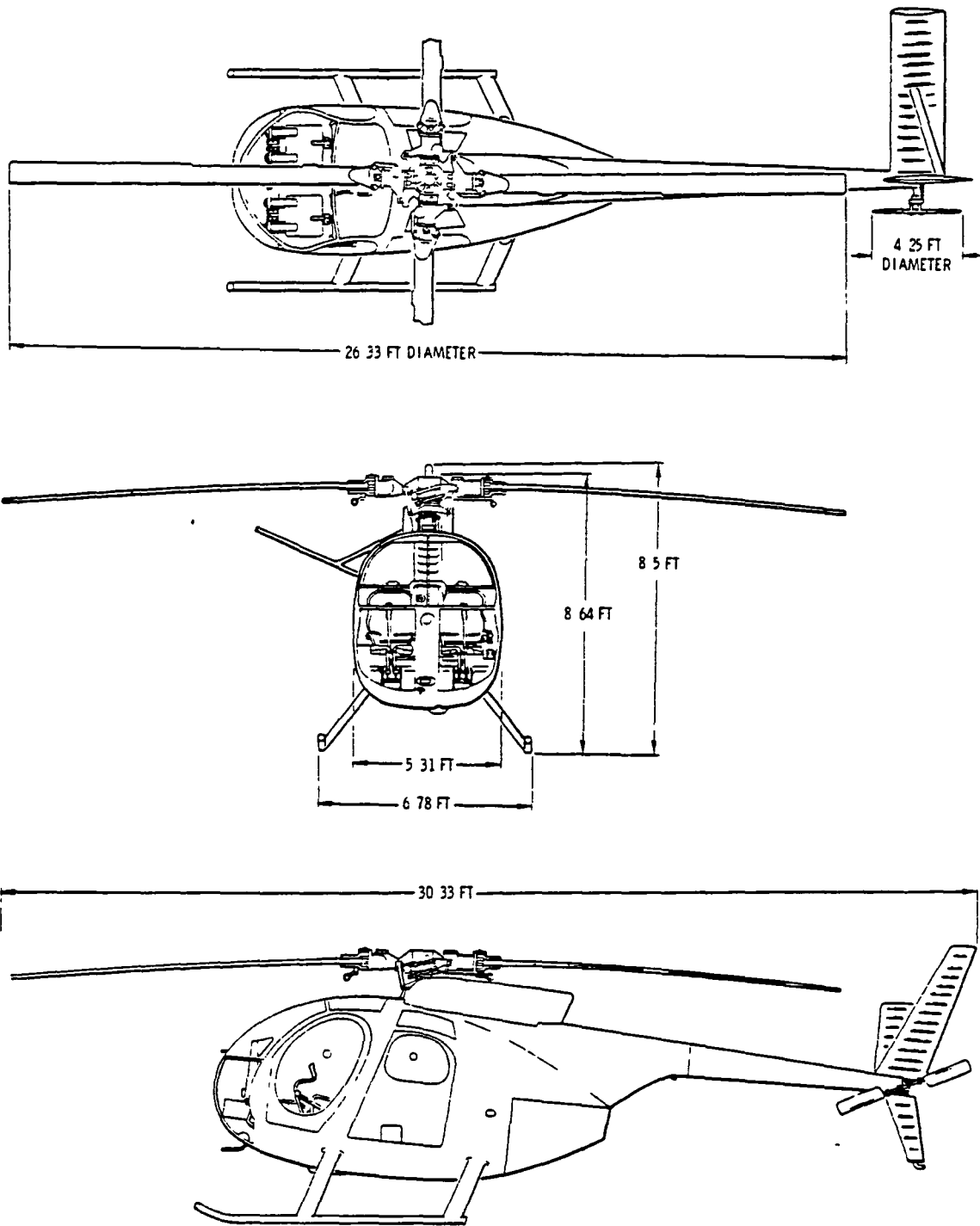
Figure 4-3 – OH-6A Helicopter Dimensions (Reproduced from ref. 9)

In adapting the helicopters to allow a single degree of freedom attachment, a welded 4130 steel tubing wedge-shaped structure is installed in the helicopter passenger compartment (Figure 4-4). This construction allows the helicopter rotor loads to be applied in compression through strong points on the seat support rails on the floor, and through brace members to the seat belt fittings. This arrangement permits ample attachment without modifying the helicopter structure.

The support structure incorporates a modular design. As shown in Figure 4-1, the outriggers can be removed for research purposes for repositioning or to substitute alternate hardware. A typical outrigger module interface fitting is shown in Figure 4-5.

4. PROPULSION UNITS

a. Rotor Systems

The FRV employs four interchangeable Hughes OH-6A helicopters for payload lifting (See Figure 4-3). It is expected the helicopters would be government-furnished equipment with all excess parts removed.

Each helicopter has a four-blade fully articulated rotor system 26.33 feet in diameter and a maximum continuous thrust at sea level of approximately 2600 pounds. The integral fuel system of each helicopter would be retained while the cargo bay would be cleared to accept the support frame attaching structure depicted in Figure 4-4.

The attaching structure has a locking feature that enables the helicopters to rigidly attach to the support frame or to roll approximately ±12 degrees about the hinge axis shown in Figure 4-4.

b. Auxiliary Propulsion Units

Four auxiliary propulsion units (APU) are attached to the support frame as shown in Figure 4-1. Two forward-facing APU's provide cruising and yaw thrust. The two side-facing units are positioned to provide lateral thrust.

The APU's consist of Allison 250 turboshaft engines rated at 317 shaft horsepower. The engines will be modified to accept variable pitch propeller systems, either by addition of a commercially available propeller reduction gearbox or conversion by an Allison distributor.

Reversible power will be provided by adaptation of AH-1T (Bell Sea Cobra) helicopter tail rotors. The tail rotors may have a portion of each blade tip removed depending on the engine conversion method selected. The engine tail rotor combination will, in either case, result in approximately 1400 pounds of fully reversible static thrust available for each APU.

Each APU will have a 62-gallon fuel tank that will utilize the gravity-feed principle. Total fuel capacity for the FRV is 3200 pounds.

Table 4-1 summarizes the physical characteristics of the proposed hybrid vehicle.

4-6

ROTOR

MAST

WL530

MODULAR
SUPPORT
FRAME

LOCKING DEVICE

FLOOR CARGO
SECTION

WL140

JACKING
POINT

HELICOPTER STRUCTURE
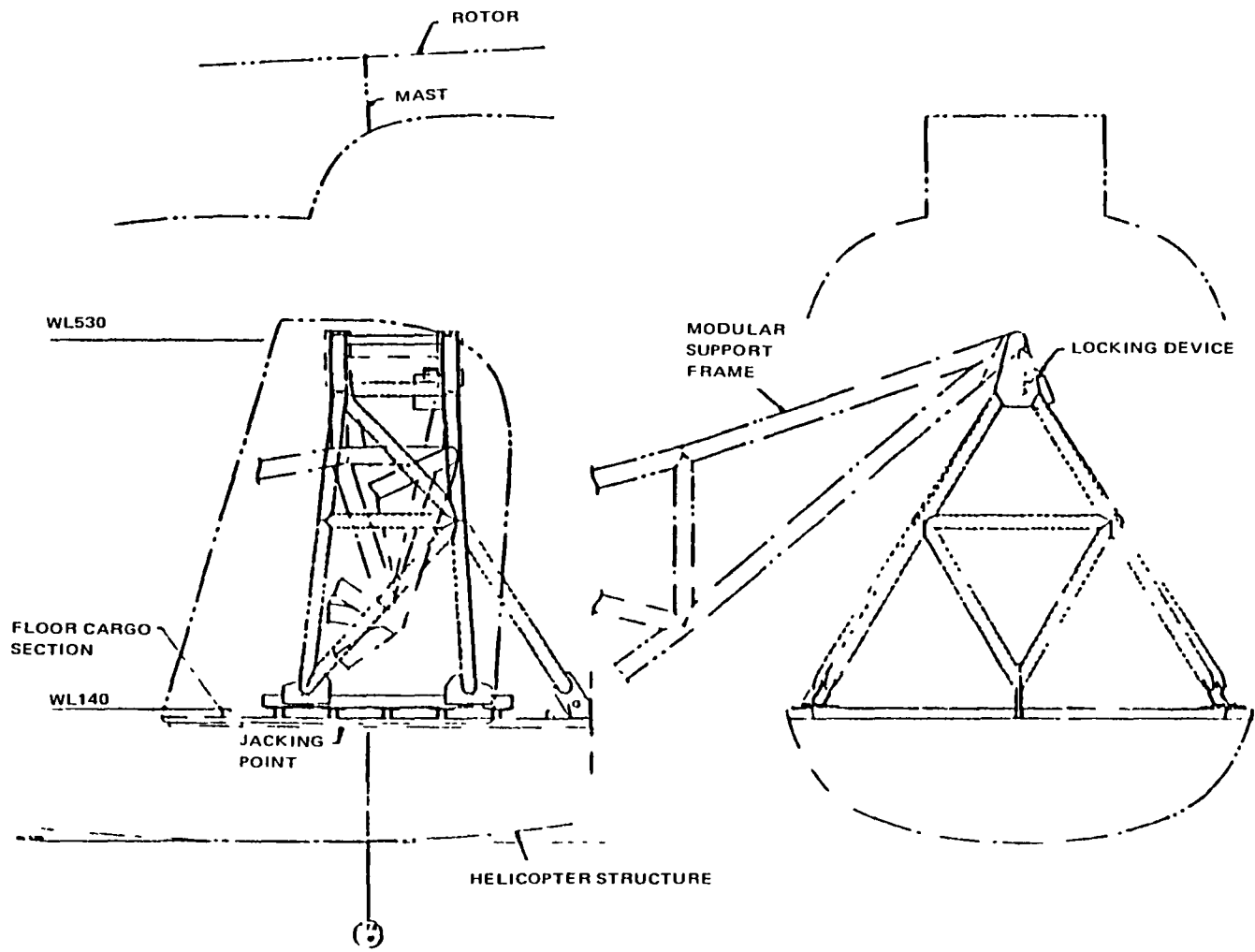
Figure 4-4 – Helicopter Attachment Detail

4-7

25

FIXED STRUCTURE

4
&
13

3

INTERFACE

5

54

REMOVABLE STRUCTURE
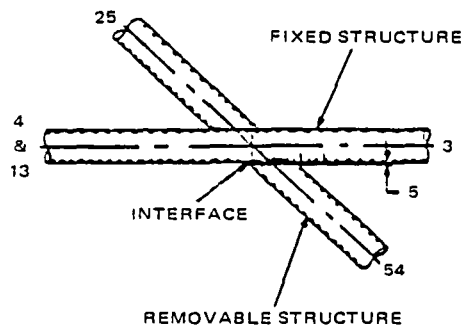
NOTE   SEE FIGURE 5 2
       FOR MEMBER LOCATIONS
       WITHIN THE STRUCTURE

4

3

54

13
&
25

LOCATION FOR
MOUNTING BOLTS

8

7 5

3 & 4

54

25

13 (BEHIND)
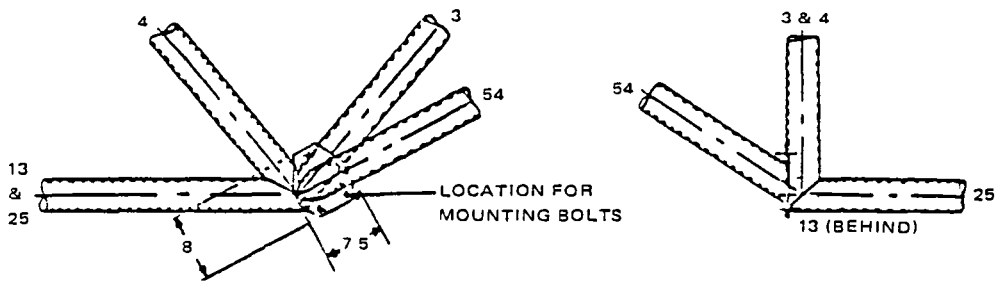
Figure 4-5 – Typical Interface Fitting in the Modular Support Structure

TABLE 4-1 - DIMENSIONS AND CHARACTERISTICS OF THE FLIGHT
RESEARCH VEHICLE

Characteristic	Dimension
Envelope:	
Volume (theoretical)	202,700 cu ft
Volume (stretched)	205,270 cu ft
Length	192.2 ft
Maximum diameter	45.9 ft
Fineness ratio	4.14
Distance to C.B. from bow	86.95 ft
Ballonet Volumes:	
Forward ballonet volume	27,400 cu ft
Aft ballonet volume	31,300 cu ft
Total volume	58,700 cu ft
Empennage arease:	
Upper fin	198 sq ft
Upper rudder	67 sq ft
Lower fin	120 sq ft
Lower rudder (including tab)	90 sq ft
Horizontal stabilizer (2)	396 sq ft
Elevators (2)	134 sq ft
Total empennage area	1005 sq ft
Propulsion:	
Helicopter (4) Hughes OH-6A:	
maximum continuous lift at 2600 lb each	10,400 lb
power plant - Allison T63-A-5A	317 shp
or Allison T63-A-700	(derated to 278 shp; 236 shp maximum continuous)
rotor	4 blades, articulated
diameter	26.3 ft
maximum continuous thrust each	2600 lb
Auxiliary power units:	
(4) Allison T250-C20B (modified to turboprop configuration or equivalent)	300 shp installed
Propellers (4):	
tail rotor from Bell Sea Cobra (AH-1T)	
number of blades	2
Diameter	
for engine mod. with 2030 rpm output	8.0 ft
for engine mod. with 1480 rpm output	9.7 ft
Chord	1.0 ft
Static thrust at sea level maximum continuous power (each)	1400 lb

TABLE 4-1 - Concluded.

Characteristic	Dimension	
Propulsion (Continued)		
Tip speed		
at 2030 rpm	850 ft/sec	
at 1480 rpm	750 ft/sec	
Weight and lift data for entire vehicle:	at sea level	at 5000 ft
Empty weight plus fuel and oil	18018 lb	18018 lb
Fuel	3200 lb	3200 lb
Static lift	13035 lb	11223 lb
Net buoyancy	-4983 lb	-6795 lb
Helicopter lift available	10400 lb	10040 lb
Payload available		
(Helicopter lift and net buoyancy)	5417 lb	3245 lb
Gross weight	23435 lb	21263 lb

5. VEHICLE AERODYNAMICS

The aerodynamic coefficients developed for this study are: (1) axial force coefficient (C_x), (2) side force coefficient (C_y), and (3) yaw moment coefficient (C_n) versus yaw angle. These coefficients are required for the range 0 deg $\leq \psi \leq$ 180 deg.

There is a limited amount of wind tunnel test data available for airships at large yaw angles. Data for the GZ20 envelope exists only for yaw angles less than 20 degrees. Ref. 3 provides aerodynamic data for the range 0 deg $\leq \psi \leq$ 180 deg for the USS Akron. The Akron had a fineness ratio (length/diameter) of 5.9. Data includes ground effects.

Aerodynamic data available for the GZ20 and data in ref. 5 were combined to provide a first order approximation of aerodynamic coefficients for the FRV. For the axial force coefficient (C_x), the Akron C_x versus ψ curve was modified slightly.

The zero-lift drag coefficient of the GZ20 envelope is 0.049. The Akron C_x versus curve was altered to reflect this at the ψ = 0 deg point. A computer program was used that employed cross flow drag theory (ref. 6) to estimate the amount of drag generated by the support frame. This drag was divided into axial and side force components that vary in magnitude with ψ. The C_x increment due to the support frame was combined with the modified Akron curve to yield the data shown in Figure 4-6.

The side force coefficient curve was modified according to the discussion in ref. 6. The side force coefficient for an airship in general varies linearly to a maximum in the vicinity of ψ = 80 deg. Ref. 3 states that ground effect on C_y has been shown to increase the coefficient by approximately 60 percent.

The slope of the C_y versus ψ curve for a GZ20 envelope is 0.015 deg^{-1}. It was assumed that the linear, nearly symmetrical shape of the C_y versus ψ curve for the Akron would apply to the GZ20 airship. A side force coefficient curve for the FRV was constructed by using the C_y slope of the GZ20 in the range 0 deg $\leq \psi \leq$ 80 deg. A slight modification was made to account for the increment of side force due to the support frame and helicopters.
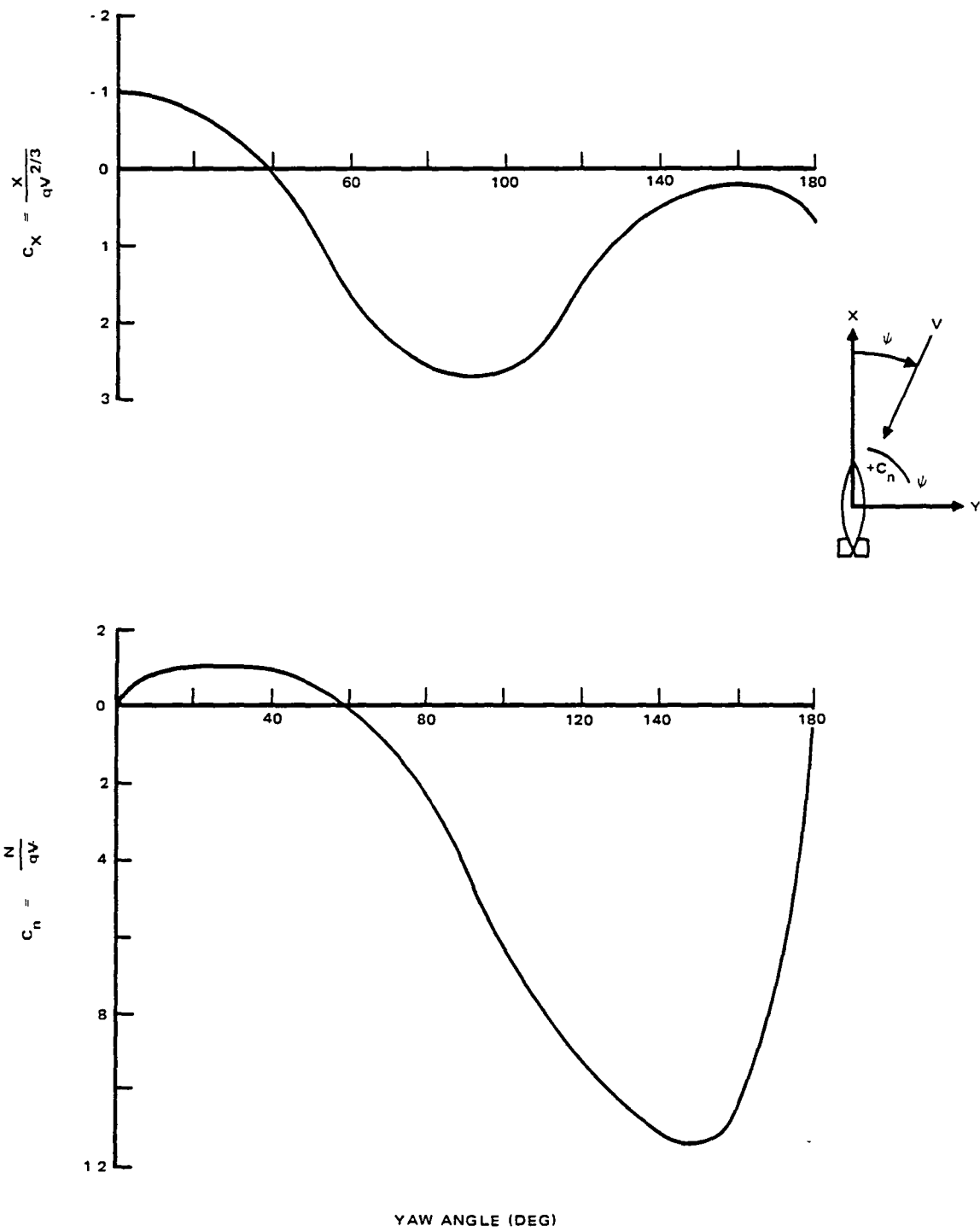
Figure 4-6 – Axial Force and Yaw Moment Vs Yaw Angle for
Flight Research Vehicle

In the range 80 deg $\leq \psi \leq$ 180 deg, the C_y curve was faired to match the trend of the Akron data.

After constructing the FRV curve, a check of peak values of C_y was made for the GZ20 and Akron curves. The peak value of the Akron C_y curve is approximately 60 percent higher than the peak C_y curve for the GZ20. This agrees with the analysis of ref. 5. It was therefore believed that this C_y curve (Figure 4-7) represented a reasonable first order approximation of the FRV's side force coefficient. For the FRV yaw moment coefficient data from refs. 5, 7, and 8 were considered. The model of refs. 7 and 8 had a fineness ratio of 4.37, which is very close to that of the GZ20 value of 4.14. Since yaw data from the three references compared favorably, the C_n curve from the Akron test was used for the GZ20.

The curve was modified in the range 0 deg $\leq \psi \leq$ 50 deg to reflect the GZ20 value of C_n = 0.017 deg^{-1} at ψ = 0 deg. Ref. 5 indicates that ground effects on C_n for an airship are generally very small. The C_n versus ψ curve for the FRV is shown in Figure 4-6.
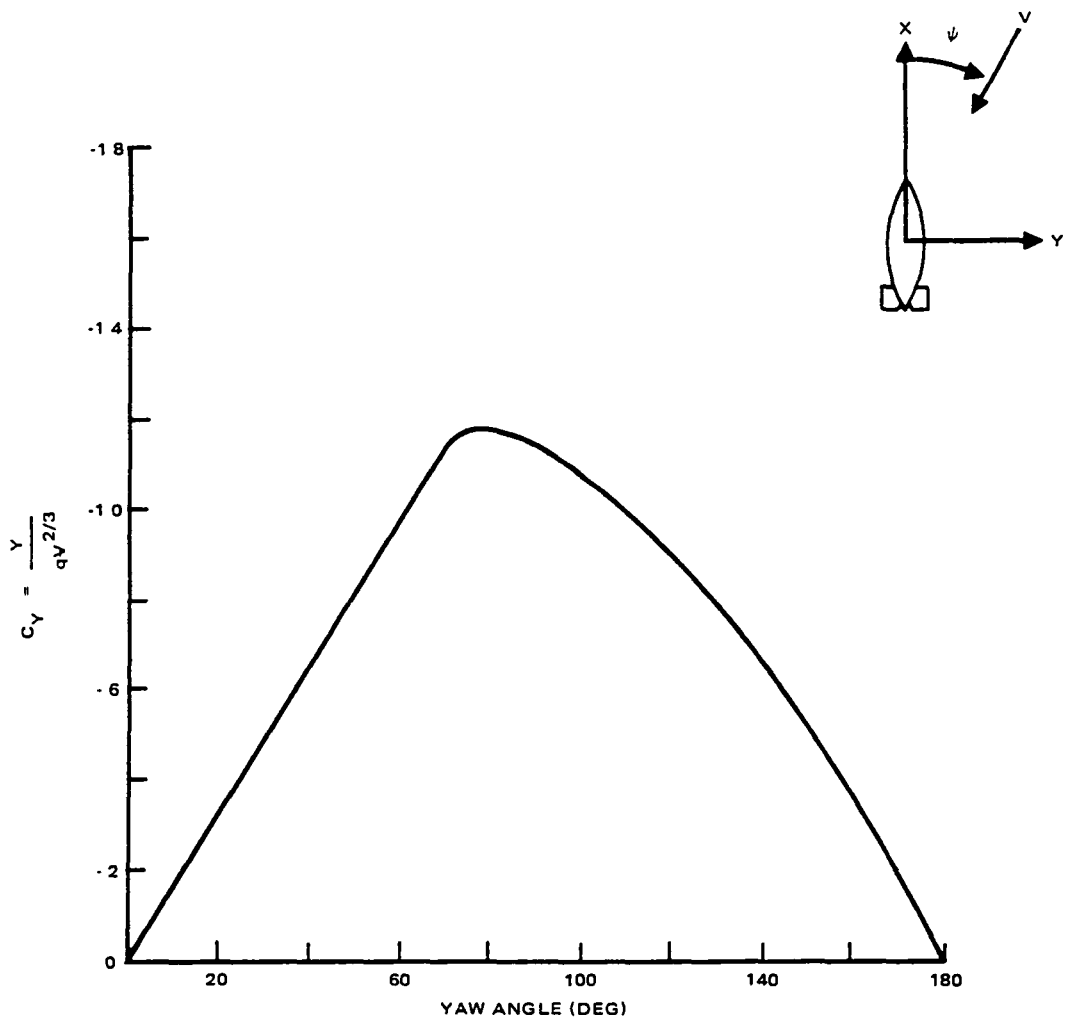
Figure 4-7 – Side Force Vs Yaw Angle for Flight Research Vehicle

SECTION V - STRUCTURAL ANALYSIS

1. MASS PROPERTIES

a. Generation of Data

A computer program developed at GAC that affords rapid, accurate mass property data was utilized for the FRV analysis.

The program determines the mass properties of a vehicle by a method similar to manual calculation. By the manual method, mass properties of a structure are calculated component by component then added to determine the mass characteristics of the complete assembly. In this approach the geometric shapes, or "building blocks," and associated equations have been programmed for computer calculation. Shapes of various orientations can be selected and added together to make an assembly. Assemblies can then be combined to obtain the mass properties of a total vehicle.

The final output of the program completely defines the mass characteristics of a vehicle and includes data on its weight, center of gravity, moments of inertia, products of inertia, location of principal axes, radius of gyration, and moment and product of inertia about the principal axes.

The determination of vehicle mass properties by the computerized building block method requires (1) determination of component mass properties, (2) summation of component properties to determine assembly mass properties, and (3) summation of assembly properties to determine vehicle mass properties.

Determination of mass properties for a component requires:

1. Selection of the oriented geometric shape and associated equations that most closely define the component.

2. Definition of parameters required for calculation of the weight and center of gravity (cg) of the component.

3. Definition of the x, y, and z dimensions, measured from the component cg to the reference axis.

This procedure may be repeated for any number of components until a total is desired. A number of components for which a total is desired constitutes an assembly. One or more assemblies make up a total vehicle for one computer run.

The computer prints totals for each assembly and grand totals for the entire vehicle. Subassembly totals for weight and cg can be summed as needed. A print-out of accumulated mass property data can be obtained at any point in the program.

If the component weight, cg, and moment of inertia are available without calculation, they can be entered as inputs. Component moment of inertia can be computed by using the parameters required for weight and cg calculations or by using the weight, cg, and component dimensions as inputs. Also, a subassembly of component weights and cg inputs can be

totaled and the moment of inertia determined for the subassembly. Mass properties can be subtracted for lightening holes or for fuel consumed or jettisoned during flight.

The output generated for the FRV is contained in Appendix A.

b. Estimated Group Weight Statement

An estimated group weight statement for the FRV as depicted in Section IV, Figure 4-1 is provided in Table 5-1. A more detailed tabulation is provided in Appendix B.

Table 5-2 indicates the loading conditions for the vehicle. The maximum allowable payload is estimated to be slightly more than 5000 pounds. The range of buoyancy ratios predicted is 0.53 to 0.68.

Table 5-3 provides center of gravity and moment of inertia data for the vehicle. Note that the horizontal distance (x) is measured from the theoretical nose of the envelope, while the lateral (y) and vertical (z) distances are measured from the center line axis of the airship.

c. Helicopter Weight Data

Information on the OH-6A helicopter weight breakdown was received from the manufacturer and estimates of the module weight were generated. Results are provided in Table 5-4, with additional detail contained in Appendix C.

The total weight of all four module installations is therefore (4 x 976.8) or 3907.2 pounds.

For the module the following represent the center of gravity reference axes:

       1.   The +x or horizontal arm is measured from helicopter station 0.0 with the center line of the rotor at 100.0

       2.   The +y or lateral arm is to the right looking forward

       3.   The +z or vertical arm is measured from the lower edge of the helicopter skid with the vertical center line of the rotor at 100.0

In this configuration , x = 107.8 inches, y = 0.05 inches, and z = 61.3 inches.

TABLE 5-1 - ESTIMATED WEIGHTS FOR FRV

Item	Weight (lb)	
Envelope group:		3635.1
Envelope	2177.7	
Ballonets	371.1	
Air lines	53.1	
Suspension systems	332.4	
Bow stiffening and mooring	315.6	
Fin suspension	62.6	
Frame fairing	50.7	
Miscellaneous	271.9	
Tail Group		757.6
Car, helicopter and frame group		7130.4
Car	334.6	
Helicopters (4)	3907.2	
Interconnecting structure	2888.6	
Alighting gear group		418.0
Pressure group		332.3
Surface control group		87.7
APU group		1300.0
Instruments and navigational equipment group		54.7
Electrical group		144.2
Electronics group:		203.7
Contractor installation	53.7	
Fly-by-wire (FBW) installations	150.0	
Furnishings and equipment group		83.0
Auxiliary gear group		79.8
Weight empty		14426.5

TABLE 5-2 - USEFUL LOAD AND GROSS WEIGHT

Item	Less payload (lb)	With payload (lb)
Crew (2)	340.0	340.0
Fuel	3200.0	3200.0
Oil	51.2	51.2
Cargo		5074.3
Useful load	3591.2	8665.7
Weight empty	14426.5	14426.5
Gross weight	18017.7	23092.0
Static lift (at 2000 ft)	12292.0	12292.0
Buoyancy ratio	0.682	0.532

TABLE 5-3 - CENTER OF GRAVITY AND MOMENTS OF INERTIA

	FRV Condition		
	less payload	with payload	with payload and helium
Gross mass (lb)	18,017.7	23,092.0	25,349.9
Center of gravity (ft)			
X	87.08	87.05	87.04
Y	0	0	0
Z	17.97	19.74	17.98
Center of buoyancy (ft)	86.95	86.95	86.95
Moment of inertia (slug·ft^2)			
I_X	436,016	444,606	418,836
I_Y	655,760	669,282	822,689
I_Z	943,062	948,651	1,077,159

TABLE 5-4 - WEIGHT ESTIMATE FOR HELICOPTER MODULE

Item	Estimated Weight (lb) OH-6A	Module
Weight empty	1232.4	976.8
Main rotor group	173.7	173.7
Tail group	23.0	-
Body group	249.7	236.3
Alighting gear group	66.6	-
Flight controls group	65.0	65.0
Nacelle group	8.2	8.2
Propulsion group	347.8	347.8
Instruments and navigation group	31.3	31.3
Electrical group	72.8	72.8
Electronics group	114.1	-
Armament group	12.3	4.5
Furnishings and equipment group	58.5	-
Air conditioning group	9.4	9.4
Attachment structure	-	27.8

2. INTERCONNECTING STRUCTURE

<u>a.</u> <u>Design</u>

(1) General

A space framework of 4130 steel tubing was chosen to reduce the complexities of design and manufacture. This is shown in the three-view drawing of the overall vehicle (See Figure 4-1) and in additional detail in Figure 5-1.

One half of the structure was modeled and analyzed using the STRUDL-II computer program (ref. 9). An exploded view of the structure is shown in Figure 5-2, wherein the joints are identified by the circled numerals and the members by the non-circled numerals. Preliminary computer results were used to size the members.

Two loading conditions were considered: lift loading and landing loading. Load values determined at the joints were inputs to the aforementioned computer model.

(2) Lift Loading

Lift loading assumes that the helicopter rotors are run up in flat pitch and then suddenly have full collective pitch applied. The resulting maximum rotor lift is assumed to be 6000 pounds per unit. Initial acceleration is calculated and applied to weight items of the configuration. Limit loads are increased by a factor of safety of 1.5.

To identify the lift loads at the point of attachment of the helicopter to the structure (joints 58 and 59 in Figure 5-2) the following procedure is followed:

- Weight Summary (Refer to Tables 5-1, 5-2)

Weight Empty	14,426.5 lb
Crew	340.0 lb
Fuel	3,200.0 lb
Oil	51.2 lb
Total	18,017.7 lb

- Maximum static lift at sea level = 13,035 pounds

- Initial Acceleration:

$$a = \frac{4(6000) + 13,035}{18017.7} = 2.06 \text{ g's}$$

- Ultimate lift of each helicopter is 1.5(6000) or 9000 pounds

- Ultimate helicopter loading is:

$$\frac{3907.2}{4} \times 2.06 \times 1.5 = 3018 \text{ pounds}$$

- Helicopter fuel and oil loading is:

$$\frac{1600 + 25.6}{4} \times 2.06 \times 1.5 = 1256 \text{ pounds}$$

- Estimated joint weight is: $61.8 \times 2.06 \times 1.5 = 191$ pounds

TOP VIEW, PORT SIDE

ISOMETRIC VIEW PORT SIDE
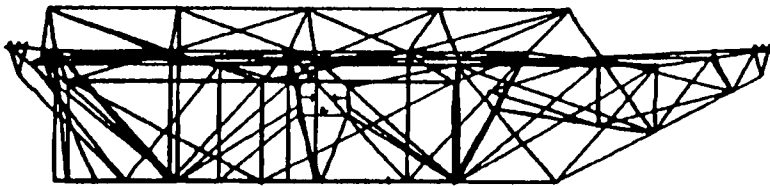
AFT VIEW, PORT SIDE

SIDE VIEW, PORT SIDE

Figure 5-1 – Interconnecting Structure Layout
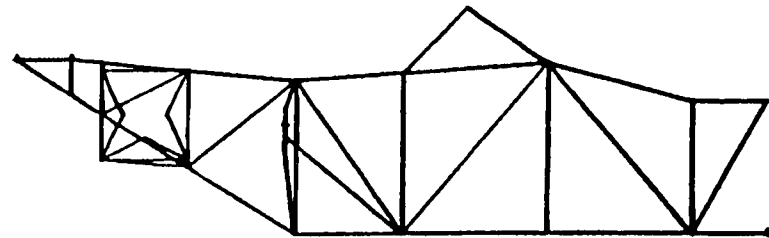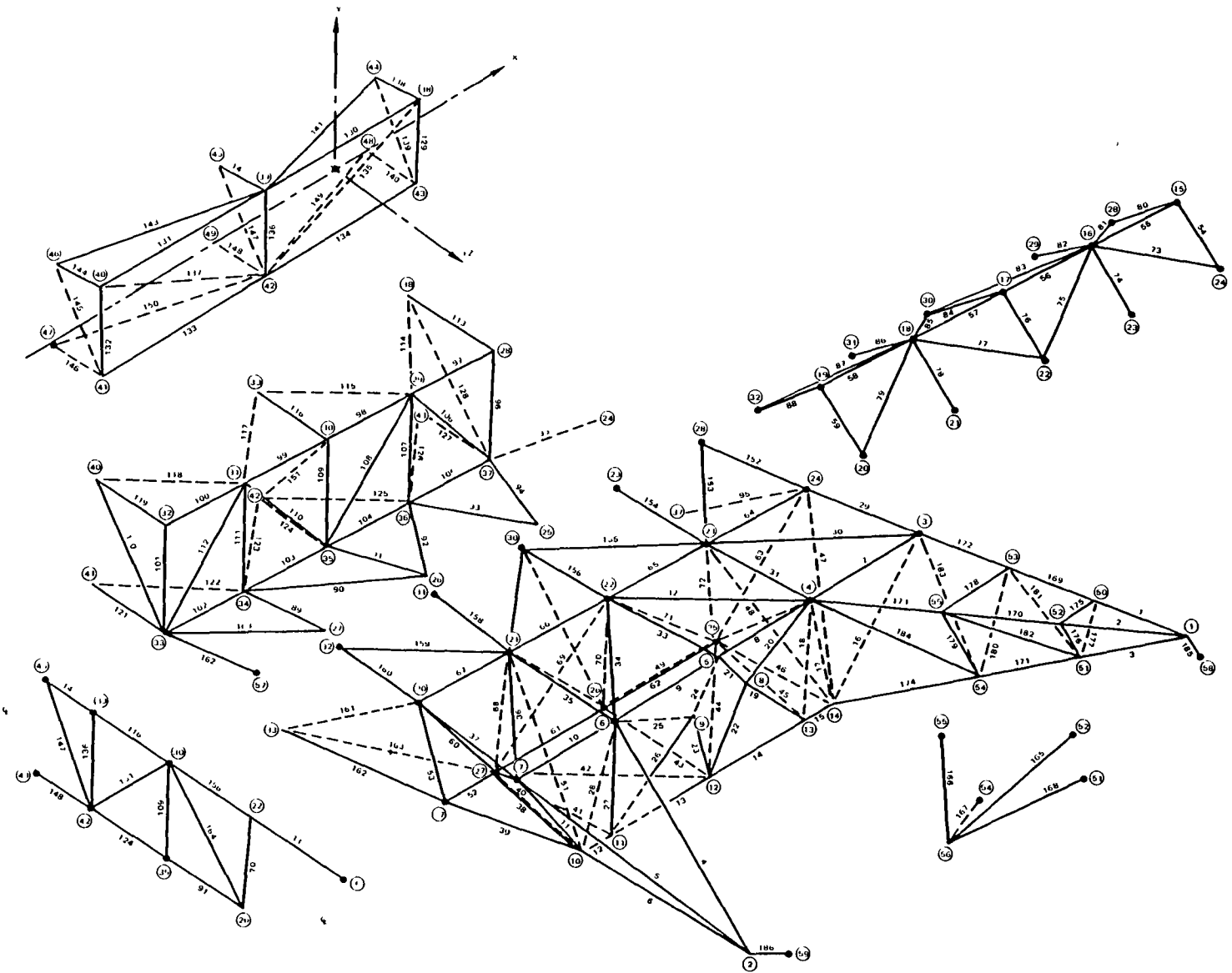
Figure 5-2 – Interconnecting Structure (Exploded View)

The load at each of joints 58 and 59 is the difference between the ultimate lift provided by by the helicopter (9000 lb) and the sum of the three weight loadings. The net result is 4535 pounds per joint.

Additional lift loadings at the appropriate joints are calculated in a like manner. These are identified in Table 5-5.

(3) Landing Loadings

A landing loading assumes the FRV makes a symmetrical landing with a sinking speed of 4 feet per second. The resulting maximum deceleration is calculated and applied to the weight items of the configuration. Again, a factor of safety of 1.5 is incorporated into the solution.

The peak landing condition g load is calculated using the above noted sinking speed and assuming a typical load deflection relationship for a non-oleo type shock absorber and tire combination. Landing the FRV symmetrically with no helicopter lift loads tends to increase the load on the structural members.

The peak load estimated for each gear is 4950 pounds. This value is premised on analytical investigations performed on the GZ20 public relations airship.

Now, using the maximum lift load together with the maximum landing gear load results in a maximum g load condition. That is,

$$a = \frac{13,035 + 4(4950)}{18017.7} = 1.82 \text{ g's}$$

Using this value, the ultimate joint loadings for the landing condition are computed in the same manner as described for the lift loadings. Results are provided in Table 5-5.

(4) Member Sizing

Long column buckling stresses are calculated using formulations developed in Summerill's "Aircraft Tubing Data" (ref. 11. Conservatively, member lengths were taken from theoretical joint-to-joint locations. Hence, c = 1.0 and L' = ℓ.

Therefore,

$$F_c = \frac{286 \times 10^6}{\left(\frac{L'}{\rho}\right)^2}$$

where F_c is the allowable column stress. The critical value of the slenderness ratio (L'/ρ) is 91.5.

The ultimate allowable column loads are calculated by multiplying the tubing cross-section area by the calculated buckling stress for various lengths and plotting the values. The resulting curves shown in Figures 5-3 and 5-4 facilitate selection of member sizes.

Appendix D tabulates the member loads for the selected loading conditions and sizes. Where the critical condition is not obvious, the calculated maximum combined stress due to axial load and end bending moments is also indicated.

<div style="text-align: center">TABLE 5-5 - JOINT LOADINGS</div>

Item	Joint (See figure 5-2)	Load per joint (lb) Lift condition	Landing condition
Forward helicopter	59	4515	-3962
Aft helicopter	58	4515	-3962
Longitudinal APU			
Engine and oil	56	-1024	-905
Fuel tank	53,54	-618	-546
Lateral APU			
Engine and oil	8,9	-512	-452
Fuel tank	5,22	-618	-546
Landing gear	10, 14	-321	4297
Structure	41,42,43	-202	-179
Structure	33,34,35,36,37	-145	-129
Structure	25,26,27,57	-277	-245
Structure	10,12,14	-415	-368
Car loads	40(Y)	-1042	-
	40(X)	-521	-
	41(X)	521	-

There are three failure modes for the members. These are identified in Appendix D as "buckling," "secondary," or "combined."

In general, the critical condition for tube size selection is the long column buckling allowable stress. Members in this category indicate "buckling".

The effect of a 255-pound ultimate load applied normal to the centerline of the member at midspan is also considered in sizing relatively lightly loaded members. Sizes selected due to this arbitrary loading condition are labeled "secondary". These minimum size members are defined as being able to support the load of a 170-pound person climbing on the structure. Thus:

$$W = 170 \times (\text{factor of safety})$$
$$= 170 \times 1.5$$
$$= 255 \text{ lb (ultimate)}$$

Now:

Maximum moment = WL/8 (at ends and center point)
Ultimate allowable stress = 67,500 psi (near welds)
Section factor k = 1.273 (for thin-walled tube)

Therefore: Bending modulus = 67,500 x 1.273

Now, solving for required section modulus "S"

$$\frac{255\ell}{8S} = 67,500 \times 1.273$$

$S_{REQ'D} = 0.00037095\ell.$

Using this factor, minimum tube sizes can be recommended for various lengths. For this particular structure, three different sizes are suggested, as shown in Table 5-6.
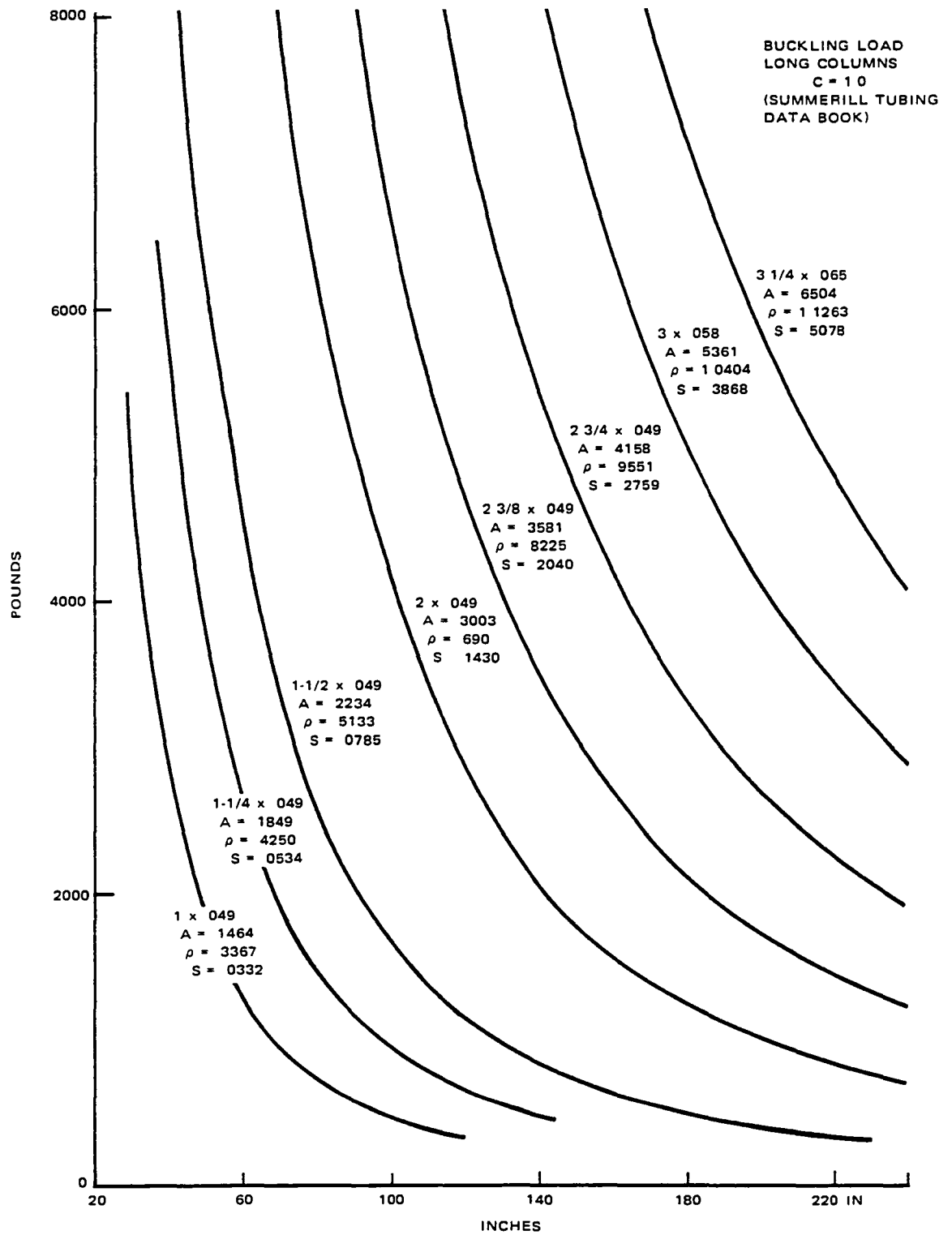
Figure 5-3 – Ultimate Allowable Column Loads (1 to 3-1/4 in. diameter)
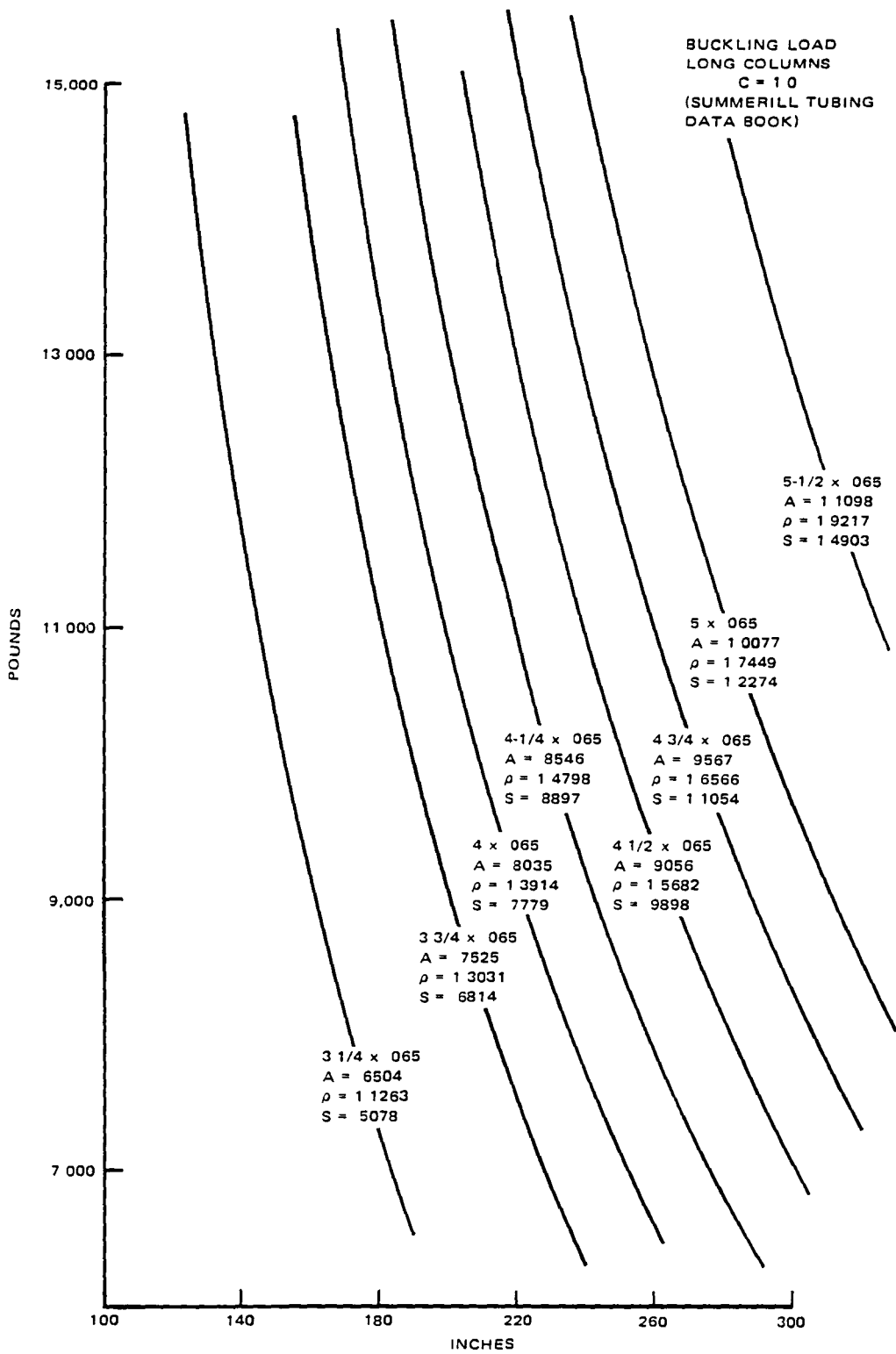
Figure 5-4 - Ultimate Allowable Column Loads (3-1/4 to 5-1/2 in. diameter)

TABLE 5-6 - MINIMUM SIZE MEMBERS

Length (inches)	S Required	Tube size (in. x in.)
60	0.02226	1 x 0.049
70	0.02597	1 x 0.049
80	0.02967	1 x 0.049
90	0.03338	1 x 0.049
100	0.03709	1.25 x 0.049
110	0.04080	1.25 x 0.049
120	0.04451	1.25 x 0.049
130	0.04822	1.25 x 0.049
140	0.05193	1.25 x 0.049
150	0.05564	1.5 x 0.049
160	0.05935	1.5 x 0.049
170	0.06306	1.5 x 0.049
180	0.06677	1.5 x 0.049

Members sized by axial loads and moments, and those that are not critical as long columns are listed as "combined" in Appendix D. The calculated loads and moments for both loading conditions are listed for each member on the same line to help isolate critical loading. The lift take-off condition load is listed above the slash, and the landing loadings below.

(5) Structure Weight

An estimate of the structure weight was made by summing the theoretical joint-to-joint member lengths of each size and multiplying these totals by the weight per inch of the tubing. The excess tubing length involved in carrying all tubes to the theoretical intersection points provides some weight for a limited number of assembly splices. These splices facilitate contemplated changes in locations of helicopters, and allow the structure to be constructed in transportable sizes.

In reviewing the original weight estimate for the structure, the listings in Table 5-7 indicate that the calculated weight is within one percent of the presumed weight. Hence, additional iteration is not required.

TABLE 5-7 - STRUCTURE WEIGHT

Tube size (in. x in.)	Total length in 1/2 structure (in.)	Unit weight (lb/in.)	Total Weight (lb)
1 x .049	3049.3	0.04143	126.33
1-1/4 x .049	4157.0	0.05233	217.54
1-1/2 x .049	3679.0	0.06322	232.59
2 x .049	4037.6	0.08498	343.12
2-3/8 x .049	1431.3	0.10134	145.05
3 x .058	302.9	0.15172	30.94
3-1/4 x .065	236.0	0.18406	43.44
3-3/4 x .065	145.5	0.21296	30.99
4 x .065	492.9	0.22739	109.81
4-1/2 x .065	91.4	0.25628	23.42
5 x .065	34.0	0.20518	9.70
		= 1/2 Structure weight =	1312.93
		Total Structure Weight =	2626 lb

b. Summary

The two loading conditions explored in this preliminary analysis of the support frame are not sufficient to totally design the structure. In addition to the dynamic collective pitch load condition (in which a conservative factor of two was used to estimate the maximum load condition), and the symmetrical landing condition (in which, again conservatively, the landing sink speed was used without rotor support load) further loadings must be investigated to ensure no single member will have higher resulting loads. The additional loadings should minimally contain:

1. One engine out operation (this results in power off on diagonally opposite helicopter).

2. Crosswind hover (results in horizontal lateral load components being applied at the copter attach points).

3. Maximum yaw (occurs when longitudinal load applications of opposite sense are applied at the copter attach points).

4.   Two-wheel landing forward, with initial landing loads taken by the forward landing gear.

5.   Two-wheel landing with initial landing loads taken by diagonally opposite landing gears.

6.   Mooring loads (when landing gear must take reactions from gust loads applied at critical angles to the airship longitudinal center line).

Although it is estimated that one engine out operation may impose higher loads on some inner shear members, many of these members have already been arbitrarily sized to minimum size tube.

3. ENVELOPE AND SUSPENSION SYSTEM

a. Loads Criteria

Suspension system load results from accelerations that occur when the airship enters a gust.

Experience has shown the airship is not instantly engulfed, but that a finite time period is required for complete engulfment. During this period the airship experiences accelerations that cause velocity changes which attenuate the gust load.

The effects of a gust on a conventional ship have been previously evaluated and a rule has been established for gust loads which is valid if the mass proportions within the ship are the same.

The heavy lift or quad rotor concept has a mass distribution that is significantly different from a conventional airship. Therefore, a method of determining transient gust-induced accelerations is described herein, enabling the evaluation of suspension system loading.

The generalized, non-dimensional longitudinal loading of the airship, flying at an angle of attack, is extracted from reference material. (Note that all control force is generated by airship controls with no variation in rotor thrust.)

The normal force coefficient angle-of-attack curve is linear to a 55-to-60-degree range of attack angles. The resultant angle-of-attack and local velocities at a series of points along the ship's length are calculated for a specific time increment. These are functions of combined local ship and air velocities. The forces resulting from this combination of velocities are applied to the ship and linear and angular accelerations obtained. These accelerations are used to determine resultant ship velocities. Each time the ship advances another time increment into the gust, the angles of attack and local velocities are calculated and used to determine forces, accelerations, and velocities. This process is repeated until the ship is totally within the gust.

This method presumes that the local load at any point along the airship is independent of the load on any adjacent section. While this is not an exact representation, the use of linear load variations between sections and making the time increments such that the product of the summation of Δt and the ship velocity does not equal the loading increments will "fair" the load with sufficient accuracy for the purposes of this analysis.

Another area of ambiguity is airship mass. When the airship is displaced in still air, a force greater than the force required to accelerate the ship's mass is needed to produce an acceleration. Ship motion requires displacement of a significant volume of the atmosphere. The required acceleration of this air mass yields an increase in force.

However, if the motion of the atmosphere induces the ship acceleration, the required atmospheric gas velocities are in part, or in total, already present and need not be produced by forces acting on the ship. Thus, past practice has been to multiply the mass of the ship by a factor and refer to the resulting mass as the virtual mass of the ship. Different factors are used for axial, translation, pitch or yawing, and roll. Since the part of the ship engulfed in the gust will have a different apparent mass than the portion of the ship in still air, three solutions to the transient problem will be used and the comparable accelerations from these will be used as the design load. The three are - no virtual mass effect, ellipsoidal virtual mass effect, and, one-half of the ellipsoidal virtual mass effect.

The described method is applied to the GZ20 and FRV airships. The design gust velocities for the GZ20 airship, shown in Figure 5-5, are used in the analysis of both ships. The resulting maximum normal accelerations are given in Figure 5-6. The virtual mass coefficients used in the analysis are given in Figure 5-7.

The GZ20 internal suspension system has a limit design load which is the load capability of this system. The effects of different mass distribution and internal to external load ratio are used to define a limit dynamic load factor for the FRV. The derived load factor is shown in Figure 5-6. A maximum forward flight velocity of 35 mph results in an internal suspension system load equal to the GZ20 design limit load for an equivalent effective mass acting on the FRV and GZ20 airships.

This analysis is only valid when the rotor thrust is constant for forward flight of the ship. Control by rotor thrust variations in forward flight can result in larger envelope lift and suspension system loads possibly to the failure level.

Assuming no decrease in forward velocity from 35 mph and no change in attitude as the ship is engulfed in a vertical 30 feet per second gust, the dynamic lift will be about 7000 pounds.

Diminishing the rotor thrust effectively transfers the load from rotors to envelope. The power required to maintain this condition exceeds the available power. Therefore, this can only happen on a transient basis. How much the ship would slow down and attenuate the load is unknown.

The recommended gust criteria for the FRV is contained in Figure 5-8.

The design limit load for the GZ20 internal suspension system is 90 percent of the acceleration transferred to the car.

5-16
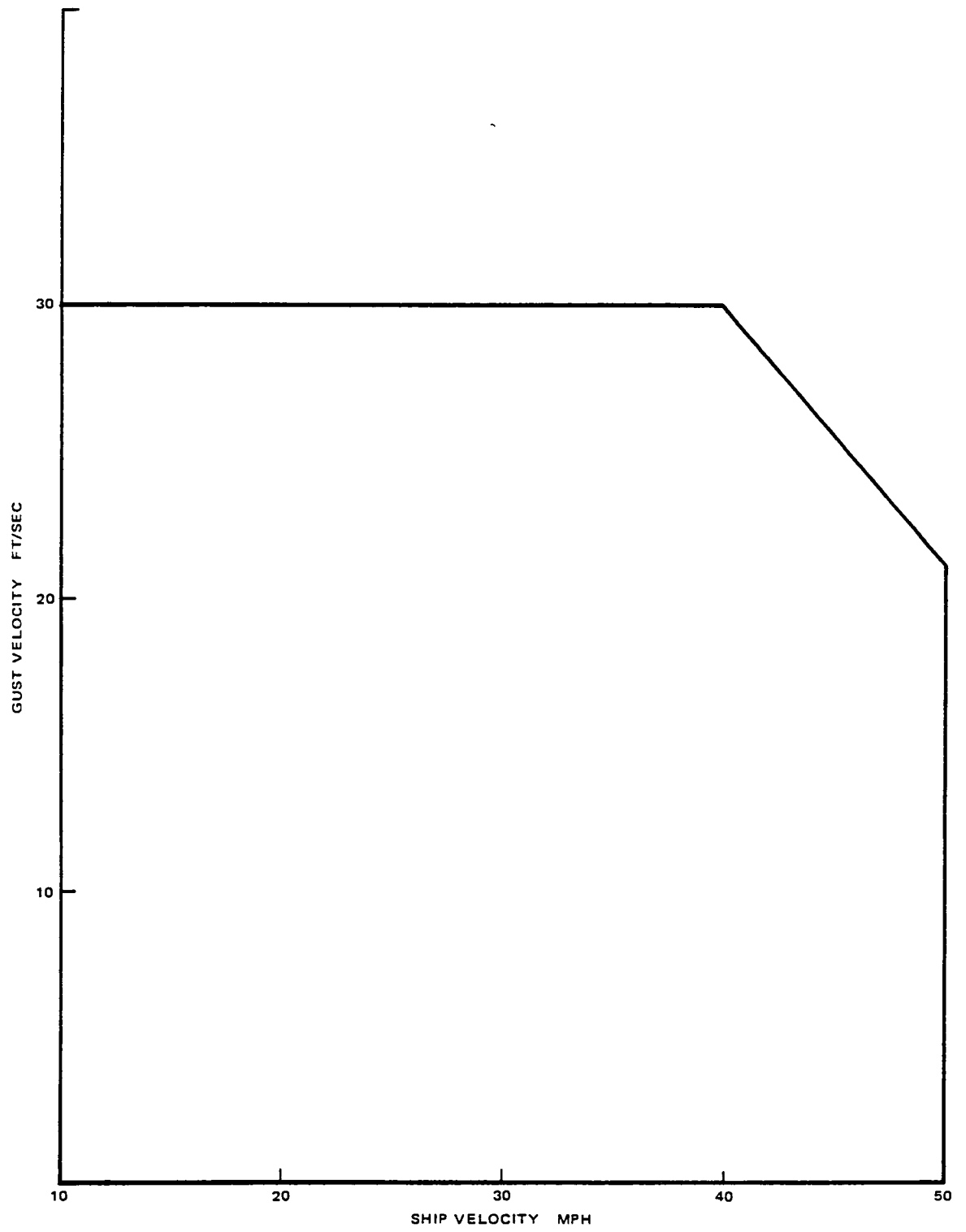
Figure 5-5 – GZ20 Design Gust Criteria

Figure 5-6 – Simulated Gust Acceleration
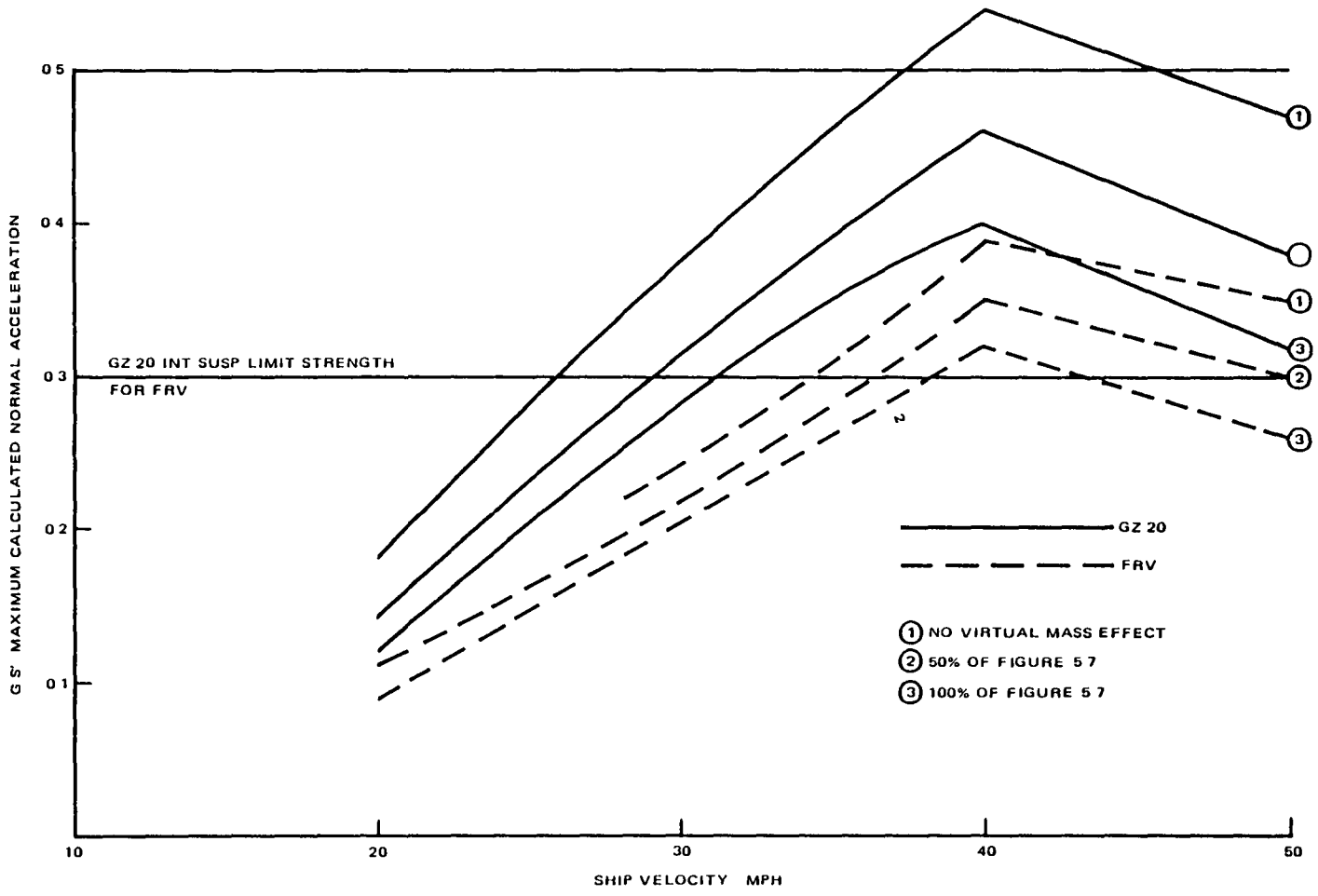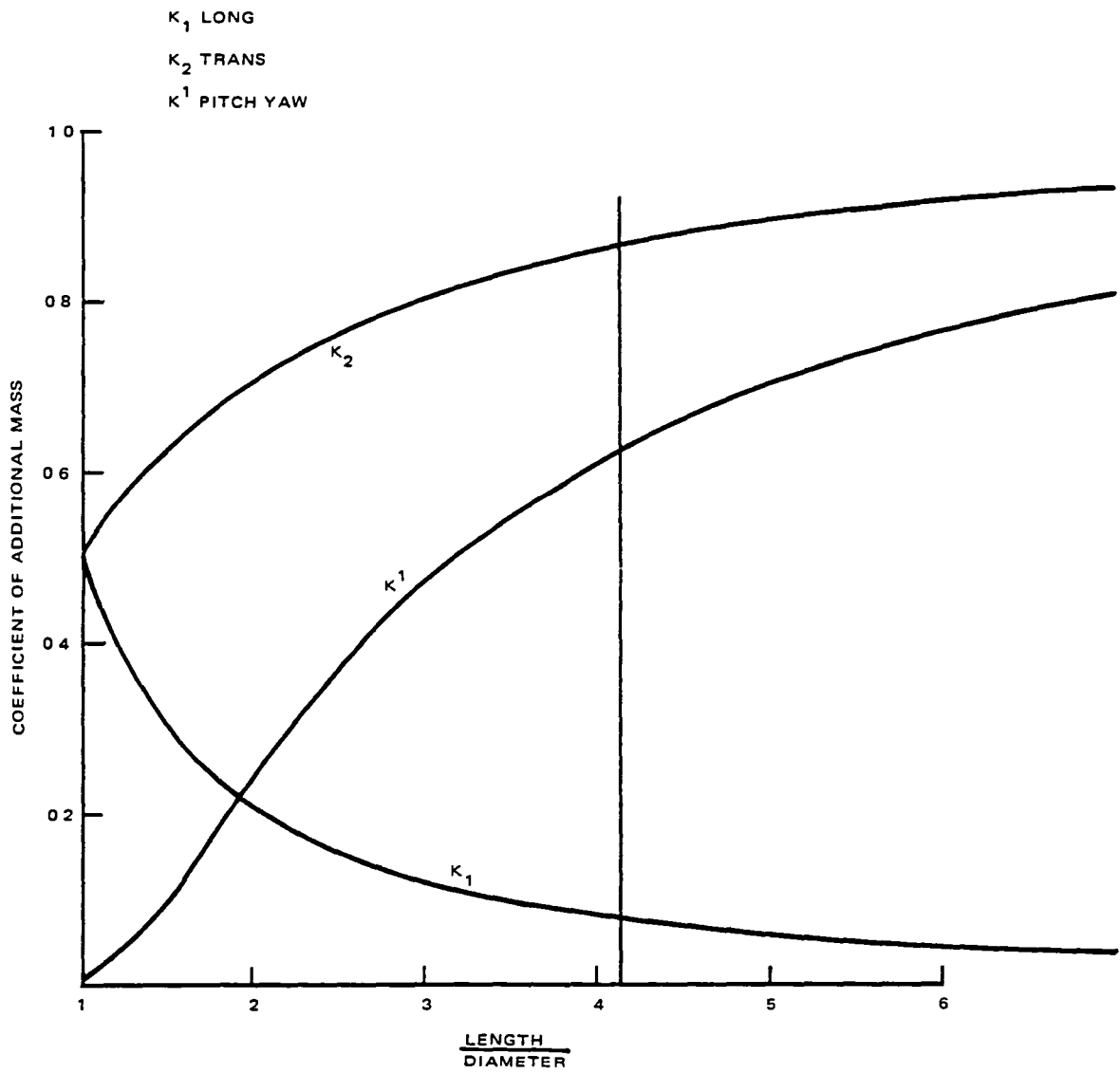
Figure 5-7 – Additional Mass of Ellipsoids
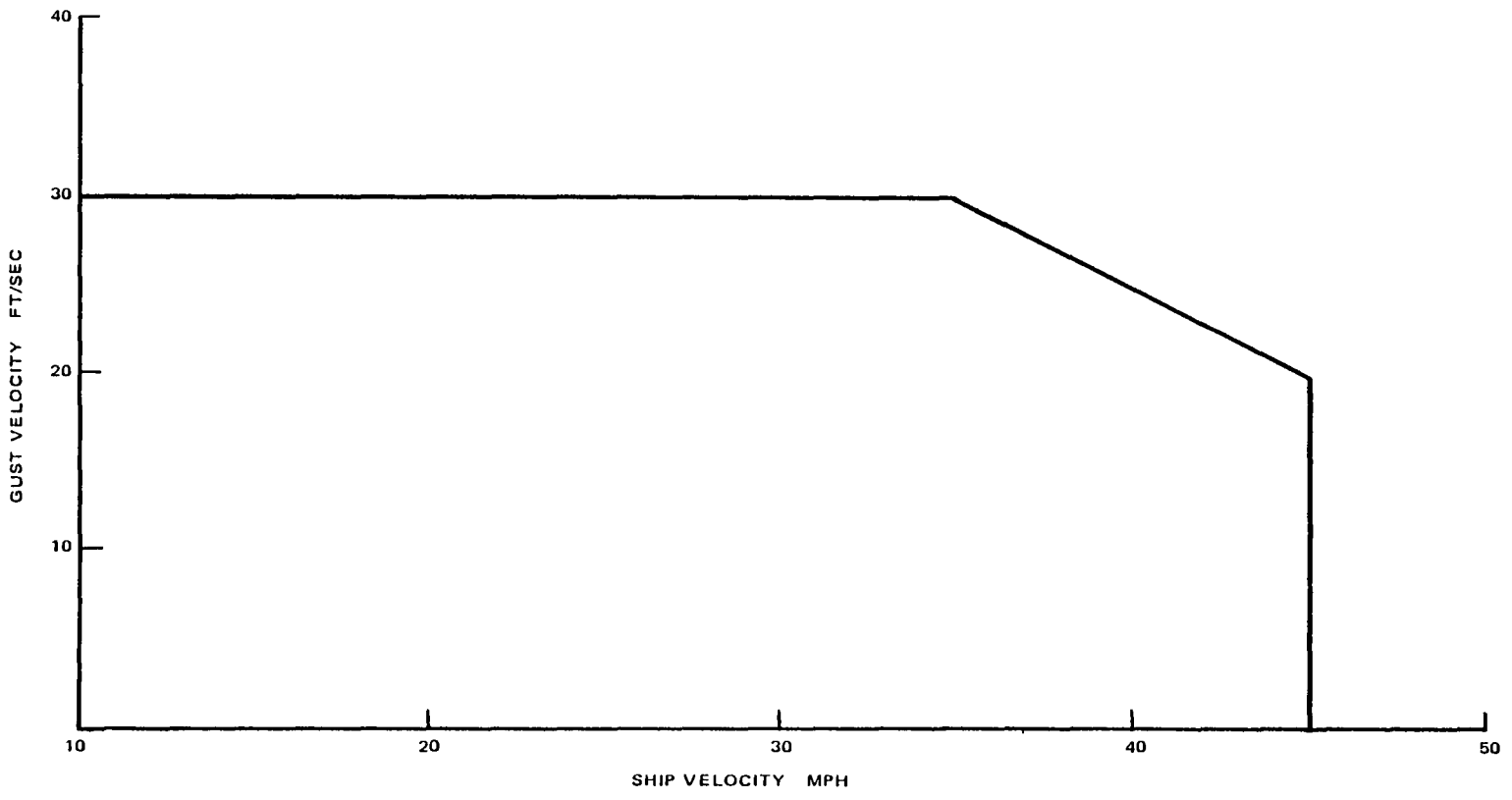
Figure 5-8 – FRV Recommended Design Gust Criteria

The internal suspension load increment for the GZ20 airship is computed as follows:

Internal suspension load GZ20 = $(M_{NGZ20} - M_E) (0.90) a_{NGZ20}$

Where M_{NGZ20} is total airship mass, M_E is envelope mass (total - car), and a_{NGZ20} is acceleration normal to long centerline.

Internal suspension load FRV = $(M_{NFRV} - M_E) (0.67) a_{NFRV}$

The curtain limit load is fixed to that of GZ20 design by reason of part utilization.

Internal suspension load (GZ20) = internal suspension load (FRV)
$$(M_{NGZ20} - M_E) (0.90) a_{NGZ20} = (M_{NFRV} - M_E) (0.67) a_{NFRV}$$

The effective envelope mass is identical for the two ships; i.e., common parts:

$$a_{N(FRV)} = \frac{M_{N(GZ20)} - M_E}{M_N(QRRV) - M_E} \frac{(0.90)}{(0.67)} a_{N(GZ20)}$$

$$= \frac{488 - 276}{752 - 276} \frac{(0.90)}{(0.67)} a_{N(GZ20)}$$

$$a_{N(FRV)} = 0.60 \, a_{N(GZ20)}$$

The design limit load factor for the GZ20 airship is the customary 0.5 g. The allowable load factor for the FRV is (0.60) (0.50 g) = 0.3 g.

b. Analysis

(1) General

The envelope analysis assumes that a Goodyear GZ20 envelope, complete with empennage and bow stiffening, is used for the FRV. An external suspension system is added to carry additional lift available from removal of the night sign. The system also provides a wider base to react to rolling moments acting on the envelope.

The static bending moment is developed in the customary manner for the envelope. Ten-foot incremental lengths of the envelope are used.

The dynamic bending moment is calculated using the maximum force loading from the dynamic gust analysis. Only the actual mass is used in the dynamic moment calculation. (This is a conservative approach.) The static and dynamic moments are added and the pressure required to resist this moment is found. The meridinal radii of curvature are treated as being infinite in comparison to the hoop radii in the membrane pressure equation. This quasi-cylinder approach is customarily used for envelope analysis.

A high value of unit lift (0.066 lb/ft^3) is used for the envelope bending analysis in place of the reduced purity lift used in the weight section of this report. Using the larger lift coefficient is conservative.

The following data are used for preliminary suspension system design:

Items	Weight (lb)
Envelope (completely new)	3,960.5
Tail (complete)	757.6
Large ballonets (modified)	130.0
5 years paint and patch at 50 lb/yr	250.0
	5,098.10
Use	5,100.0
Additional external suspension	70.0
	5,170.0
Design static lift 2000-ft pressure ceiling (205270) (0.066) (0.943)	12,780.0
Net static lift	7,610.0
Gas pressure load	1,532.0
Load, static on suspension systems	9,142.0
Internal suspension design load (0.90) (6800)	6,120.0 (67% of total)
External suspension load (new)	3,020.0 (33% of total)
External suspension load (existing)	0.0

The added external suspension system lies in a 45 degree plane. A true view of the system is shown in Figure 5-9.

Assuming the axial load P_E is distributed over the bottom 45 degree of arc and using the approximate radius in this area as 22 feet,

The axial load per foot is:

$$w_{A,E} = 31 \text{ lb/ft}$$

The nominal pre-stress is:

$$F = [(5.2)(1.75) + (0.063)(5.0)] \frac{22}{2}$$
$$= 103 \text{ lb/ft.}$$

This is considered a reasonable level of load for this area of envelope.

The loads and lift on basically 10 foot envelope sections are used to develop the shear and bending moment for load and lift. The gas pressure load is included in this calculation and is summarized in Table 5-8.

Figure 5-9 — Added Extension Suspension System Rigging Load

$W_{\Delta,K}$

$W_{E,T}$

$W_{\Delta,E}$

P_E

1 68 FT

38 66 DEG

8 4 FT TYP

39 00 DEG

P_E

F F F F F

10 FT (APPROX)

8 75 FT TYP

10 FT (APPROX)

P_E

P_E
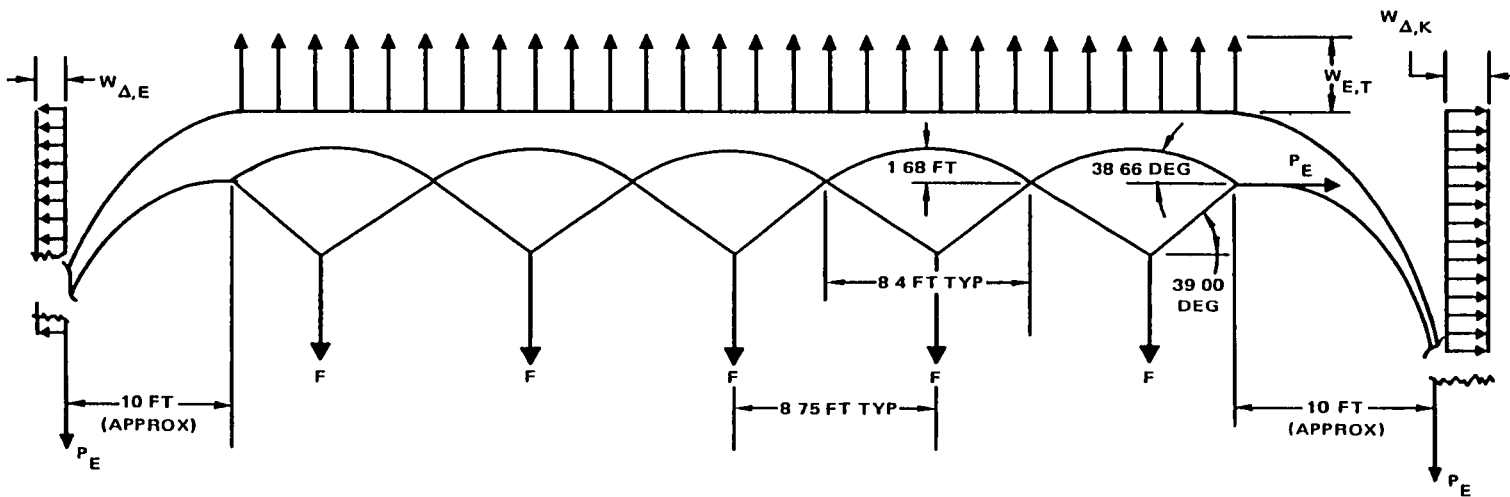
$$W_{E\ T} = \frac{3020}{2\ (COS\ 45\ DEG)\ 42}$$

$$= 50\ 8\ LB/FT$$

$$F = 8\ 4\ (50\ 8)$$

$$= 426\ 7$$

$$PE = \frac{F}{2}\ (COT\ 39\ 0\ DEG + COT\ 38\ 66\ DEG)$$

$$= 1\ 24F$$

$$= 1\ 24\ (426\ 7)$$

$$= 530\ LB$$

TABLE 5-8 – ENVELOPE STATIC-LOAD, LIFT AND GAS PRESSURE LOAD, SHEAR AND BENDING MOMENT

Env sta (ft)	Env wt (lb)	React (lb)	Gas load (lb)	Lift (lb)	Lift-re (lb)	Shear (lb)	ΔX (ft)	ΔMom (ft-lb)	Mom (ft-lb)
0	80			0	-80	-80			0
							2.5	-286	
2.5	107			38	-69	-149			-286
							5	-745	
7.5	106			106	0	-149			-1031
							7.5	-338	
15	183			391	208	59			-1369
							10	2545	
25	199			590	391	450			1175
							10	7110	
35	224			746	522	972			8286
							10	9880	
45	197	633		862	32	1004			18166
							10	9175	
55	242	870		939	-173	831			27341
							10	5240	
65	231	1534	167	984	-614	217			32581
							10	1300	
75	329	1534	686	1003	-174	43			33881
							10	-460	
85	326	1534	679	1003	-178	-135			33421
							10	-5580	
95	272	1534		960	-846	-981			27841
							10	-10770	
105	197	904		909	-192	-1173			17071
							10	-11685	
115	238	591		838	9	-1164			5386
							10	-8860	
125	195			751	556	-608			-3474
							10	-3820	
135	202			654	452	-156			-7294
							10	235	
145	189			548	359	203			-7059
							10	2910	
155	256			432	176	379			-4149
							10	3065	
165	458			313	-145	234			-1084
							10	-1125	
175	433			190	-243	-9			41
							10	-45	
185	54			63	9	0			-4
Σ=	4718	9134	1532	12320					
C.G.@	97.53	79.93	78.34	86.90					

(2) Rigging Moment

The effects of the longitudinal components of suspension system loads on the longitudinal bending capability of the envelope is given in the equation:

$$M_{rig} = \pm \Sigma HY + \frac{R}{2} \Sigma H;$$

where H is horizontal force, Y is vertical distance to centerline, and R is radius.

The first term transfers the longitudinal force to center line with resulting moment. The second term represents the reduction in envelope bending capability from the total axial load acting on the envelope. The rigging moment from the external system is given in Table 5-9. The internal rigging moment is in Table 5-10 and the two are combined in Table 5-11 to obtain the total rigging moment.

The longitudinal load, P_E is expected to be developed over a 10-foot length in the x direction and a 45 degree arc length between $\theta = -45$ degrees and the bottom centerline of the envelope. θ is the angle between horizontal centerline plane and the point on the envelope. The load centroid is at the -65.5 degree point on the arc.

TABLE 5-9 – RIGGING MOMENT EXTERNAL/SYSTEM

Station	H	ΣH	R	$\Sigma HR\cos 67.5$	$\frac{R}{2} \Sigma H$	M_{-rig}	M_{rig}
49.25	1058	1058	22.26	-21758	11775	-9982	0
59.25	-	1058	22.79	-22276	12055	-10220	-9982
69.25							-10220
75.25	-	1058	23.03	-22511	12182	-10328	-10328
81.25	-	1058	22.91	-22393	12119	-10273	-10273
91.25	-	1058	22.32	-21817	11807	-10009	-10009
101.25	1058	-	21.68	-21191	11468	-9722	-9722
111.25	-	1058					0

TABLE 5-10 - INTERNAL SYSTEM RIGGING MOMENT

Station	R	H	ΣH	HRcos30	ΣHRcos30	$\frac{R}{2}$ ΣH	Moment rigging moment
32.25	19.44	576	576	9697	9697	5598	15295
		116					
42.25	21.15	-	692	-	12674	7317	19991
		338					
52.25	22.09	-	1030	-	19704	11376	31080
		196					
62.25	22.79	-	1226	-	24197	13970	38167
		34					
67.58	22.91	-	1260	-	24999	14433	39432
79.90	23.03	-	1209 1209	-	24112	13921	38033
89.88	22.67	-	1158	-	22734	13125	35859
		62					
97.55	21.73	-	1009	-	18988	10962	29950
		248					
107.55	21.56	-	848	-	15833	9141	24974
		324					
117.55	20.62	-	524	-	9357	5402	14759
		94					
127.55	19.56	430	430	-	7283	4205	11488

TABLE 5-11 - TOTAL RIGGING MOMENT

Station	Internal rigging moment	External rigging moment	Rigging moment	1.5 x rigging moment
32.25	15295	-	15295	22943
42.25	19991	-	19991	29986
49.25	-	0	27753	41629
52.25	31080	-	28084	42127
59.25	-	-9982	26059	39088
62.25	38167	-	28113	42169
67.58	39432	-	29251	43876
69.25	-	-10220	28992	43488
75.25	-	-10328	28233	42349
79.90	38033	-	27747	41620
81.25	-	-10273	27465	41197
89.88	35859	-	25814	38721
91.25	-	-10009	24794	37191
97.55	29950	-	20121	30181
101.25	-	-9722	18387	27580
107.55	24974	-	18849	28273
111.25	-	0	21070	31605
117.25	14759	-	14759	22136
127.55	11488	-	11488	17232

(3) Gas Gradient Moment

The gas gradient moment for the GZ20 envelope is shown in Figure 5-10. The static load lift and a 1.3 g rigging moment are also shown. The transverse dynamic loads, shears and moments are calculated separately. The dynamic load effect on the rigging moment is approximated by multiplying the static rigging moment by the dynamic load factor.

The moments are added algebraically and the summation referred to as the static moment is included in Figure 5-10.

(4) Dynamic Moment

The maximum normal force from the gust response analysis is used to develop the preliminary envelope dynamic moment. The transverse and angular forces, moments and accelerations are reacted by inertia forces which are proportional to the static loads on the envelope lengths.

The helium weight is added to the envelope weight and reactions. Only the WX^2 terms are used in the rotational inertia term. The I_0 term is excluded. The transverse acceleration load is provided in Table 5-12. The angular acceleration load and the dynamic lift are combined with the transverse acceleration load and the resulting shear and moments are shown in Table 5-13.

(5) Operating Pressure

The pressure required at the envelope center line is given by the equation:

$$P = \frac{2M}{\pi R^3}$$

The manometer is approximately 28 feet below the envelope center line. Thus:

$$P_o = P - 0.0635\ (28)$$
$$= P - 1.78$$

The manometer reads in inches of water

$$P_o = \frac{1}{5.2}\left[\frac{2M}{\pi R^3} - 1.78\right]$$
$$= 0.122\ \frac{M}{R^3} - 0.34$$

5-28

Figure 5-10 – FRV Static Moments
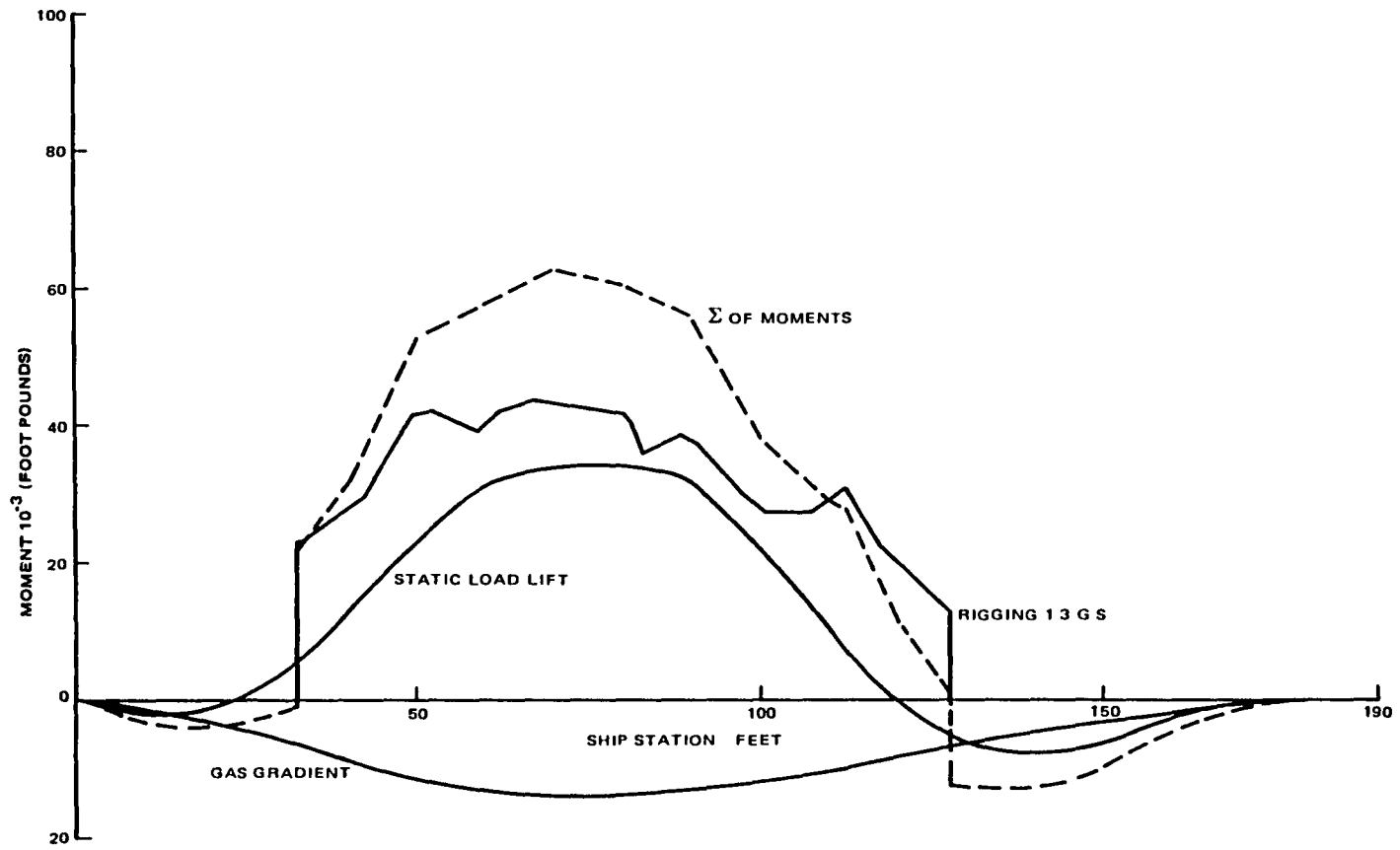
TABLE 5-12 - TRANSVERSE ACCELERATION LOAD

Envelope station	A	Envelope weight	B	C	Load (B+C)
0	0	82	25.9		25.9
2.5	7.1	110	37.0		37.0
7.5	19.1	109	40.4		40.4
15	72.4	188	82.2		82.2
25	109.2	205	99.2		99.2
35	138.2	231	116.5		116.5
45	159.6	203	114.4	373.4	487.8
55	173.9	249	133.5	513.3	646.8
65	182.6	238	132.7	905.1	1037.8
75	185.8	339	165.6	905.1	1070.7
85	185.8	335	164.4	905.1	1069.5
95	177.8	280	144.5	905.1	1049.6
105	168.3	203	117.2	533.3	650.5
115	155.1	245	126.3	348.7	475.0
125	139.1	201	107.3		107.3
135	121.1	208	103.9		103.9
145	101.5	194	93.3		93.3
155	80.0	263	108.3		108.3
165	58.0	471	167.0		167.0
175	35.2	446	151.9		151.9
185	11.7	56	21.4		21.4
Total	2281.5	4856	2253.0	5389	7642.0

Notes: 1. A is the effective gas weight = 0.1856 x lift

2. $B = \dfrac{7642}{(752)(32.2)}$ x (A + envelope weight)

3. $C = \dfrac{7642 - 2253}{9134}$ x reaction = 0.59 x reaction

TABLE 5-13 – DYNAMIC SHEAR AND MOMENT

Envelope Station	X (ft)	W	$WX \times 10^{-2}$	Aero-lift	$-0.011WX$	Accel load	ΣF_N	V_{Aero}	ΔX	ΔM	M_{Aero}
0	-86.71	80	-69.37		79	25.2	54	54			
2.5	-84.21	114	-96.00	181	108	36.0	253	307	2.5	451	451
7.5	-79.21	125	-99.01	466	111	39.5	538	845	5	2880	3331
15	-71.71	256	-183.58	690	207	80.7	816	1661	7.5	9398	12729
25	-61.71	309	-190.68	674	215	97.4	792	2452	10	20565	33294
35	-51.71	363	-187.71	557	211	114.4	654	3106	10	27790	61084
45	-41.71	884	-368.72	434	416	489.1	361	3467	10	32865	93949
55	-31.71	1140	-361.49	191	407	648.8	-51	3416	10	34415	128364
65	-21.71	1691	-367.12	154	415	1042.0	-473	2943	10	31795	160159
75	-11.71	1792	-209.84	19	237	1074.0	-818	2125	10	25340	185499
85	-1.71	1789	-30.59	-59	35	1073.0	-1097	1028	10	15765	201264
95	-8.29	1727	143.17	-95	-161	1053.0	-1309	-281	10	3735	204999
105	18.29	1118	204.48	-212	-231	653.0	-1096	-1377	10	-8290	196709
115	28.29	885	+250.37	-327	-283	475.7	-1086	-2463	10	-19200	177509
125	38.29	334	127.89	-342	-144	105.5	-592	-3054	10	-27585	149924
135	48.29	323	155.98	-301	-176	102.1	-579	-3633	10	-33435	116489
145	59.29	291	169.62	-286	-191	91.7	-569	-4202	10	-39175	77314
155	68.29	336	229.45	1147	-259	106.1	+782	-3420	10	-38110	39204
165	78.29	516	403.98	1766	-455	162.9	1149	-2271	10	-28435	10744
175	88.29	468	413.20	2948	-467	147.8	2333	+62	10	71045	-296
185	58.29	66	64.87	15	-74	20.7	-80	-18	10		-76
Totals		14507		7620		7642					

Notes:
1. $\overline{X}_{Aero} = \dfrac{881202.5}{7620} = 115.64$

2. $\overline{X}_{Load} = \dfrac{636738}{7642} = 83.31$

3. $\dfrac{(115.64 - 8331)\ 7620}{\Sigma WX^2} = 0.01128$

The static and dynamic moments are added over the central portion of the envelope and the pressure required at each station is calculated. The maximum is the required operating pressure as shown in Table 5-14.

TABLE 5-14 - REQUIRED PRESSURE CAR MANOMETER

STA	$10^{-3}M_{stat}$ [1]	$10^{-3}M_{dyn}$ [2]	0.1 R [3]	P_o (in. of water)
45	42	93.9	2.15	1.37
55	55	128.3	2.23	1.68
65	60	160.2	2.29	1.90
75	61.8	185.5	2.31	2.11
85	58	201.3	2.29	2.30
95	47	205.0	2.24	2.40
105	33.5	196.7	2.17	2.42
115	22.3	177.5	2.09	2.34
125	4.5	149.9	1.97	2.13
135	-13	116.5	1.85	1.66
145	-12	77.3	1.69	1.31

(1) Reference Figure 5-10
(2) Reference Table 5-13
(3) Stretched radius

The required operating pressure for 35 mph gusty weather is therefore 2.42 inches at the manometer.

c. Transverse Load Effects

Conventional airships experience negligible transverse loads. The metacentric height causes the airship to roll so that the resultant of the combined lateral and vertical acceleration vectors (including gravity effects) lies in the nominal airship vertical center line plane.

The quad-rotor concept introduces the ability to develop side loads and rolling moments. The application of these loads to the envelope, and reacting them by a conventional type suspension system, deforms the transverse envelope sections in a manner which could result in significant differences between the maximum and minimum section diameters. The magnitude of these differences is dependent upon the design crosswind velocity as well as the suspension system geometry.

The required envelope pressure is a function of the longitudinal stress in the envelope. Significant differences from the manufactured theoretical circular shape of the envelope sections result in a variable longitudinal pressure stress distribution around sections. At some point, as the section deforms, section arc lengths become slack in the longitudinal direction. The presence of these slack lengths has several major detrimental impacts on the envelope structural characteristics.

The presence of the arc lengths with no longitudinal pressure stress indicates the stress in the arc lengths having longitudinal stress is increased. Assuming a linear stress variation in the loaded arc lengths, the maximum longitudinal stress is increased by,

$$\frac{2 \text{ Total section length}}{\Sigma \text{ Tensioned arc length}}$$

Studies of collapsing moments for pressure-stabilized cylinders indicate the ratio of maximum stress to theoretical uniform stress is a function of the working stress-to-stiffness ratio of the material which becomes infinite at a "0" stress-to-stiffness ratio. Using a working stress-stiffness of 0.025, the proposed envelope's approximate ratio, the maximum stress at the collapsing moment is approximately seven times the nominal uniform pressure stress. If sufficient arc lengths become slack, the section will buckle and a deep wrinkle will form with stresses approaching those of the collapsing moment.

The presence of arc lengths with no longitudinal tension will reduce the envelope stiffness both in shear and bending. The transfer of shear across areas having only hoop tension is done by geometrical deformation rather than material strain as in a biaxial stress field.

The geometric deformations are large, compared to material strain deformations under the same load. The bending stiffness about the axes perpendicular to the mid-radii of the slack arcs is also greatly reduced from that of a uniformly pre-stressed section. The magnitudes of the initial wrinkling and collapsing moments are also much reduced.

Excessive cross-section deformations can cause some suspension cables to become slack. Past practice has been to design in a manner which will prevent cables from becoming slack under any condition. The reason for avoiding cable slackness is the relatively low energy-absorbing capability of steel cables compared with their breaking strength. The energy equal to the cable design load acting unrestrained over a relatively small percentage of the cable length can easily exceed the cable's ability to absorb energy. Whether such energies will develop when cables become slack is not known, but, if possible, prevention of this condition is desirable.

Past practice has been to maintain the "circular" shape as closely as practical. Considerable effort was expended to minimize differences between the loaded sections and the theoretical circular sections. This assured a minimum deviation from the theoretical uniform longitudinal pressure stress in the envelope. The shear and bending stiffness of the envelope are ensured to loads equal to theoretical wrinkling values.

At this time, there is no simple analytical method to evaluate the effects of cross-section deformation on the longitudinal stress distribution in the envelope. Several two-dimensional (quasi-cylindrical) methods exist to predict the envelope-loaded section shapes. These are used to control the design of the ship, i.e. minimizing section distortion under load.

The FRV is designed to hold against small velocity crosswinds. This implies that some level of "antisymmetrical" section deformation is acceptable. How large this level is requires further analysis and verification.

The basic item not currently available is the external pressure distribution over the airship at large incidence angles. A finite element program for airship envelope analysis is currently being developed and may aid in defining acceptable crosswind load levels for the FRV.

At this time a cautious approach to these flight conditions, with a careful evaluation of performance, may enable the FRV to explore holding in a crosswind with adequate safety and a reasonable expectation of success.

d. Summary

A Goodyear GZ20 envelope can be used for the FRV.

An increase in operating pressure is required for forward flight. The FRV recommended operating pressure is 2.4 inches of water, compared to the GZ20A recommended operating pressure of 1.75 inches of water. The envelope can safely sustain pressures up to 3.0 inches of water car manometer pressure.

The effect of increasing the operating pressure is to shorten the safe life of the envelope. If this vehicle is to be built, the envelope life model will be modified to obtain a safe life prediction which requires a good estimate of operating and storage time and conditions. For the present, a minimum safe life of two years is probable. Depending on operating and storage conditions, it could be extended.

4. DYNAMIC CONSIDERATIONS

The quad rotor research vehicle consists of four helicopters and four auxiliary propellers run by eight power plants. Based on rotorcraft technology, a vehicle of this type is subject to several aeroelastic and vibration problems. If not prevented, some of them can lead to rapid destruction of the vehicle.

The rotorcraft technology is well-known as is the airship technology, but the aeroelastic problems that arise as a result of coupling these technologies are not known and can produce catastrophic failures. The instabilities are not necessarily bad as long as they are identified, analyzed and sufficient dampings are provided to stabilize the otherwise unstable modes. The following structural dynamic problems are identified as potential problems for hybrid airships with quad rotors.

a. Ground Resonance

Ground resonance can be caused by the in-plane motion of the rotor blades interacting with any other body modes when the vehicle is on the ground. The vehicles with soft in-plane rotors are prone to this type of instability and no aerodynamic forces are required for this phenomena to occur.

Ground resonance, if it occurs, often results in total destruction of the vehicle within a matter of seconds. Several helicopters have been destroyed by this phenomena.

b. Air Resonance

Air resonance can be caused by the in-plane motion of the rotor blades interacting with the body modes when the vehicle is in the air. Aerodynamic forces also enter into the picture.

For typical helicopter with articulated rotor the flapping frequency is around 1/rev and this yields very low body modes.
It is very unlikely for these low body modes to be in resonance with rotor lead-lag modes in the body-fixed system at the normal rotor operating speeds. If the rotor is stopped during the flight, the possibility of air resonance exists. If the helicopter is restrained on the airship interconnecting structure, then the body frequencies may be high enough to be in resonance with the rotor lead-lag modes.

c. Whirl Flutter

If propellers are employed for generation of direct side forces, then the possibility of whirl flutter has to be examined. The gyroscopic moments of the propeller couple its pitch and yaw modes and these coupled modes are called whirl modes.

The whirl motions associated with these modes produce changes in angle-of-attacks of blade elements. The changes in these blade element incidences generate perturbation aerodynamic forces and these forces provide the mechanism for whirl flutter.

d. Outrigger Stability

When a rotor is installed on a cantilever, the rotor modes may be coupled with cantilever modes giving rise to self-excited oscillations.

During the flight tests of several experimental tail rotors, the end of tail boom gave rise to an instability problem known as tail wagging.

There could be other problems associated with rotor-outrigger coupling and it is important to identify these problems and make sure that the vehicle is free of them.

e. Blade Stability

The rotor blade has several aeroelastic stability problems. The most common ones are:

1.   Pitch-lag stability

2.   Pitch-flap stability

3.   Flap-lag stability

Even though the existing rotors, which are free from these instabilities, are employed for the quad rotor research vehicle, they have to be re-evaluated since the blade is very sensitive to small changes in structural and aerodynamic parameters.

f. Frequency Placement

It is very important to establish guidelines on frequency placement of supporting structures, rotors, and propellers. The guidelines should consider the following:

- Resonant or nearly resonant responses

- Support stiffeners

- Fixed-rotating system transfer

- Fixed-system excitations

- Aerodynamic excitations of rotors and or propellers

g. Drive System Dynamics

A drive train dynamic analysis is necessary to make sure the following problems will not surface:

- Critical shaft conditions

- Drive system torsioned mode resonance

- Large torsional excursions

- Large shaft transverse excursions

- Coupled engine/drive system

- Fuel control system instability

SECTION VI - CONTROL SYSTEM CONCEPT FOR QUAD ROTOR FLIGHT RESEARCH VEHICLE

1. CONFIGURATION

The baseline design of the FRV is presented in Figure 4-1. It consists of four Hughes OH-6A helicopters and four auxiliary engine-propellers attached to the star frame to provide propulsive, control, and lifting forces. In addition, the conventional tail control surfaces are used to control the airship in cruise flight.

The helicopters are attached to the starframe with a hinge along the longitudinal axis and are free to roll ±12 degrees. They are restrained in pitch and yaw. A mechanism is provided such that this feature can be locked at 0 degrees rigidly attaching it to the starframe. The helicopter tail rotors are removed to reduce the number of control functions. Main rotor reaction torque is nominally compensated by tilting the left side helicopters forward and the right side helicopters aft approximately 1.5 degrees.

The auxiliary thrustor rotors are variable pitch and provide fully reversible thrust.

The use of hinge-mounted helicopters to provide additional side thrust is an optional feature and will probably only be used if sufficent lateral control is not achieved with the auxiliary thrustors and lateral cyclic with the helicopters rigidly attached. In the hinged mode, lateral cyclic pitch is used to torque the helicopters in roll. Angular sensors provide feedback for closed loop position control. In effect, the helicopters fly on the gimbals to the desired angular position.

2. FLIGHT CONTROL CONCEPT

a. Hover

In hover, provisions are made for controlling the FRV in six degrees-of-freedom as follows:

1. Longitudinal - forward facing auxiliary thrusters with variable pitch and main rotor longitudinal cyclic in unison.

2. Lateral - side facing auxiliary rotors with variable pitch and main rotor lateral cyclic (roll attitude in hinged configuration) in unison. An option would be to: roll the airship instead of, or in addition, to generate side forces.

3. Yaw - differential longitudinal auxiliary thrusters, differential main rotor longitudinal cyclic and differential lateral cyclic (roll attitude in hinged configuration).

4. Vertical - main rotor collective pitch in unison

5. Pitch - differential collective with ballonet trim

6. Roll - differential collective

In hover, pitch and roll automatic attitude control decouples the adverse roll and pitch moments from the lateral and longitudinal translational control forces. It is desirable to operate the airship with no angle-of-attack or sideslip during hover to minimize the aerodynamic forces and moments which are balanced by the control forces and moments. The recommended hover control method is shown in Figure 6-1 (ref. 12).

Yaw and longitudinal control use the same control forces. The control logic was designed such that yaw has authority over longitudinal control. Pitch and roll control were each limited to 10 percent of the main rotor collective as the baseline system, but some additional tests and data were recorded with different levels of authority. These authorities were selected based on some previous work and are not necessarily the recommended design. Additional work needs to be done in this area.

b. Ground Handling

The same control forces are available for taxiing and ground handling as for hover.

c. Cruise

In the cruise flight the airship is controlled with the conventional tail surfaces. Transition occurs at about 20 to 25 knots. Collective pitch is retained to provide vertical thrust, but it can be augmented by flying at some angle-of-attack to carry some of the load with aerodynamic lift.

In cruise flight the following controls are used:

> Longitudinal - Auxiliary thrusters and longitudinal cyclic in unison
> Lateral - None
> Yaw - Vertical tail control surfaces
> Pitch - Horizontal tail surfaces and differential collective pitch

Roll control is not required because of the inherent metacentric stability.

d. Pilot's Controls

A separate set of controls will be used for hover and cruise. This is logical from a hardware standpoint and also ease of pilot control.

In cruise flight, the GZ20 conventional controls are retained minimizing hardware changes. The flight controls are shown in Figure 6-2. The yaw pedals control the vertical tail control surfaces. The pitch control wheel at the right side of the pilot's seat controls the horizontal tail control surfaces and differential main rotor collective pitch. A conventional throttle lever is used to control the auxiliary thrusters pitch and longitudinal cyclic in unison for forward thrust. In the hover mode, the pitch wheel is locked in the neutral position and the yaw pedals are disconnected from the tail vertical control surfaces. These surfaces are also locked in a neutral position.

In hover, a right side arm controller is used to provide longitudinal and lateral control like a helicopter. A roll/pitch trim switch is mounted on this controller which controls the roll and pitch attitude if these autopilots are engaged. A conventional helicopter collective stick is provided on the left side of the pilot's seat. Yaw control is retained with the yaw pedals.

6-2
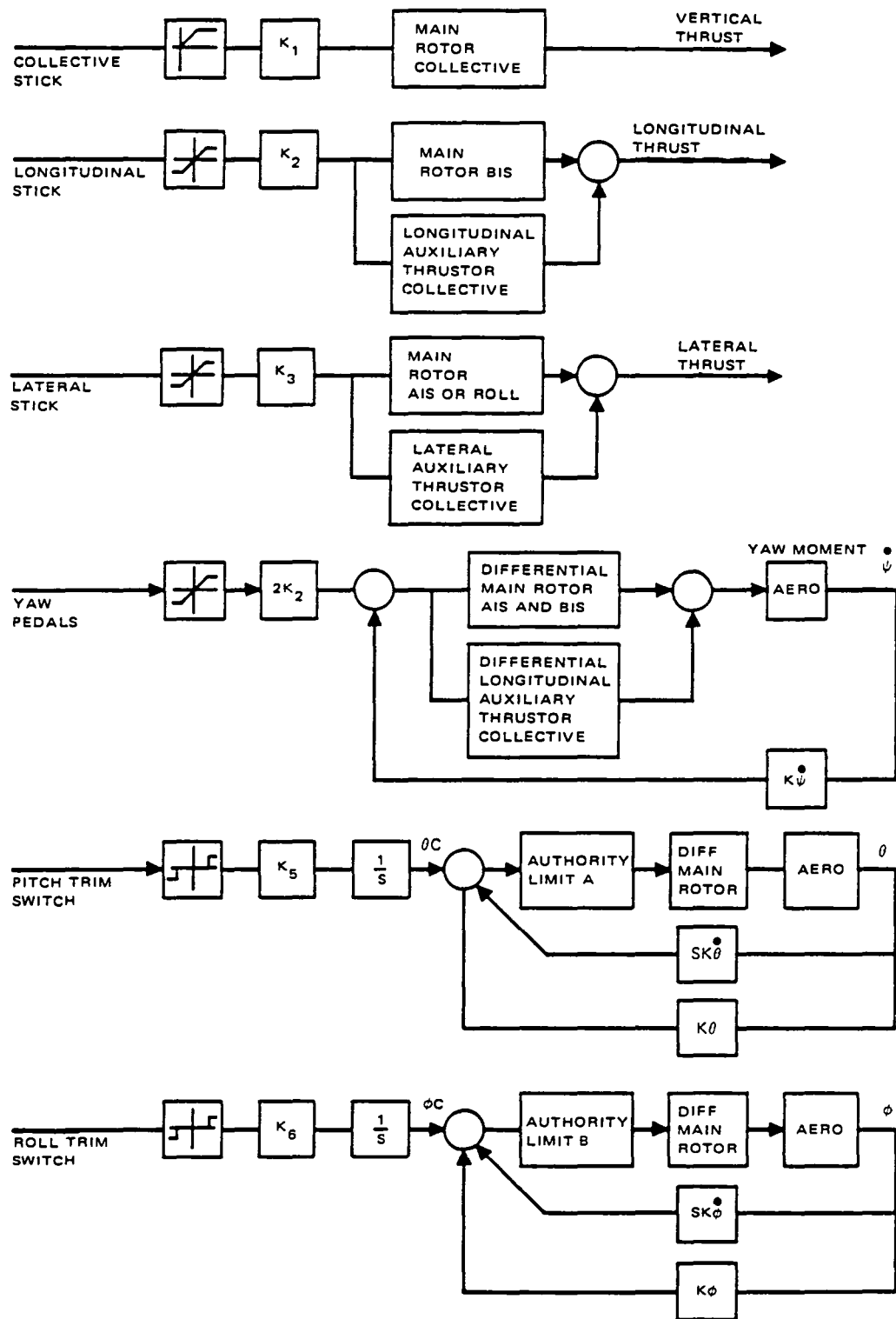
Figure 6-1 - Hover Control Logic
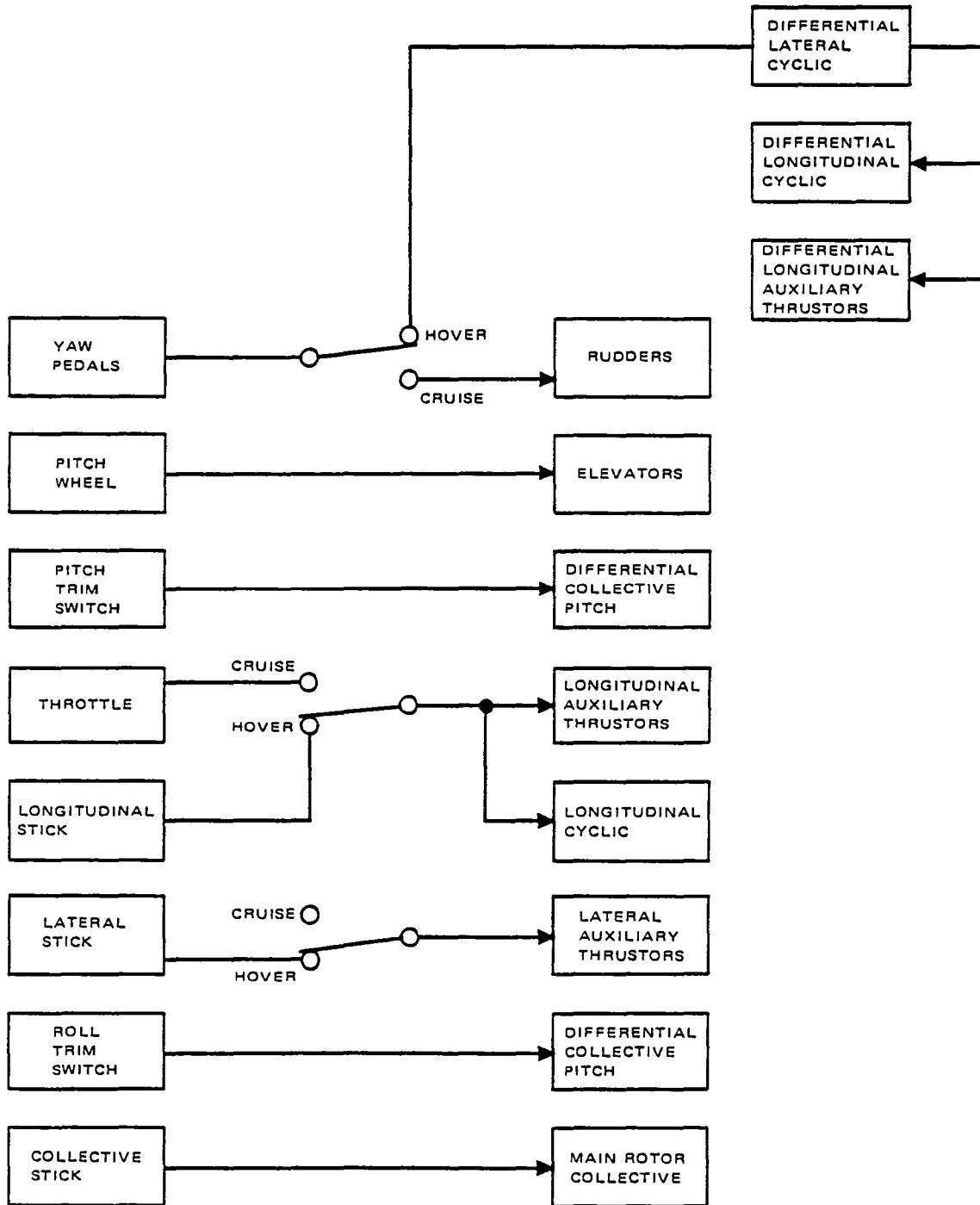
Figure 6-2 - Flight Controls

The logic for having separate controls is that in hover, FRV control is similar to that of a helicopter, while in cruise, it is like an airship.

A flight engineer will be used to monitor and control all the engine functins for the auxiliary thrusters and the helicopters.

3. FLY-BY-WIRE CONTROL SYSTEM

a. General

The fly-by-wire (FBW) system consists of three main groups, the primary flight controls and vehicle state sensors, the computers, and the flight control actuators. In addition, there is the remote starting, and management and monitoring of all eight engines (four helicopter and four auxiliary engines) from the flight engineer's station. Standard GZ20 envelope pressure and ballonet controls will be used and operated by the flight engineer.

General Electric Aircraft Equipment Division, Binghamton, New York, was a consultant on the FBW concepts.

One of the baseline assumptions is that the FRV will have the ability to jettison the payload in an emergency, such as a loss of an engine control function to stay aloft. Most control mode failures degrade the flying qualities or the ability to hover but will not result in total loss of control. Examples of a single control failure and its effects are presented in Table 6-1.

Since the loss of a single cyclic control does not endanger flight safety, the concept of using a control actuator without redundancy for cyclic is a possibility.

All of these failures involve the loss of an engine or a rotor control. The loss of a single main rotor or auxiliary thruster control or a single engine failure would not result in an unsafe flight condition if the proper pilot action is taken.

The most critical condition is the loss of a main rotor when carrying a payload. If the pilot jettisons the payload, the rotor lift is sufficient to gain or hold altitude giving the pilot time to assess the failure and make the best decision on what corrective action needs to be taken to make a safe landing.

The loss of an engine would be immediately detected at the flight engineer's station where the proper corrective action to shut down the diagonally opposed could be taken.

It should be noted that the loss of a control function would not necessarily be apparent to the pilot.

b. Fly-By-Wire Control System Candidates and Recommendations

Table 6-2 lists the candidate components which would provide a suitable FBW system for the FRV. It is recommended that all components, except the state sensors, have the fail-operate mode to ensure flight safety.

TABLE 6-1 – POTENTIAL CONTROL FAILURES AND PILOT RESPONSE

Control Failure	Effect	Pilot Action
Loss of forward auxiliary thruster engine during cruise or hover	Loss of airspeed and adverse yaw	Cut forward power and hover. Coordinate yaw and forward thrust to land.
Loss of lateral auxiliary thruster engine during hover	Reduction in lateral control	Be aware of reduction in lateral control. Landing not required.
Loss of collective control on forward auxiliary thruster. Fails in maximum forward or reverse thrust.	Gain or loss in airspeed and an unwanted yaw	Shut down defective engine and follow procedure described in first listing.
Loss of collective control on lateral auxiliary thruster. Fails in maximum port or starboard thrust.	Unwanted side force generated	Shutdown defective engine and be aware of reduced lateral control. Landing not required.
Loss of main rotor collective. Fails in maximum collective position.	Start to gain altitude with unwanted pitch and roll attitude	Jettison payload. Shut down failed rotor and diagonally opposed rotor and land.
Loss of a main rotor engine	Start to lose altitude with unwanted pitch and roll	Jettison payload. Shutdown diagonally opposite main rotor, stabilize at altitude and land.
Loss of main rotor cyclic. Hard over lateral cyclic.	Unwanted yaw and sideforce	Compensate with yaw and lateral stick control. Land normally.
Loss of main rotor cyclic. Hard over longitudinal cyclic.	Unwanted yaw and longitudinal force	Compensate with yaw and longitudinal stick control. Land normally.

TABLE 6-2 - CANDIDATE FBW CONTROL SYSTEMS

Augmentation or State sensors	Primary flight control sensors	Computer	Actuators
*Non-redundant sensors self-monitored lective	*Dual sensors self-monitored RVDTS or or LVDTS	Self-monitored digital computer with analog backup	OH-6A autopilot actuators for pitch and yaw. Dual redundant for main rotor and auxiliary thruster col-
Dual redundant sensors self-monitored	Triple redundant RVDTS or LVDTS with majority vote	Dual digital computers self-monitoring	*Dual redundant actuators with model comparison
Triple redundant sensors		*Dual digital computers with self-monitoring, and wrap-around	Triple redundant actuator with majority vote
		Dual digital computers with self-monitoring, wrap-around and analog backup	
		Triple redundant computers with majority vote	

*Selected components for baseline system

A block diagram of the selected FBW system is shown in Figure 6-3. The concept uses dual redundancy in the primary flight controls, digital computers, control actuators and power supplies.

This system has the added feature that a single failure does not shut down one complete channel. It allows primary channel operation with more than one failure if it is not the same function. This is accomplished by the steering capability in the digital computers. The steering capability is shown on a more detailed block diagram of the digital computers in Figure 6-4. The input and output interfaces are dual. All inputs go through both interface A/D channels and CPU's. If a single A/D fails the redundant channel, A/D input #2, is used, but it is steered back to CPU #1 keeping channel 1 still operative. If the channels were completely independent, a failure in channel 1 and channel 2 would result in some non-operative function.

DIGITAL COMPUTERS

SELF MONITOR

PRIMARY CONTROL SENSORS NO 1

PRIMARY CONTROL SENSORS NO 2

SELF MONITOR

WRAP AROUND TESTS

INPUT INTERFACE

COMPUTER NO 1

COMPUTER NO 2

OUTPUT INTERFACE

DUAL REDUNDANT ACTUATORS

FLIGHT CONTROL MECHANISM

ACTUATOR MODEL

AUGMENTATION OR STATE SENSORS

WRAP AROUND TESTS

SELF MONITOR

Figure 6-3 – Fly-by-Wire Block Diagram
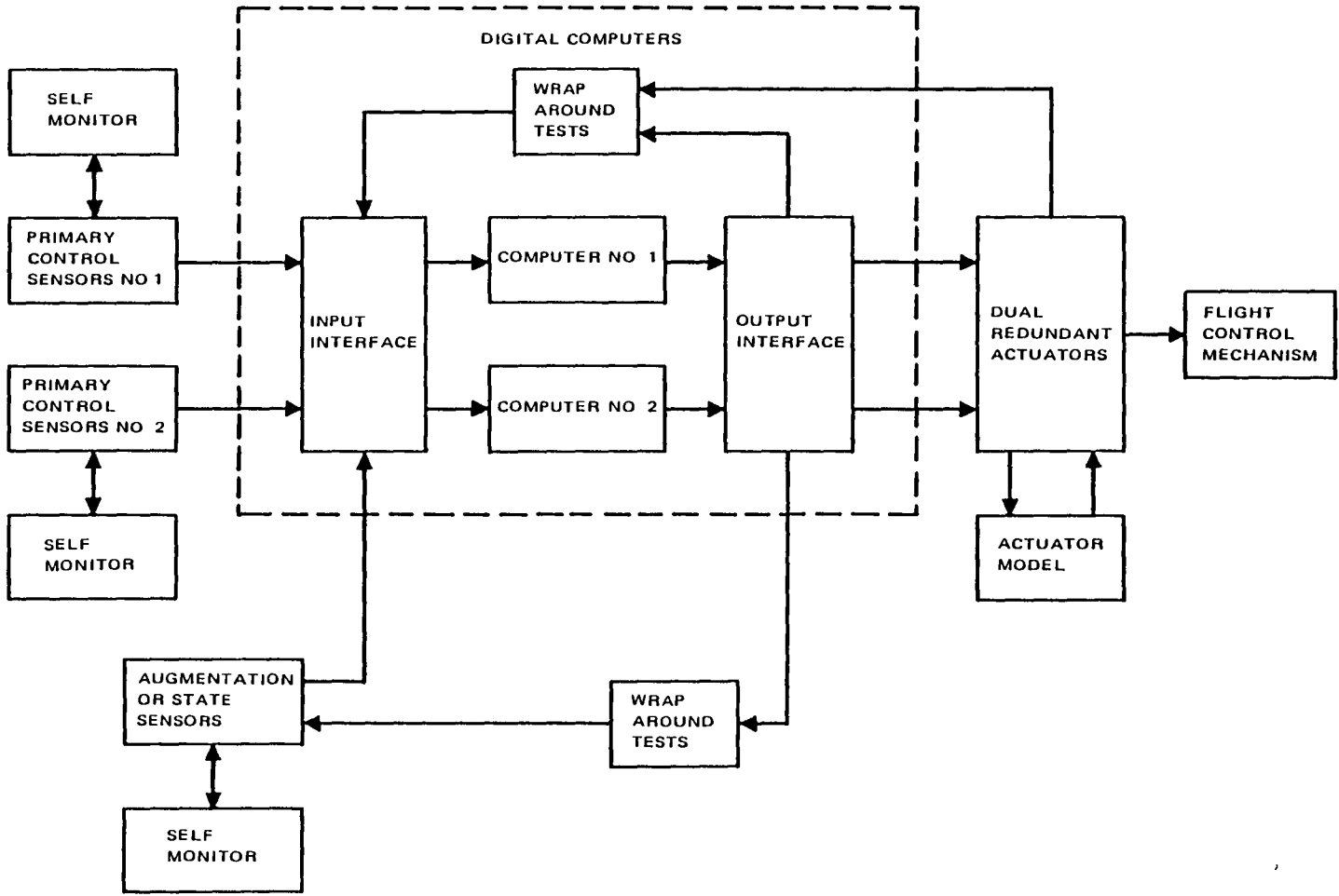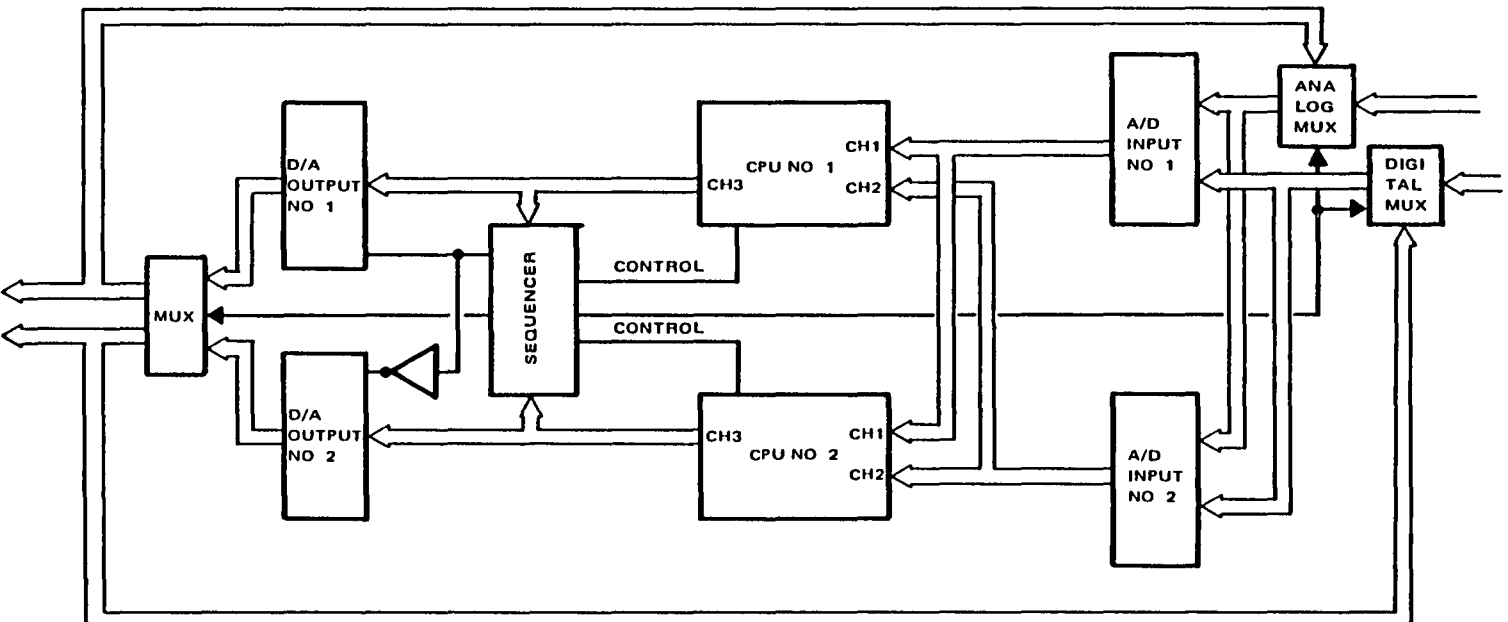
Figure 6-4 – Dual Digital FBW Computers

(1) Augmentation Sensors

Preliminary analysis indicates that flight control augmentation is not mandatory for flight safety although it improves handling qualities. Therefore, the augmentation or state sensors for the primary flight control system need not be redundant. They will contain a self-monitoring technique which would indicate a faulty measurement. If a faulty sensor is detected, it can be disconnected from the flight control system and flown without augmentation.

A strapdown inertial measuring unit (IMU) is recommended. It can measure all states of the FRV which might be useful for both augmentation and an automatic hover sensor.

(2) Primary Flight Control Sensors

In hover, the pilot's controls are:

       (a)   Longitudinal stick electric) (critical)

       (b)   Lateral stick (electric)

       (c)   Collective stick (electric) (critical)

       (d)   Yaw pedals (electric) (critical)

       (e)   Pitch (electric switch)

       (f)   Roll (electric switch)

In cruise flight, the pilot's controls are:

       (a)   Yaw pedals (cables to rudders)

       (b)   Elevator wheel (cables to elevators)

       (c)   Collective stick (electric) (critical)

       (d)   Throttle (electric) (critical)

Many of these controls are critical to flight safety, particularly main rotor collective which is required to remain airborne. Because of their importance it is recommended that all of the pilot's electric controls be at least dual redundant.

The recommended primary flight control sensors are rotary variable differential transformers (RVDTS) or linear variable differential transformers (LVDTS) and trim switches. A triple redundant LVDT is shown in Figure 6-5.

(3) Flight Control Computer

The flight control computer takes the input signals from the primary flight controls and state sensors and implements the control mixing, signal conditioning and the control laws as required and outputs the control signals to the flight control actuators.
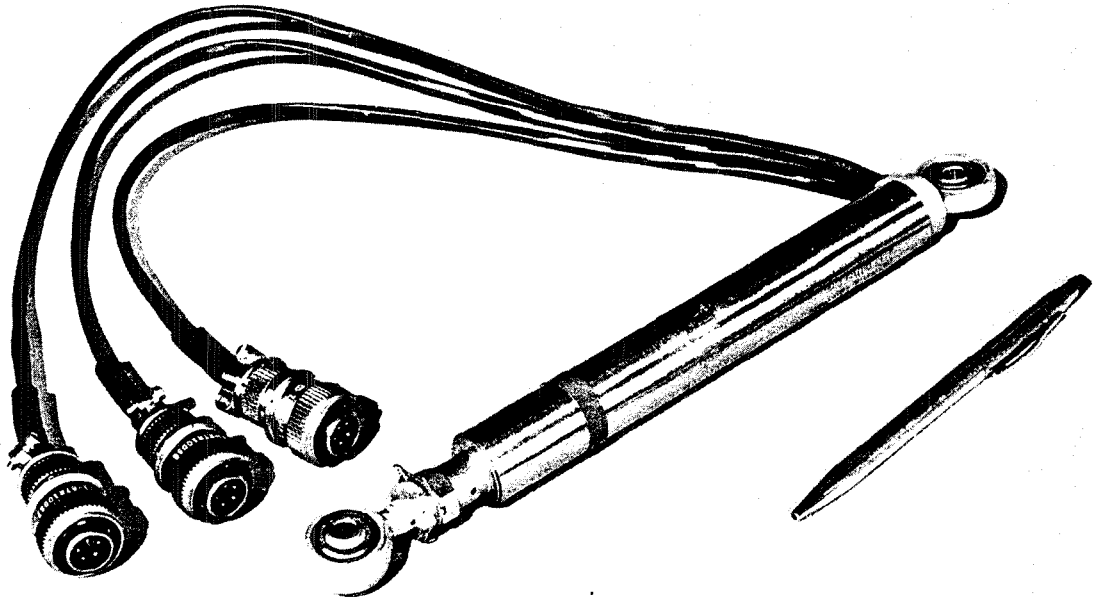
Figure 6-5 - Triple Redundant LVDT

An all analog flight control computer was not considered to be practical for the FRV because it would not have the flexibility to be easily reprogrammed and thus would not meet the objectives of a flight test program. A digital flight computer is ideal for the FRV because of the accuracy of implementation and ease with which program changes can be made in the field.

The lowest level of redundancy would be to have a digital computer with an analog backup. This concept was not selected because the dual digital computer was considered to be more versatile and not require an additional analog design.

Dual digital computers, with the addition of the wrap-around techniques to check the computer I/O's and actuators, were selected as the baseline because that system provides the additional fault monitoring for a totally redundant system.

The dual redundant digital computer with analog backup and the triple redundant digital systems are considered to be beyond what is required to ensure FRV flight safety. In addition, to implement the control mixing and stability augmentation, the digital computer does self-testing and wrap-around tests of the entire system from the computer input interface to the actuator outputs.

On initial power up the computers will do a self-test. Then the interface hardware will be checked by each computer to verify the dual I/O control logic in a closed loop using the outputs of the flight control actuators.

This wrap-around or closed-loop test checks the integrity of everything beyond the primary input sensors. The augmentation sensors can also be checked in the same way. Self-monitor signals from the flight control sensors and actuators are also sent back to the computers for total system verification. The wrap-around tests within the computer are performed during flight which provides continuous closed loop integrity testing.

Any failure(s) are automatically removed from the loop and substituted with the redundant channel. The failure(s) is indicated on the pilot's or engineer's status panel.

The anticipated flight control mixing logic and iteration rates are not excessive so that a number of general purpose computers could be used in this application.

(4) Flight Control Actuators

The OH-6A has an optional autopilot which is manufactured by Astronautics. The autopilot actuators are not redundant and would only be useful for the cyclic controls since the autopilot has no collective control. In the interest of commonality and safety, it was decided that the dual redundant actuator should be used for all flight controls.

The dual redundant flight control actuators were also selected for their consistency with the baseline concept of having a fail-operate concept throughout the FRV.

The flight control actuators are dual redundant electric AC servos which are capable of providing enough torque to react to all the flight loads on the helicopter controls. Based on information from Hughes, it is assumed that all flight loads will not exceed 80 percent of the limit loads. The actuators will be designed to provide full control travel in one second.

The actuator consists of parallel redundant motor-brake-tachometers driving an output gear through a differential gear. Figure 6-6 shows a preliminary design of a dual actuator without the tachometers. An output RVDT is provided for each motor loop for position feedback.

Normally both motor loops are driven simultaneously and the summation of the tachometer outputs provides an indication that both motor loops are functioning. If one of the loops fails, each tachometer is compared with the electronic actuator model tach to determine which is faulty. The faulty loop is then braked via the actuator control logic and an indication of the loop failure is fed back to the computer.

In addition to this logic, the actuator wrap-around tests are checked each computer cycle to determine total closed-loop integrity.

(5) Control Signals

The control actuators for the helicopters and auxiliary thrusters are remote from the control car. Ideally, it would be desirable to transmit commands and output status signals to and from the actuators with serial digital fiber optics. This would minimize the effects of electromagnetic interference (EMI) and provide lightweight cables to these units. However, use of fiber optics would require additional digital processing electronics at each station and would unnecessarily complicate the FBW system.

Figure 6-6 – Preliminary Design of a Dual Actuator

MOTOR CHARACTERISTICS AT UNIT TEMPERATURE OF + 125°C		FIXED PHASE(NT)	CONTROL PHASE(NT)
EXCITATION AT 400 Hz(VOLTS RMS)		*	*
ZERO SPEED POWER	(WATTS)	35	35
TUNING CAPACITOR	(mfd)		
TORQUE AT 3 RPM	(LB-IN)	400	
POWER OUT AT 3 RPM	(WATTS)	14.2	

BRAKE CHARACTERISTICS AT UNIT TEMPERATURE OF +25°C		
POWER AT 28 VOLTS	(WATTS)	4.0
PULL IN VOLTAGE	(VOLTS DC)	16
DROP OUT VOLTAGE	(VOLTS DC)	1.0
BRAKE TORQUE (DE-ENERGIZED)	(LB-IN)	500

EACH RVDT CHARACTERISTICS AT UNIT TEMPERATURE OF + 25°C		
EXCITATION AT 400 Hz	(VOLTS)	*
SCALE FACTOR	(MV/DEG)	250
ANGULAR RANGE	(DEG)	±40

PINION DATA	
NUMBER OF TEETH	53
DIAMETRAL PITCH @ 20° P.A.	24
PITCH DIAMETER	2.2083
AGMA QUALITY CLASS	12

* INVERTER POWERED

ELECTRONIC CHARACTERISTICS AT UNIT TEMPERATURE OF +25°C			
INPUT	AMPLITUDE	(VDC)	+28±10
	POWER	(WATTS)	82
	FREQUENCY	(Hz)	400
OUTPUT	AMPLITUDE		NOTE #1
	POWER PER PHASE	(WATTS)	35
	PHASE RELATIONSHIP	(DEG)	90

CONNECTOR CHART			
PIN	FUNCTION	PIN	FUNCTION
1	N/C	9	DC POWER RTN
2	N/C	10	+DC POWER INPUT
3	DOR SELECT (NOTE2)	12	MOTOR (RED)
4	POWER DISABLE (NOTE3)	13	MOTOR (BLK)
5	LOGIC HIGH SOURCE	14	MOTOR (YEL)
8	CASE GROUND	15	MOTOR (WHT)

FOR CUSTOMER USE ONLY

PROPOSAL NO: R-8870
(FOR IDENTIFICATION ONLY)

NOTES:

8 - CHARACTERISTICS SHOWN ARE WITH ONE MOTOR BRAKE FULLY ENERGIZED AND ONE FULLY DE-ENERGIZED.
7 - PINS 2 AND 9 MUST BE TIED TOGETHER EXTERNALLY.
6 - PINS 5,12,13,14, AND 15, MUST NOT BE GROUNDED.
5 - UNIT TO BE HEAT SUNK. (X) SURFACE NOT TO EXCEED +100°C.
4 - MATING CONNECTOR IS CANNON DAHM-15S. (SUPPLIED BY CUSTOMER)
3 - OUTPUT IS DISABLE WITH LOGIC HIGH ON PIN 4. FOR NORMAL OPERATION TIE PIN 4 TO PIN 9.
2 - D.O.R. IS SELECTABLE ON PIN 3. LOGIC HIGH=CW, LOGIC LOW=CCW.
1 - DEPENDENT UPON SUPPLY VOLTAGE, MATCHED TO MOTOR FOR OPTIMUM PERFORMANCE. (SQUAREWAVE)

ISSUE		CUST. GIXID YEAR	DESCRIPTION	ACCT. NO.	PROD. CODE	PART NO.
		SPEC.	**FLIGHT CONTROL ACTUATOR**	01R	227	
		I.D.				
		(2)6-E-35-35-C/118K		APPROVALS		
		28V/11 DIP (2)11-22.4DF)	MPC PRODUCTS CORPORATION			
		(2)1.0RT D-1	CHICAGO, ILLINOIS U.S.A			

Fiber optics would also require unwarranted additional development. Proof of flight concept, not the development of new technology FBW systems, is the intent of the FRV.

The baseline concept is to use analog and discrete signals to the rotor modules and auxiliary thrusters for simplicity and cost. A block diagram of the interconnection system is shown in Figure 6-7.

c. Fly-By-Wire Power Supplies

The power supply concept is shown in Figure 6-8. The prime power comes from a 28 vdc 150 amp generator, standard equipment on each helicopter. This is adequate to supply all the electrical systems. The largest power requirement is for the four ballonet blowers. Twenty amps each is required because ram air is not easily accessible with the remote location of the rotor modules.

Figure 6-8 shows that Power System No. 1 supplies Flight Control System Channel 1 and Power System No. 2 supplies Flight Control System No. 2. Each power system is dual redundant supplied by two isolated DC generators and dual 400 Hz inverters.
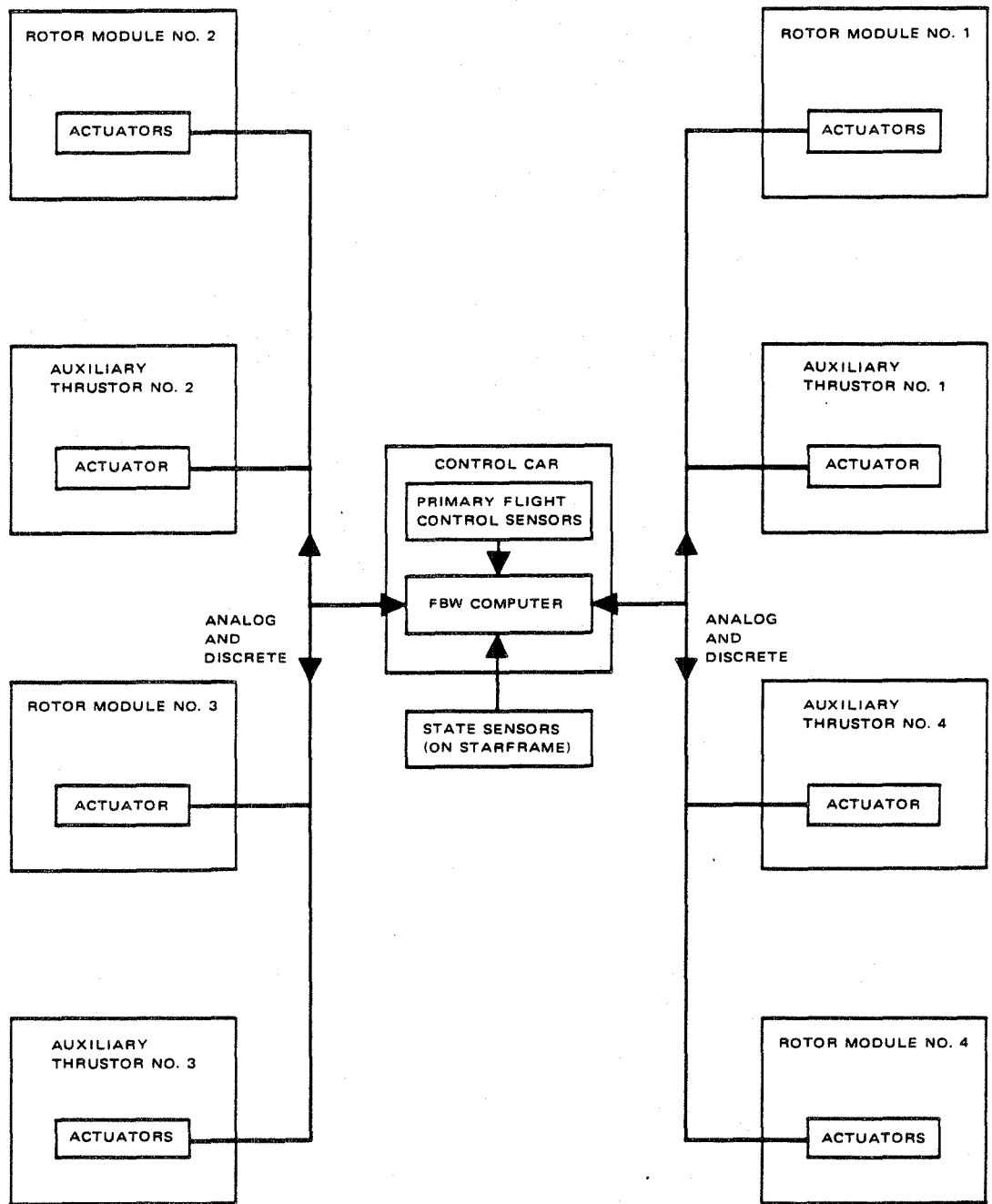
Figure 6-7 - Fly-by-Wire Interconnection System
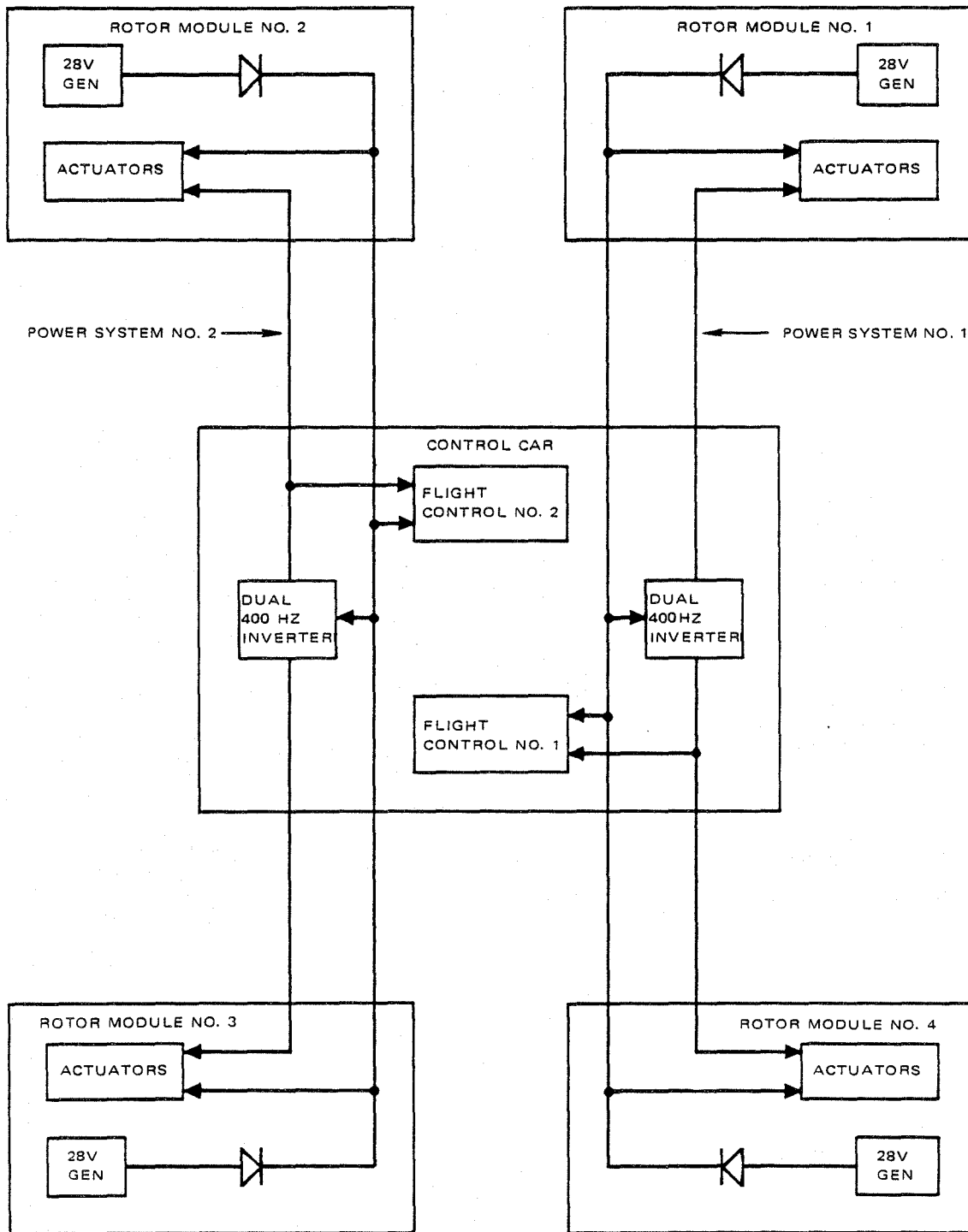
Figure 6-8 - Dual Redundant Power System

SECTION VII - PERFORMANCE CHARACTERISTICS

1. GENERAL

The performance characteristics of the vehicle in typical flight conditions corresponding to hover, climb, and forward flight have been estimated in terms of its helicopter and airship components. The performance data pertinent to the OH-6A helicopter in this vehicle configuration were obtained from the manufacturer, while that related to the airship components were generated by Goodyear Aerospace. The following describes the methods used and results obtained.

2. HOVER PERFORMANCE

a. Hover Ceiling

To predict ceiling altitudes for hover out of ground effect (HOGE) as a function of ambient temperature, the corresponding rotor thrust available from the four OH-6A helicopters (Figure 7-1) as well as the static lift available from the airship envelope (Figure 7-2) was calculated.

The total contribution from the four helicopters, including individual helicopter thrust data for various altitudes and ambient temperature conditions, was calculated by the helicopter manufacturer. The static lift of the airship envelope was calculated by Goodyear Aerospace by the following method:

Sample calculation:

static lift at 2000 ft pressure altitude
= (stretched volume of envelope) (unit lift of helium) (envelope inflation for 2000 ft   pressure height)
where,

$$\text{envelope inflation for 2000 pressure height} = \frac{\text{weight of air at 2000 ft}}{\text{weight of air at sea level}}$$

consequently,
static lift at 2000 ft = (205270 ft^3) (0.0635 lb/ft^3) (0.943) = 12292 lb.

This lift is corrected for temperature effects based on absolute temperature ratio with standard sea level conditions. For instance, static lift at 2000 ft at 80 degrees F is given by

$$(12,292) \frac{(59 + 459.4)}{(80 + 459.4)} = 11,813 \text{ lb.}$$

Similar calculations were made for other temperature and altitude conditions, shown in Figure 7-2. These results were combined to determine the maximum permissible gross weight of the vehicle during hover at a given altitude and ambient temperature.

Figure 7-3 shows hover ceiling in a case where the helicopters were assumed to be operating at maximum take-off power, while Figure 7-4 shows similar data corresponding to operation at maximum continuous power.
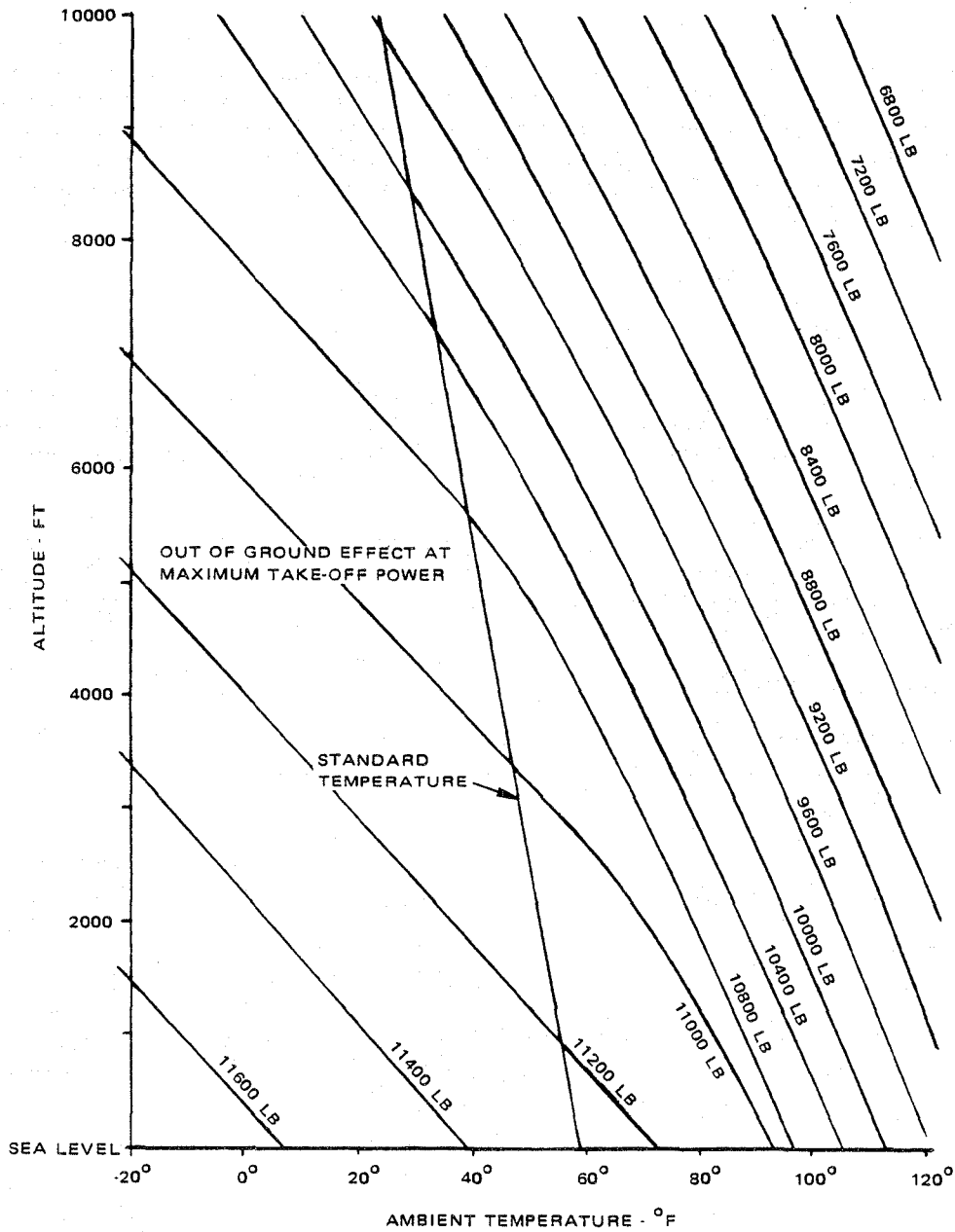
Figure 7-1 – Effect of Altitude and Ambient Temperature On Total Helicopter Thrust

7-2
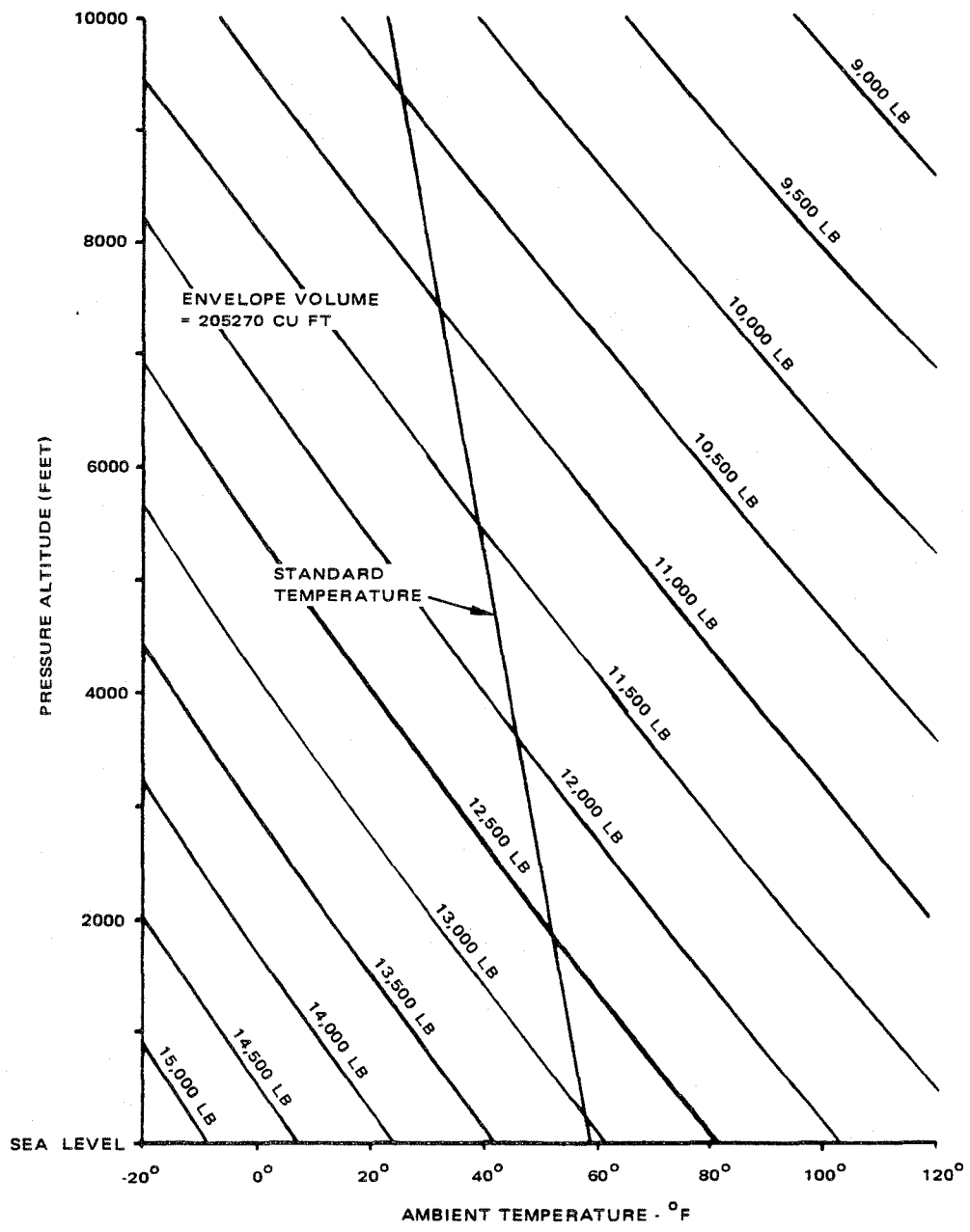
Figure 7-2 – Altitude and Ambient Temperature Effects on Airship Envelope Static Lift
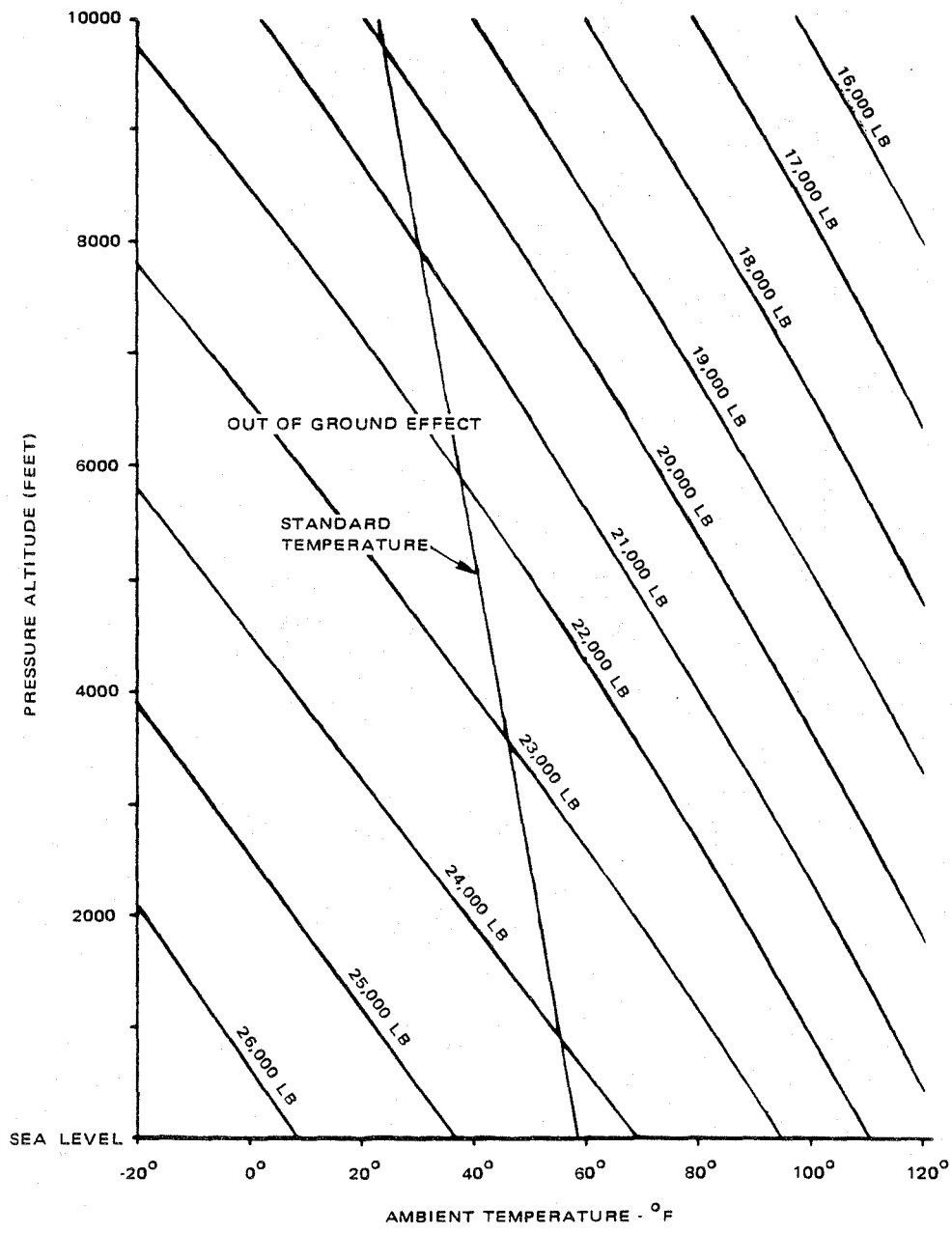
Figure 7-3 - Hover Ceiling at Maximum Take-Off Power Vs Ambient Temperature
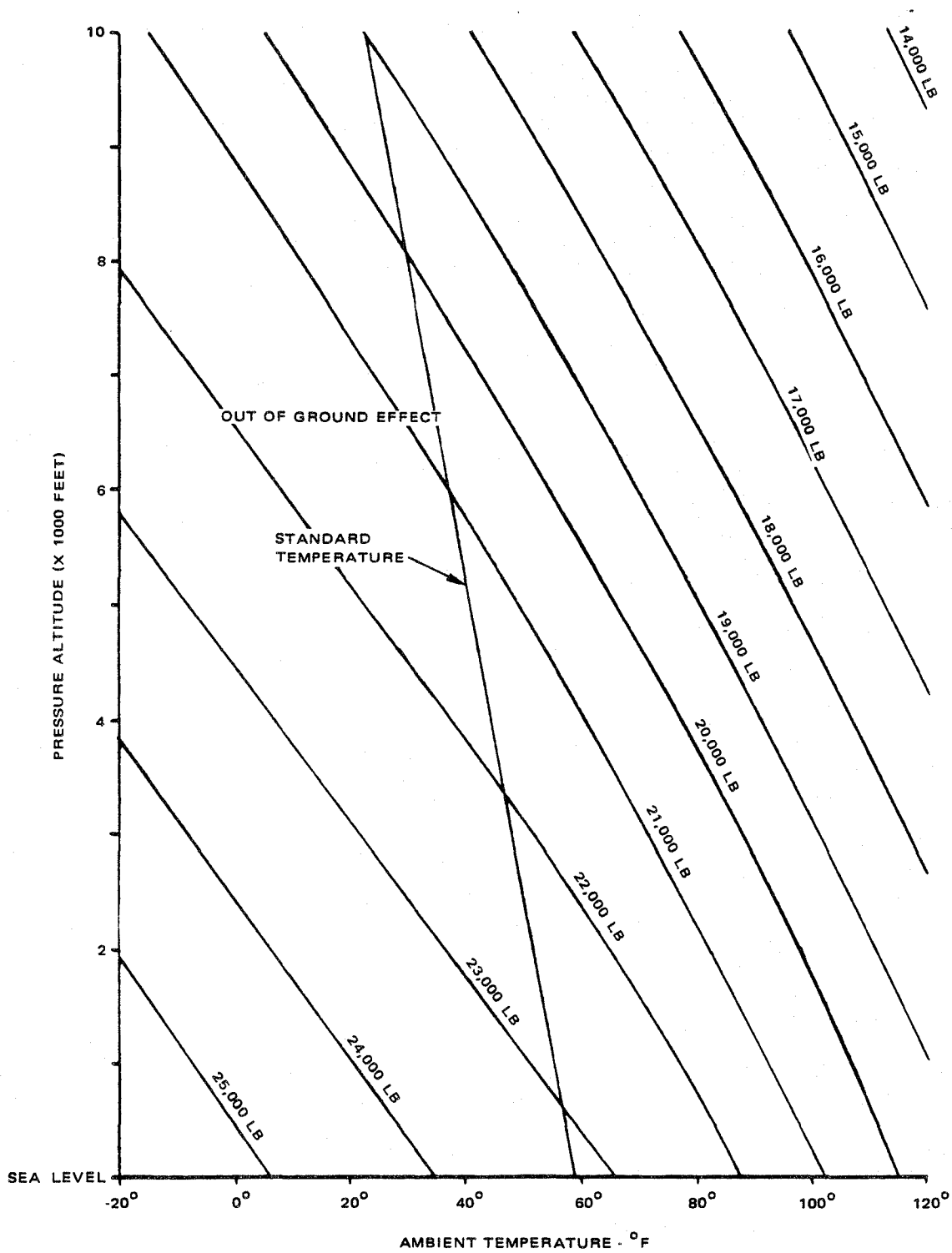
Figure 7-4 – Hover Ceiling at Maximum Continuous Power Vs Ambient Temperature

Hover ceiling with one engine out, or in this vehicle, one helicopter unit out, is shown in Figure 7-5.

Note that in hovering at maximum take-off power, the gross weights shown in Figure 7-3 correspond to the maximum gross lift that can be generated. Consequently, no allowance has been made here for thrust required for maneuvers from hover at these gross weight conditions.

Hover ceiling in ground effect is perhaps not significant to this aircraaft, since the helicopter rotors are located nearly out of ground effect.

b. Power Requirements

The power requirements for hovering were obtained by considering the power requirements of ecah of the helicopters for a specified operating condition, as shown in Figure 7-6.

The maximum permissible gross weights for both the maximum take-off and maximum continuous power limits is a standard day operation are shown. Note that the power available to the helicopter is transmission-limited. The T63 engine on the OH-6A is derated from 317 shaft horsepower to 236 shp (maximum continuous) when installed. Consequently, the engine is capable of delivering 236 shp at 5000-feet density altitude.

c. Hover Endurance

The eight engines in the proposed vehicle configuration could consume significant amounts of fuel in a relatively short time in comparison to other aircraft. Consequently, hover endurance is important for operational consideration.

For a given payload the hover endurance has been calculated by considering the corresponding power required (see Figures 7-6 and 7-7) and the associated fuel consumption rate (Figure 7-8). Typically, the power requirements of the aircraft in hover are calculated by combining the power requirements of the individual helicopters, at a given operating condition.

A similar approach is used to calculate the power requirements in forward flight as explained subsequently (see section on Forward Flight Power Requirements). In all cases, maximum available fuel is fixed at 3200 pounds with a 10 percent allowance for warmup, taxi, take-off, and climb and a 10 percent reserve at the end of flight. Consequently, usable fuel per flight is assumed to be 2560 pounds.

Typically, as the fuel is consumed, the weight of the vehicle decreases causing a drop in required power, hence, fuel consumption is less.

Thus a piece-wise, decremental approach is taken in accounting for the effect of decreasing fuel weight on vehicle hover endurance.

The endurance resulting from burning the first 500 pounds of fuel is calculated in one step by using constant values of power required and resulting fuel flow rates corresponding to the initial gross weight of the vehicle. Subsequently, the gross weight is decremented by 500 pounds for the next step.

For example, consider the vehicle with a full payload and fuel corresponding to maximum gross weight of 23,435 pounds (Figure 7-7). Since 10 percent of the available fuel is consumed

7-6
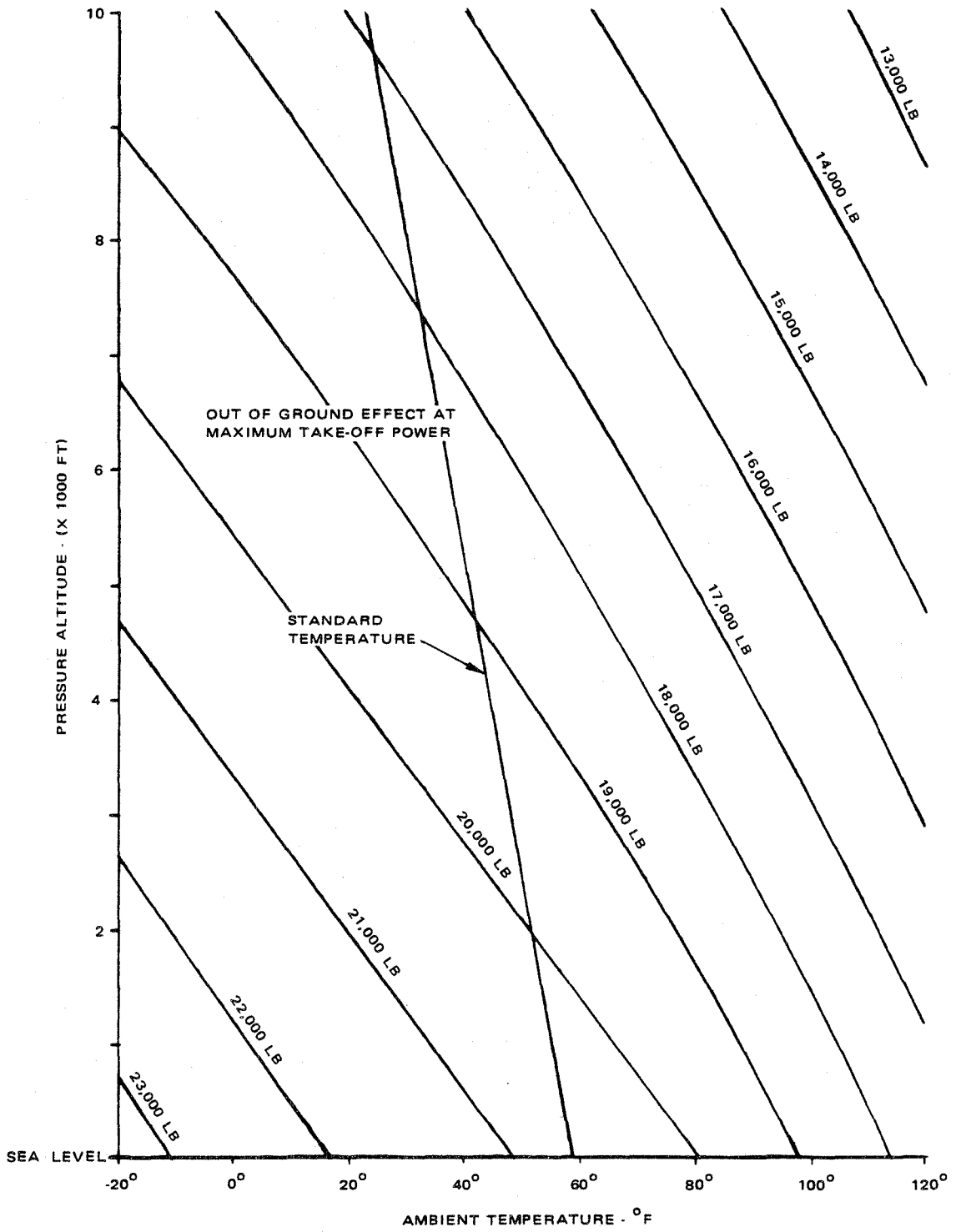
Figure 7-5 - Hover Ceiling With One Helicopter Power Out Vs Ambient Temperature
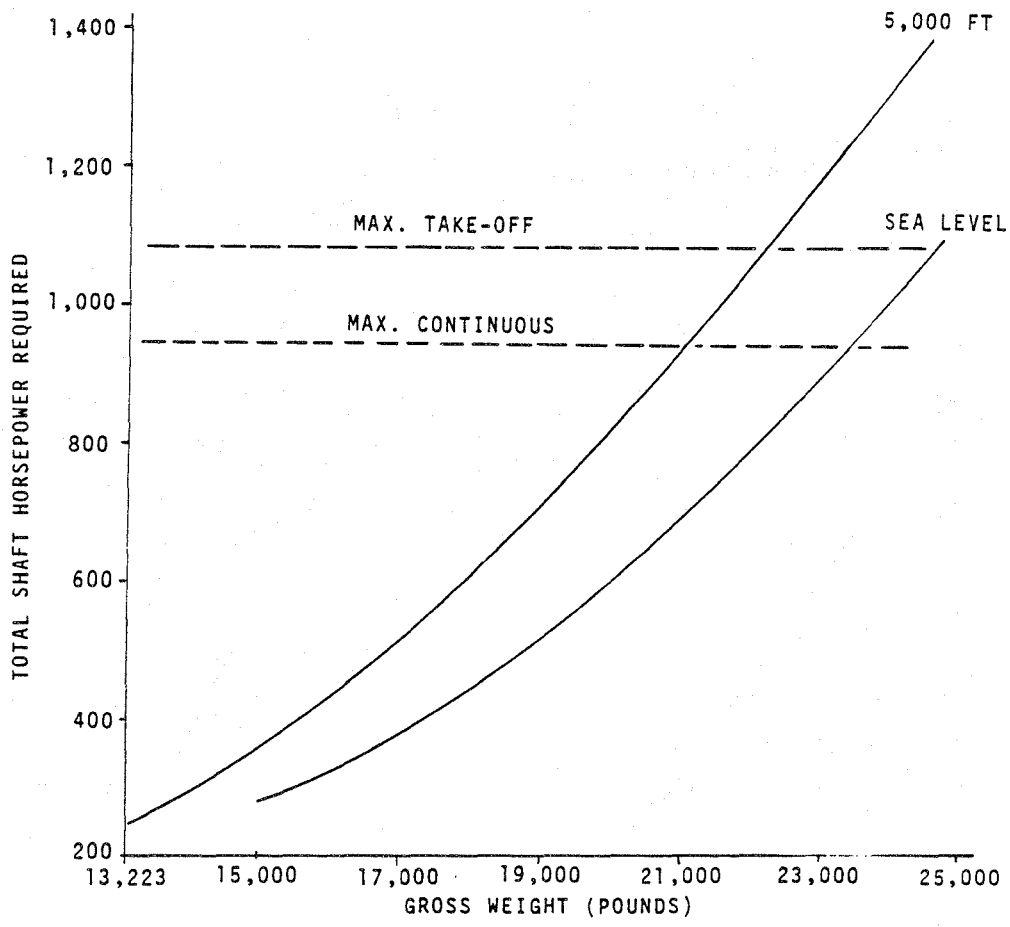
Figure 7-6 – Shaft Horsepower Required for Hover Vs Gross Weight at
Sea Level and 5000-Foot Density Altitude
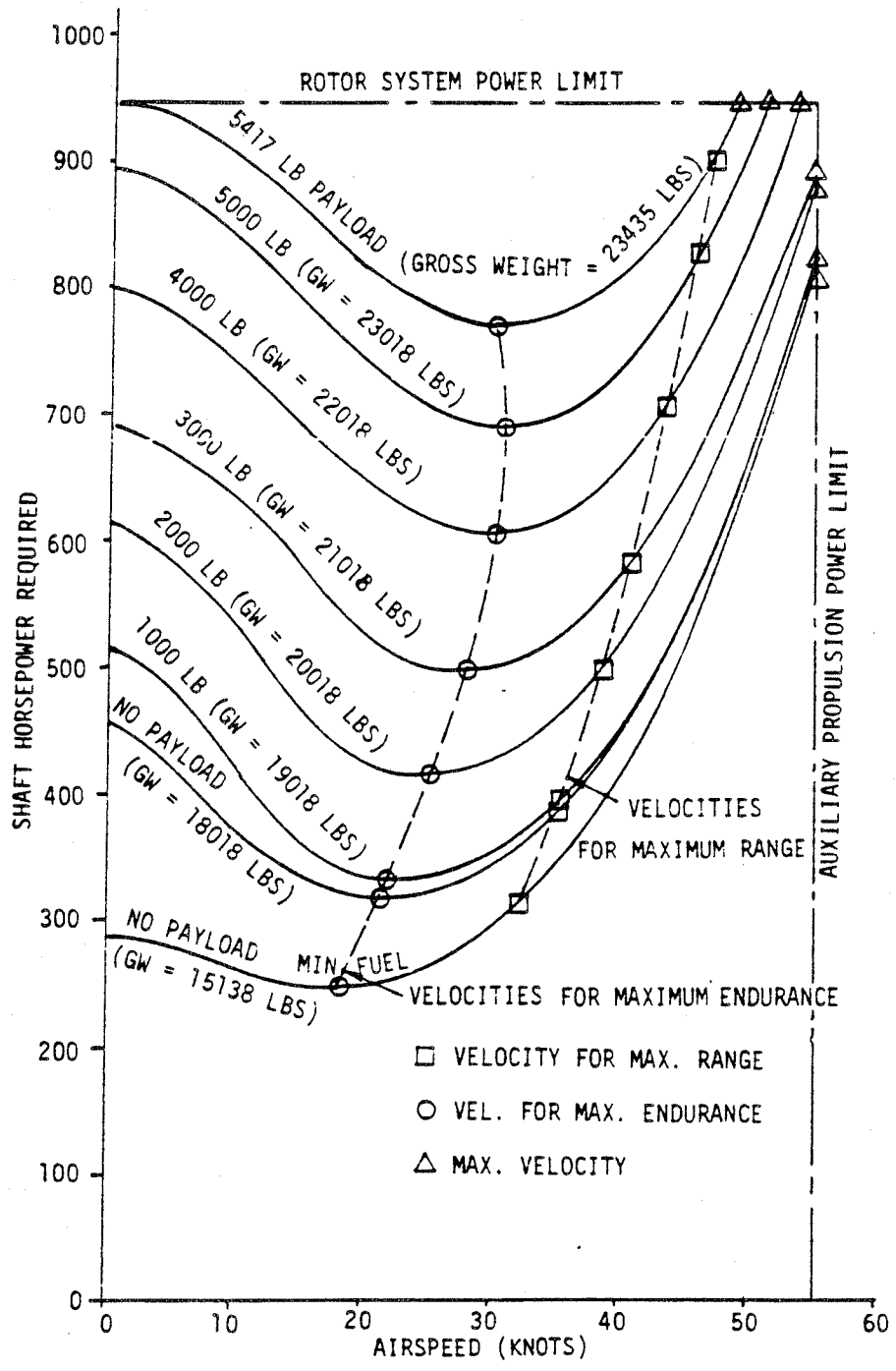
Figure 7-7 – Vehicle Power Requirements in Forward Flights for
Various Gross Weights at Sea Level
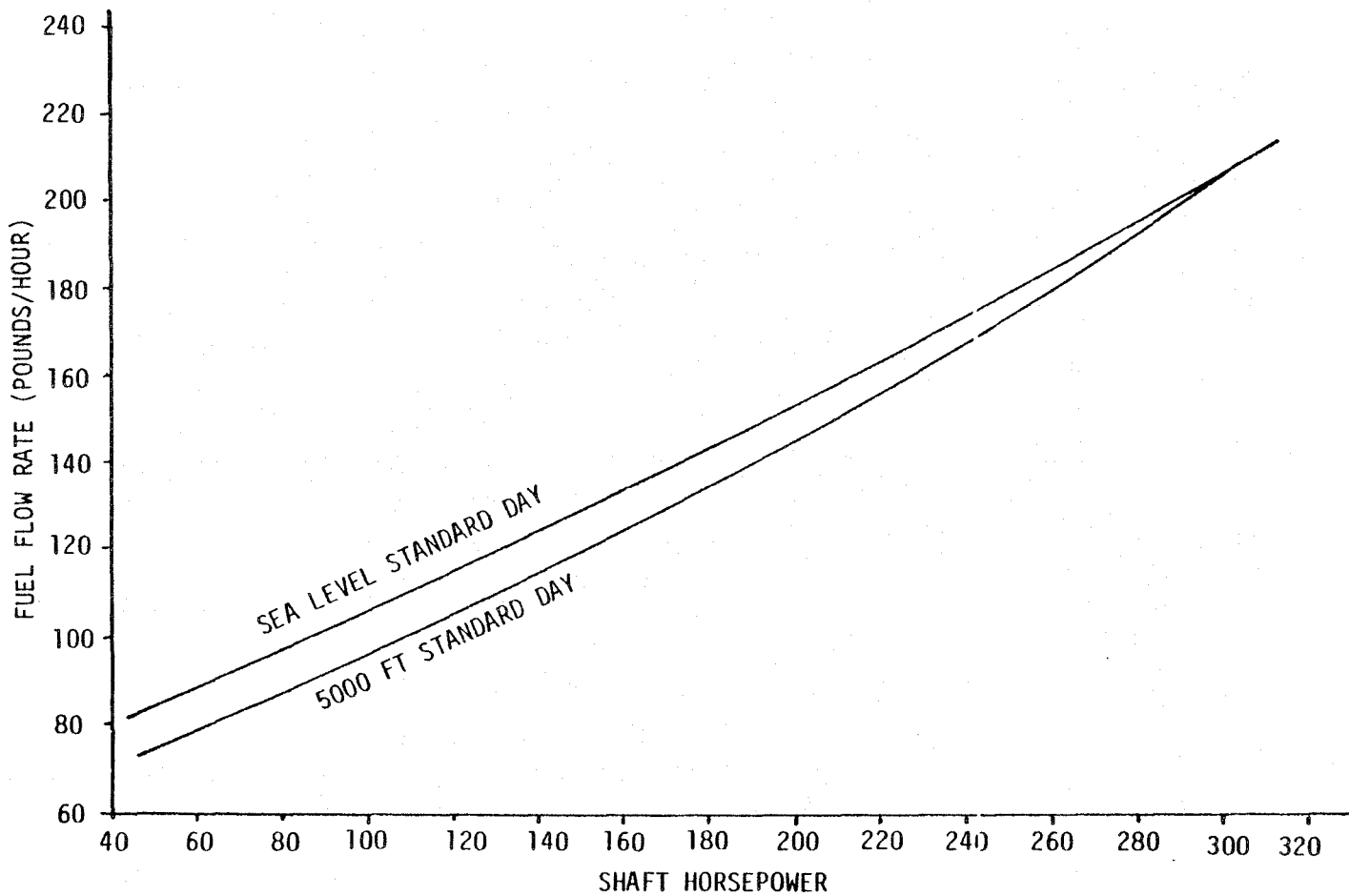
prior to hover the vehicle begins to hover at a gross weight of 23,115 pounds. As the fuel is consumed the vehicle would in effect progress down the locus of zero velocity points for various gross weight conditions.

For this example, the power curve for a gross weight of 23,435 pounds corresponds to the "5417 pound payload" curve. Since 10 percent of the fuel is considered consumed prior to beginning hover, the weight of the vehicle at the start of hover is 320 pounds less than that represented by the 5417 pound curve. Interpolating between the 5417 pound and 5000 pound curves gives an initial required hover power of 908 shp.

This 908 shp is shared by the four rotor systems. Each engine must therefore provide:

$$\frac{908 \text{ shp}}{4 \text{ engines}} = 227 \text{ shp/engine}$$

Figure 7-8 shows the fuel flow requirements per shaft horsepower for the T63 engine. At sea level, to develop 227 shp, each engine's fuel flow rate (w) must equal 166 lbm/hr. It is also assumed that in the hover condition, the four auxiliary propulsion units (APU) are running at idle. At sea level, w_{idle} = 60 lbm/hr for each engine. Therefore, the four APU's consume 4 (60 lbm/hr) = 240 lbm/hr.

This fuel rate is considered constant throughout the flight.

Fuel consumption for the total system then becomes: 4 (166 lbm/hr) + 240 lbm/hr = 904 lbm/hr. Assuming 97 pounds of fuel are burned at this rate, the time required to consume the fuel is:

$$\frac{97 \text{ lbm}}{904 \text{ lbm/hr}} = 0.107 \text{ hr}$$

At the end of this time increment, the vehicle is 97 pounds lighter. For the next iteration, the shaft horsepower required should be taken from the zero velocity line of Figure 7-7 at a point 97 pounds lighter than the previous point. This iterative procedure is continued until 2560 pounds of fuel have been consumed.

For ease of interpolation, the fuel was incremented in 500 pound steps except for the first and last increments. Calculations for this hover performance flight are listed in table 7-1.

Using this approach the total endurance of the vehicle with various payloads is calculated both at sea level and 5000-foot density altitude (Figure 7-9).

It can be observed that the endurance in the case of 2000 pound payload is not sensitive to altitude change. Typically, with an increase in altitude the power required increases and the static lift decreases, both conditions that lead to lower endurance. However, as the engines operate more efficiently, less fuel is demanded and this yields higher endurance. Apparently, for a larger payload the latter effect dominates.
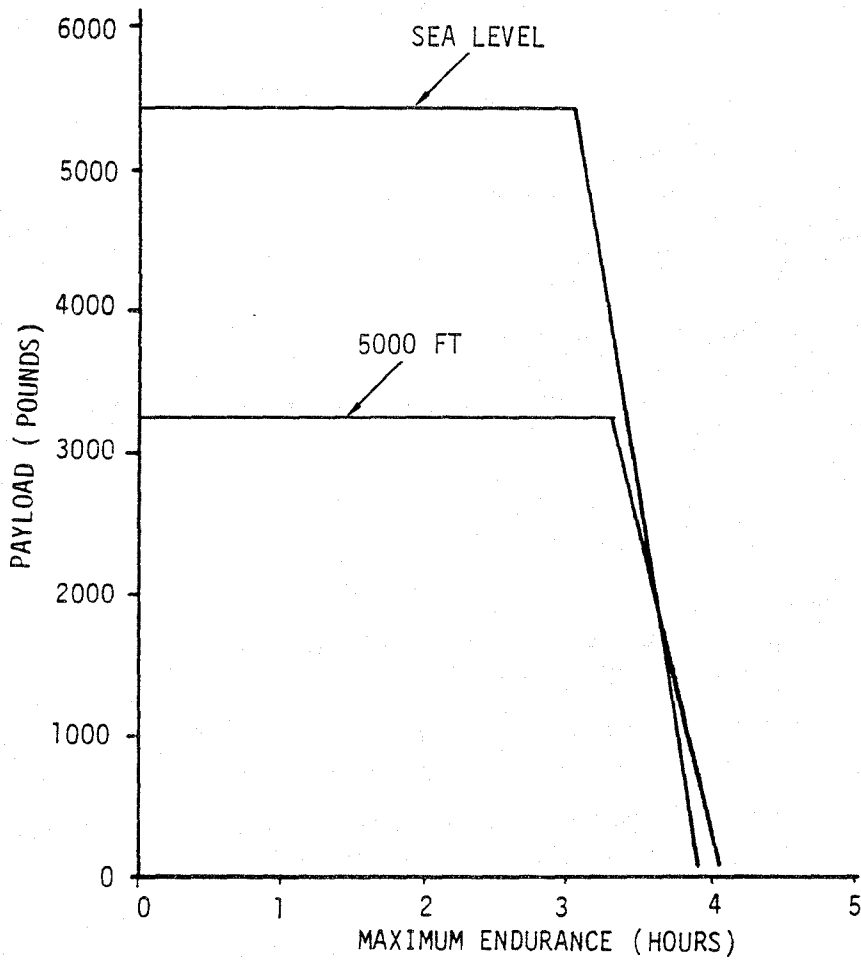
Figure 7-9 – Payload Effect on Hover Endurance at Sea Level
and 5000-Foot Density Altitude

TABLE 7-1 – SAMPLE CALCULATION OF HOVER ENDURANCE FOR FLIGHT RESEARCH VEHICLE

Density Altitude: sea level								Fuel capacity: 3200 pounds	
Payload (lbm)	Gross vehicle wt (lbm)	Fuel wt (lbm)	Total SHP reqd	SHP reqd each rotor	$\dot{\omega}$ each rotor (#/hr)	$\dot{\omega}$ Rotor system (#/hr)	$\dot{\omega}$ Rotor +$\dot{\omega}$ APU** (#/hr)	Δ Fuel (lbm)	Time to burn Δ fuel (hr)
5417	23115	2880*	980	227	166	664	904	97	0.107
5417	23018	2783	895	224	165	660	900	500	0.556
5417	22518	2283	850	213	159	636	876	500	0.571
5417	22018	1783	800	200	152	608	848	500	0.590
5417	21518	1283	745	186	145	580	820	500	0.610
5417	21055	783	690	173	139	556	796	463	0.582
5417	20592	320							
							Totals:	2560 lb	3.01 hr

* 320 pound assumed consumed prior to start of hover.
** Four APU at idle consume 240 lb/hr; constant for flight.

3. CLIMB AND FORWARD FLIGHT PERFORMANCE

a. Vertical Rate of Climb

The ability of the vehicle to climb vertically has been determined by considering the corresponding performance of the individual OH-6A helicopters and the airship component.

It was assumed that each of the helicopters would overcome 25 percent of the parasite drag of the airship envelope and support structure in vertical climb. The corresponding power requirements of each helicopter for nominal climb rates of 500 feet per minute and 1000 feet per minute were calculated and used to determine the overall vehicle power requirements.

Figure 7-10 shows the corresponding power requirements for nominal climb rates of 500 fpm and 1000 fpm at sea level while Figure 7-11 shows similar data at 5000-foot density altitude.

b. Forward Flight Power Requirements

To predict the maximum speed, maximum range and endurance of the vehicle, it is necessary to determine the power required to cruise at various airspeeds and gross weight conditions. This is done by calculating the power required to drive the airship envelope and support structure at various airspeeds (Figure 7-12).
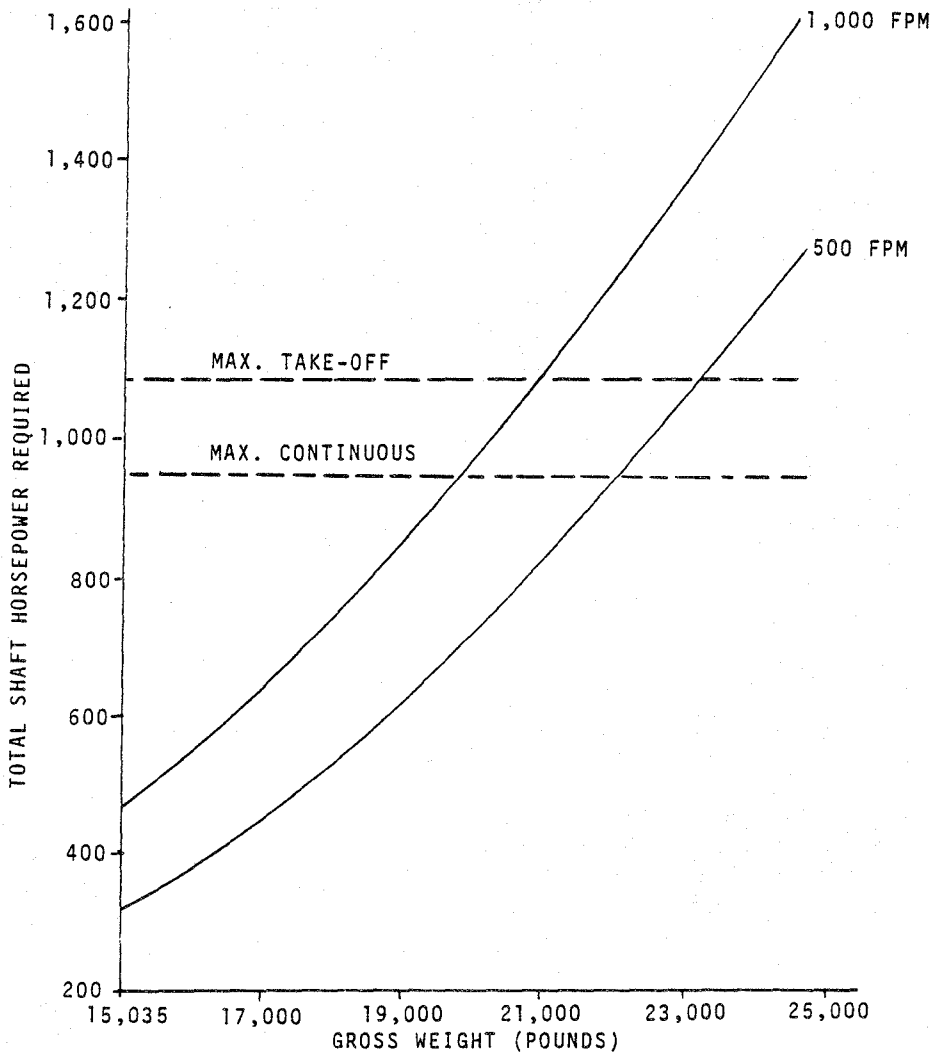
Figure 7-10 - Typical Gross Weight Effect on Climb Power Requirements at Sea Level
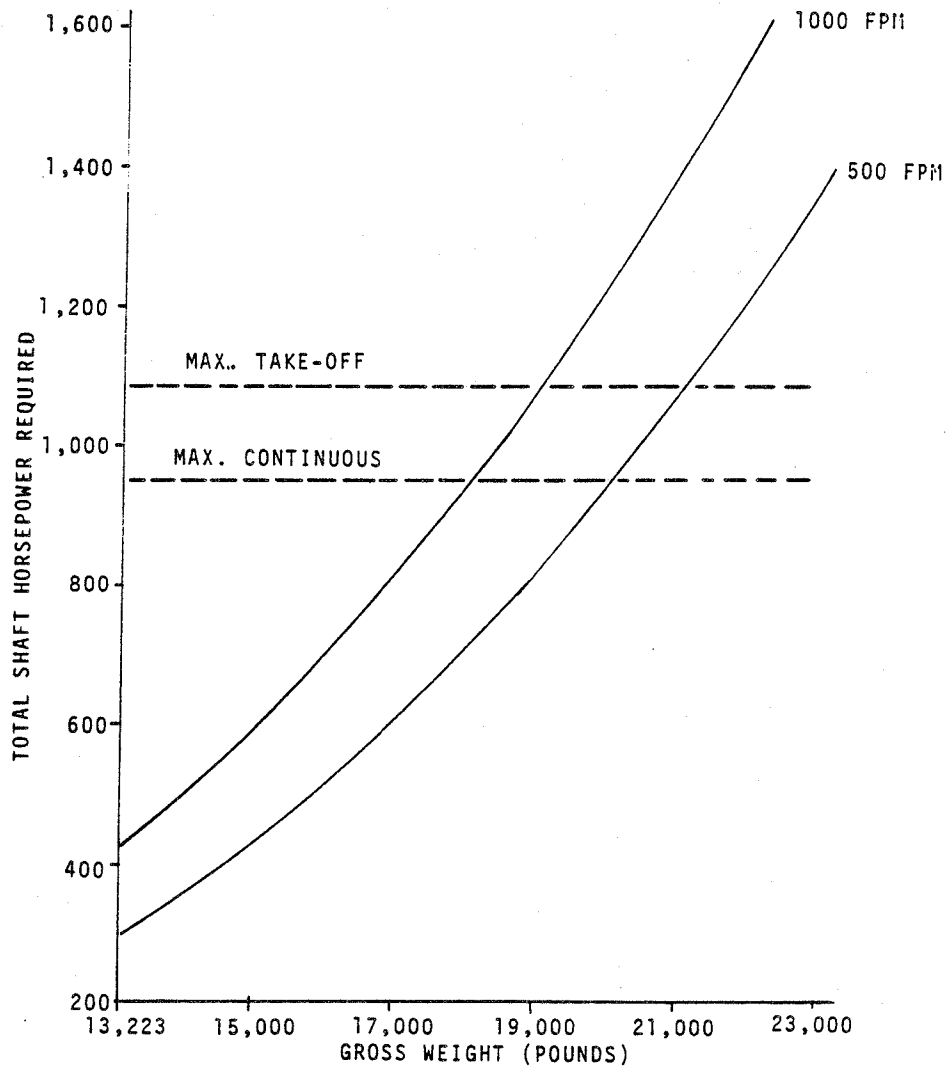
Figure 7-11 – Gross Weight Effect on Climb Power Requirements at
5000-Foot Density Altitude
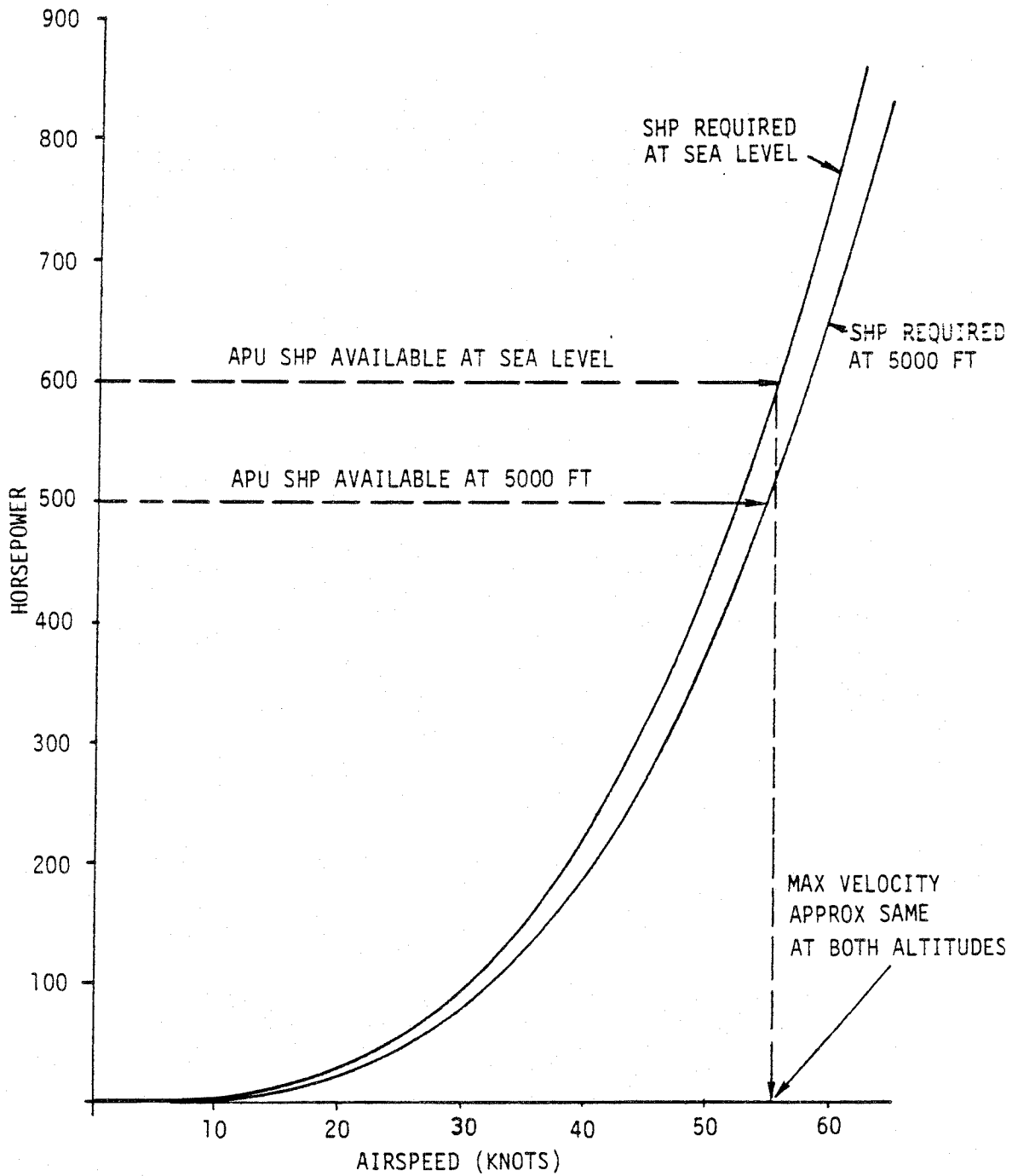
Figure 7-12 - Forward Flight Power Requirements for
Airship Envelope and Support Frame

Similarly, the power required to drive the individual helicopters at various airspeeds, while operating at various thrust conditions (Figures 7-13 and 7-14), has also been calculated.

It has been assumed for simplicity that in cruise mode the power required by each helicopter is limited to its own induced profile and parasite power losses. The power plants with the longitudinal auxiliary thrusters have been selected such that they provide the necessary power to overcome the envelope and support frame drag at all airspeeds.

Based on these factors, the results of the above calculations were combined to determine the overall power requirements of the vehicle at various airspeeds and gross weight conditions. Figure 7-7 shows the power requirements of the vehicle at sea level on a standard day. Figure 7-15 shows similar data at 5000-foot density altitude.

The power limitations of the rotor systems and the auxiliary thruster power plants are also indicated in these figures. It can be observed that the power requirement characteristics of the FRV at various gross weights are similar to that of a conventional helicopter.

c. Maximum Speed

For a conventional aircraft the maximum speed in cruise mode is typically given by the airspeed at which power available is equal to power required for the same operational condition. However, with the FRV configuration, there are two power sources available. The constraint is the power limit on the auxiliary propellers since they are assumed to be the source for overcoming envelope drag.

It is assumed that the AH-1T tail rotor acts as a constant speed propeller which will allow the APU to develop its rated horsepower at all forward speeds. Since an untwisted helicopter tail rotor will undoubtedly operate less efficiently with increasing forward speed, the validity of this assumption would be assessed in a more rigorous investigation.

It should also be noted that performance predictions contained herein are premised only on aerodynamic considerations. Predicted speeds and loads may not be achievable due to structural limitations such as the one identified in Section V. A more detailed analysis would be required to collectively consider all factors affecting the FRV's performance (e.g., aerodynamic structural, environmental, operational).

Assuming a nominal efficiency of 90 percent for the auxiliary propulsion system, the maximum speed for this vehicle should be 50 knots or better, depending on the power available from the helicopter power plants to overcome envelope drag.

Note that the power available from the longitudinal auxiliary propulsion units is decreased by 50 shp at 5000 feet. The power required to overcome the envelope-frame drag at 5000 feet is also reduced by 14 percent. Therefore, there is no significant change in the maximum speed at the higher altitude (Figure 7-12).

d. Payload versus Maximum Range

In Figure 7-7 each curve represents the power required by the vehicle to carry the indicated payload with a full tank of fuel. For a particular value of gross weight corresponding to a specified payload, the speed for maximum range is given by a line drawn through the origin and tangent to the power-speed curve as shown.

ROTOR SPEED = 470 RPM

N_2 = 100%

HORIZONTAL PARASITE DRAG AREA = 6 FT^2

NO TAIL ROTOR LOSSES

DENSITY ALTITUDE = SEA LEVEL
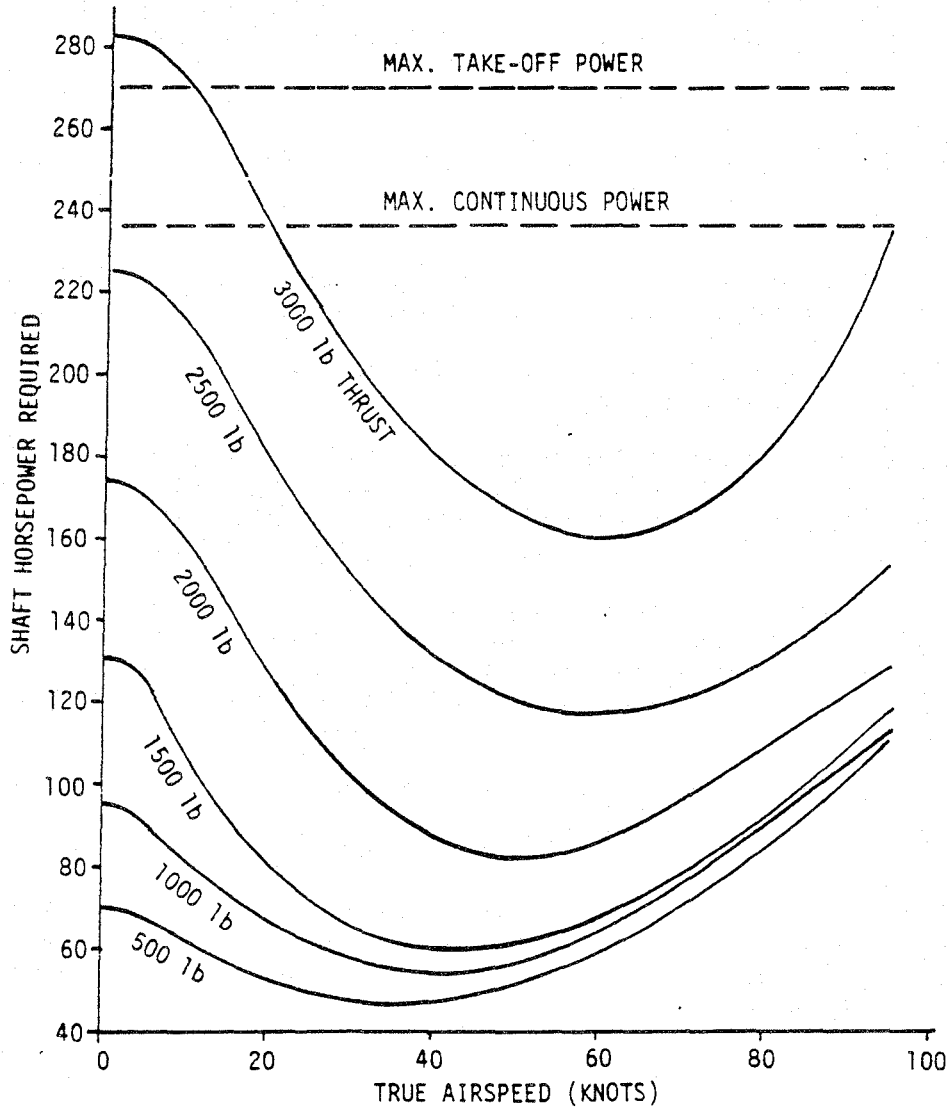
Figure 7-13 - Typical Forward Flight Power Requirements for
OH-6A Helicopter at Sea Level

ROTOR SPEED = 470 RPM

N_2 = 100%

HORIZONTAL PARASITE DRAG AREA = 6 FT^2

NO TAIL ROTOR LOSSES

DENSITY ALTITUDE = 5000 FT
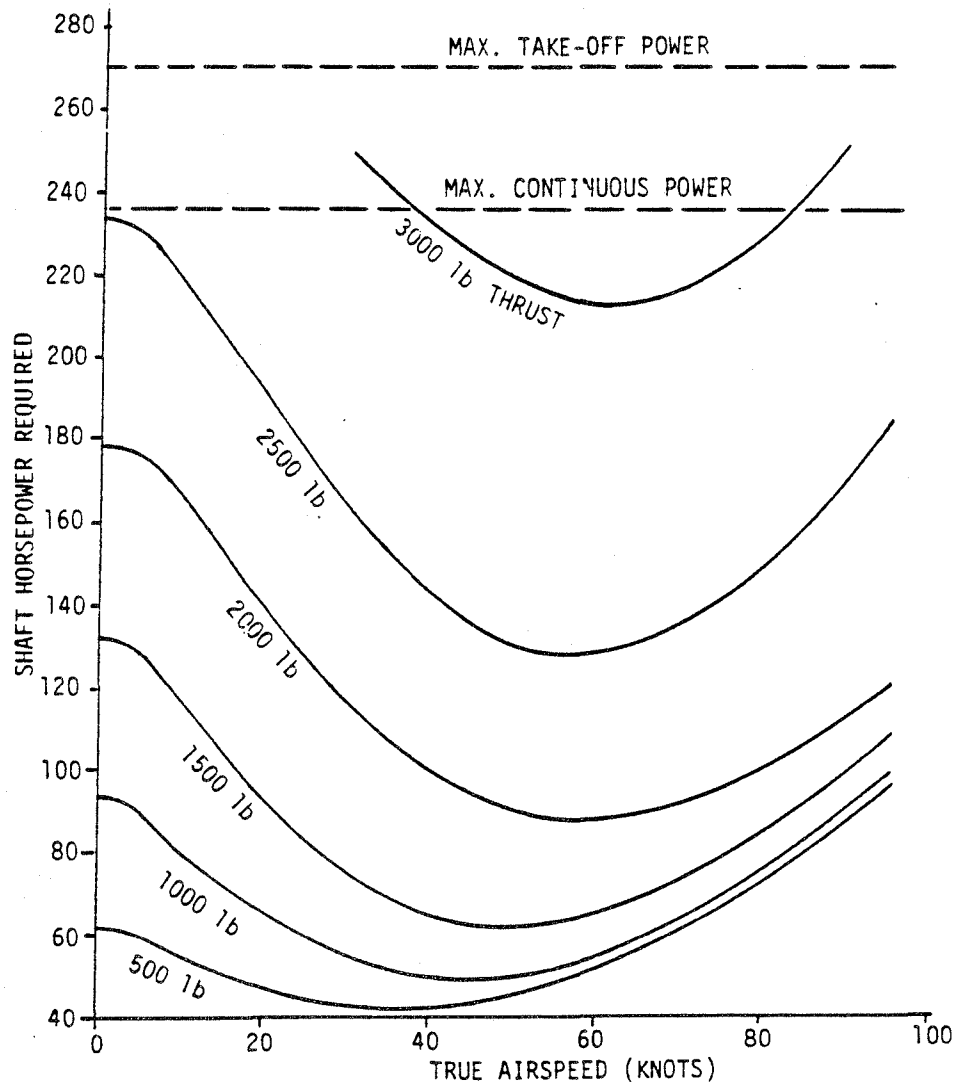
Figure 7-14 – Typical Forward Flight Power Requirements for
OH-6A Helicopter at 5000-Foot Density Altitude
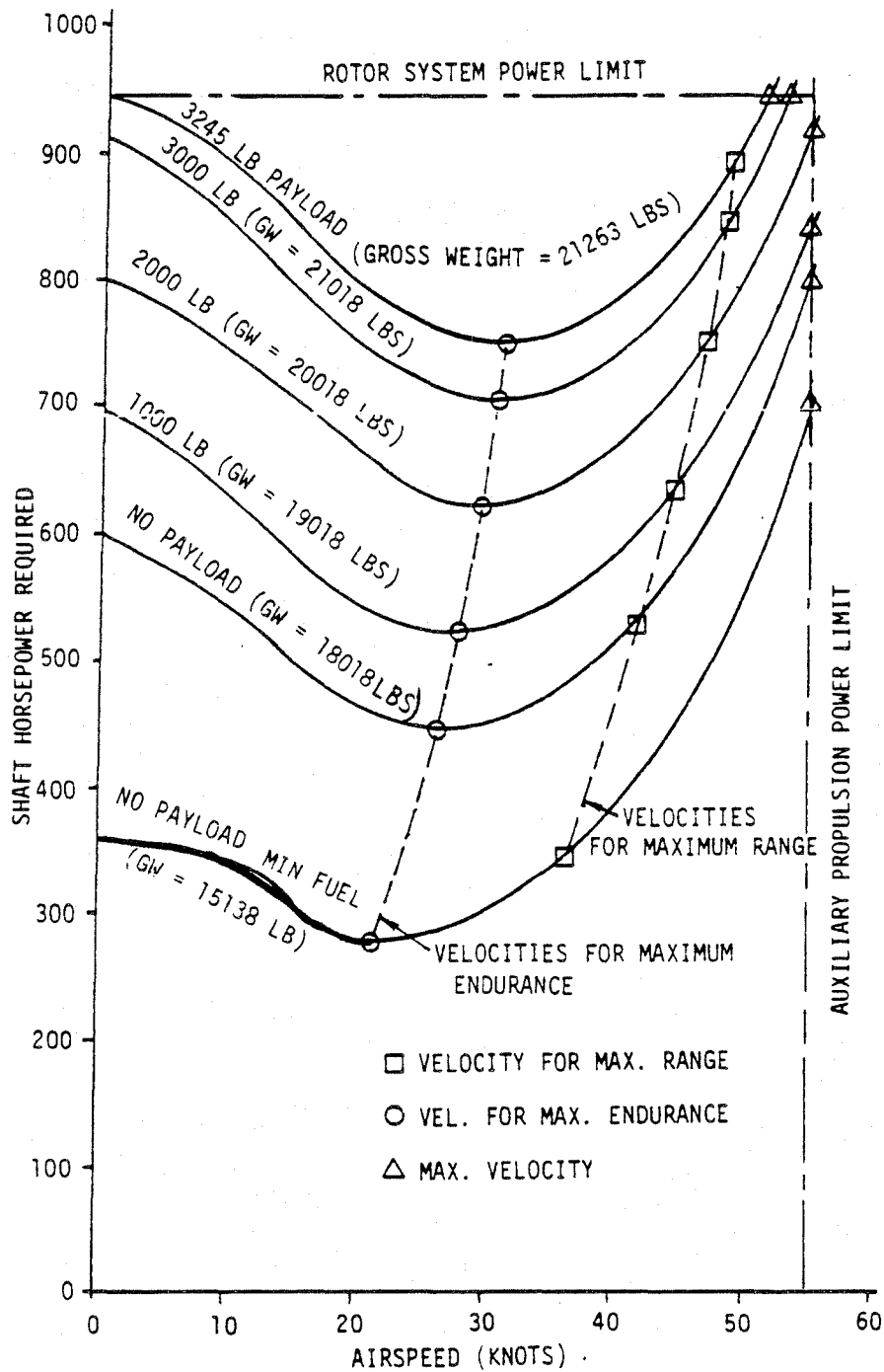
Figure 7-15 – Vehicle Power Requirements in Forward Flight for
Various Gross Weights at 5000-Foot Density Altitude

Typically, a maximum range flight profile of the FRV at sea level consists of initially cruising at the speed for maximum range corresponding to payload. As the fuel is consumed, the weight of the vehicle decreases and its power requirements are lowered. In effect, this requires flying at a lower speed for maximum range, as the vehicle progresses down the locus of maximum range velocity (see Figure 7-7) until all fuel is consumed.

As an example, consider a maximum range flight of the FRV at sea level, carrying the maximum payload of 5417 pounds (see Table 7-2).

Since 10 percent of the fuel is considered consumed prior to beginning cruise, the weight of the vehicle at the start of cruise is 320 pounds less than that represented by the 5417 pound payload curve in Figure 7-7. Interpolating between the 5417 pound and 5000 pound curves of Figure 7-7 gives an initial maximum range velocity of 46 knots at a required power of 840 shaft horsepower.

It is also assumed that in cruise, the two laterally directed APU's are shut down. The 840 shp is then shared by six engines. Thus, each engine supplies 140 shaft horsepower.

Figure 7-8 shows the fuel flow requirements per shaft horsepower for the T63 engine. Note that equal power output assumed from each engine does not influence the fuel flow calculation, since the fuel flow variation rate with shp is linear.

At sea level, to develop 140 shp, each engine's fuel flow rate (w) must equal 124 lbm/hr. The total system w is then:

$$6 \text{ engines } (124 \text{ lbm/hr/engine}) = 744 \text{ lbm/hr.}$$

TABLE 7-2 – FLIGHT RESEARCH VEHICLE WEIGHT AND LIFT DATA

Item	At sea level (lbs)	At 5000 feet (lbs)
Empty weight plus fuel and oil	18,018	18,018
Fuel	3,200	3,200
Static lift	13,035	11,223
Net buoyancy	-4983	-6795
Helicopter lift available	10,400	10,040
Payload available	5,417	3,245
(Helicopter lift and net buoyancy)		
Gross weight	23,435	21,263

Assuming 597 pounds of fuel are burnt at this rate, the time required to consume this fuel is:

$$\frac{597 \text{ lbm}}{744 \text{ lbm/hr}} = .802 \text{ hr.}$$

Cruising at a velocity of 46 knots for .802 hr, the vehicle travels:

$$46 \text{ kt } (.802 \text{ hr}) = 36.91 \text{ nautical miles.}$$

At the end of this time increment, the vehicle is 597 pounds lighter.

For the next iteration, the maximum range velocity should be selected from a point on the maximum range velocity curve 597 pounds lower than the previous point. This procedure is continued until 2560 pounds of fuel have been consumed. For ease of interpolation, the fuel was incremented in 500 pound steps except for the first and last increment. Calculations for this flight profile are listed in Table 7-3.

Similar calculations were performed for other gross weight conditions corresponding to various payload conditions. Maximum range in each case was determined both at sea level and at 5000 foot density altitude as shown on Figure 7-16.

It appears that for the flight at sea level there is an optimal payload of 2000 pounds at which best range can be achieved. Apparently, with gross weight decrease the power required by the helicopter rotors decreases along with the maximum range speed. The former effect tends to increase the range while the latter tends to decrease it. For payloads from maximum value to 2000 pounds, the range increment due to the reduced power requirement overrides the decrement because of the slower speed for maximum range. The converse is true for payloads smaller than 2000 pounds.

e. Payload versus Maximum Endurance

In Figures 7-7 and 7-15, speed for maximum endurance of the FRV at various gross weights were identified. For a given payload the maximum endurance was calculated in a manner similar to that used for maximum range calculation. The corresponding results are shown on Figure 7-17. As previously observed in hover endurance, if the payload is approximately 1250 pounds, the vehicle is not found to be sensitive to altitude changes.

TABLE 7-3 - SAMPLE CALCULATION OF MAXIMUM RANGE VS. PAYLOAD

Density Altitude· sea level									Fuel Capacity. 3200 lb.	
Payload (lbm)	Gross veh wt. (lbm)	Fuel wt (lbm)	Velocity (kt)	Total HP required	HP each engine required	ὠ each engine (lb/hr)	ὠ Total (lb/hr)	ΔFuel (lbm)	Time to burn Δ fuel (hr.)	Dist. for Δ fuel (Nm)
5417	23115	2880*	46	840	140	124	744	597	.802	36.91
5417	22518	2283	44.5	770	128	118	708	500	.706	31.43
5417	22018	1783	43.5	710	118	114	684	500	.731	31.80
5417	21518	1283	42	650	108	109	654	500	.765	32.13
5417	21018	783	41	590	98	105	630	463	.735	30.13
5417	20555	320				Totals.		2560	3.74	162.4

* 320 lbm assumed consumed prior to start of cruise.
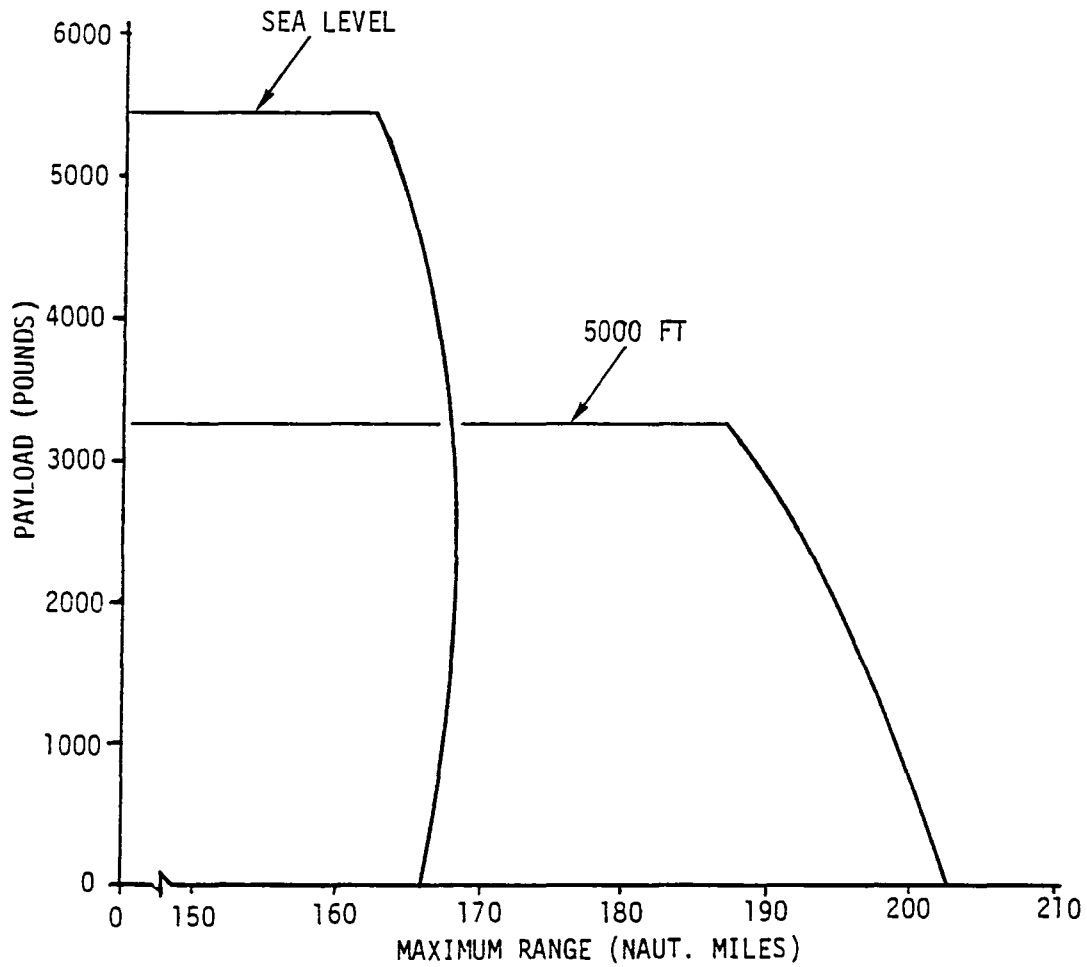
RANGE VS PAYLOAD PERFORMANCE FOR FLIGHT RESEARCH VEHICLE

Figure 7-16 – Payload Vs Maximum Range at Sea Level and 5000-Foot Density Altitude

7-24
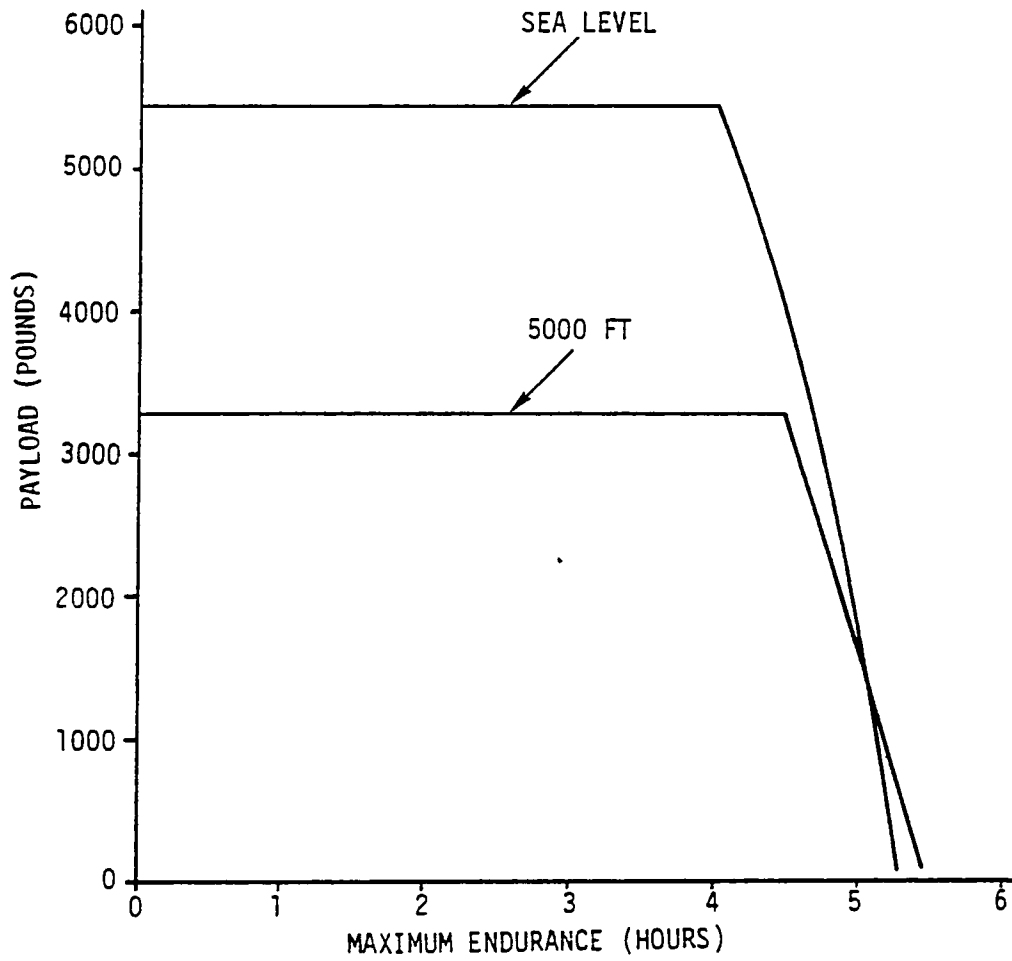
CRUISE ENDURANCE PERFORMANCE VS PAYLOAD

Figure 7-17 - Payload Vs Maximum Endurance at Sea Level
and 5000-Foot Density Altitude

SECTION VIII - STABILITY CHARACTERISTICS

1. GENERAL

The extent of stability and control augmentation desirable for this aircraft depends on the inherent stability characteristics of the vehicle configuration. Stability has been evaluated in typical flight conditions of hover and cruise.

The effects of carrying a sling load on the vehicle dynamics have been predicted by considering a linear, state-variable model of the coupled system. Typical operational conditions that could lead to vehicle instability have been determined by a piloted flight simulation of the aircraft. A description of the analytical model used and the determined stability characteristics of the vehicle are given below.

2. VEHICLE SLING LOAD STATE-VARIABLE MODEL

A linear system model that describes the coupled motion of the vehicle sling load configuration has already been derived by linearizing the corresponding non-linear equations of motion about trim conditions in hover and forward flight (ref. 13).

In this model the hull is assumed to be a buoyant, rigid body from which a payload, modeled here as a point mass, is suspended from an arbitrary point on the vehicle by means of a rigid, nonextensible link. The rotor modules in the configuration are assumed to be rigidly connected to the hard structure and are implicit devices that produce forces and moments on the vehicle for a specified flight path of the HLA and appropriate control inputs.

Translation of the vehicle is described in terms of its velocity components u, v, and w along the x, y, and z axes, respectively, of a body axes system whose origin is located at an arbitrary point, while the rotational motion of the vehicle is described by the angular velocity components p, q, and r about the x, y, and z axes, respectively, of the same reference frame. The orientation of the vehicle is described by the Euler angles φ, θ, and ψ, which locate the body axes reference frame with respect to a local horizon system.

Motion of the payload relative to the vehicle is described in terms of its coordinates x_L, and y_L, which are defined in the reference body axes system of the vehicle. Note that only two independent coordinates are required to describe the payload motion, since it is assumed here that the payload remains at a constant distance equal to the cable length from the suspension point.

These perturbation equations can be rearranged in a state-variable form:

$$\dot{\bar{x}} = \underline{A}\bar{x},$$

where $\bar{x}^T = (uwq\ \theta\ u_p\ x_p\ v\ p\ \varphi\ r\ \psi\ v_p\ y_p)$ is the state vector consisting of perturbations in state-variables and $\underline{A}$ is the system matrix.

Typically, the stability characteristics of the system are determined by examining the eigenvalues of the system matrix. Stability characteristics of the vehicle alone, without a sling load, can also be examined by appropriately partitioning the overall system matrix and using corresponding input data in the evaluation.

To examine the stability of the vehicle with an internal or external payload of 5000 pounds while hovering or cruising, it is necessary to determine the corresponding aerodynamic derivatives of the vehicle. These have been synthesized by combining the aerodynamic derivatives of the quad-helicopter configuration with those of the airship component. (refs. 14 and 15.)

The contribution from the former has been determined by kinematically relating the individual helicopter derivatives to those of the overall vehicle. (refs 16 and 17). In the present case, since the helicopter tail rotors are absent, their contribution to the aerodynamic derivatives of individual helicopters has been omitted. Consequently, as a first approximation, the yaw moment derivatives of individual helicopters have been neglected. These results are shown in Tables 8-1 to 8-4.

The acceleration derivatives corresponding to the airship component of the vehicle have been estimated using the classical approach. (refs. 15 and 18.) These results are shown in Table 8-5.

3. HOVER STABILITY

For a case in which the vehicle was hovering in still air with an internal payload of 5074 pounds, the corresponding system matrix was evaluated. It was found that the vehicle is inherently stable in this operating condition and has the following modal characteristics:

Mode 1 - This is a stable oscillation of the vehicle in the pitch plane with a time period of 16.1 seconds and time to half amplitude $(T_{1/2})$ of 37.1 seconds. The corresponding mode-shape (Figure 8-1) indicates a phase relationship in which a change in forward velocity of 1 ft/sec is associated with a change in pitch angle of 2.1 degree, the former leading the latter by 90 degrees. The phase relationship observed here is similar to that of the pitch plane oscillation of the OH-6A helicopter in free flight.

Mode 2 - This mode represents heave subsidence with a $T_{1/2}$ of 7.8 seconds. It consists of vertical motion of the vehicle, which is damped by the helicopter rotors.

Mode 3 - This mode represents surge subsidence with a $T_{1/2}$ of 70 seconds. It consists of convergence of the forward velocity of the vehicle resulting from the surge damping of individual helicopters.

Mode 4 - This is a stable oscillation of the vehicle in the lateral vertical plane. It is well-damped and has a time period of 8.9 seconds with $T_{1/2}$ of 5.8 seconds. The corresponding modeshape (Figure 8-2) indicates that the resulting motion is predominantly rolling. A change in roll attitude of 10.3 degrees is associated with a change in lateral velocity of 1 ft/sec.

Mode 5 - This is a heavily damped, weak oscillation of the vehicle in the horizontal plane. It has a time period of 560 seconds and a $T_{1/2}$ of 62.3 seconds. The corresponding modeshape (Figure 8-3) indicates coupled motion of the vehicle in which nearly equal changes occur in surge and sway velocities that are 180 degrees out of phase. Small drift in heading was also observed in this mode.

TABLE 8-1 - STABILITY DERIVATIVES* OF OH-6A
HELICOPTER WITHOUT TAIL ROTOR

Hover at sea level:

	X	Y	Z	L	M	N
u	-2.04	1.25	-3.34	.10	11.33	-
v	.03	-3.45	-3.49	-15.20	-2.34	-
w	.90	-1.54	-26.98	-.63	-5.39	-
p	-64.85	-106.71	4.61	-1618.61	338.29	-
q	103.28	-66.90	1.30	-373.74	-1586.29	-
r	-4.82	27.17	116.88	-94.52	64.64	-

Forward flight at 20 knots at sea level:

	X	Y	Z	L	M	N
u	-1.32	.63	-15.03	.16	14.02	-
v	.19	-3.88	-2.93	-14.64	-1.71	-
w	1.71	-.48	-34.38	-2.24	-2.70	-
p	-61.76	-125.19	-.15	-1701.32	314.38	-
q	120.25	-63.18	12.56	-375.19	-1689.49	-
r	-7.84	38.33	121.02	-86.30	85.76	-

Forward flight at 40 knots at sea level:

	X	Y	Z	L	M	N
u	-2.14	.32	-7.46	-.63	11.69	-
v	.06	-5.38	-1.85	-15.76	-9.71	-
w	.99	-.95	-49.93	-5.72	-3.06	-
p	-59.41	-152.92	-32.31	-1792.49	256.39	-
q	134.94	-70.74	-41.06	-405.49	-2015.65	-
r	-4.38	37.89	114.82	-71.20	165.69	-

*From Reference 16. All derivatives are dimensional.

TABLE 8-2 - QUAD-HELICOPTER CONTRIBUTION TO VEHICLE STABILITY DERIVATIVES

Hover at sea level:

	u	v	w	p	q	r
X	-8.15	.1268	3.582	-261.6	270.2	-19.276
Y	5.009	-13.79	-6.15	-184.93	-179.75	108.68
Z	-13.38	-13.95	-107.92	263.13	-229.47	467.54
L	-87.47	181.1	105.38	-134367.	1664.8	14105.
M	-97.6	-7.125	41.26	-3071.76	-55445.4	6982.5
N	-	-	-	-4388.6	3113.7	-16963.

Forward flight at 20 knots at sea level:

	u	v	w	p	q	r
X	-5.295	.7609	6.848	-260.38	388.12	-31.355
Y	2.536	-15.54	-1.934	-228.28	-208.23	153.32
Z	-60.11	-11.73	-137.5	205.15	-1004.1	484.09
L	-43.83	213.92	24.973	-170212.	2163.05	70601.2
M	-36.77	6.514	109.33	-3189.77	-68575.9	5731.65
N	-	-	-	-8388.86	979.06	-14350.4

Forward flight at 40 knots at sea level:

	u	v	w	p	q	r
X	-8.56	.2536	3.963	-242.1	389.62	-17.532
Y	1.3	-21.527	-3.804	-234.08	-260.16	151.58
Z	-29.834	-7.419	-199.7	.8994	-687.54	459.26
L	-25.3	314.55	43.833	-246595.	2897.35	33602.5
M	-103.4	-34.39	57.29	-2539.7	-101509.	4110.95
N	-	-	-	-4854.7	1926.01	-21384.1

TABLE 8-3 - STABILITY DERIVATIVES OF GZ20 AIRSHIP

Forward flight at 20 knots at sea level:

	X	Y	Z	L	M	N
u	-22.04	7.15	7.15	-	-	-
v	-	-142.26	-	-	-	6790.7
w	-	-	-142.26	-	-9251.5	-
p	-	-	-	-	-	-
q	-	-	5522.6	-	-770529	-
r	-	-7662.7	-	-	-	-662459.

Forward flight at 40 knots at sea level:

	X	Y	Z	L	M	N
u	-44.08	14.3	14.3	-	-	-
v	-	-284.52	-	-	-	13581.4
w	-	-	-284.52	-	-18503.	-
p	-	-	-	-	-	-
q	-	-	11045.2	-	-1541058.	-
r	-	-15325.4	-	-	-	-1324918.

TABLE 8-4 - ESTIMATED STABILITY DERIVATIVES
OF THE COMPLETE VEHICLE

Hover at sea level:

	u	v	w	p	q	r
X	-8.15	.1268	3.582	-261.6	270.2	-19.276
Y	5.009	-13.79	-6.15	-184.93	-179.75	108.68
Z	-13.38	-13.95	-107.92	263.13	-229.47	467.54
L	-87.47	181.1	105.38	-134367	1664.8	14105.
M	-97.6	-7.125	41.26	-3071.76	-55445.4	6982.5
N	-	-	-	-4388.6	3113.7	-16963.

Forward flight at 20 knots at sea level:

	X	Y	Z	L	M	N
u	-27.335	7.911	13.998	-260.38	388.12	-31.36
v	2.536	-157.795	-1.934	-228.28	-208.23	6944.02
w	-60.1l	-11.73	-279.76	205.15	-10255.6	484.09
p	-43.829	213.92	24.973	-170212	2163.05	70601.2
q	-36.77	6.5137	5631.93	-3189.77	-839104.9	5731.65
r	-	-7662.7	-	-8388.86	979.06	-676809.

Forward flight at 40 knots at sea level:

	X	Y	Z	L	M	N
u	-52.64	14.554	18.263	-242.1	389.62	-17.532
v	1.3	-306.047	-3.804	-234.08	-260.16	13732.98
w	-29.834	-7.419	-484.22	.8994	-19190.54	459.26
p	-25.3	314.55	43.833	-246595.	2897.35	33602.5
q	-103.4	-34.39	11102.49	-2539.7	-1642567.	4110.95
r	-	-15325.4	-	-4854.7	1926.01	-1346302.

TABLE 8-5 - ACCELERATION DERIVATIVES OF THE VEHICLE

	X	Y	Z	L	M	N
u	-37.1	-	-	-	-	-
v	-	-438.6	-	-	-	1489.8
w	-	-	-438.6	-	-1489.8	-
p	-	-	-	-	-	-
q	-	-	-1489.8	-	-687357	-
r	-	1489.8	-	-	-	-687357

4. VEHICLE STABILITY IN FORWARD FLIGHT

In straight and level flight with increasing speed up to 40 knots, the pitch plane oscillation or Mode 1 (Figure 8-4) tends to have a larger time period with greater damping. This behavior is similar to that of a conventional airship as shown in Figure 8-5. For reference, the corresponding mode of a conventional helicopter is also shown in the same figure.

The increase in time period or decrease in natural frequency of oscillation for the FRV at higher speeds can perhaps be explained as follows: As flight speed increases, the resulting aerodynamic pitch stiffness is destabilizing and hence tends to offset the inherent metacentric stability of the airship envelope. The net result is a reduction in the overall pitch stiffness of the vehicle, which leads to an increase in the period of oscillation.

However, the pitch damping resulting from the empennage, as well as the quad-helicopter configuration, increases with speed. This results in a more dynamically stable vehicle at higher speeds. The heave subsidence (Mode 2) tends to have greater damping at higher speeds, since the inherent heave damping of the individual helicopters increases with flight speed.

The convergence of the longitudinal velocity component (Mode 3) observed in hover was found to become weakly divergent with time to double amplitude of 166 seconds in a flight at 20 knots. However, at higher speeds around 40 knots this mode was again found to be convergent.

The oscillatory mode of the vehicle in the lateral vertical plane (Mode 4) remains stable in forward flight, with increasing damping at higher speeds up to 40 knots. (Note that this increase in damping results from the increased roll damping of the quad-helicopter configuration at higher speeds.) The corresponding modeshape is shown in Figure 8-6 for a flight speed of 40 knots. The effect of varying flight speed on this mode has been found to be similar to that of a conventional airship as shown in Figure 8-7. The corresponding mode of a helicopter in free flight is included in this figure for reference purposes.

$\Delta\theta = 0.037$

$\Delta u = 1.0$

$\Delta q = 0.014$

$\Delta w = 0.04$
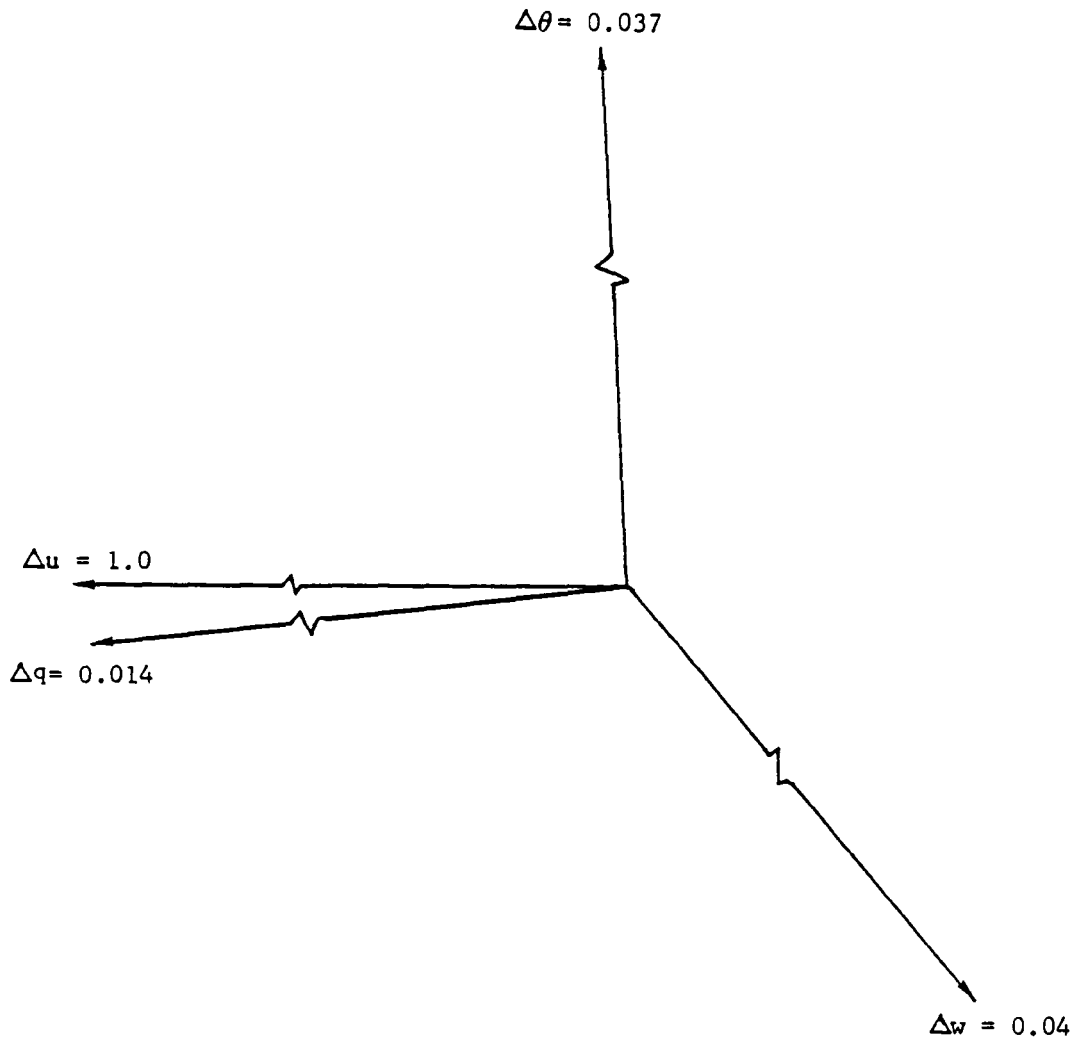
Figure 8-1 - Modeshape of Inherent Longitudinal Oscillation (Mode 1)
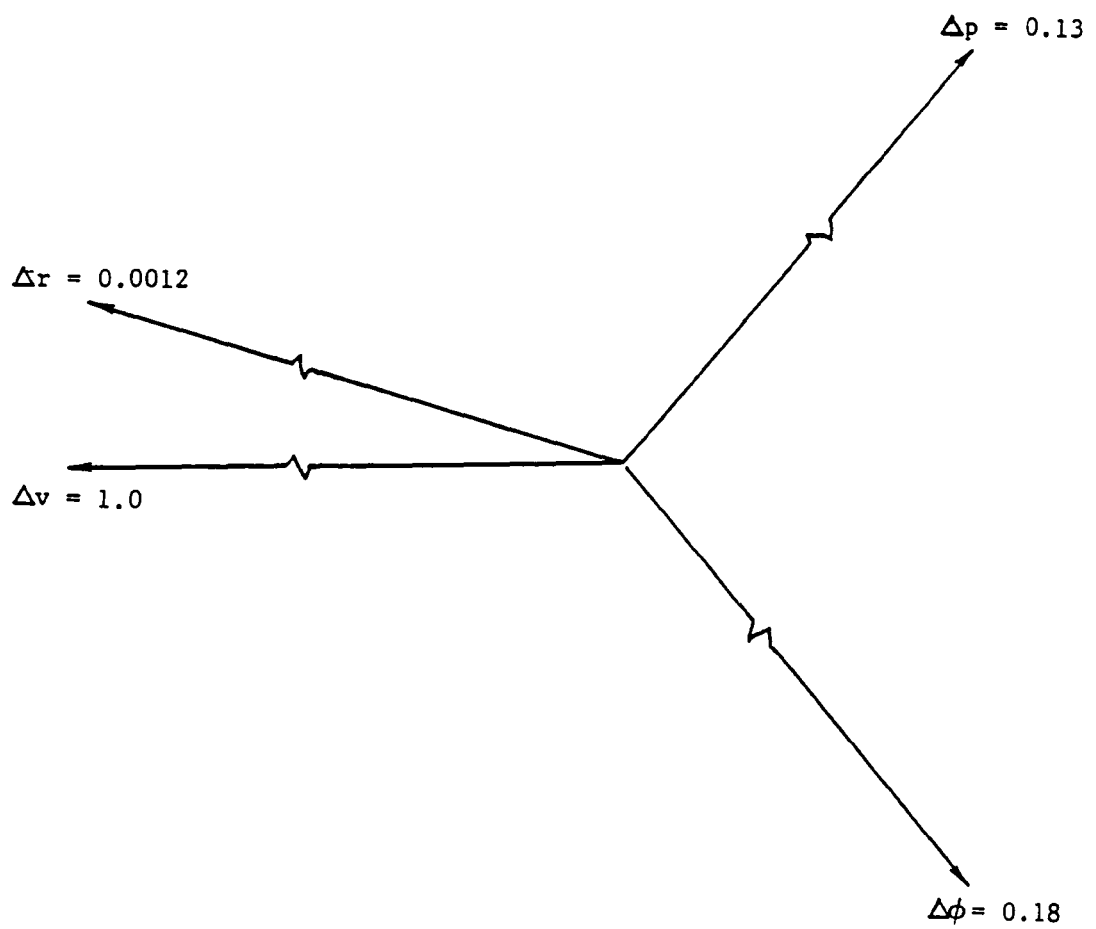
Figure 8-2 – Modeshape of Inherent Lateral Oscillation (Mode 4)
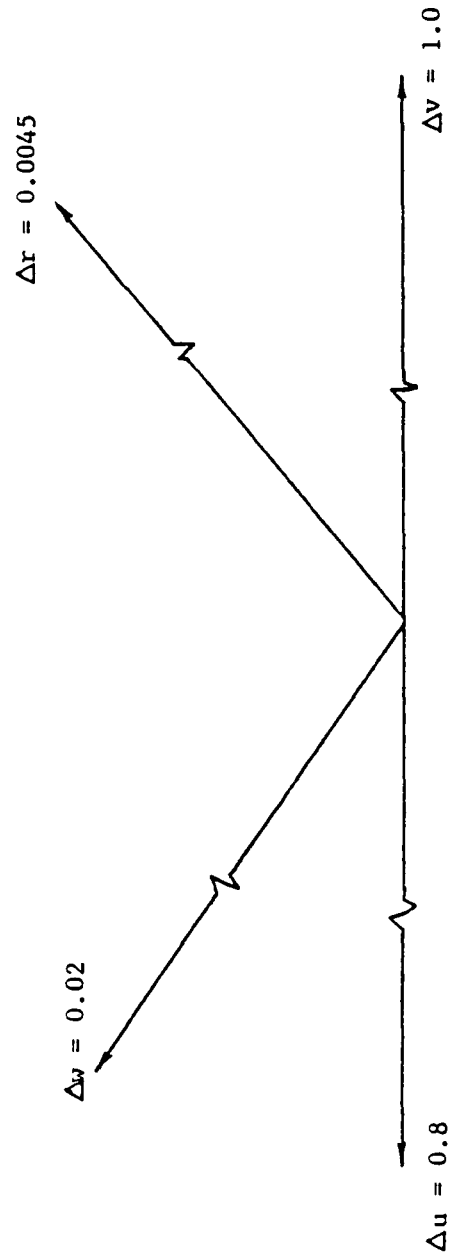
Figure 8-3 - Modeshape of Inherent Coupled
Longitudinal/Lateral Oscillation (Mode 5)

$\triangle\theta= 0.015$

$\triangle u = 1.0$

$\triangle w = 0.27$

$\triangle q = 0.003$
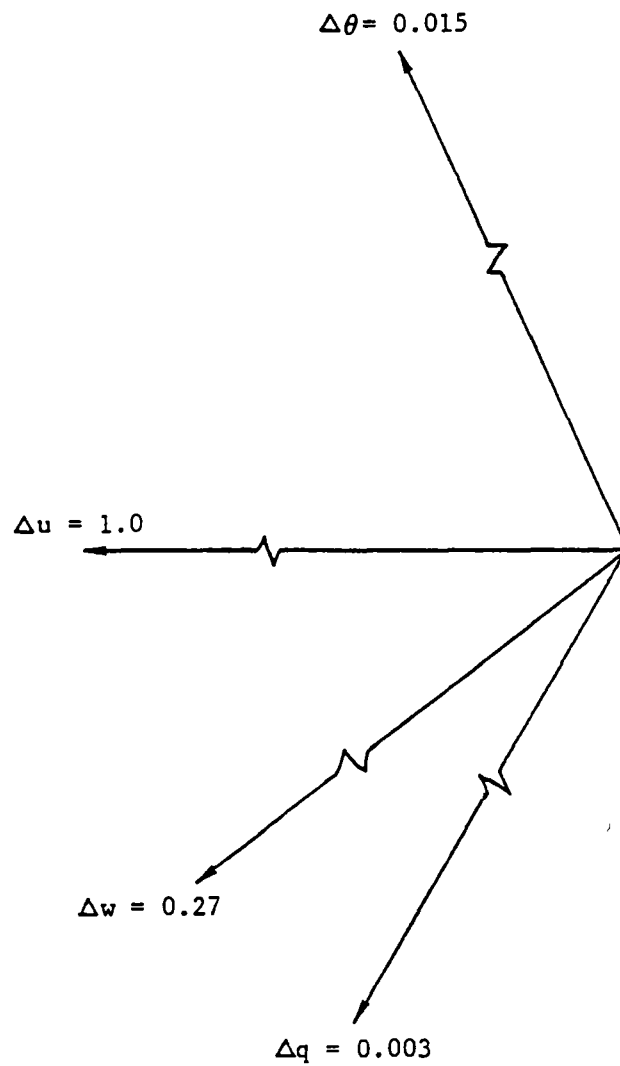
Figure 8-4 - Modeshape of Inherent Longitudinal Oscillation (Mode 1)
in Forward Flight at 40 Knots
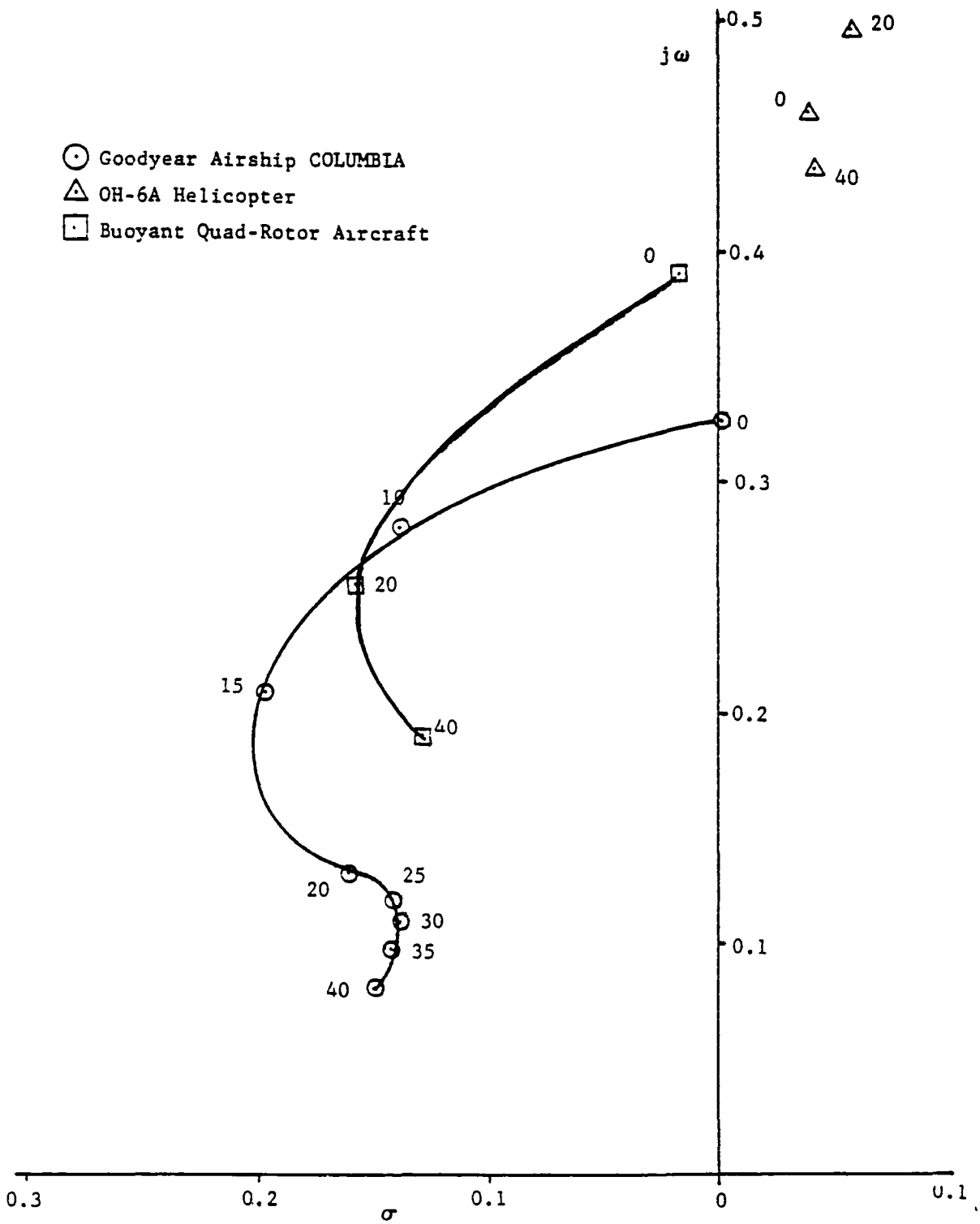
Figure 8-5 – Flight Speed Effect on Pitch Plane Oscillation

$\Delta\phi = 0.15$

$\Delta r = 0.01$

$\Delta v = 1.0$

$\Delta p = 0.1$
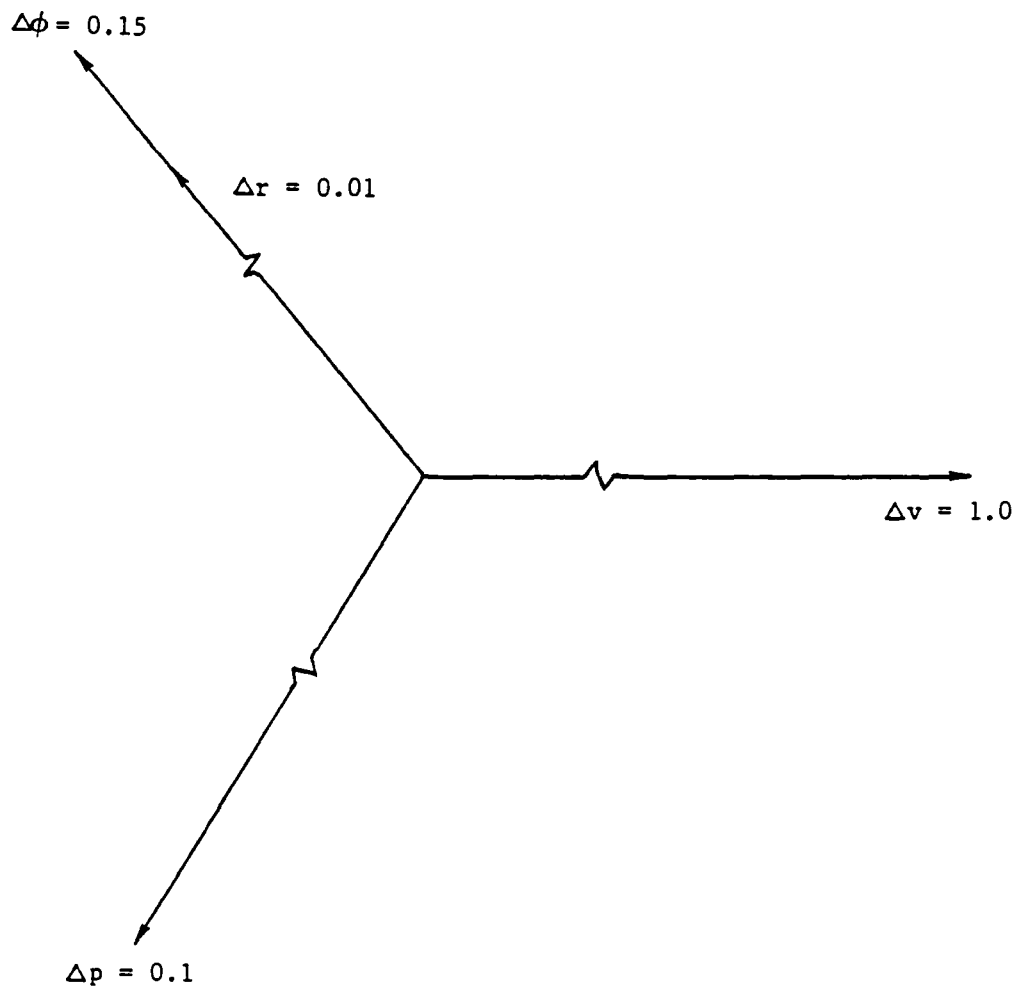
Figure 8-6 – Modeshape of Inherent Lateral Oscillation (Mode 4)
in Forward Flight at 40 Knots
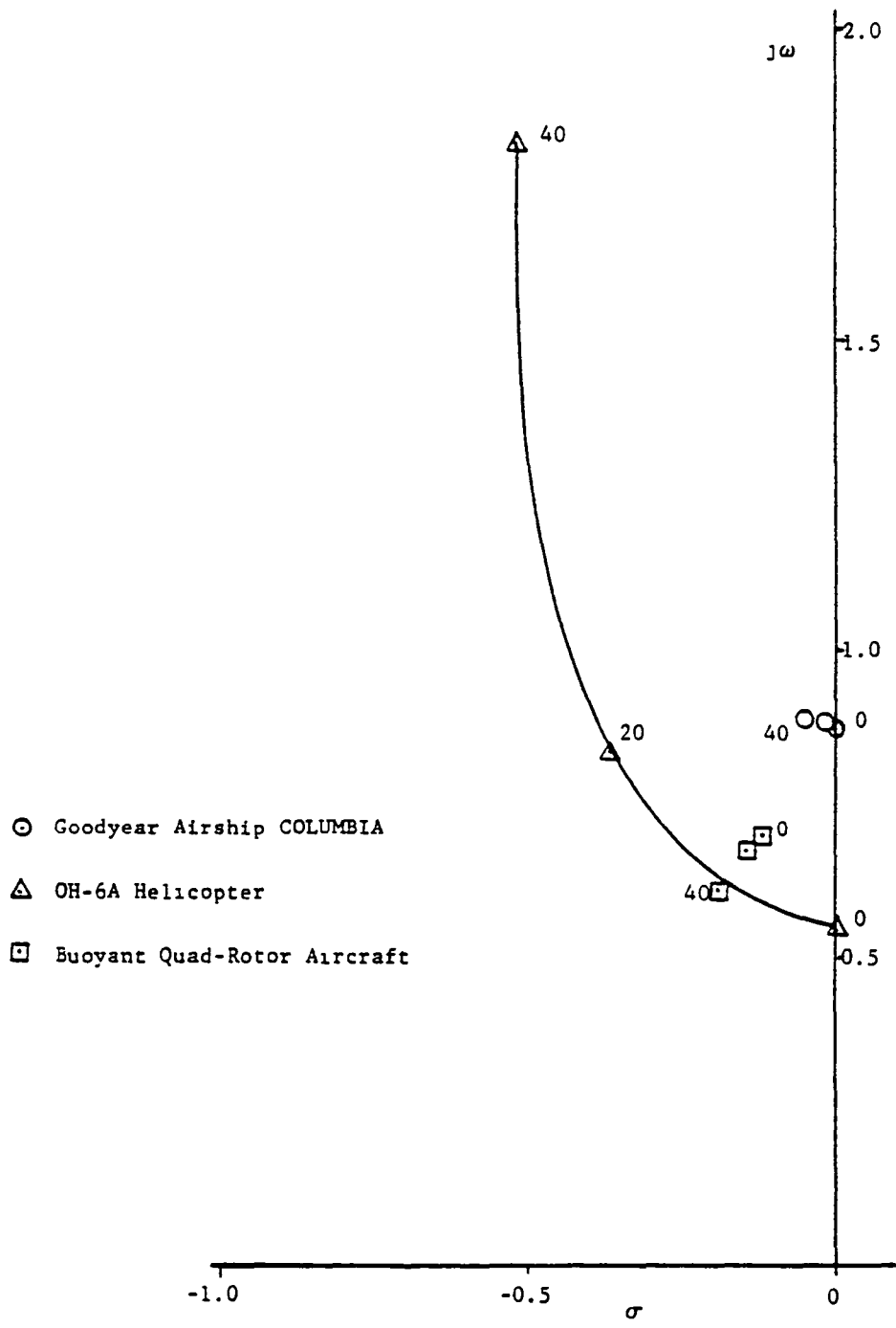
Figure 8-7 – Flight Speed Effect on Lateral Oscillation

The coupled longitudinal-lateral oscillation (Mode 5) observed in hover was found to decompose in forward flight into aperiodic convergences of yawing, and lateral-roll velocity components. These tend to be more stable at higher flight speeds due to the increased damping in each case.

It should be observed that the basic modes of the vehicle described here have already been predicted for similar configurations of this vehicle concept (refs. 19 and 20). However, the aerodynamic data used in all cases are preliminary in nature.

For instance, the aerodynamic interference between airship and helicopter components has not been accounted for. Consequently, a detailed stability analysis should be conducted after pertinent aerodynamic data have been generated for this vehicle.

5. EFFECT OF SLING LOAD ON VEHICLE STABILITY

Corresponding system modes have been determined for a case in which the FRV was hovering in still air with a sling load of 5074 pounds at the end of a 200-foot cable. It was found that introduction of a sling load results in two additional oscillatory modes of vehicle sling load motion in the longitudinal plane (Figure 8-8) and in the lateral plane (Figure 8-9). In addition, the inherent oscillatory modes of the vehicle were also found to become coupled with the corresponding sling load motions without causing any change in their modal properties. It was observed that in hover the sling load induced longitudinal oscillation (Mode 6) tends to be more unstable for increasing suspension cable lengths up to 500 feet, while it remains stable in forward flight (Figure 8-10). (Also see ref. 18).

The lateral oscillation induced by the sling load (Mode 7) was found to be stable both during hover and forward flight with heavier damping occurring at higher forward speeds (Figure 8-11).

6. POTENTIAL INSTABILITIES OBSERVED IN FLIGHT SIMULATION

Typical operational conditions anticipated for this vehicle such as those occurring during sling load pickup and dropoff, and V/STOL modes of flight and cruise were simulated to gain insight into potential stability problems. (A description of the piloted flight simulation used is given in Appendix E).

It has been determined that the vehicle is sensitive to pitch disturbances while hovering and climbing, and that this could eventually cause the aircraft to pitch over if not properly controlled. This aspect of vehicle stability needs further evaluation before flight safety can be ensured.

Similarly, backward motion of the vehicle, if not properly-controlled, has also been found to eventually lead to aircraft pitch over. However, piloted simulations involving these flight conditions have been conducted successfully both with and without stability augmentation (ref. 12 and 21).
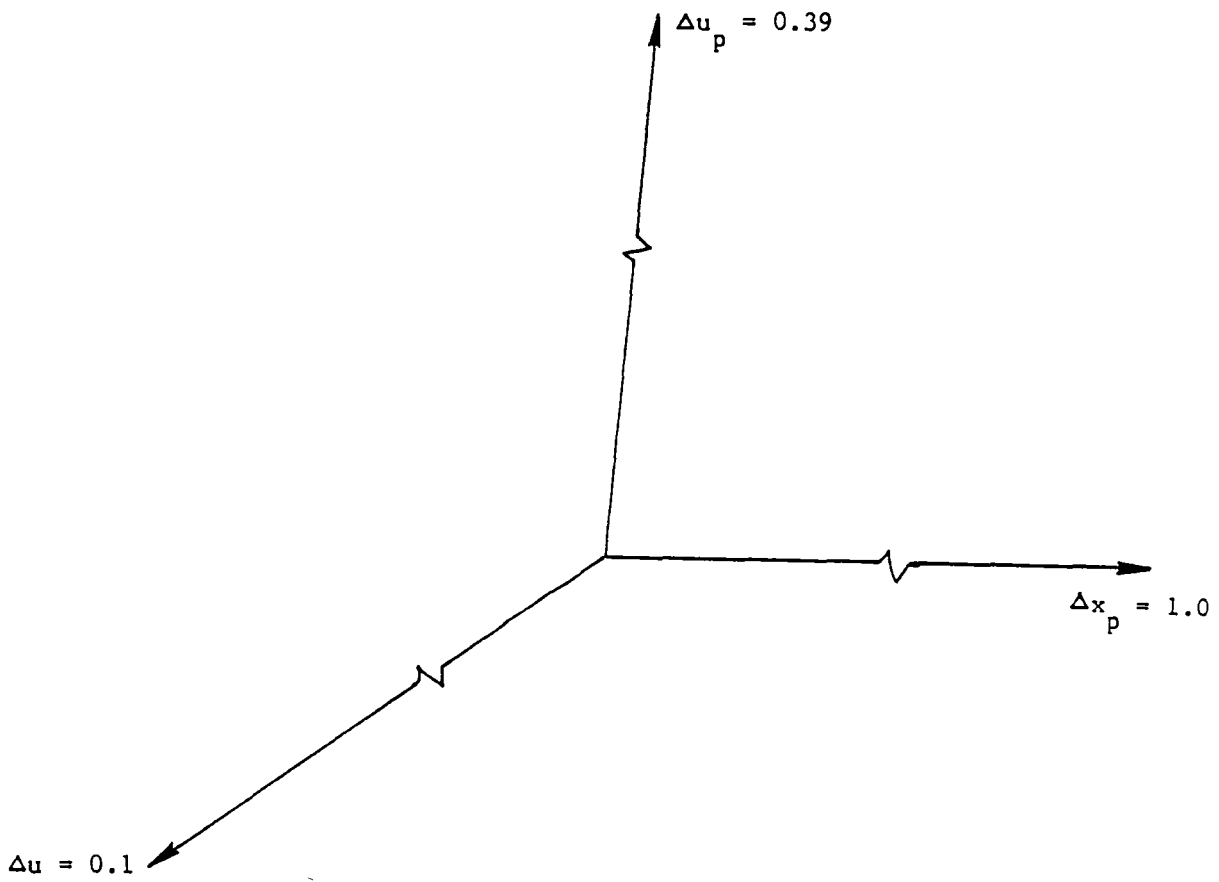
Figure 8-8 - Modeshape of Sling Load Induced Longitudinal Oscillation
(Mode 6) in Hover

$\Delta v = 0.03$

$\Delta y_p = 1.0$

$\Delta v_p = 0.40$
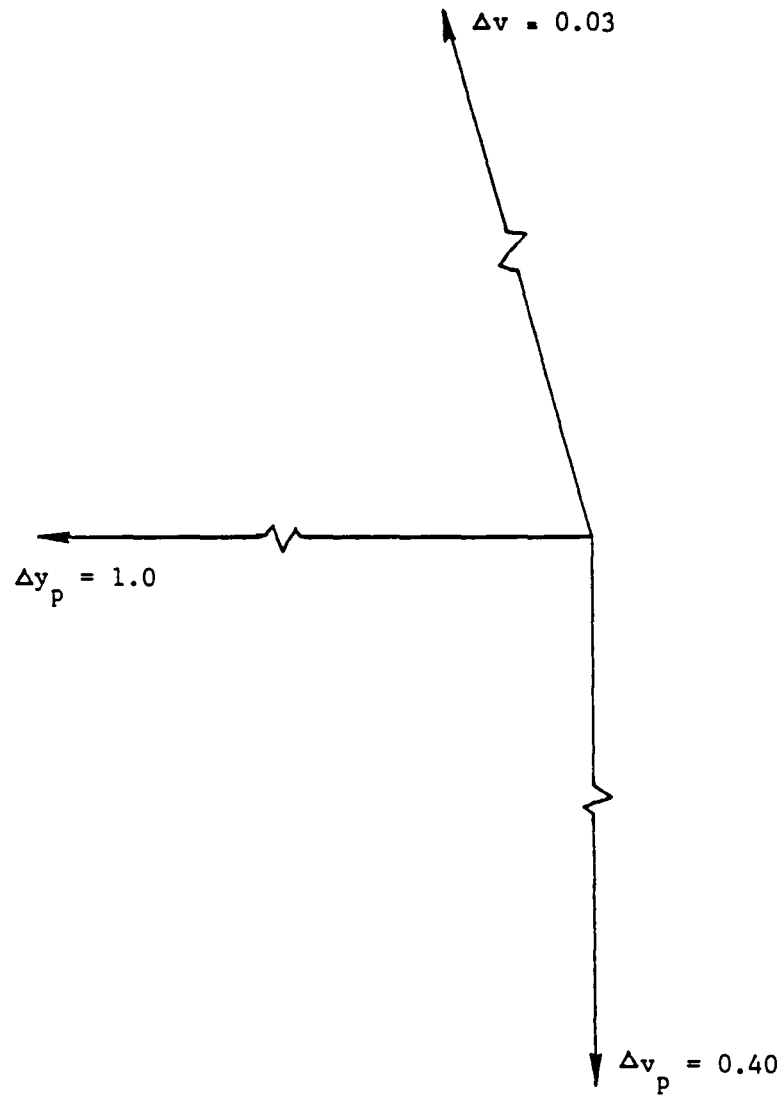
Figure 8-9 – Modeshape of Sling Load Induced Lateral
Oscillation (Mode 7) in Hover
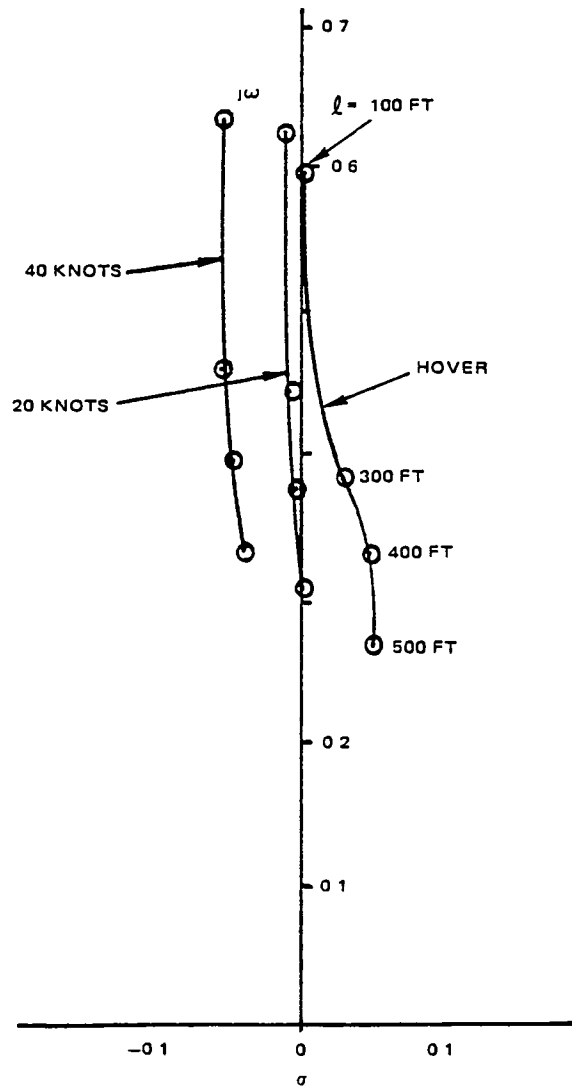
Figure 8-10 – Cable Length Effect on Sling Load
Induced Longitudinal Oscillation (Mode 6)
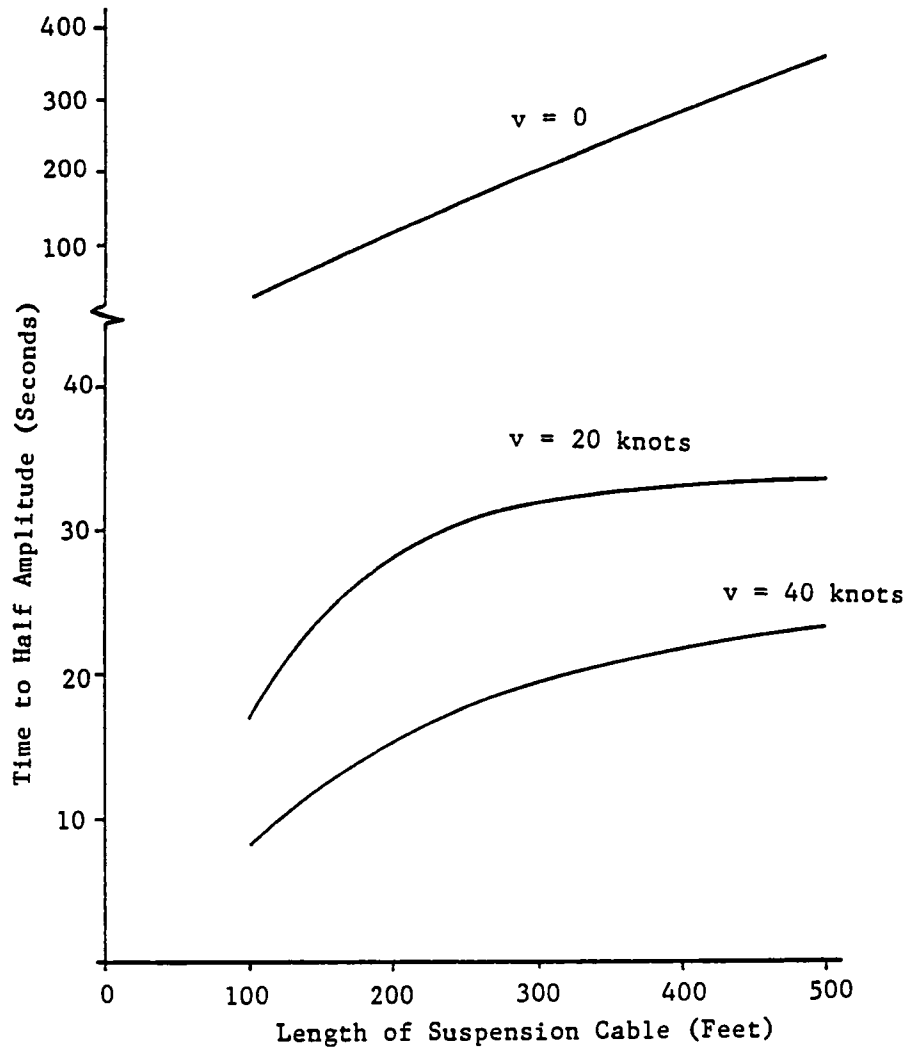
Figure 8-11 – Cable Length Effect on Sling Load Induced Lateral Oscillation

SECTION IX – CONTROL CHARACTERISTICS

1. GENERAL

Unlike the airplane or helicopter, handling qualities criteria for hybrid airships are nebulous. Consequently the control requirements for this vehicle have been interpreted in terms of specific tasks such as ability to maneuver from hover, stationkeeping ability, ability to accelerate into a headwind or crosswind, and ability to counter wind disturbances while hovering over a point on the ground. These characteristics are examined in the following sections (ref. 22).

2. OPEN LOOP RESPONSE TO CONTROL ACTUATIONS

A six-degree-of-freedom flight dynamics simulation previously developed for hybrid airships was adapted to simulate the proposed flight research vehicle configuration (ref. 18). A description of this simulation is given in Appendix A.

Complete rigid body motion of the vehicle was simulated by using estimated values of the overall physical and aerodynamic properties of the vehicle (see Section V), which are defined in terms of its airship and helicopter components. (refs 5, 13, and 16)

Significant insight into hover maneuverability was obtained by considering vehicle response to control inputs in open loop. Initially, the vehicle by itself (gross weight = 18,018 pounds) was trimmed in hover and subjected to individual unit step inputs to each of its controls with the open loop results recorded on strip charts. A similar procedure was repeated for a case in which the vehicle was carrying an internal payload of 4274 pounds.

Vehicle response to a unit step input of collective pitch. (Figure 9-1) illustrates the presence of aerodynamic and dynamic crosscouplings in vertical and pitching motions, which lead to longitudinal motion as well.

This can perhaps be explained as follows: As the vehicle climbs vertically, it experiences an aerodynamic noseup pitching moment and forward directed axial force. This results in a pitch velocity which, in conjunction with the prevailing vertical velocity, produces forward motion of the vehicle. These effects tend to decrease the angle-of-attack and hence, the nosedown pitching moment on the vehicle until steady state is reached.

However, the vehicle with payload (shown by the dotted line in the figure) responded by pitching up while drifting upward and backward, until it turned over. The backward motion in this case is perhaps due to the vehicle weight in excess of static lift, which tends to accelerate the climbing vehicle backwards if not countered. The net effect on the vehicle is a continuous noseup tendency.

A careful examination of the corresponding flight path reveals that vehicle motion in such a case is aerodynamically unstable. A detailed analysis should be conducted to verify this tendency. In any event, control and piloting techniques can be evolved that would overcome this problem. For instance, inherent vehicle trim in hover can be made to occur with a negative pitch attitude, which eliminates this flight regime, as demonstrated by the simulation and subsequently discussed.
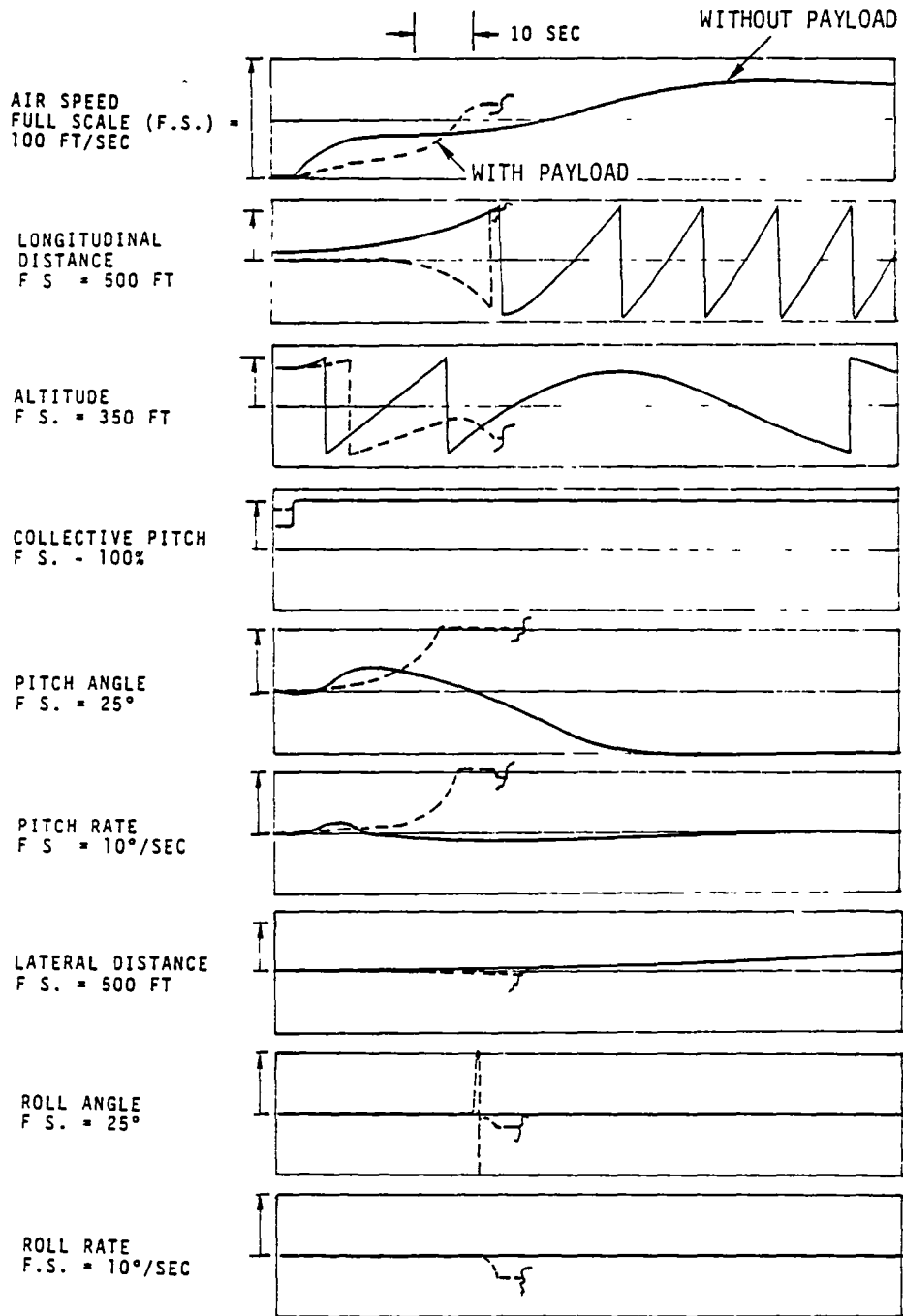
Figure 9-1 - FRV Open Loop Response to a Unit Step Input to Collective Command

Vehicle response to a unit step input to longitudinal stick (Figure 9-2) consists of forward flight in which the vehicle develops a noseup pitch attitude of 16 degrees, also resulting in climb. The pitch up tendency of the vehicle can be explained by noting that the line of action of the longitudinal control force has a large vertical offset from the envelope aerodynamic center. Therefore, the control application results in a noseup pitch attitude that gives rise to aerodynamic pitching moment. This tends to increase the pitch attitude of the vehicle until a steady state is reached. The vehicle with payload responded similarly by climbing with a pitch attitude of 11 degrees.

However, a negative unit step input to longitudinal stick (Figure 9-3) resulted in the vehicle developing an initial nosedown attitude while drifting upward and backward, thus leading to the pitch up tendency described earlier. Similar response was also observed when the vehicle was with payload.

The vehicle responded to a lateral stick input (Figure 9-4) by moving laterally while oscillating in roll, a result of the control crosscoupling. In this case the lateral control force tends to roll the vehicle adversely so that it decreases the effectiveness of the lateral control. The application of this control also results in a stable, roll oscillation in which the metacentric moment generates the roll stiffness and the helicopters generate the damping moment.

The FRV was also found to drift forward and upward during lateral stick input and to change its heading at the slow rate of one degree per second.

A unit step input to roll command (Figure 9-5) tends to oscillate the FRV in roll while it drifts laterally. In addition, the FRV drifts forward and downward. The latter results from a decrease in net vertical component of rotor thrust following a roll command input. This can be alleviated by limiting the authority of the roll command to generate differential collective pitch on the rotors.

The vehicle responded to a unit step input to pitch command (Figure 9-6) by oscillating in pitch with peak amplitude of 12 degrees while drifting backward and downward. Simultaneously, the FRV oscillated in roll while developing a steady yaw rate of five degrees per second.

In addition, even a slight change in trim causes the vehicle to move upward and pitch over following this step input. Consequently, it is essential that pitch attitude of the hovering vehicle be controlled with appropriate augmentation of the control loop.

A negative unit step input to this control (Figure 9-7) causes the vehicle to oscillate in pitch and finally take a nose dive. This perhaps indicates the sensitivity of this control for maneuvering near hover.

A unit step input to yaw command (Figure 9-8) leads to the vehicle developing a steady yaw rate of 13 degrees per second.
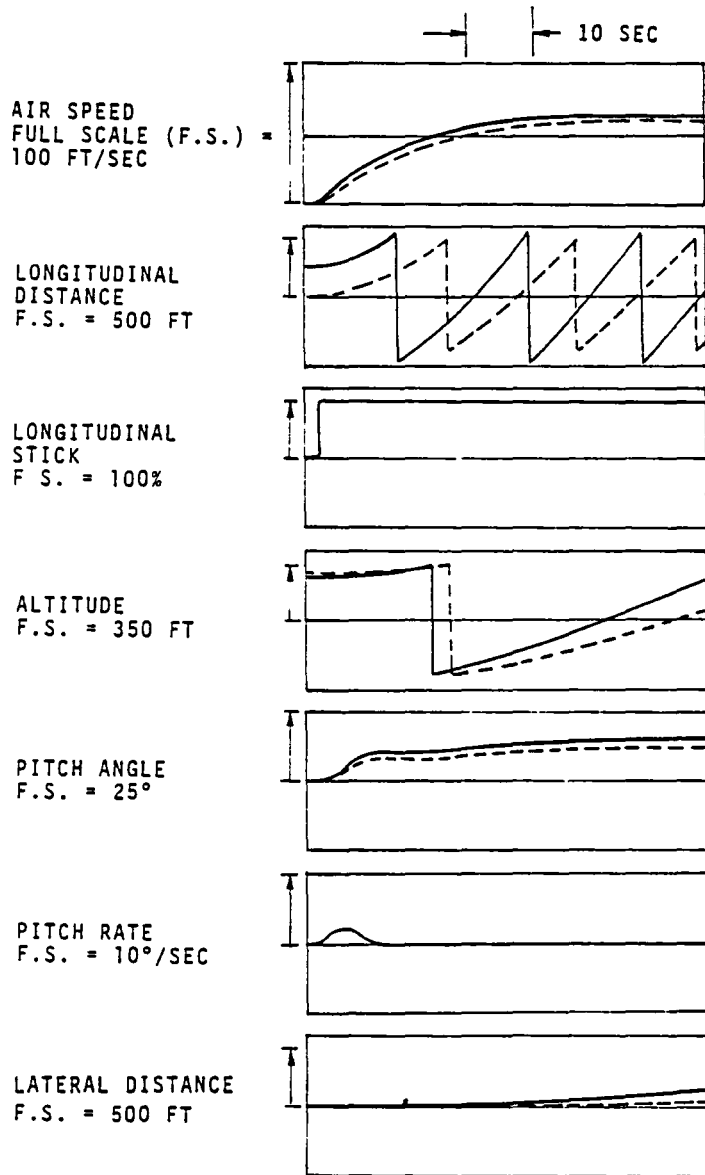
Figure 9-2 - FRV Open Loop Response to a Unit Step Input to Longitudinal Stick

AIR SPEED
FULL SCALE (F.S.) =
100 FT/SEC

— |— 10 SEC

LONGITUDINAL
DISTANCE
F S. = 500 FT

LONGITUDINAL
STICK
F.S = 100%

ALTITUDE
F.S. = 350 FT

PITCH ANGLE
F S. = 25°

PITCH RATE
F S = 10°/SEC

LATERAL DISTANCE
F.S. = 500 FT

ROLL ANGLE
F.S. = 25°

ROLL RATE
F S. = 10°/SEC

YAW ANGLE
F.S = 180°

YAW RATE
F.S = 20°/SEC
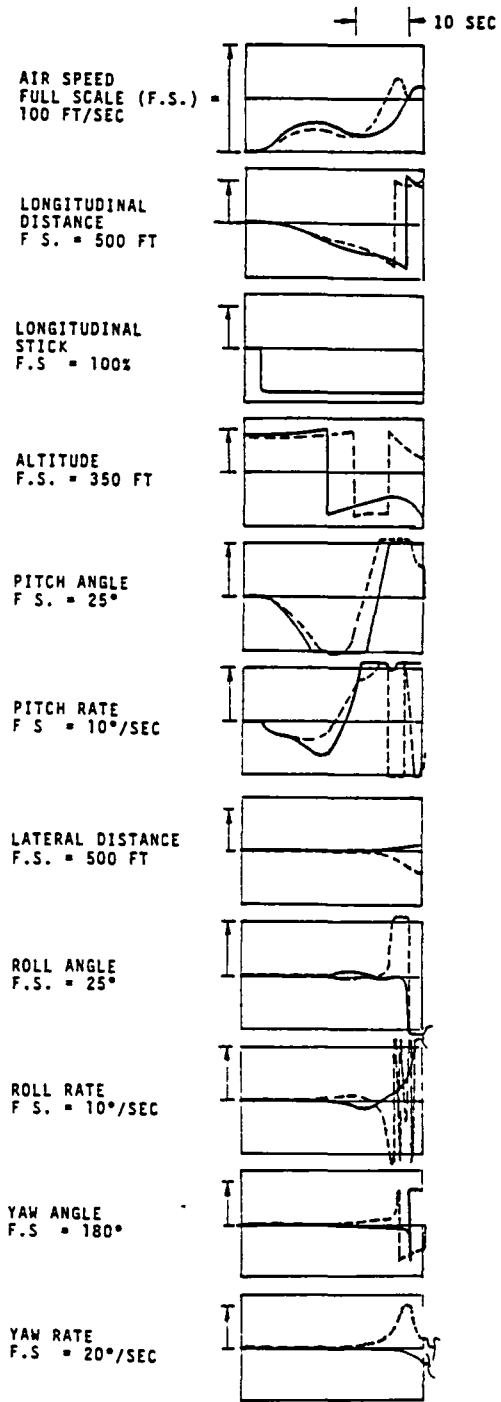
Figure 9-3 - FRV Open Loop Response to a Unit Step Input to Negative Longitudinal Stick
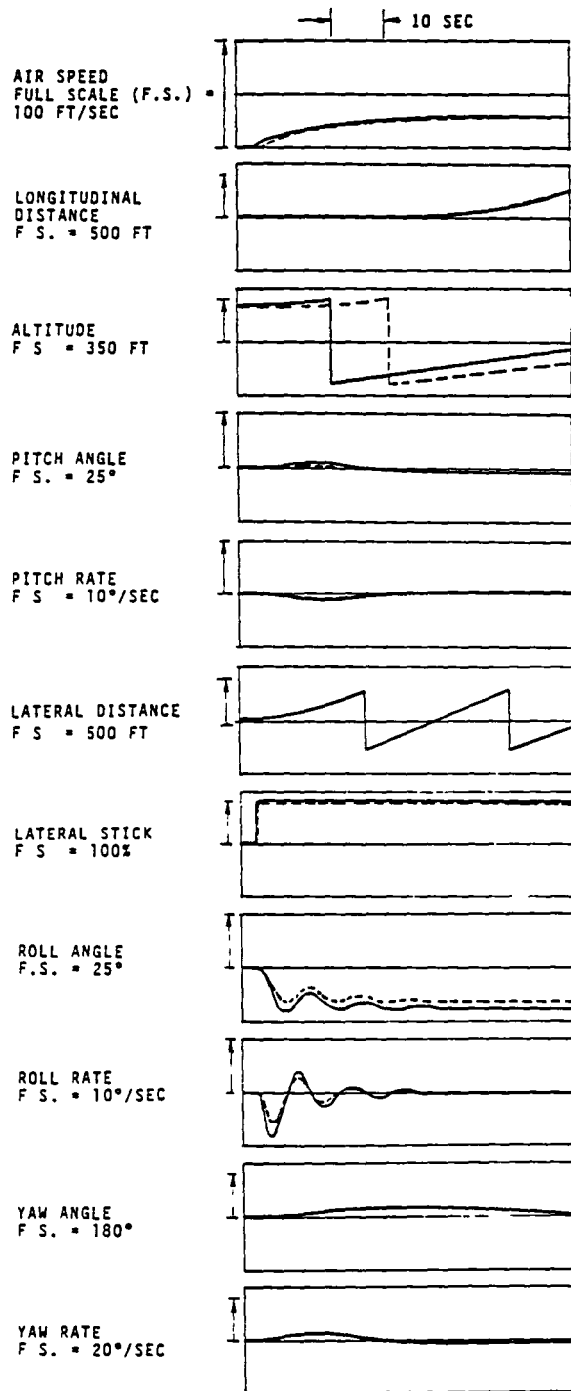
Figure 9-4 - FRV Open Loop Response to a Unit Step Input to Lateral Stick
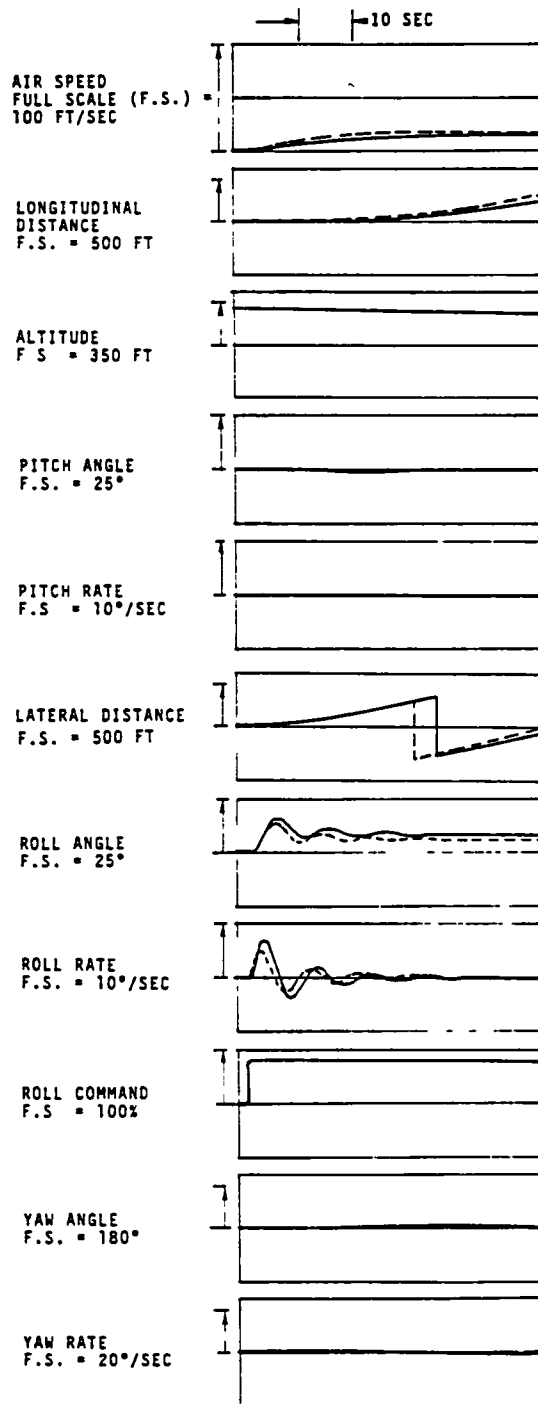
Figure 9-5 – FRV Open Loop Response to a Unit Step Input to Roll Command
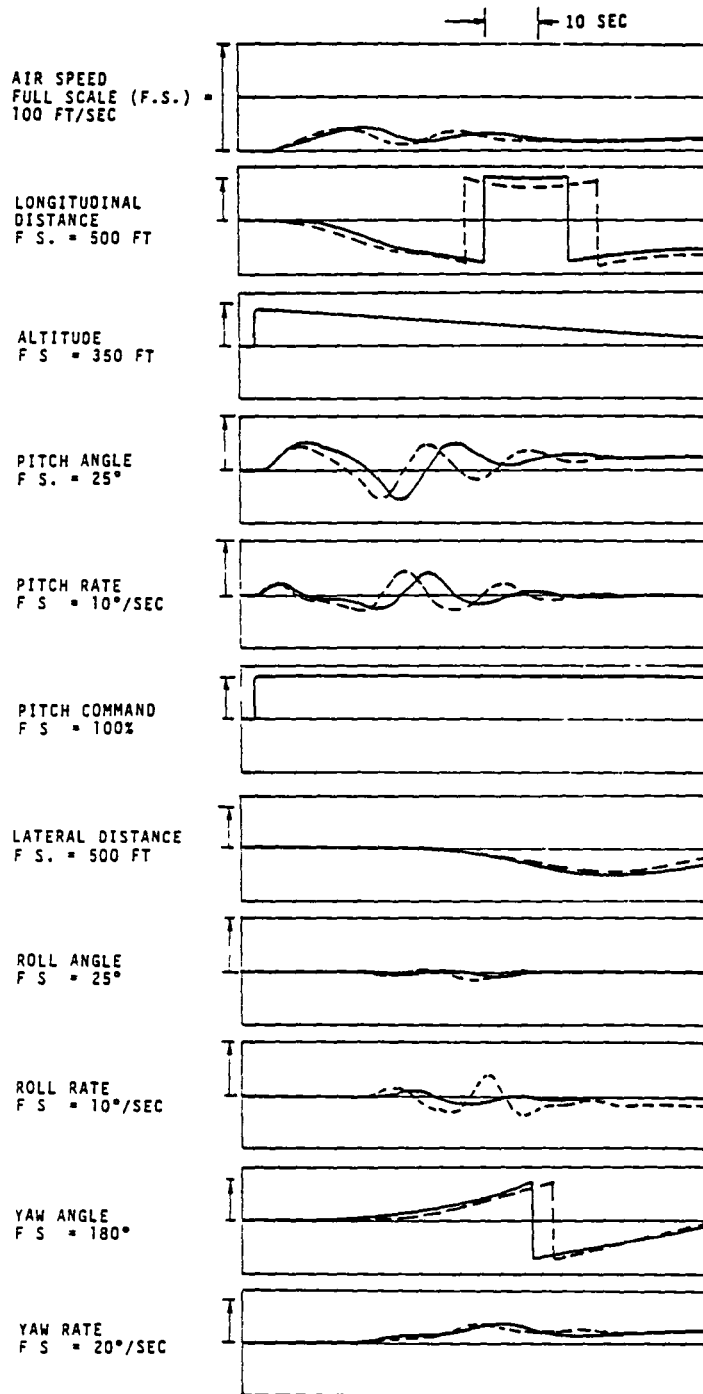
Figure 9-6 - FRV Open Loop Response to a Unit Step Input to Pitch Command

AIR SPEED
FULL SCALE (F.S.) =
100 FT/SEC

LONGITUDINAL
DISTANCE
F.S. = 500 FT

ALTITUDE
F.S. = 350 FT

PITCH ANGLE
F.S. = 25°

PITCH RATE
F.S. = 10°/SEC

PITCH COMMAND
F.S. = 100%

LATERAL DISTANCE
F.S. = 500 FT

10 SEC
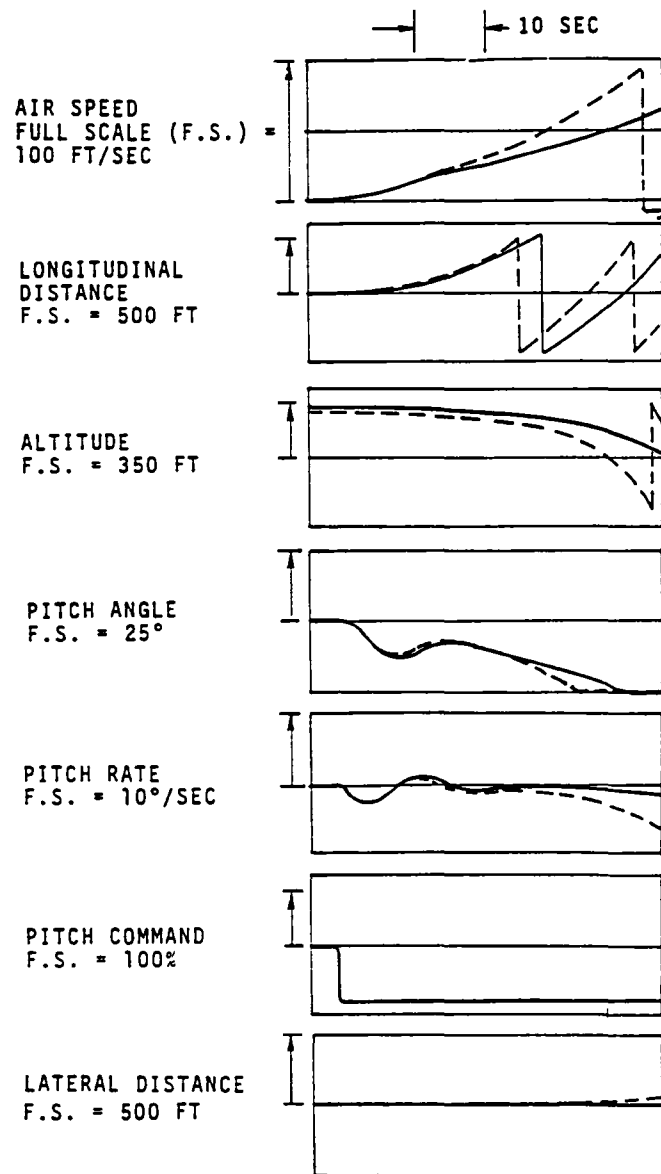
Figure 9-7 - FRV Open Loop Response to a Unit Step Input to Negative Pitch Command

YAW ANGLE
F.S. = 180°

YAW RATE
F.S. = 20°/SEC
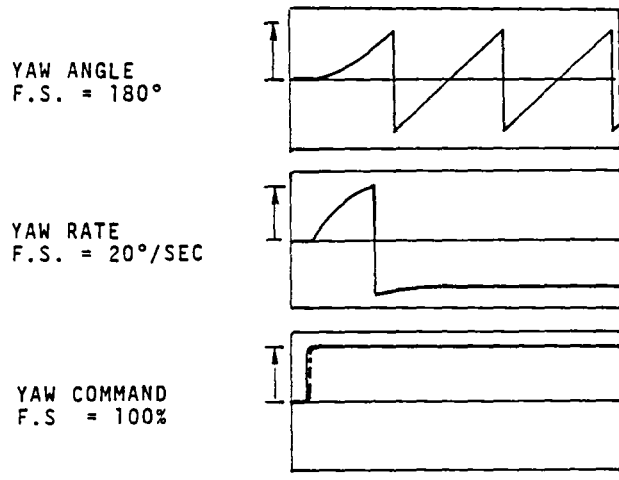
YAW COMMAND
F.S = 100%

Figure 9-8 - FRV Open Loop Response to a Unit Step Input to Yaw Command

3. CLOSED LOOP RESPONSE TO CONTROL ACTUATIONS

The open loop resonse of the hovering vehicle to control inputs indicated strong cross-couplings in control forces and control moments which could result in undersirable motion of the vehicle. Consequently, closed loop responses of the vehicle have been determined for various values of control authority parameters and initial trim conditions preceding the control actuations (Table 9-1).

A value of parameter A = 0.1 implies a 10 percent authority on the differential collective pitch that can be generated by full roll command input. Similarly, B = 0.4 implies a 40 percent authority on the differential collective pitch that can be generated by full pitch command. Note that in a given trim condition these control authorities apply only to the extent of net 100 percent collective pitch on any one of the rotors.

TABLE 9-1 - TRIM CONDITIONS FOR CLOSED LOOP
RESPONSE OF THE VEHICLE

Run no.	Gross weight	A	B	ref (deg)	Collec- tive stick	Longi- tudinal stick	Lateral stick	Remarks
1	18018	0.1	0.1	0	1	0	0	
2	18018	0.1	0.1	-5	1	0	0	
3	18018	0.1	0.1	0	0.477	1	0	
4	18018	0.1	0.1	0	0.477	0	1	
5	18018	0.1	0.1	5	0.477	0	0	
6	18018	0.1	0.1	-10	0.477	0	0	
7	18018	0.4	0.4	0	1	0	0	
8	18018	0.4	0.4	-5	1	0	0	
9	18018	0.4	0.4	0	0.477	1	0	
10	18018	0.4	0.4	0	0.477	1	1	
11	18018	0.4	0.4	-10	0.477	1	0	
12	22292	0.1	0.1	0	1	0	0	Unstable
13	22292	0.1	0.1	-5	1	0	0	Stable
14	22292	0.1	0.1	0	0.833	1	0	
15	22292	0.1	0.1	0	0.833	0	1	
16	22292	0.1	0.1	5	0.833	0	1	
17	22292	0.1	0.1	-10	0.833	0	1	
18	22292	0.4	0.4	0	1	0	1	Unstable
19	22292	0.4	0.4	-5	1	0	1	Stable
20	22292	0.4	0.4	0	0.833	1	1	
21	22292	0.4	0.4	0	0.833	1	1	
22	22292	0.4	0.4	-10	0.833	1	0	

A = pitch control authority
B = roll control authority

In each case given in Table 9-1, the FRV was initially trimmed in hover while the pitch, roll, and heading angles were commanded to desired values via autopilots (See Appendix A). In all cases the roll and heading were referenced to zero. All control inputs thus correspond to the proposed pilot inputs. The corresponding responses of the vehicle are shown in Appendix E.

When the vehicle is hovering at a gross weight of 22,292 pounds a step input to collective control tends to tip over the vehicle even at higher pitch control authority. However, this unstable situation can be avoided by trimming the vehicle to a negative pitch attitude before the collective control input. A reference input of -5 degrees to the pitch autopilot provides enough negative pitch attitude of the vehicle to prevent the unstable situation. It may therefore be desirable to partially slave the pitch control to the collective pitch input so that the vehicle tends to develop a nosedown attitude simultaneously with the collective pitch input. The resulting vehicle motion would be similar to that of a conventional helicopter's response. In all cases the higher authority in pitch and roll commands tend to decouple the adverse crosscoupling effects as illustrated by these results.

4. STATIONKEEPING ABILITY

The hover flight envelope at sea level on a standard day out of ground effect is calculated, for various wind conditions assuming the baseline configuration has the following features:

1. Each OH-6A main rotor produces 2,700 pounds maximum thrust at all speeds.

2. Four degrees of longitudinal cyclic are available for the rigid mounted OH-6A's.

3. The OH-6A's are mounted on a roll hinge with ±12 degrees of travel to produce side forces.

4. The OH-6A's are tilted differentially in the longitudinal direction to counteract main rotor reaction torque.

5. Each auxiliary thrustor produces 1,400 pounds of fully reversible static thrust. This thrust was assumed to decrease at 5.8 pound-feet per second for axial velocity.

The objective is to determine the hover operating envelope for winds from zero to 90 degrees sideslip. A six-degree-of-freedom computer trim program was used to compute the operating envelopes for various methods of control. It is assumed that maximum heaviness is 90 percent of the main rotor thrust and 50 percent when empty. The thrust available in the body axes are given below with the components of main rotor thrust (MRT) and auxiliary thrust (AT).

Body axis	90% MRT	50% MRT
X (longitudinal)	678 lb MRT	376 lb MRT
	2800 lb AT	2800 lb AT
	3478 lb Total	3176 lb Total

Body axis	90% MRT	50% MRT
Y (lateral)	2021 lb MRT	1122 lb MRT
	2800 AT	2800 lb AT
	4821 lb Total	3922 lb Total
Z (vertical)	9720 lb	5400 lb

The main rotors are not very effective in the longitudinal direction but are retained for proof of concept.

Each point on the operating envelope is defined as the maximum wind that the vehicle can hover in at a given sideslip angle. The program operates by incrementing the wind speed at a given sideslip angle until the control force or moment for any of the six-degrees-of-freedom reaches a limit. The control logic was selected to maximize the use of each control function.

For sideslip angles greater than about 30 degrees the lateral control force available is the limiting control function. At zero degrees sideslip the longitudinal control force is obviously the limiting control function. Between zero and 30 degrees the summation of yaw and longitudinal control is the limiting factor.

The summation of the percent of longitudinal force for yaw and the percent of longitudinal force for forward velocity cannot exceed 100 percent without starting to lose forward force.

To help alleviate this limitation, the control logic priority is assigned such that, initially, the yaw moment requirement is satisfied using differential lateral cyclic to the extent that it is not being used for lateral side force. This maximizes the use of the lateral force leaving less of a yaw moment to be compensated by differential longitudinal cyclic. Overall, this increases the hover envelope in the zero to 10-degree sideslip range.

Figure 9-9 shows the flight envelopes for the FRV with and without differential lateral cyclic for yaw control for 90 percent and 50 percent main rotor thrust. In both cases, the increased capability is about five knots at two degrees sideslip. This probably would never be needed in the steady state condition, but it may be advantageous to have this additional capability for longitudinal or yaw acceleration in the dynamic requirements of stationkeeping. All data presented use (if available) differential lateral thrust for yaw.

A typical hover performance envelope is shown on Figure 9-10. Figure 9-11 shows the limiting control functions in determining the hover flight envelope. From zero to 2 degrees the longitudinal stick is used 100 percent to produce forward velocity. The yaw command is provided by differential lateral thrust and does not require any differential longitudinal force. Between two degrees and about 30 degrees the sum of the longitudinal stick and the yaw pedals expressed by the dashed line equals 100 percent. Thus, the longitudinal force continues to be the limiting control force.

Beyond 30 degrees to about 85 degrees the lateral force is the limiting control factor. At 90 degrees the yaw moment has become quite large again and the limiting control factor is the longitudinal force. Figure 9-12 shows the control forces and moments for this hover envelope.

FLIGHT RESEARCH VEHICLE
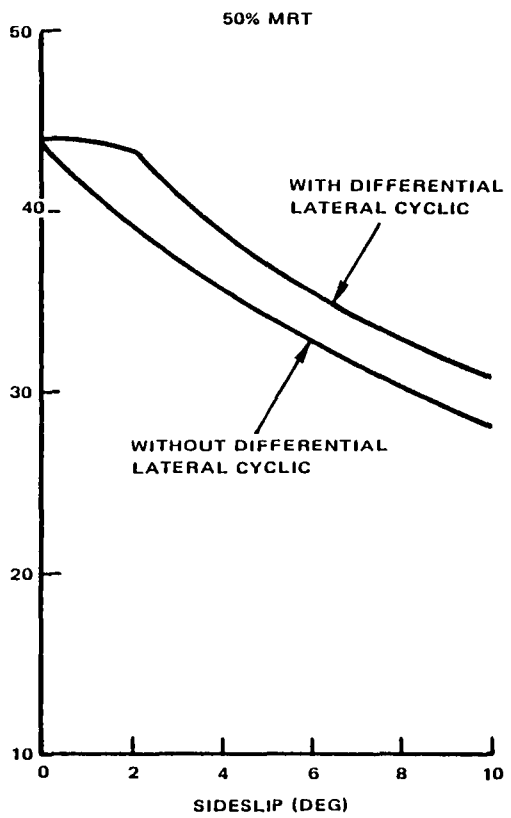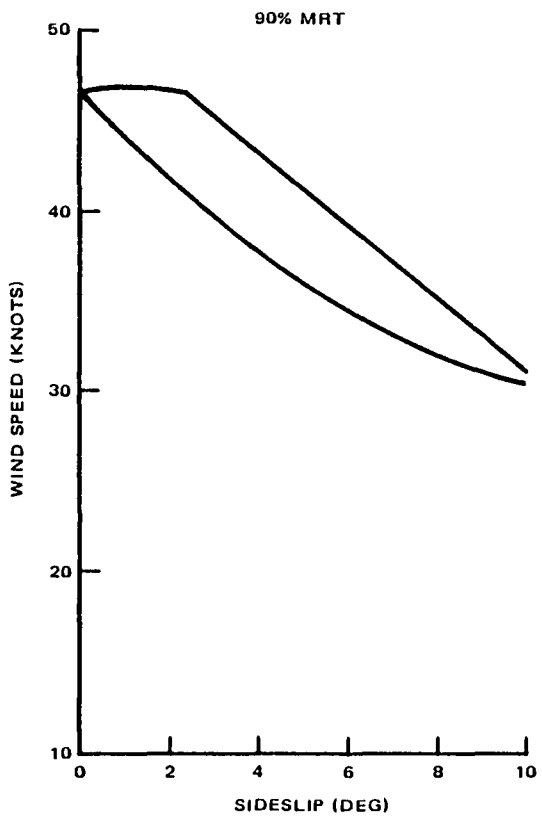
Figure 9-9 – Hover Flight Envelope With and Without Differential Lateral Cyclic for Yaw Control
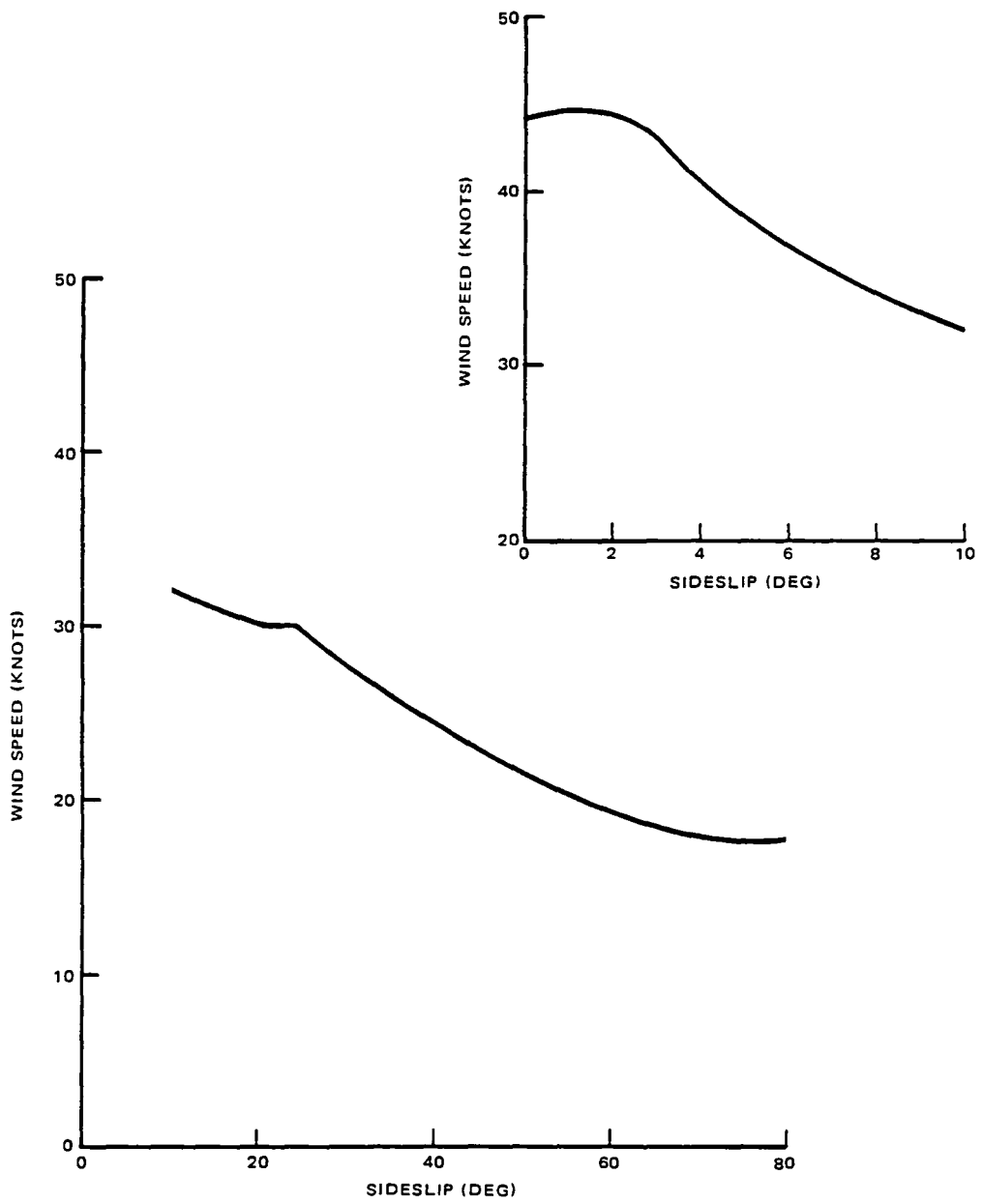
Figure 9-10 - Hover Flight Envelope with 50% Rotor Thrust Condition
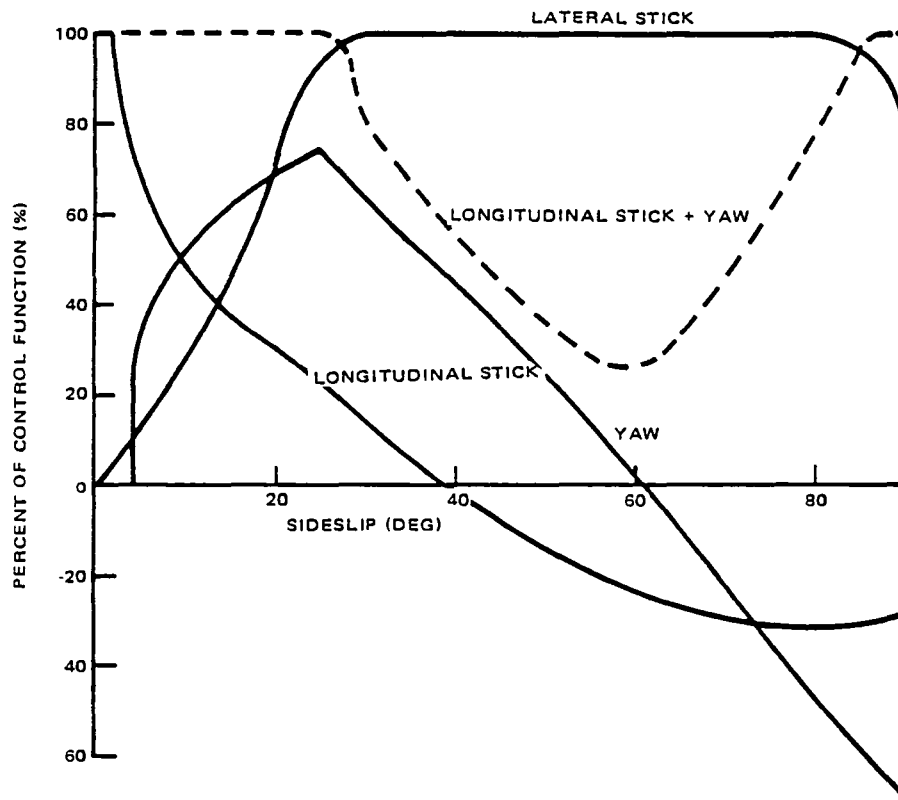
Figure 9-11 - Limiting Control Function Effect on Hover Flight Envelope
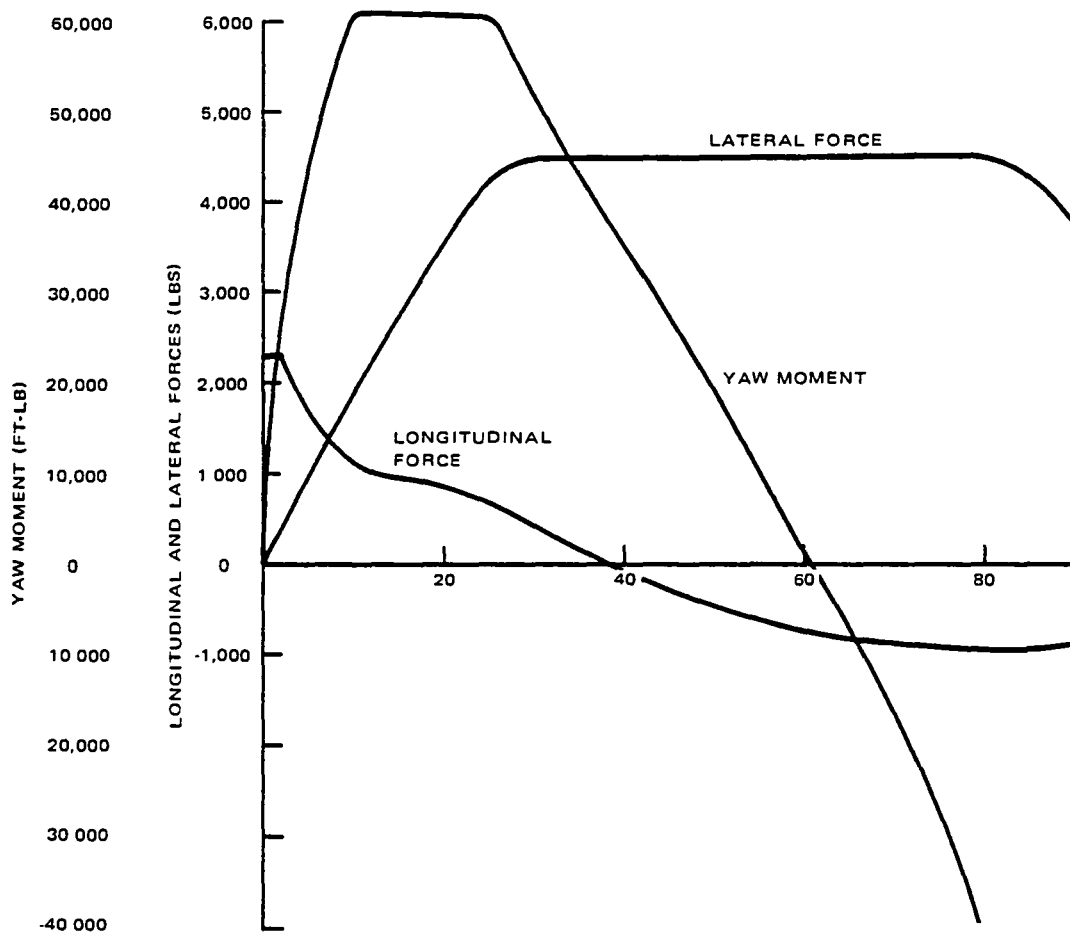
Figure 9-12 - Control Forces and Moments in a Hover Flight Envelope

a. Crosscoupling

Some control crosscoupling effects in hover are important to note. The aerodynamic center-of-pressure is not in line with the control forces for pitch and roll. Thus hovering into a wind causes adverse pitching and rolling moments. This effect is shown in Figure 9-13.

In each case, to stationkeep and remain level, the thrust on the downwind main rotors is increased and decreased on the upwind side. For example, if these moments were not compensated the FRV would pitch up 0.6 degrees and roll counter clockwise 14 degrees for relative winds of 10 knots at zero and 90 degrees respectively. The change in thrust on each rotor is 24 pounds to maintain pitch, and 361 pounds to maintain roll level.

A secondary crosscoupling into yaw results from the differential main rotor thrust. This accounts for less than 10 percent of the total yaw moment. The cause of this crosscoupling is shown in Figure 9-14.

For any significant sideslip the roll differential thrust exceeds the pitch differential thrust and the resultant yaw moment is positive. In general, this tends to reduce the aerodynamic yaw moment. For most situations this crosscoupling is not significant but it is important to be aware of it. The magnitude of this effect is plotted in Figure 9-15.

At higher velocities, above 20 knots, the elevator can be used to provide the pitching moment for sideslip angles from zero to ± 30 degrees. This feature was used throughout this study. The rudder could also be used to compensate for yaw moments under these same conditions but this results in an adverse side force. This option was not used in this study.

b. Stationkeeping Methods

The most difficult hover condition is to stationkeep into a crosswind. The drag in this direction is large and requires a large control force that results in a large coupling moment into roll. If this moment is not counteracted, the FRV tends to roll away from the direction requiring the control force. This tends to reduce the side force from the main rotor.

The auxiliary thrustors are effected only slightly because the degradation in thrust is a $(1 - \cos \phi)$ function. Since a large proportion of the thrust is produced by the auxiliary thrustors, the adverse roll effect is not as critical as a quad rotor configuration which uses only main rotors.

There are several control options to be evaluated for hovering into a crosswind. (See Figure 9-16).

The first option is not to provide any roll control and let the vehicle roll. The second is to use differential collective thrust on the main rotors to maintain the vehicle level providing a stable platform for lateral translation.

The third option is to roll into the relative wind thereby increasing the lateral component of the side force. If the differential thrust is not sufficient to provide the commanded roll angle, the vehicle is permitted to roll back to the position which provides the maximum crosswind hover capability.

FXA   =   LONGITUDINAL AERODYNAMIC DRAG FORCE

TAUX   =   AUXILIARY THRUST

FYA = LATERAL AERODYNAMIC DRAG FORCE
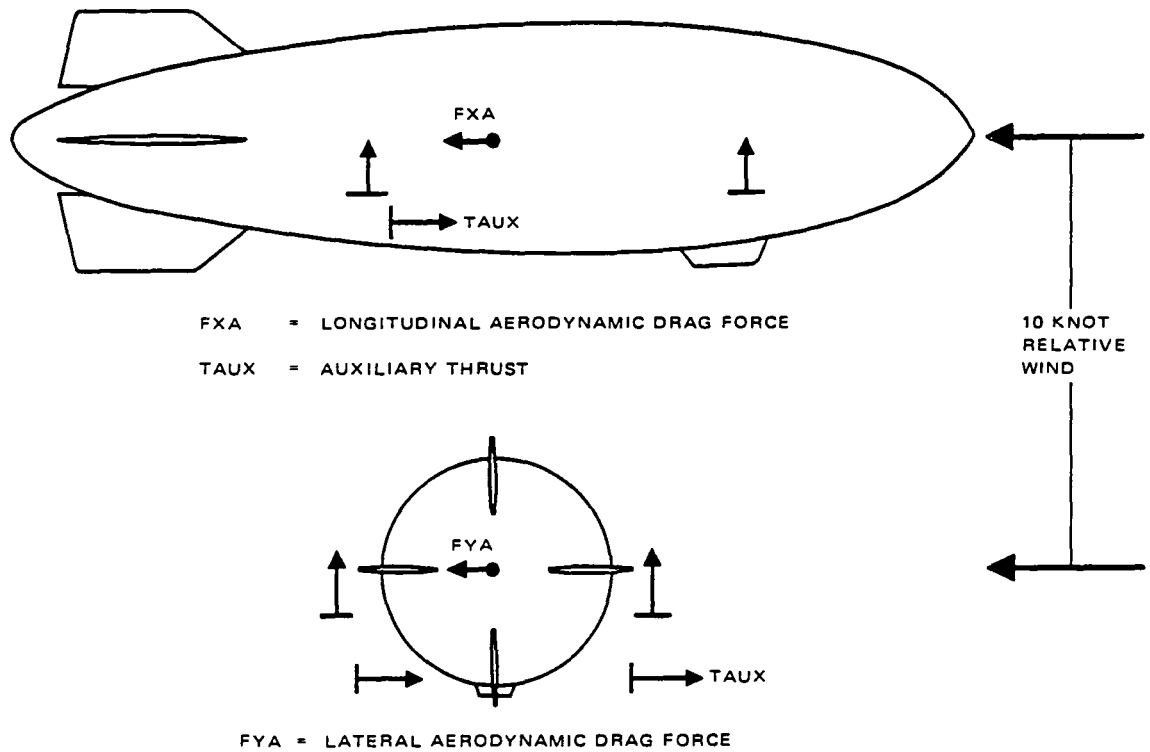
Figure 9-13 - Pitch and Roll Crosscoupling Effects

PITCH DIFFERENTIAL
THRUST AND LATERAL
CYCLIC COUPLE INTO
A NEGATIVE YAW

ROLL DIFFERENTIAL
THRUST AND LONGITUDINAL
CYCLIC COUPLE INTO A
POSITIVE YAW
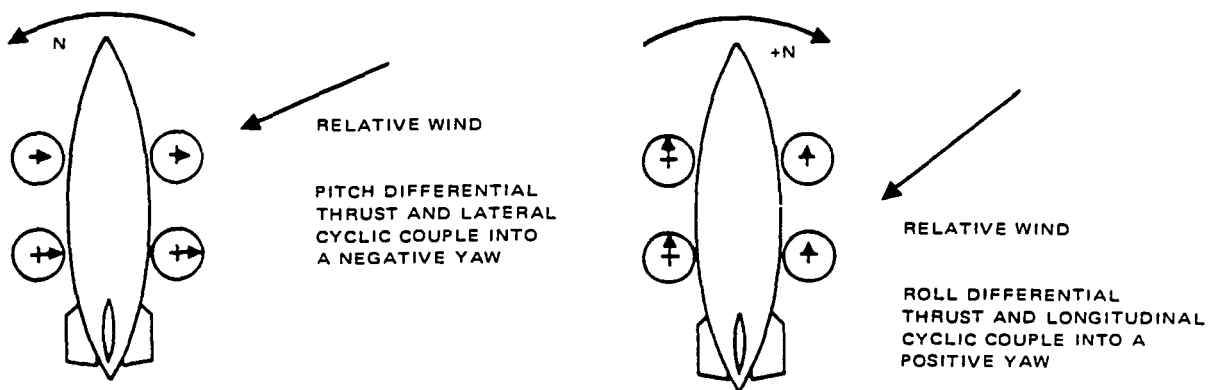
Figure 9-14 - Yaw Crosscoupling Effects
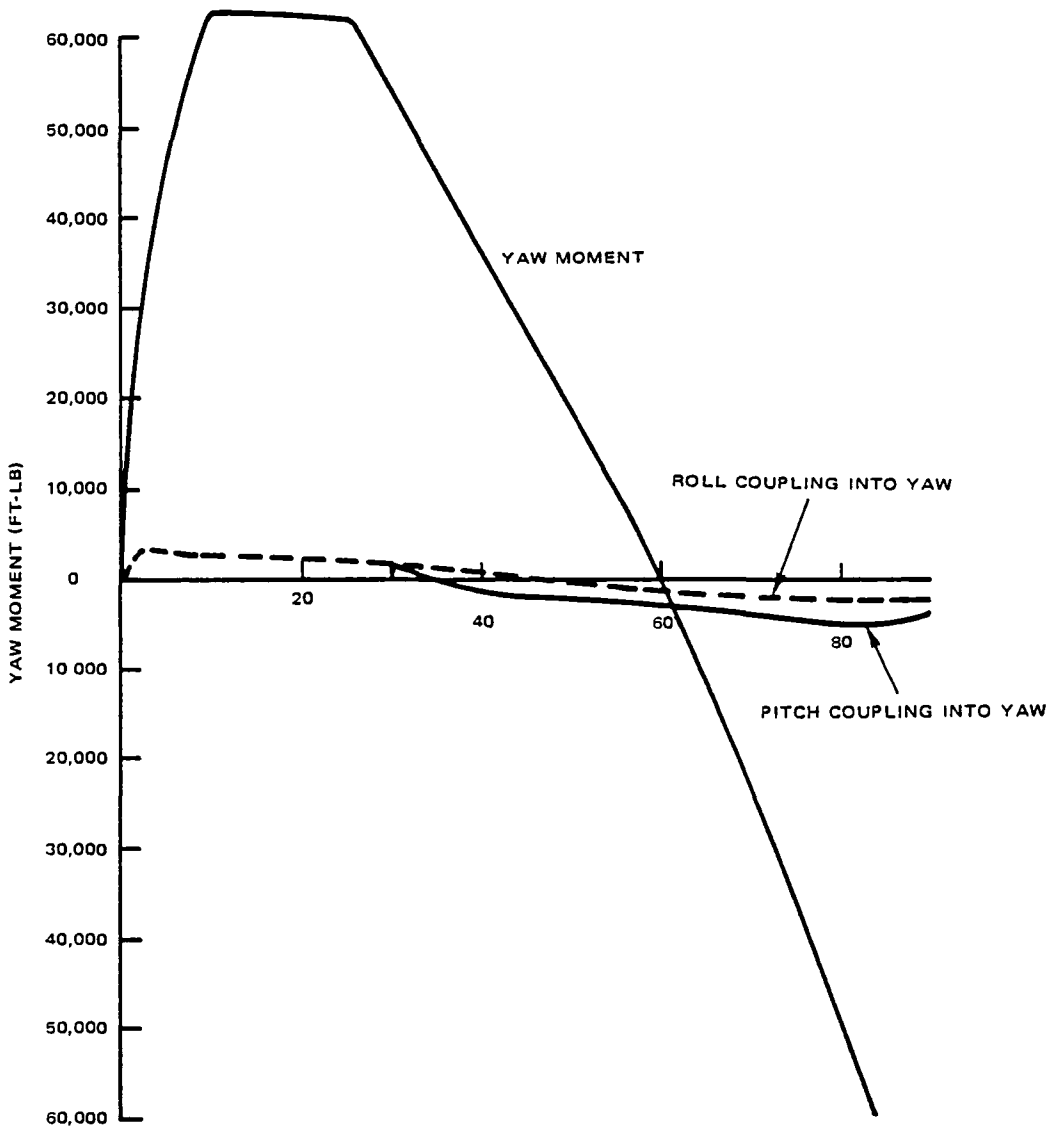
Figure 9-15 - Pitch and Roll Crosscoupling Effect on Aerodynamic Yawing Moment
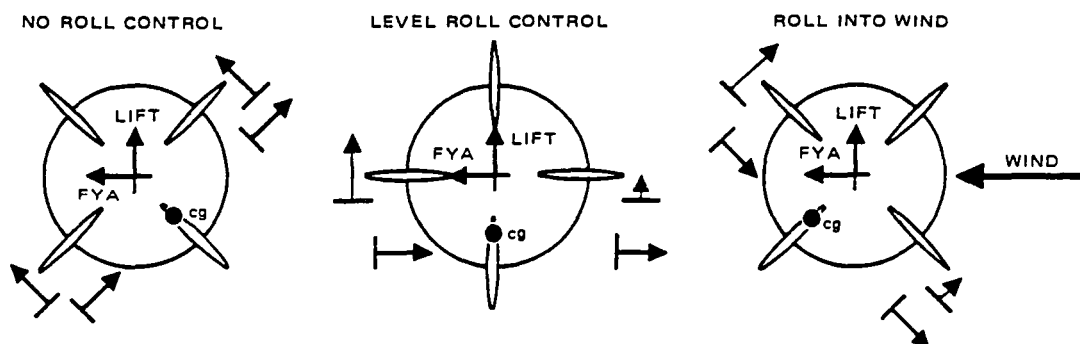
Figure 9-16 - Control Options for Crosswind Hover

The last option should obviously provide the most control, but the increase in control may not be enough to justify the disadvantages of having the vehicle roll.

These various lateral control options were evaluated at 90 percent main rotor thrust (maximum load) and 50 percent main rotor thrust (empty). The results follow.

(1) Lateral Control by Roll

This concept rolls into the wind to develop side forces. It relies totally on the main rotor thrust and does not use lateral cyclic or the lateral auxiliary thrustors. Figure 9-17 for 50 percent MRT shows the hover envelope for 5, 10, and 15 degrees roll. The 15 degree roll is obviously the best, stationkeeping in a 27 knot wind at 10 degrees and a 9.5 knot wind at 90 degrees.

In Figure 9-18 for 90 percent MRT, the commanded roll angle is 5 degrees, but because of the limited amount of differential main rotor thrust (+270 pound per rotor) the FRV can only achieve about 3.5 degrees roll into the wind. Performance is considerably degraded compared to 50 percent MRT as the FRV stationkeeps into an 18 knot wind at 10 degrees sideslip and a six knot wind at 90 degrees.

(2) Lateral Control with Lateral Thrust and Maintain Level

This concept uses differential thrust to maintain a level roll attitude and the lateral auxiliary thrustors and main rotor lateral cyclic (hinged +12 degrees in roll) to develop lateral side forces. Figure 9-19 shows the results for both 90 percent and 50 percent MRT. At 10 degrees both have a 31 knot hover capability. At 90 degrees the 50 percent MRT hovers in a 16 knot wind and the 90 percent MRT hovers in a 9.5 knot wind.

The hover capability beyond 10 degrees is better for 50 percent MRT. In 90 percent MRT, the MRT margin is insufficient to maintain the vehicle level without losing altitude.

Beyond 20 degrees lateral force is the limiting factor for 50 percent MRT. The 90 percent curve has a lump at about 40 degrees which is caused by the longitudinal drag coefficient going through zero. This eliminates the thrust required to maintain pitch, allowing more thrust to maintain roll, resulting in a higher wind trim capability.
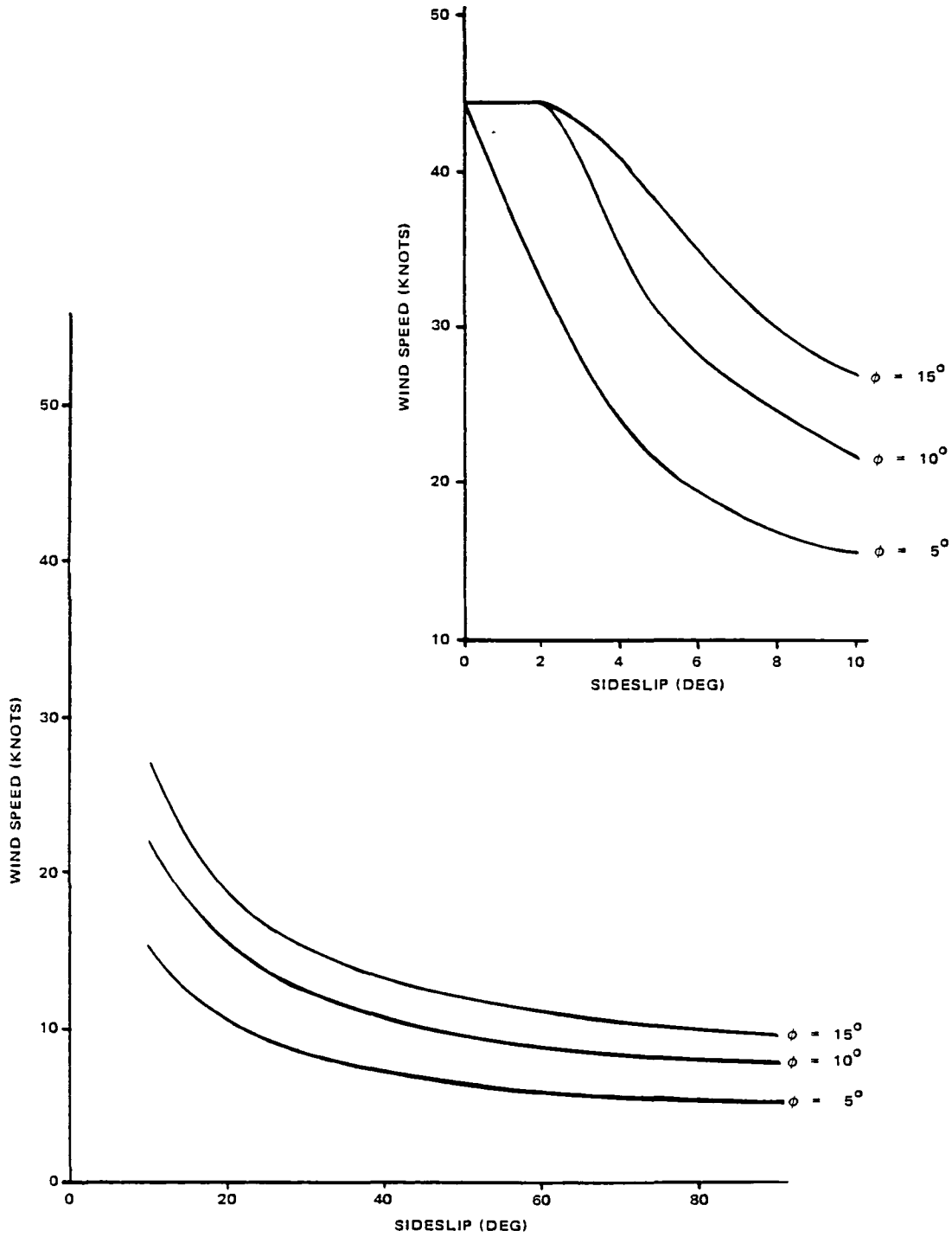
Figure 9-17 - Hover Flight Envelope with Roll-Induced
Lateral Control at 50% Thrust Level
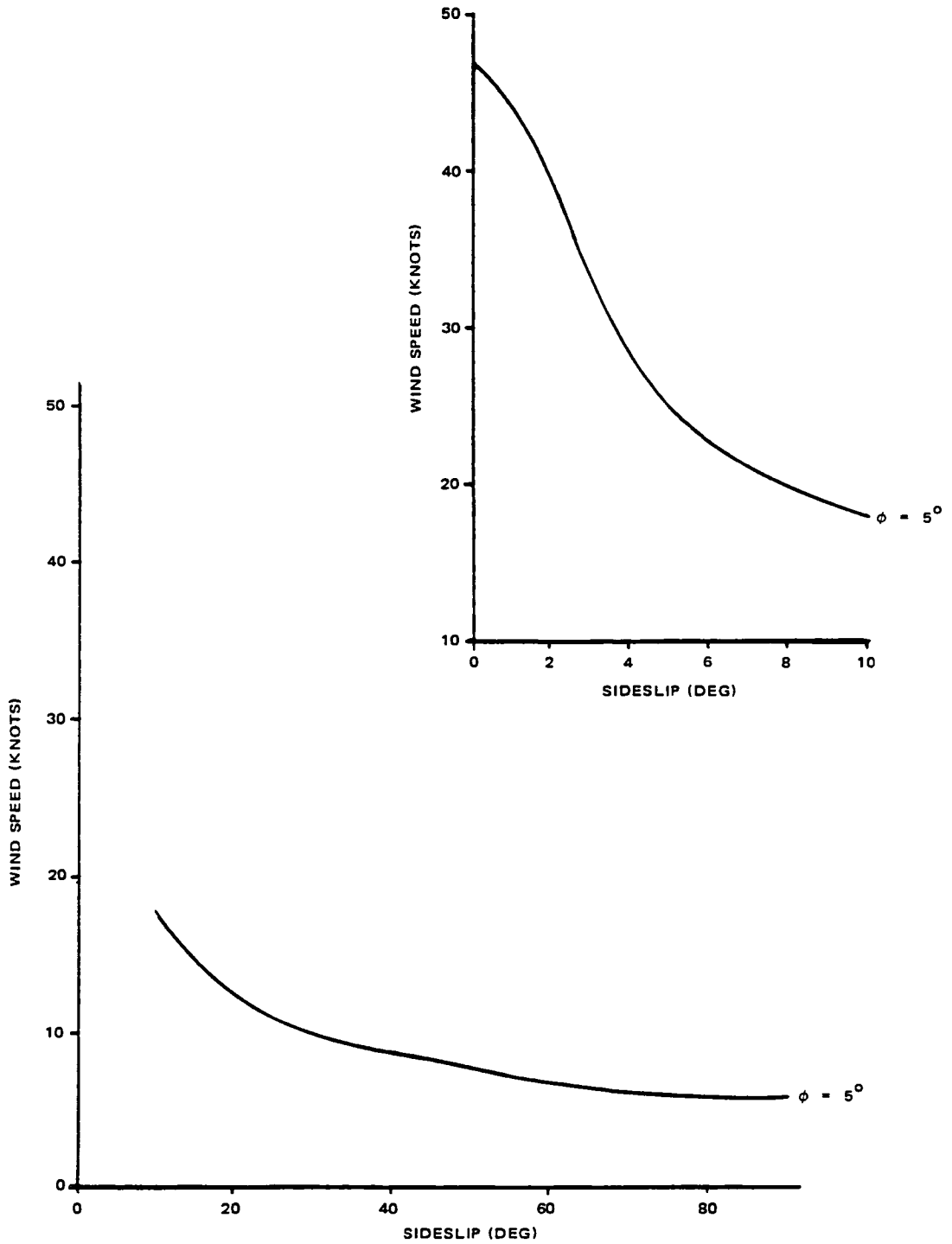
Figure 9-18 – Hover Flight Envelope with Roll-Induced
Lateral Control at 90% Thrust Level
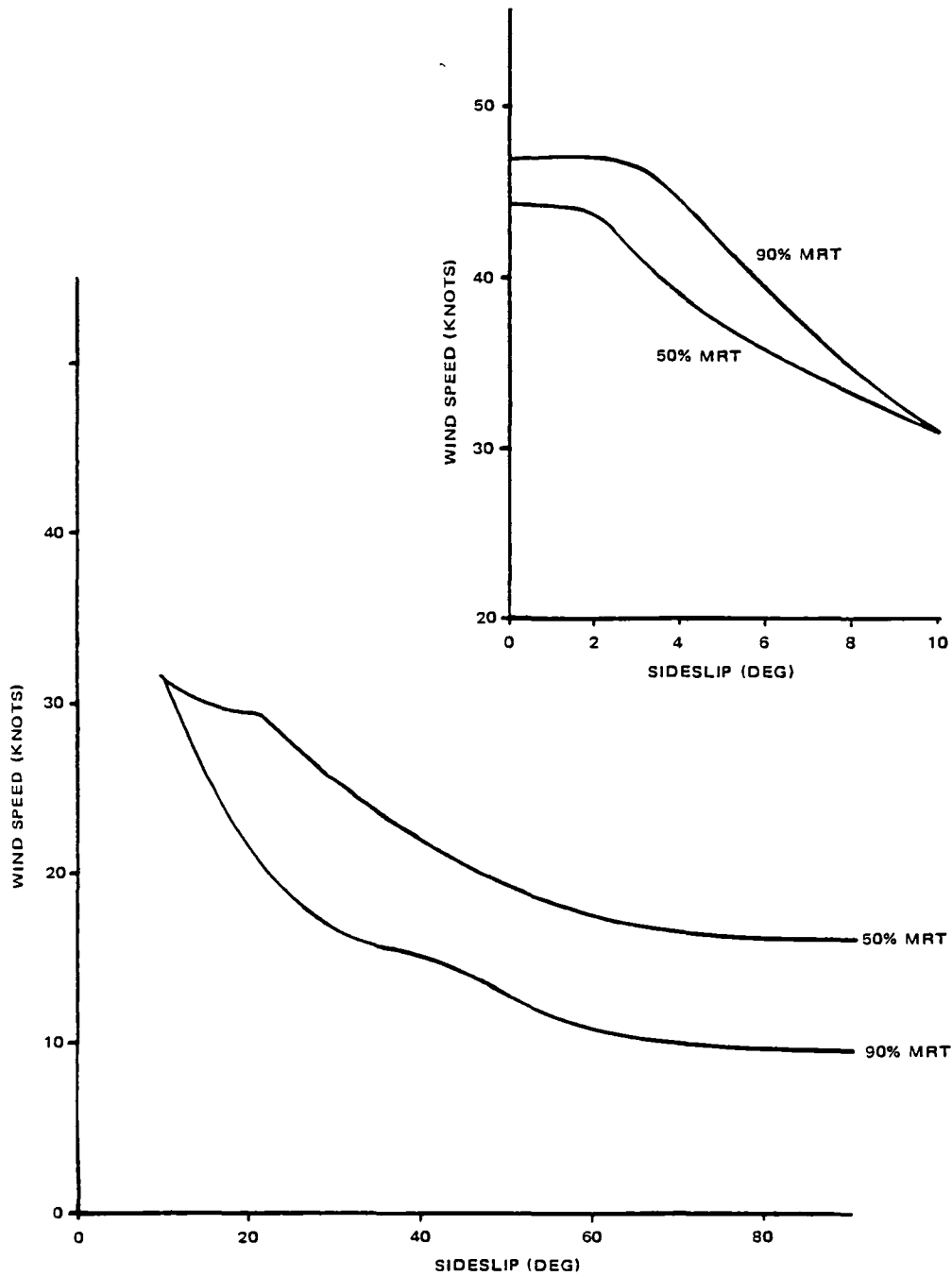
Figure 9-19 - Hover Flight Envelope with Lateral Control and Zero Roll Attitude

(3) Lateral Control with Lateral Thrust and Roll Into Wind

This concept uses lateral thrust and rolls into the wind to increase the lateral thrust. Figure 9-20 for 50 percent MRT shows the effect of rolling into the wind 5, 10, 15, and 20 degrees. The difference is small. This is because most of the lateral thrust is being provided by the auxiliary thrustors so that the added thrust from increasing the roll angle is small.

The fact that the wind velocity increases as the square root of the force is also a factor. On the average the wind velocity is 32 knots at 10 degrees and 17 knots at 90 degrees.

Figure 9-21 for 90 percent MRT shows the effect of trying to roll into the wind. In these examples the differential thrust is not sufficient to hold the commanded angle so it rolls away from the prevailing wind. The program is structured such that the FRV is not permitted to roll in either direction more than the commanded angle. At 10 degrees the windspeed is 33.5 knots. At 90 degrees the average wind speed is 12.5 knots.

The curves are identical below 10 knots because none of the commanded angles can be attained and the limiting factor is longitudinal thrust, not lateral thrust.

(4) Lateral Control with Lateral Thrust and No Roll Control

Figures 9-22 and 9-23 show a comparison of the three options of lateral control: no roll control, level roll altitude, and roll into the wind 10 degrees if possible.

Figure 9-22 at 50 percent MRT shows no control results in a 29.5 knot capability at 10 degrees and 12.5 knots at 90 degrees. No roll control is inferior to using one of the other methods of control, particularly beyond about 20 degrees. The difference between level control and rolling 10 degrees into the wind is insignificant.

Figure 9-23 for 90 percent MRT shows a different trend. Beyond 10 degrees the concept of maintaining level is not as effective as the other methods because the differential thrust to hold level is the limiting factor.

In both cases, 50 percent and 90 percent MRT, it is best to try to roll into the wind 10 degrees.

(5) Lateral Control with Helicopter Rigidly Attached

The addition of the helicopter on the roll hinge would be a costly and complicated mechanism. Figures 9-24 and 9-25 compare the concept of having the helicopters rigidly attached and using 4 degrees of lateral cyclic with the helicopters hinged $\pm$12 degrees. In general, the difference is only a loss of 1 to 2 knots capability. This is small and probably not worth the expense of putting the helicopters on the hinge, except possibly to demonstrate the performance of a moving rotor near the envelope.

(6) Control Margins in Hover

In the previous examples the curves were generated assuming 100 percent of the auxiliary thrust is available for countering winds. Figure 9-26 shows the hover envelopes for 90, 70 and 50 percent of main and auxiliary rotor thrusts.
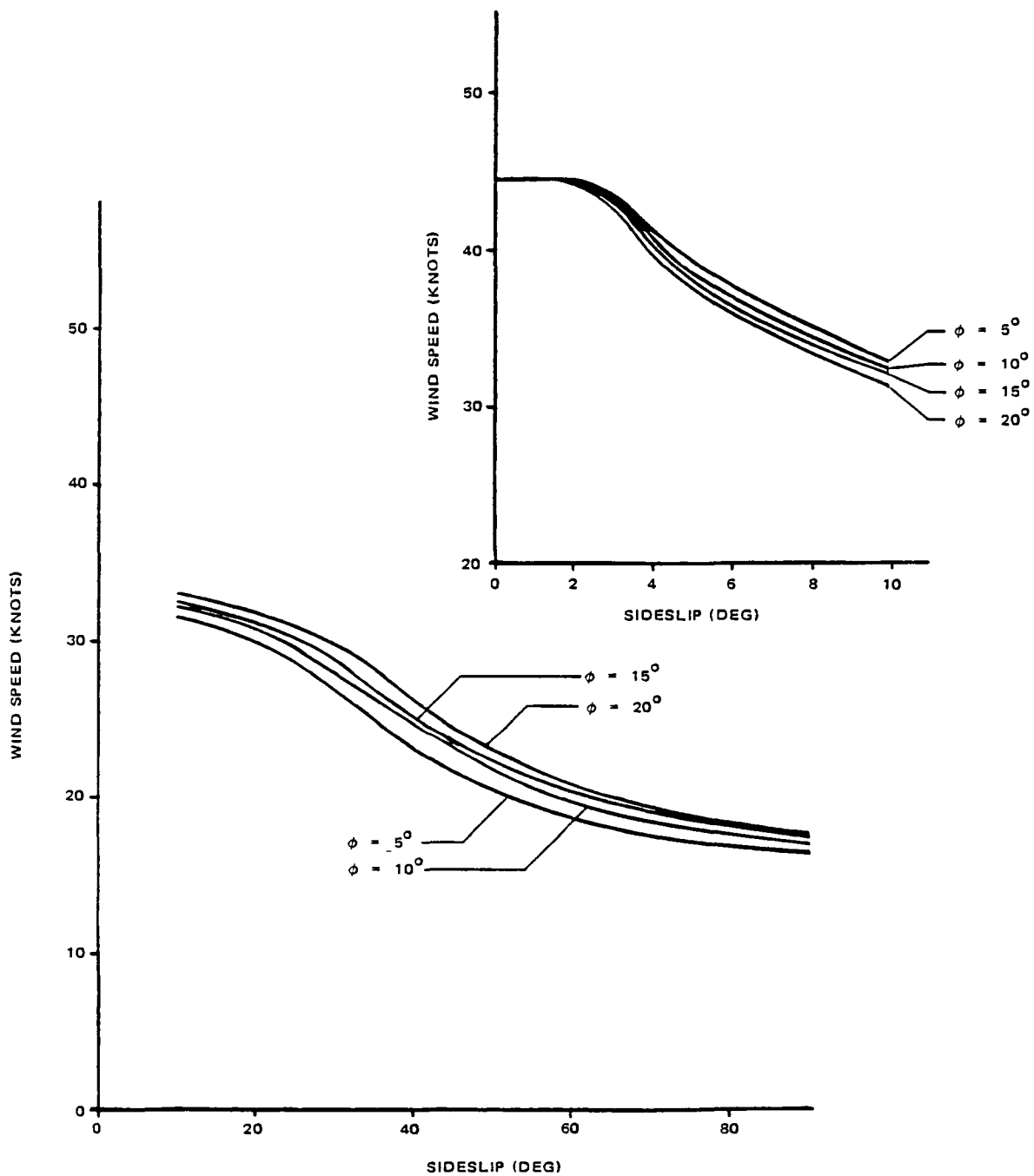
Figure 9-20 – Hover Flight Envelope with Lateral Control and
Rolling into the Wind at 50% Thrust Level
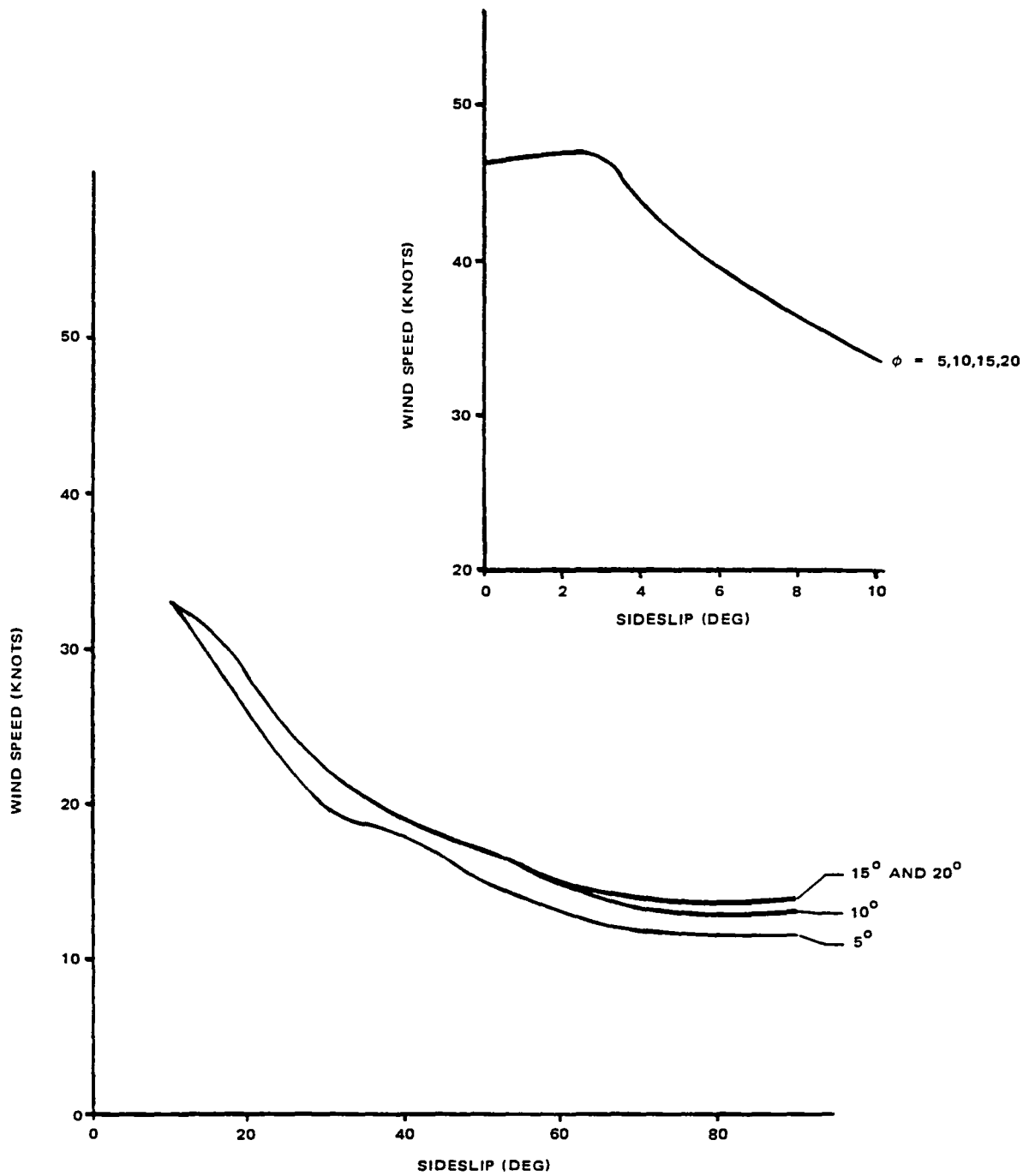
Figure 9-21 – Hover Flight Envelope with Lateral Control and
Rolling into the Wind at 90% Thrust Level
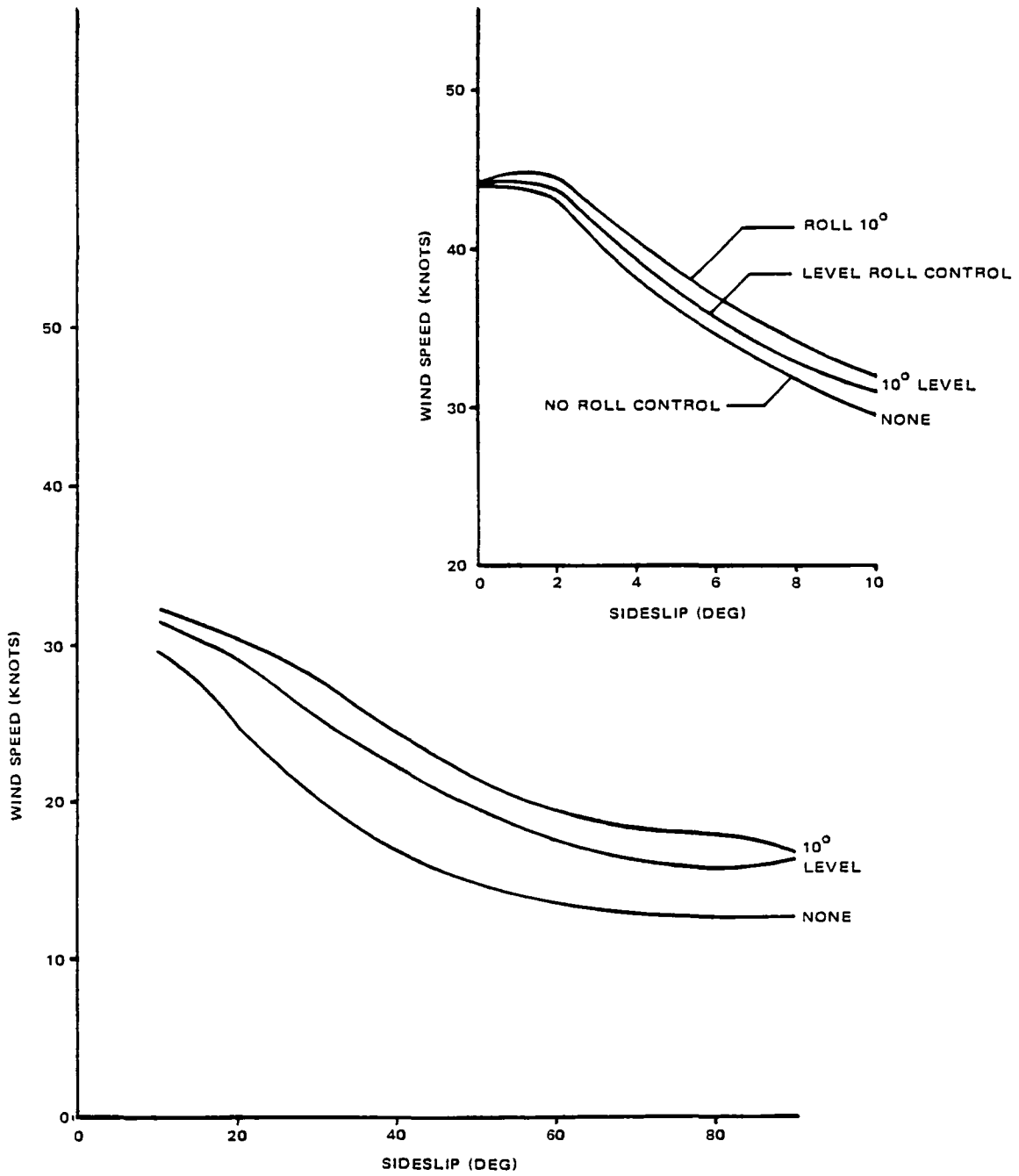
Figure 9-22 - Hover Flight Envelope for Various Modes of
Lateral Control at 50% Thrust Level
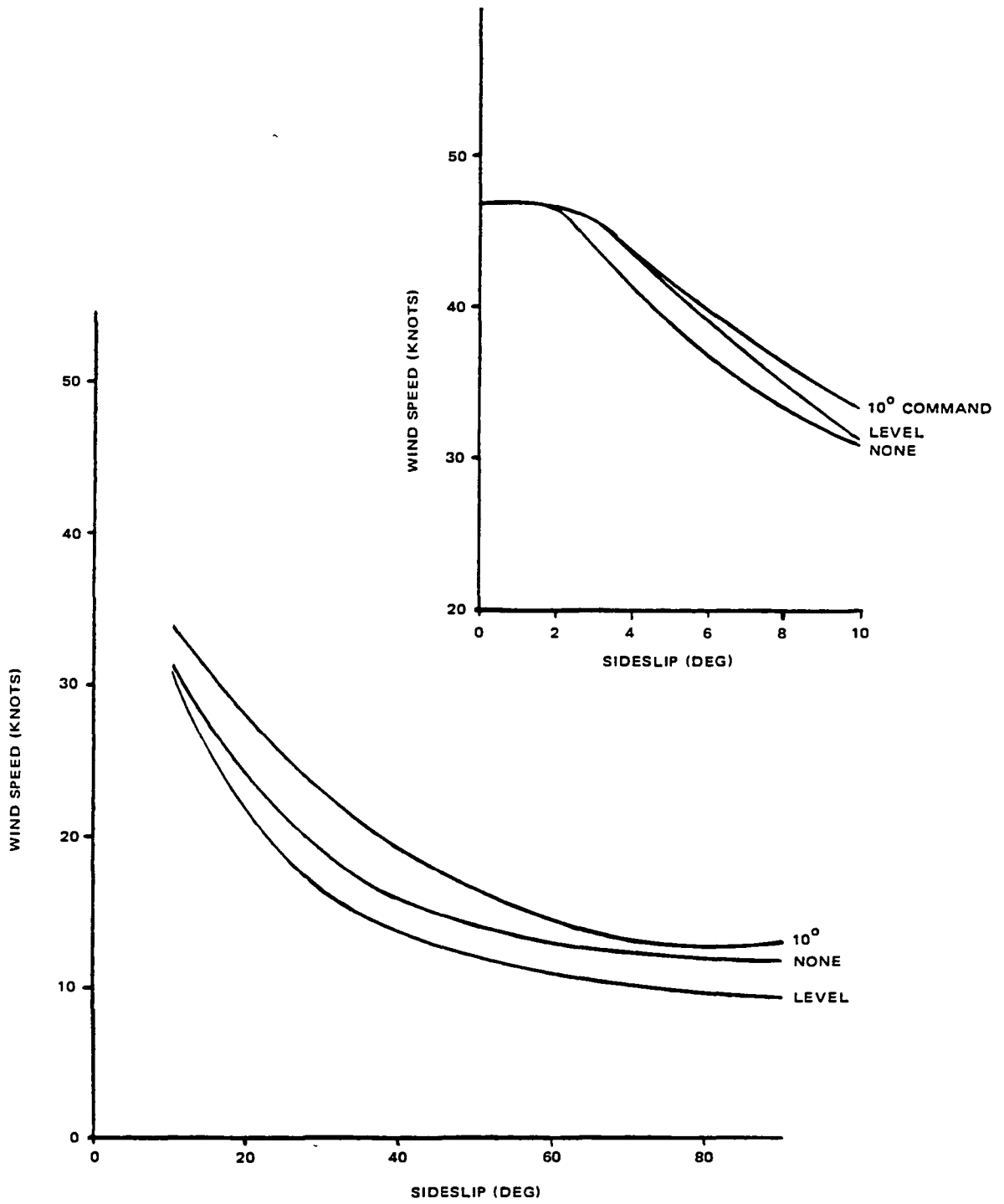
Figure 9-23 – Hover Flight Envelope for Various Modes of
Lateral Control at 90% Thrust Level
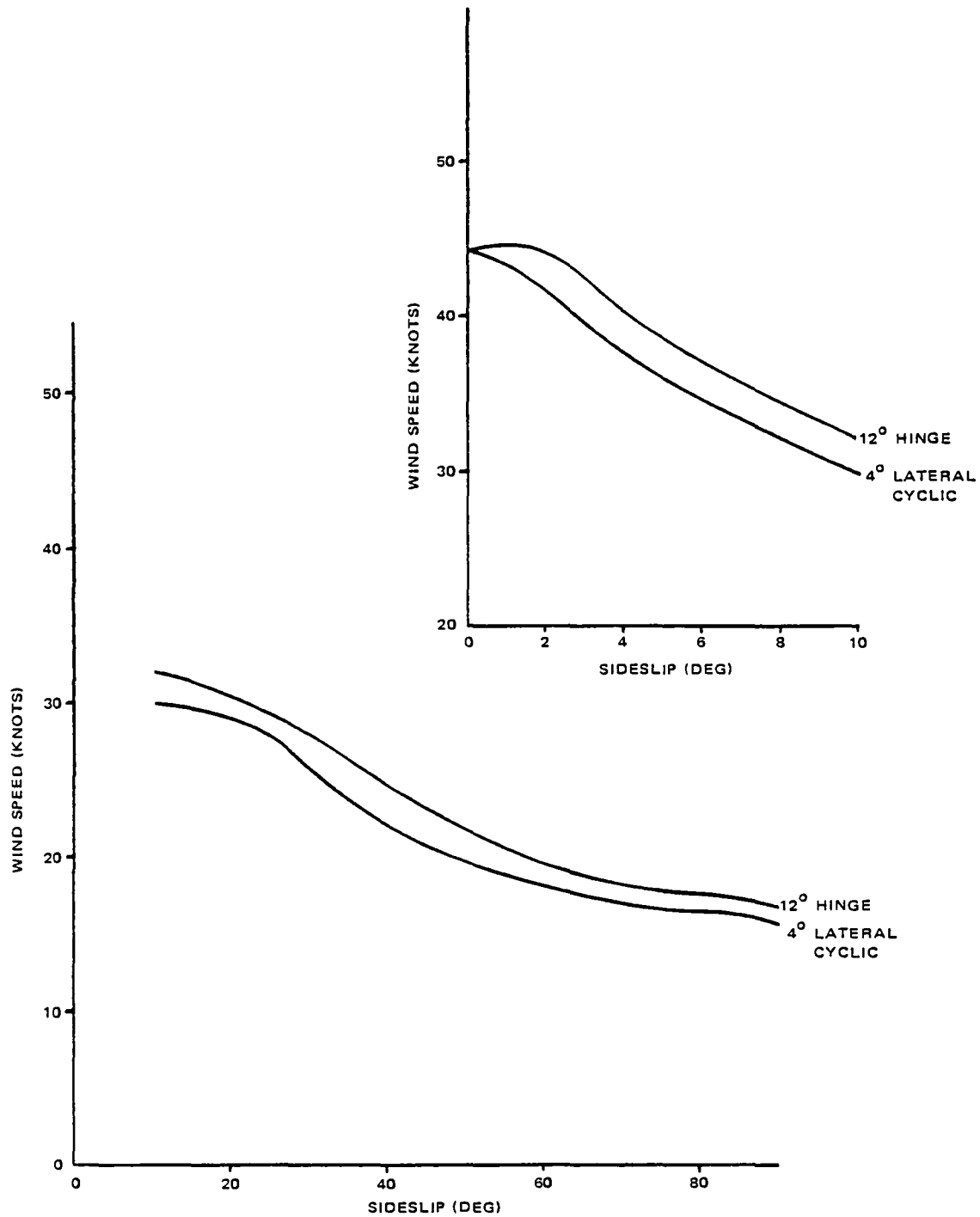
Figure 9-24 - Hover Flight Envelope Comparison for Rigidly Attached and Hinged
Helicopters at 50% Thrust Level
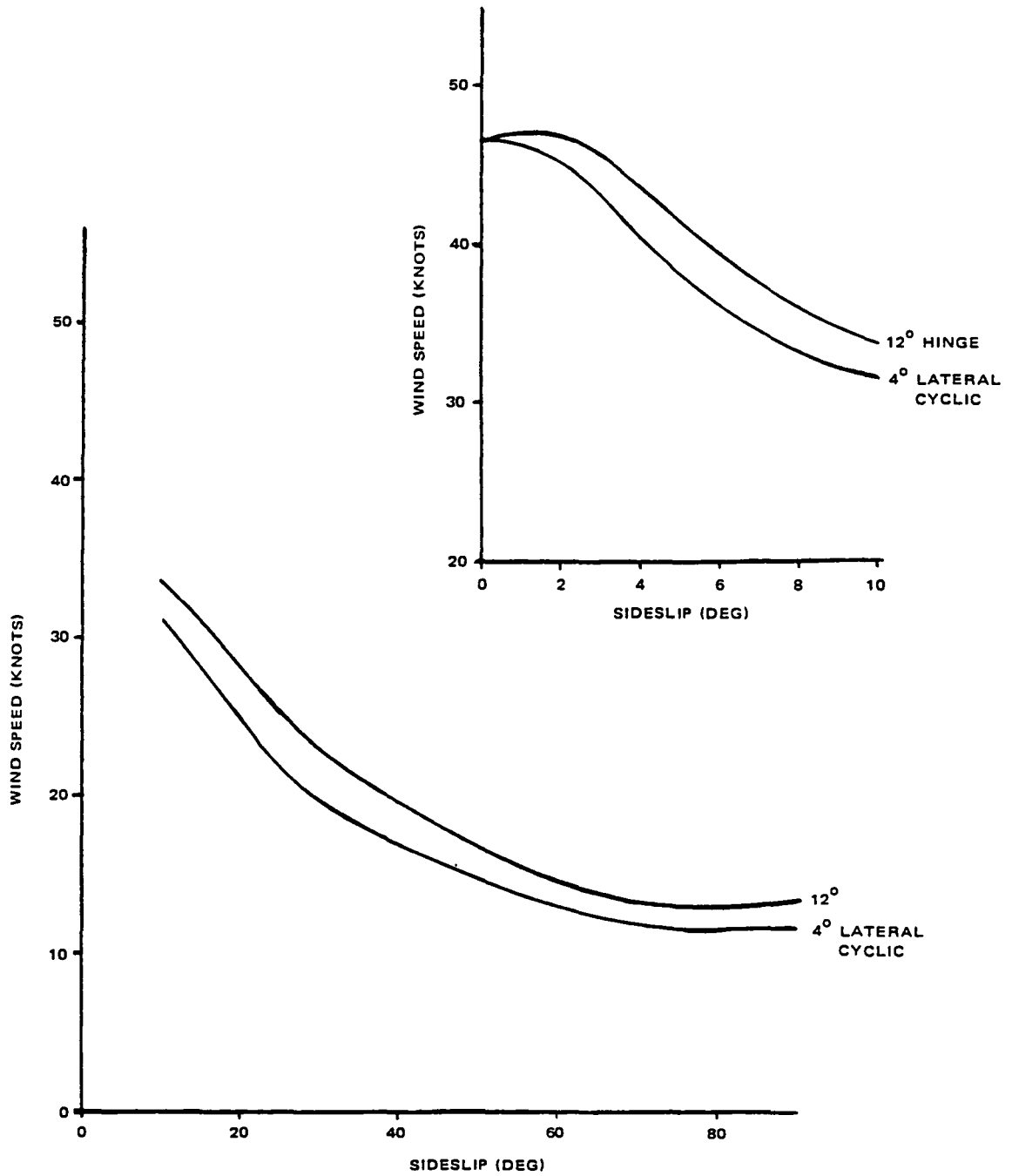
Figure 9-25 - Hover Flight Envelope Comparison for Rigidly Attached and Hinged
Helicopters at 90% Thrust Level
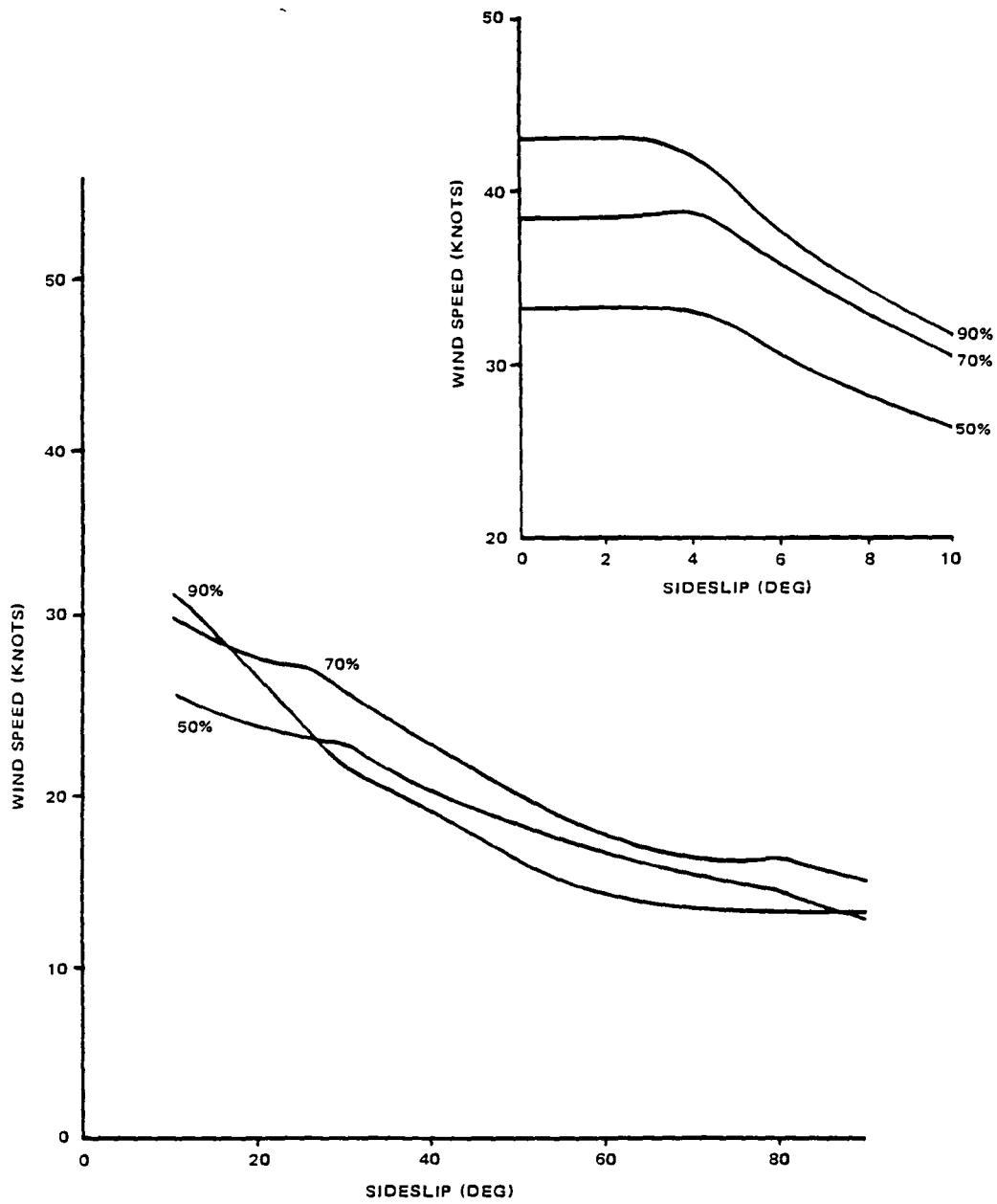
Figure 9-26 - Control Margin Effect on Hover Flight Envelope

(7) Summary of Lateral Control Results

Table 9-2 is a brief summary of the relative capabilities of the lateral control methods. This was computed by averaging the flight envelope operating points at 10 and 90 degrees sideslip for 50 and 90 percent MRT. This "figure of merit" shows that using roll only is very ineffective and all other methods are almost equal.

The method of rolling into the wind 10 degrees has some advantage over holding level, particularly at 90 degrees and 90 percent MRT. It also has a definite advantage over no roll control at 90 degrees and 50 percent MRT.

All of these methods should be evaluated on the flight simulator and in FRV flight tests to determine the best method of hover control.

TABLE 9-2 – SUMMARY OF LATERAL CONTROL METHOD CAPABILITIES

Lateral control method	90% MRT		50% MRT		Figure of merit average
	10 deg	90 deg	10 deg	90 deg	
Roll only 10 deg	18 kt	6 kt	21.5 kt	8 kt	13.4 kt
Level	31	9.5	31	16	21.9 kt
Roll into wind 10 deg	33.5	12.5	32	17	23.8 kt
No roll control	31	12 kt	29.5	12.5	21.3 kt

5. CONTROL POWER REQUIREMENTS

One of the principal operational requirements of the FRV is to be able to hover in a prevailing wind and have adequate control power to trim the vehicle following its disturbance from a steady state.

To examine the control power available while operating in a windy environment, the vehicle is initially trimmed while it is hovering into a headwind. Subsequently, a unit step input to its longitudinal stick is applied and the resulting increment in ground speed in five seconds is determined by considering complete motion of the vehicle (Figure 9-27).

In this case autopilots were used to maintain constant altitude as well as zero heading and pitch attitude. It is found that the vehicle without its payload tends to accelerate better in lower headwinds. With its payload, it tends to accelerate better at higher headwinds. This indicates a trade-off between the additional inertia of the vehicle due to its payload and the incremental aerodynamic drag at higher wind speeds.

The response of the vehicle to a unit step input to its lateral stick while the vehicle is hovering in a crosswind was also examined (Figure 9-28). Here the vehicle was rolled into the wind by applying roll command simultaneously. Albeit the isolated lateral control power available is larger for the vehicle with a payload rather than by itself, in operation the same could not be realized, because of the significant crosscoupling between the lateral and roll motion of the aircraft.
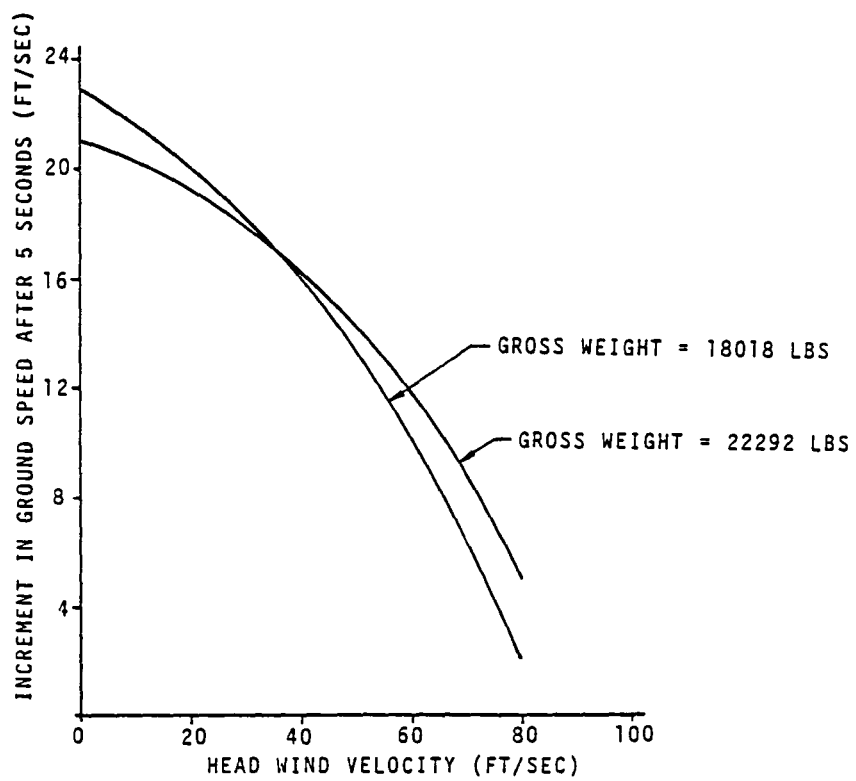
Figure 9-27 - Vehicle Response to a Unit Step Input to its
Longitudinal Control in a Prevailing Headwind
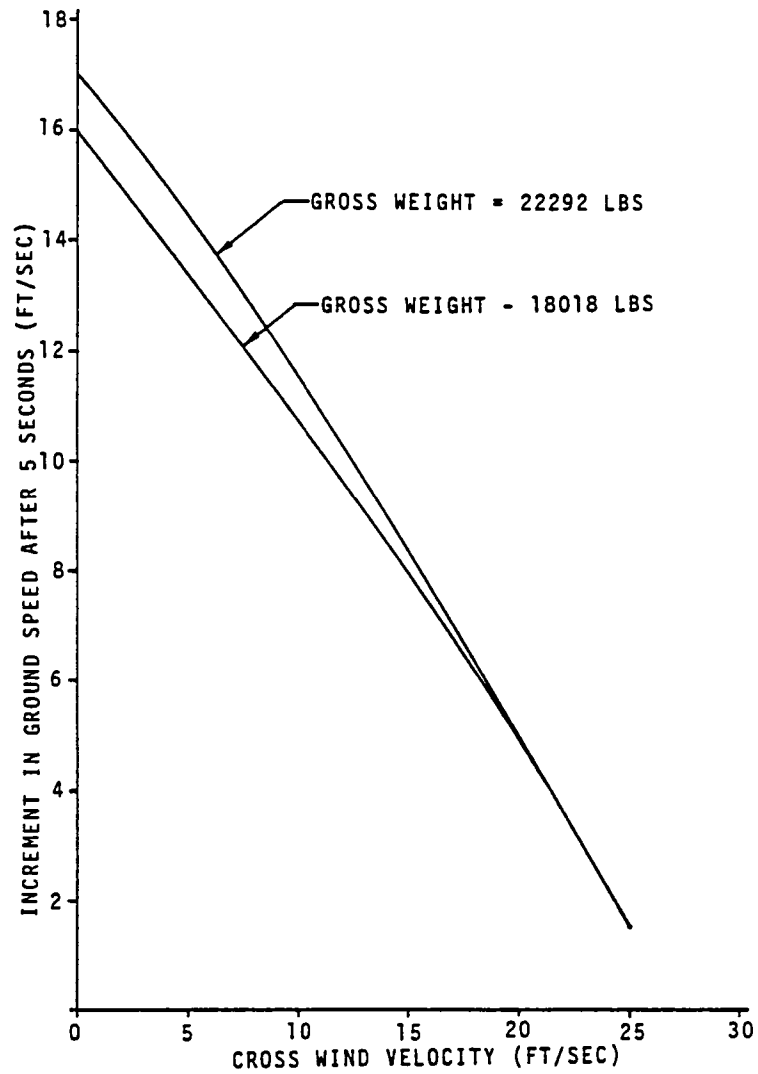
Figure 9-28 - Vehicle Response to a Unit Step Input to its
Lateral Control in a Prevailing Crosswind

6. RESPONSE TO WIND DISTURBANCES

The capabilities of the FRV and hence, the quad-rotor hybrid airship concept itself, to perform under adverse weather conditions depends upon the adequacy of its control for satisfactory operation. To evaluate the selected control logic in meeting the required vehicle performance in hover, various operational flight conditions involving step changes in wind magnitude and shifting wind direction were chosen.

Initially, the vehicle is trimmed in hover in still air or a prevailing wind. Simple autopilots consisting of position and rate feedback are used to form a closed loop control logic that would come into play when the vehicle is disturbed from its trim. The pitch and roll atti tudes are commanded to zero value while maintaining constant heading. An altitude autopilot is used to maintain a reference height of 300 feet. The position on the ground is maintained by longitudinal and lateral position autopilots.

Table 9-3 shows the closed loop response of the FRV to several wind disturbances without a payload.

In comparing maximum excursions of the vehicle, it was found that presence of the payload has no favorable effect on vehicle response, albeit larger control forces and moments are produced. This can be explained by noting the control power lost in decoupling the inherent crosscouplings of longitudinal-pitch and lateral-roll controls, which tend to offset the increment in control forces and moments due to the payload.

The relatively short excursions could perhaps be attributed to the large time constant of the vehicle or its sluggishness and the assumption of instantaneous tilting of the thrust vectors and availability of vehicle motion cues.

7. VEHICLE RESPONSE TO SYSTEM FAILURES

Since the FRV is a unique, experimental aircraft, its failure modes need a thorough investigation both on ground and in flight. The hybrid nature of the vehicle lends itself to a combination of emergency modes of operation associated with power failure in a conventional airship and helicopter.

When the vehicle is hovering without any payload and low on fuel, it is approximately 3000 pounds heavy, which permits it to maintain altitude and land safely in the event of power failure in one of the helicopters. However, when the vehicle is hovering with a 5000 pound payload and full fuel of 3200 pounds and has power failure in one of the helicopters, it would descend quickly and develop significant pitch or roll attitude which could be uncontrollable. Consequently, several failure modes of the vehicle were simulated to determine the severity of the effect of helicopter power failure on the vehicle flight safety.

In a case where the FRV with a payload of 4175 pounds, hovering at an altitude of 300 feet in still air, experienced right front helicopter power failure, the vehicle developed peak roll rate of 10 degrees per second and peak roll altitude of 30 degrees before reaching a steady roll angle of 10 degrees (Figure 9-29). Meanwhile, it also developed a steady nosedown pitch attitude of 3 degrees and a descent rate of 1200 feet per minute.
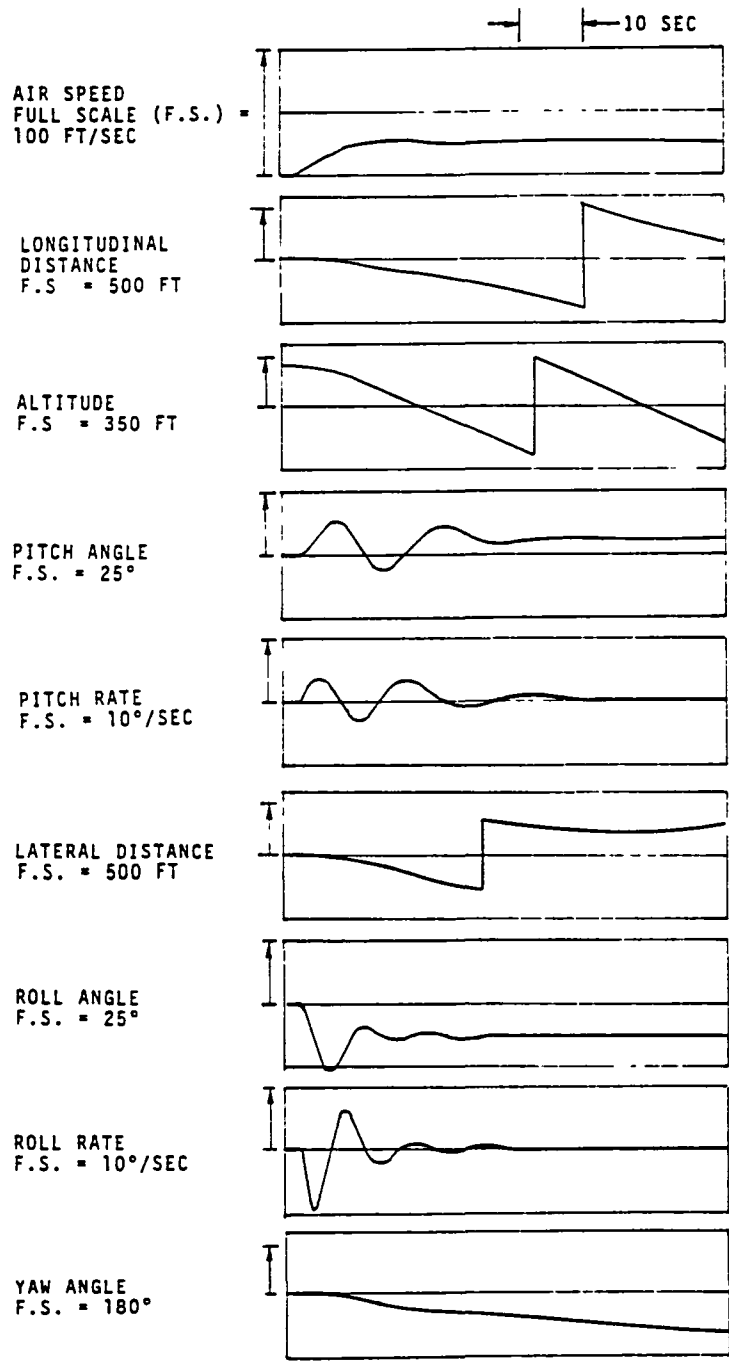
Figure 9-29 – FRV Open Loop Response to Power Failure
in the Right Front Helicopter

TABLE 9-3 - CLOSED LOOP RESPONSE TO WIND DISTURBANCES

HOVER TRIM	STEP INPUT	VEHICLE WITHOUT PAYLOAD (GW - 18018 LBS)					
		MAXIMUM ERROR			CONTROL INPUT		
		x (FT)	y (FT)	ψ(DEG)	LONSTK(%)	LATSTK(%)	YAWC(%)
$V_W = 15$ KTS $\psi_W = 30°$	$\Delta\psi_W = 10°$	0	-4.9	-1 35°	-0 5	67	7.5
$V_W = 0$	$\Delta V_W = 10$ KTS $\Delta\psi_W = 30°$	-0.2	-1 4	-0.9°	1	20	5
$V_W = 10$ KTS $\psi_W = 30°$	$\Delta\psi_W = 10°$	0	-2.1	-0 9	-1	27.5	3
$V_W = 5$ KTS $\psi_W = 30°$	$\Delta V_W = 10$ KTS	-0.2	-1.4	-0.9	1	20	5
$V_W = 0$	$\Delta V_W = 10$ KIS $\Delta\psi_W = 90°$	1 3	-3 3	4 5	-15	45	-15

When a similar failure occured on the rear left helicopter (Figure 9-30), the vehicle responded similarly in roll and also developed a noseup pitch attitude of six degrees. In this case, it also descended at a rate of 1200 feet per minute.

However, when the power of the rear left helicopter was automatically shut off simultaneously with the right front helicopter power failure, the vehicle developed a steady noseup pitch attitude of 3 degrees while descending at a rate of 1750 feet per minute (Figure 9-31).

A failure in the control system of the vehicle that resulted in maximum thrust on the right front helicopter rotor while others remained at their trim values, was also simulated. The consequent response of the vehicle (Figure 9-32) indicates strong pitch and roll oscillations with peak amplitudes of 35 degrees and 20 degrees, respectively, accompanied by climb in altitude and lateral drift. Meanwhile, the vehicle was also found to develop a steady yaw rate. It should be possible to control the vehicle in this situation by shutting off the power to the failed rotor.

A similar control failure of the rear left helicopter rotor caused the vehicle to develop a nosedown pitch attitude of 13 degrees and right roll attitude of 9 degrees with a descent rate of 330 feet per minute (Figure 9-33).

It is anticipated that a pilot on board could intervene following these failures, recover the vehicle in flight, and be able to land safely. This might involve shutting down the failed and diagonally opposed rotor. Maximum safety can be ensured in this situation by jettisoning the payload as part of the recovery procedure.
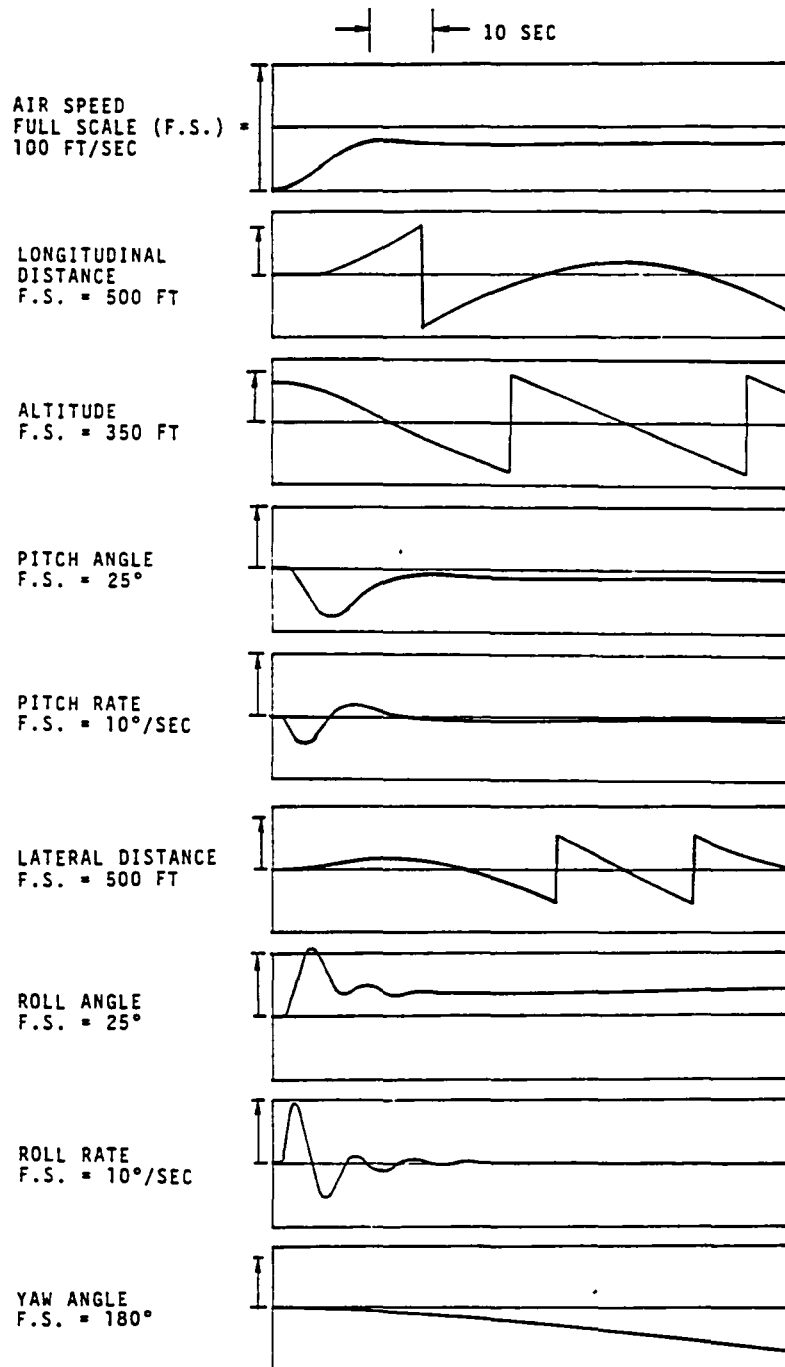
Figure 9-30 - FRV Open Loop Response to Power Failure
in the Left Rear Helicopter
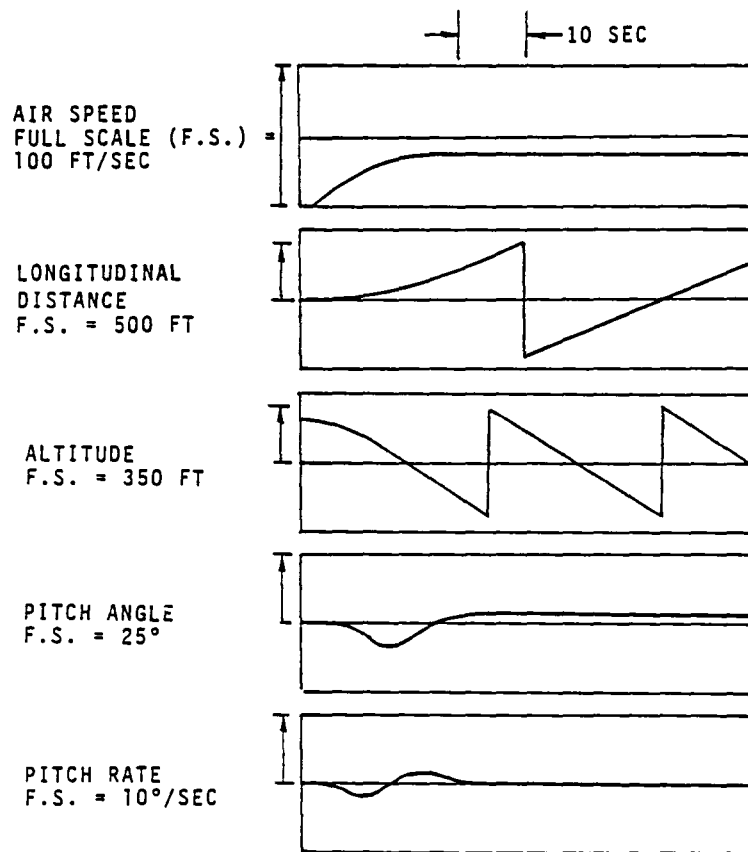
Figure 9-31 – FRV Open Loop Response to Power Failure in Right Front Helicopter
and Simultaneous Power Shut-Off in Left Rear Helicopter
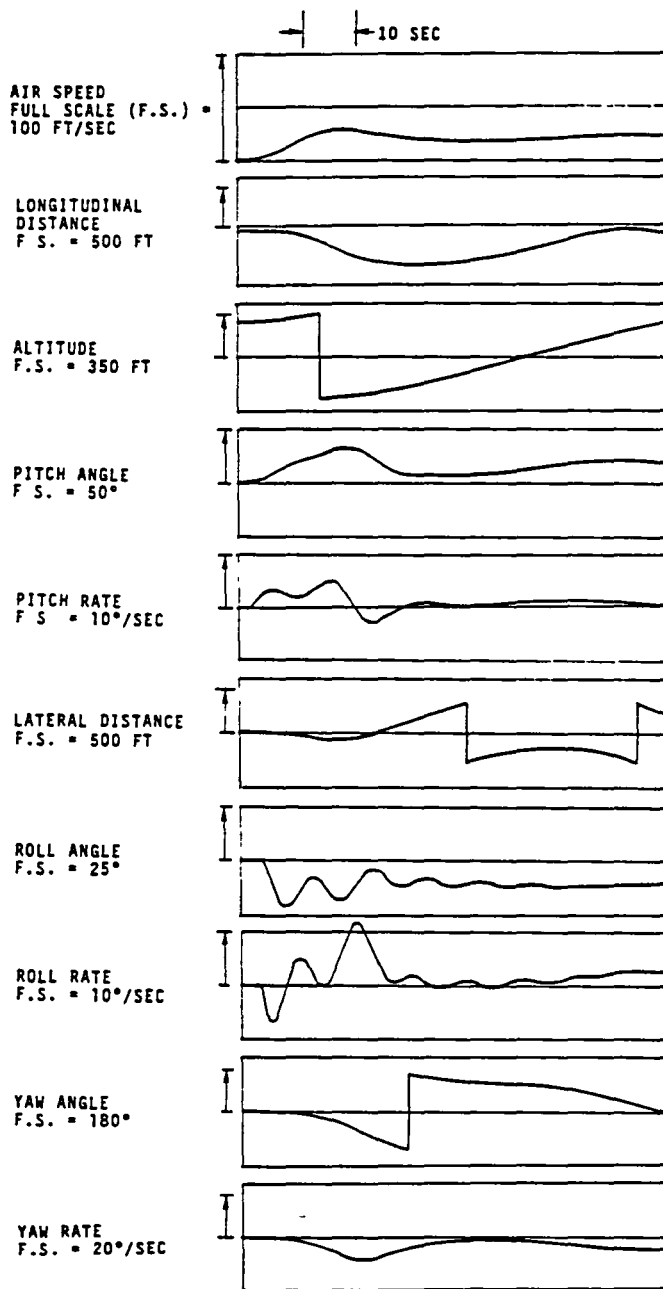
Figure 9-32 - FRV Open Loop Response to Control System
Failure in Right Front Helicopter
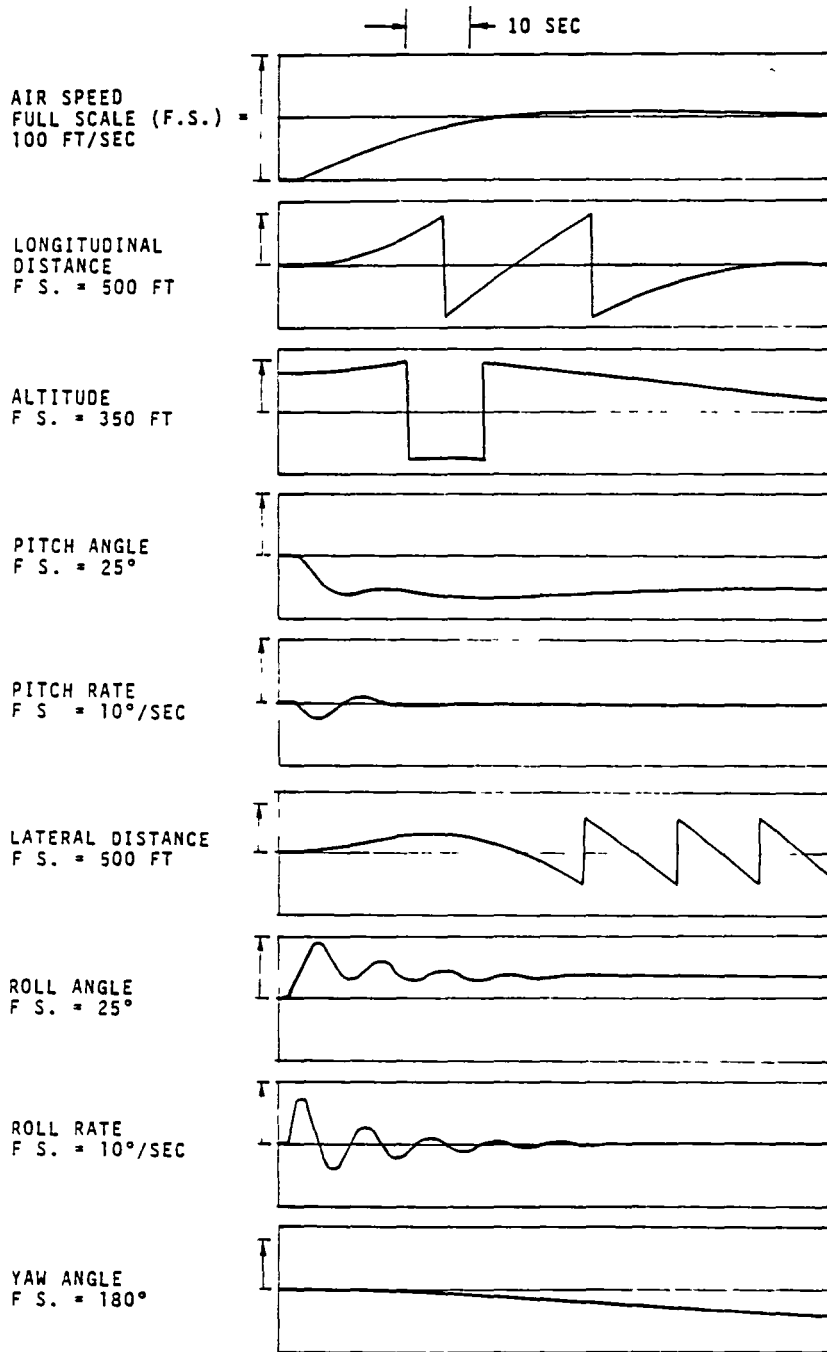
Figure 9-33 - FRV Open Loop Response to Control System Failure in Left Rear Helicopter

SECTION X - ACQUISITION COST AND SCHEDULE

1. GENERAL

The vehicle resulting from this preliminary design study has been configured to take maximum advantage of existing hardware and major components. As such, a sophisticated approach to acquisiton cost utilizing in-house computer programs would not result in the most meaningful or realistic values. The more conventional approach to estimating vehicle cost therefore will be followed. Acquisition cost is defined herein as the sum of research, development, test and evaluation (RDT&E) plus fabrication.

As the vehicle system is essentially an integration of a collection of existing hardware assets, a building block approach to the estimation of acquisition cost is used to establish an overall figure. This approach permits various cost options to be considered.

2. MAJOR COST ELEMENTS

The major cost elements of the vehicle are presented in Figure 10-1. A brief description of the composition of each is presented.

Note that the cost figures quoted in this section do not reflect an authorized quotation of vehicle development and manufacturing costs. They are provided merely as a reasonable approximation of the FRV's predicted acquisition cost.

Concurrent with the vehicle design and fabrication phases, an intensive training program will be carried out for all ground and flight crews.

a. Engineering

This element will include all the engineering design, development, and analytic effort.

Preliminary design work has been accomplished to the extent that the configuration has been established. The stress and structural dynamics problems have been sufficiently identified for solution in the detail design phase. Preliminary control and performance analyses have established vehicle feasibility and will be further developed in the advanced phases of the program.

The major areas of investigation together with identifiable tasks that will be required in the continued development of the FRV are listed in Table 10-1.

All engineering effort to prepare detail drawings on all major subsystems as well as the analyses to support the design are included in this area. Development effort such as flight control system design, and flight and structural dynamics simulations are also described. Data requirements include technical, operational, and training manuals necessary to support test, evaluation and training operations.

AIRSHIP/HELICOPTER
SYSTEM
FRV

ENGINEERING

— SUBSYSTEM DEVELOPMENT

— DETAIL DESIGN

— DETAIL ANALYSES

— DATA

— PROJECT MANAGEMENT

FABRICATION

— MANUFACTURING

— QUALITY ASSURANCE

— TOOLING

— MANUFACTURING PLANNING

— ERECTION

— SPARES

TESTING

— TEST STANDS AND FIXTURES

— STATIC TESTS

— GROUND TESTS

— FLIGHT TESTS

— FLIGHT OPERATIONS

Figure 10-1 – Major Cost Elements
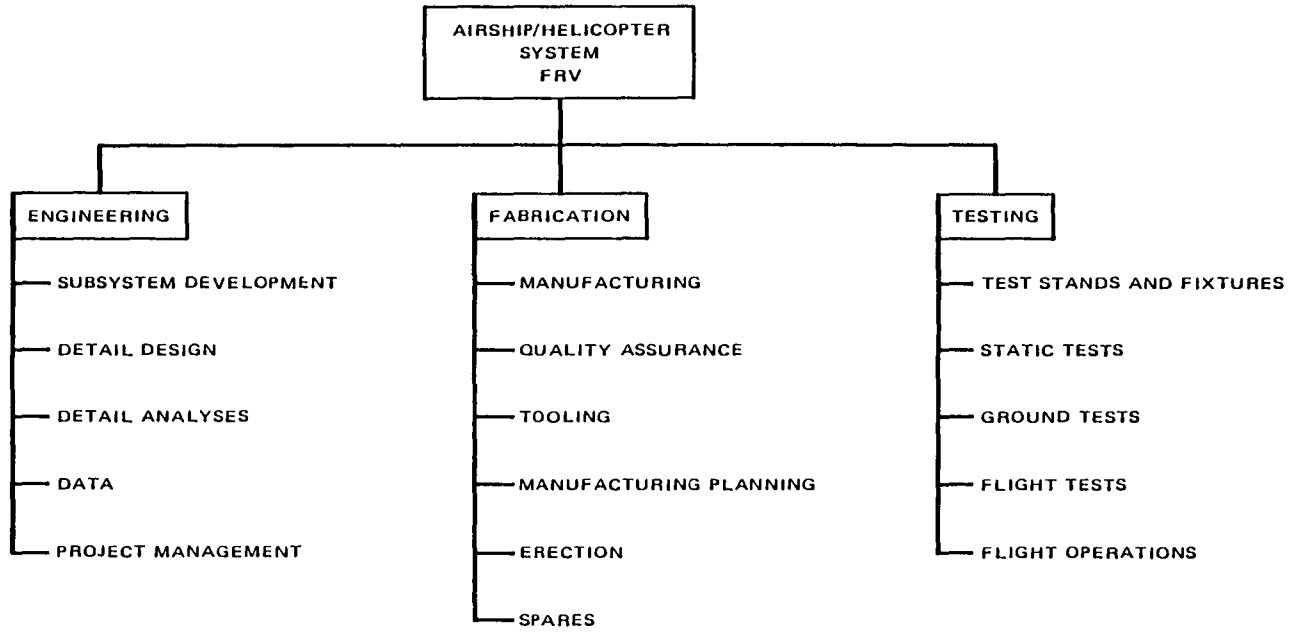
TABLE 10-1 - ADVANCED ENGINEERING REQUIREMENTS

Discipline	Key Tasks	Task sub-elements
Aerodynamics	Define component characteristics and derivatives (wind tunnel tests)	Rotors, propellers, module fuselage, envelope, payload.
	Model the vehicle to assess impacts on system derivatives	Rotor location, propeller location, envelope radius of curvature, empennage size and configuration, ground effects, turbulence response.
Structural Dynamics	Validate envelope finite element model	
	Model and validate interconnecting structure using NASTRAN	
	Compute and validate natural vibrational characteristics of the outrigger structure	
	Develop rotor force model	
	Perform aeroelastic stability analysis	Ground resonance model, air resonance model whirl flutter model, mechanical instabilities model, static aerodynamic instabilities model.
	Estimate fatigue of structural components	
Flight Controls	Design pilot's controls, rotor module requirements power supply and installation	
	Fabricate and laboratory test	
Flight Simulation	Enhancement of real-time piloted simulation	

b. Fabrication

This element involves parts manufacturing, quality assurance (inspection), manufacturing planning, and tooling. The manufacturing effort incorporates the cost of raw materials and purchased parts.

Final assembly of the complete vehicle is actually a two-phase effort consisting of the final assembly of all major subsystems and the erection of the vehicle. This is the final marriage of the aerostat and the helicopter/framework subassemblies into a completed FRV. Due to the overall width of the vehicle a large hangar such as Goodyear's airdock, the facility at Santa Ana or the hangar at Ames would be needed for erection.

The identification of spares for this estimate will be, at least at this time, a best guess and will be limited to major spares only. Meaningful allocations of spares in any vehicle system involves analytical procedures which are not justified on a one-of-a-kind vehicle.

c. Testing

The third major cost element is the total test program for the entire vehicle. There are three major testing scenarios that will be required: a test stand, ground testing, and flight testing.

During the detail design phase of the program, several models will be required to predict or substantiate analytical prediction of vehicle and component behavior. This would encompass wind tunnel testing and major subsystems tests as defined in Table 10-1.

The FRV test stand analysis would be conducted in the hangar. Primary investigation would address the following:

- Structural interface

- Main rotor/envelope dynamics

- Propeller and drive shaft performance

- Structural and vibrational characteristics - frequencies, moments, stresses, torsional modes

The tests would progress from static loadings to rotor and propeller engagement with varying collective pitch and rpm.

FRV ground tests would encompass the following:

- Static and dynamic evaluation of the interconnecting structure

- Envelope and ballonet pressure controls

- LTA controls functioning

- Helicopter controls functioning and synchronization

- Engine controls functioning and synchronization

10-4

- Vehicle weighoff, static trim, and lift

- Pitot static system

- Electrical and electronic systems

- Payload suspension system functioning

- Emergency systems functioning

- Compass calibration

- Ground operations (undocking, docking, ground handling mooring system, taxi tests)

Flight tests will demonstrate vehicle structural integrity as well as overall flight performance. Proposed flight test tasks are listed below:

- Pilot familiarization
    - Undocking and docking - taxi
    - Liftoff - vertical and forward run
    - First flight within airfield area (takeoff, landing, pressure height check, trim at pressure height, ballast dumping)

- Ground resonance and effects

- Hover capability - various static conditions

- Control in horizontal flight

- Directional stability and turning radius

- Maximum speed - normal and military rated power

- Airspeed calibration

- Control characteristics - various heaviness conditions

- Takeoff and landings - various heaviness conditions

- Powerplant synchronization

- Rapid ascents - air valve capacity

- Rapid descents - damper valve capacity

- Rapid ascent above pressure height

- Turn entry and climb

- Turn entry and dive

- Turn recovery and climb

- Turn recovery and dive

- Heavy descent and pullup

- Transient turn and reversal

- Auxiliary blower capacity

- Vibration

- Noise level - on-board and on-ground measurements (various altitudes)

- Electrical and electronic systems

- Load-handling characteristics - payload pickup and discharge

- Emergency procedures characteristics
  - Various engine out conditions
  - Engine air starts
  - Payload emergency drop
  - Autorotation
  - Fuel dumping

3. ESTIMATED COSTS

The total estimated FRV program cost (excluding spares) is estimated to be $13,424,800. As indicated in earlier sections the availability of major systems as government-furnished equipment would have a significant cost impact. With GFE considerations, the total estimated cost is $11,425,800.

Table 10-2 summarizes the predicted program costs. Figures in parenthesis reflect the costs if GFE is utilized.

TABLE 10-2 - PREDICTED FRV COSTS

Item	Cost ($1981)
Engineering	3,259,400
Fabrication	6,254,400 (4,255,400)
Testing	3,911,000
Total	13,424,800 (11,425,800)
Spares	704,000 (243,000)
Grand Total	14,128,800 (11,668,800)

Details of each cost item are provided in Tables 10-3 through 10-6.

TABLE 10-3 - SUMMARY OF ENGINEERING COST

Item or subsystem	Estimated Cost
Envelope	$ 49,000
Empennage	65,000
Nose stiffening	39,400
Control car	134,000
Interconnecting structure	340,000
Auxiliary propulsion (less GFE)	504,000
Flight control system	629,000
Landing gear	33,000
Pressure control system	97,000
Instruments and avionics	49,000
Electrical and electronics installation	85,000
Stress and mass properties analyses	399,000
Aerodynamics, flight dynamics	138,000
Design services during fabrication	389,000
Publications	309,000
Total Estimated Engineering	$3,259,400

TABLE 10-4 - SUMMARY OF FABRICATION COST

Item or subsystem	Estimated Cost
Manufacturing	
Envelope refurbishment	$326,100
Empennage modification	349,900
Nose stiffening	65,100
Control car	103,500
Interconnecting structure	620,000
Auxiliary propulsion (less GFE)	684,000
Flight control system	552,600
Landing gear	50,400
Pressure control system	181,400
Instruments and avionics	61,600
Electrical and Electronics installations	49,800
Subtotal Manufacturing (less GFE)	$3,044,400
Tooling	$330,000
Quality Assurance	84,000
Manufacturing planning	120,000
Erection	434,000
Spares (less GFE)	243,000
Total Estimated Fabrication Cost (less GFE)	$4,255,400
(Add the following items if no GFE:)	
Engines 250C20B (4 at $70,000)	280,000
Tail rotors AH-1T (4 at $6,500)	26,000
Helicopters 500D (4 at $308,000)	1,232,000
Spare engines (2)	140,000
Spare tail rotors (2)	13,000
Spare rotor drive train (helicopter)	308,000
Total Estimated Fabrication Cost - No GFE	$6,254,400

TABLE 10-5 – SUMMARY OF ESTIMATED TESTING COSTS

Test or operation	Estimated Cost
Structural Tests	
Planning	$ 64,000
Design and fabricate fixtures and stand	540,000
Run tests	320,000
Data reduction	97,500
Ground tests	
Planning	64,000
Run tests	340,000
Data reduction	65,500
Flight tests	
Planning	80,000
Instrumentation design	165,000
Instrumentation fabrication	94,000
Installation and calibration	320,000
Run tests	490,000
Data reduction	384,000
Flight operations/training	
Organization	69,000
Crew training and familiarization	416,000
Ground tests	106,000
Flight tests	296,000
Total Estimated Testing Cost	$3,911,000

TABLE 10-6 - MAJOR SPARES REQUIREMENTS

Quantity	Description	Estimated Cost
1	Helicopter rotor drive train	GFE ($308,000)
2	Engines 250C20B	GFE ($140,000)
2	Tail rotors AH-1T	GFE ($13,000)
2	Propeller reduction gear boxes	$ 34,000
1	Lower fin and rudder	$137,000
2	Air/gas valves	$ 60,000
1	Landing gear	$ 12,000
Total:	Considering GFE	$243,000
	All Contractor Furnished	$704,000

4. PROJECTED SCHEDULE

The overall program, including engineering, fabrication, and testing would take approximately six years from the point of initiation. Figure 10-2 represents the anticipated schedule.

The timetable is established to permit periodic review of the program prior to commitment to additional phases. These decision points represent key milestones for the program and include the following:

1. Initiation of Detail Design
   At this point, the detail design process commences. All necessary tests in support of the design would be conducted during this phase.

2. Design Review
   After 18 months of design effort, a program review is indicated. Up to this point all effort would be directed to engineering only. At this juncture, commitments to proceed with fabrication would be required.

3. Program Review
   Three years into the program, all engineering and manufacturing effort will be complete. A program review prior to the erection process is indicated at this point.

4. First Flight
   Though the FRV will be erected after 42 months, first flight will not be until six months later. This will permit adequate structural and ground testing to be conducted.

Figure 10-2 – Projected FRV Program Schedule

Activity	Scheduled Span (Year / Quarter)
ENGINEERING	
DESIGN	Yr 1 Q1 – Yr 3 Q4
FABRICATION SUPPORT	Yr 2 Q4 – Yr 4 Q2
PUBLICATIONS	Yr 2 Q3 – Yr 4 Q1
FABRICATION	
ENVELOPE, EMPENNAGE, NOSE	Yr 2 Q3 – Yr 4 Q1
CAR FAB AND ASSEMBLY	Yr 3 Q1 – Yr 3 Q4
INTERCONNECTING STRUCTURE	Yr 3 Q3 – Yr 4 Q1
PROPULSION	Yr 3 Q3 – Yr 4 Q1
ERECTION	Yr 4 Q1 – Yr 4 Q2
TOOLING	Yr 2 Q3 – Yr 3 Q3
QUALITY ASSURANCE	Yr 2 Q3 – Yr 4 Q1
MANUFACTURING PLANNING	Yr 2 Q3 – Yr 4 Q1
TESTING	
STRUCTURAL	Yr 4 Q1 – Yr 4 Q4
GROUND	Yr 4 Q3 – Yr 5 Q2
FLIGHT OPS/TRAINING	Yr 4 Q3 – Yr 6 Q4
FLIGHT TESTS	Yr 5 Q2 – Yr 6 Q4

KEY MILESTONES: △1 (Yr 1 Q1), △2 (Yr 2 Q1), △3 (Yr 3 Q1), △4 (Yr 4 Q1)

The time table is sufficiently flexible to permit schedule changes. If, for example, no overlap between engineering design and fabrication was mandated, this could be accommodated by extending the overall performance period by 18 months.

5. GROUND HANDLING CONSIDERATIONS

There is an obvious requirement to be able to adequately handle and secure the FRV when it is on the ground. Though not specifically a part of the vehicle, ground handling equipment is a necessity.

a. Docking and Undocking

After completing the erectiona nd final assembly of the vehicle within a hangar, it must be moved outside in order to perform specific ground and flight tests. (Under ideal weather conditions.) Airships of this size have successfully been undocked and docked using manpower alone. However, any significant crosswind at the hangar door would make this an unviable option.

A more rational and proven technique is to employ a mobile mast conncted to the bow of the airship with two ground handling mules attached to stern lines.

This approach provides adequate support to counteract prevailing winds at the time of egress. The estimated equipment costs would total to approximately $1,200,000 with $500,000 attributable to the pairs of mules and the remainder to the mobile mast.

The time required to design and manufacture the equipment would parallel the fabrication phase of the FRV.

b. Mooring Out

If all flights of the FRV are restricted to the area adjacent to the erection hangar, the FRV can be assumed to return to this base at the termination of a flight and the mobile mast can be used for mooring out.

If, however, flights to more distant sites are anticipated, then a transportable stick mast would be needed. This mast could be erected at a suitably flat, clear location and the FRV could be adequately secured by the bow.

The estimated cost of a stick mast is $100,000.

10-12

SECTION XI - SUMMARY, CONCLUSIONS AND RECOMMENDATIONS

A preliminary design study of a hybrid airship for flight research was undertaken to determine the best combination of four small helicopters and an aerostat. This vehicle design was subsequently subjected to analysis and redesign.

Several candidate helicopters and envelope sizes were identified and various combinations of equiment were examined. A baseline configuration employing OH-6A helicopters and a GZ20 envelope was developed to establish basic geometric relationships. Other vehicles investigated were extensions of this concept.

Initial evaluations were based on four issues: overall cost, helicopter adaptability to the FRV design, safety, and control power. The best compromise was identified as a vehicle with four OH-6A rotor systems, four auxiliary propulsion units, a GZ20 envelope, and tail rotors from the Sea Cobra helicopter for the reversing propellers on the APU's.

Having selected the basic components, the baseline design was more accurately defined. The GZ20 envelope was retained and hence, its dimensional properties were not altered. An additional external suspension system was provided to supplement the existing internal and external systems. The interconnecting structure incorporates a modular design to permit repositioning of the propulsion units.

As indicated earlier, the main rotor system is the OH-6A while the APU system is comprised of four Allison T250-C20B modified engines and tail rotors from the AH-1T. Estimated maximum thrusts are 2600 pounds and 1400 pounds per unit respectively, with the latter being capable of full reversal.

The mass properties of the FRV were developed and indicate a vehicle empty weight of 14,426.5 pounds. Maximum useful load is estimated to be 8665.7 pounds with a total cargo capability of 5074.3 pounds. Buoyancy ratios in the range 0.53 to 0.68 are achievable.

The interconnecting structure was designed based on lift and landing loading conditions. A framework of 4130 steel tubing was developed with a total of 186 members.

The envelope and suspension system analysis incorporated a study of the effects of in-flight gust loads. Results indicate that while a GZ20 envelope can be utilized for the FRV, an increase in envelope operating pressure would be necessary. Though this requirement is within the safe operating range of the envelope, it will reduce envelope life. At this point, a minimum of two years operation is predicted.

Several structural dynamic problems were identified as potential areas of concern for a hybrid airship. These would require appropriate investigation during a detailed design phase.

The control system concept for the FRV was defined. In cruise flight, the conventional airship controls are retained minimizing hardware changes. In hover, however, these controls are locked in the neutral position and controls similar to helicopter components are engaged.

The performance characteristics of the FRV in typical flight conditions corresponding to hover, climb, and foreward flight were estimated.

The extent of stability and control augmentation desirable is dependent on the inherent stability characteristics of the FRV configuration. Stability was evaluated in typical flight conditions of hover and cruise. The effects of carrying a sling load on the vehicle dynamics were predicted by using a linear, state-variable model of the coupled system. A piloted flight simulation of the FRV was utilized to investigate typical operational conditions that could lead to vehicle instability.

Due to the rather nebulous state of the FRV handling qualities criteria, control requirements for the vehicle were interpreted in terms of specific tasks. These included: the ability to maneuver from hover, stationkeeping ability, the ability to accelerate into a headwind or crosswind, and the ability to counter wind disturbances while hovering over a point on the ground. Failure modes were also addressed.

In terms of a cost and development schedule, an estimated expenditure of $11,425,800 over a six-year period is envisioned. This cost would include all engineering design, fabrication and testing. An additional spares inventory requirement of $243,000 is also identified. Note that these estimates reflect the assumed availability of the helicopter and APU systems as GFE.

Since the overall results of this study, particularly in terms of performance and control, tend to support the viability of this configuration as a manned flight research vehicle, the following tasks are recommended for continued vehicle development. These elements would be considered part of the detailed design investigation:

- Wind tunnel model tests to accurately define the aerodynamic coefficients and derivatives (static and dynamic) of the vehicle. These tests should also show interference effects due to the rotor and propulsion unit in order to provide direction for continued iteration of the design in terms of rotor and propeller placement with respect to each other and the hull.

- Validation of GAC's finite element model through experimentation

- Development of a structural model incorporating a single outriger and propulsion system in order to assess structional dynamics considerations

- Design, fabrication, and lab testing of the flight controls system

- Enhancement of the real-time piloted simulation

APPENDIX A

FRV MASS PROPERTIES

	WT.	X	Y	Z	WX	WY	WZ
ENVELOPE COMPLETE							
ENVELOPE ASSY							
ENVELOPE - FWD SECTION	1010.300	45.172	.000	.612	45637.3	.0	618.3
ENVELOPE - AFT SECTION	1490.500	117.298	.000	.612	174832.6	.0	912.2
ENVELOPE ASSY TOTAL	2500.800	88.161	.000	.612	220469.9	.0	1530.5
BALLONETS							
BALLONET - FWD	182.100	37.500	.000	13.800	6828.8	.0	2513.0
BALLONET - AFT	189.000	131.700	.000	13.900	24891.3	.0	2627.1
BALLONETS TOTAL	371.100	85.476	.000	13.851	31720.0	.0	5140.1
AIR LINES	53.100	87.700	.000	20.500	4656.9	.0	1088.6
SUSPENSION SYSTEM							
CATENARY CURTAIN-PORT	57.100	80.000	-10.000	-18.300	4568.0	-571.0	-1044.9
CATENARY CURTAIN-STB.	57.100	80.000	10.000	-18.300	4568.0	571.0	-1044.9
SUSPENSION CABLES - PORT	36.700	79.800	-6.700	9.600	2928.7	-245.9	352.3
SUSPENSION CABLES - STB.	36.700	79.800	6.700	9.600	2928.7	245.9	352.3
OUTSIDE SUSPENSION	44.800	77.478	.000	22.612	3471.0	.0	1013.0
EXTERNAL SUPPORT CURTAINS(LH)	50.000	82.000	-16.000	18.000	4100.0	-800.0	900.0
EXTERNAL SUPPORT CURTAINS(RH)	50.000	82.000	16.000	18.000	4100.0	800.0	900.0
SUSPENSION SYSTEM TOTAL	332.400	80.218	.000	4.295	26664.3	.0	1427.8
BOW STIFFENING & MOORING							
MOORING CONE	69.000	-.500	.000	.300	-34.5	.0	20.7
BATTENS AND ATTACH.	222.800	9.260	.000	.000	2063.1	.0	.0
UNDER NOSE MOORING STIFFENING	23.800	24.160	.000	17.300	573.6	.0	411.7
BOW STIFFENING & MOORING TOTAL	315.600	8.245	.000	1.370	2602.2	.0	432.4
FIN CATENARIES	62.000	165.000	.000	.000	10329.0	.0	.0
CAR COVER	43.200	77.500	.000	22.500	3348.0	.0	972.0
CAR FAIRING	7.500	78.800	.000	22.800	591.0	.0	171.0
ENVELOPE COMPLETE TOTAL	3686.200	81.486	.000	2.920	300381.1	.0	10762.3
PRESSURE SYSTEM							
AIR VALVE - NO.1	29.400	31.900	.000	20.300	937.9	.0	596.8
AIR VALVE - NO.2	29.400	47.700	.000	20.300	1402.4	.0	596.8
AIR VALVE - NO.3	29.400	113.500	.000	20.300	3336.9	.0	596.8
AIR VALVE - NO.4	29.500	137.700	.000	20.300	4062.1	.0	598.8
GAS VALVE - NO.1	33.300	69.200	-20.000	3.100	2304.4	-666.0	103.2
GAS VALVE - NO.2	33.300	69.200	20.000	3.100	2304.4	666.0	103.2
BLOWER - NO.1	74.000	91.700	-5.000	24.100	6785.8	-370.0	1783.4
BLOWER - NO.2	74.000	91.700	5.000	24.100	6785.8	370.0	1783.4
PRESSURE SYSTEM TOTAL	332.300	84.019	.000	18.545	27919.6	.0	6162.6
HANDLING LINES							
STERN HANDLING LINES	16.600	181.600	.000	10.700	3014.6	.0	177.6
GROUND HANDLING BRIDLE	30.800	144.100	.000	13.380	4438.3	.0	412.1
NOSE LINES	32.400	-2.200	.000	25.000	-71.3	.0	810.0
HANDLING LINES TOTAL	79.800	92.501	.000	17.540	7381.6	.0	1399.7
TAIL ASSY							

	WT.	X	Y	Z	WX	WY	WZ
FIN AND RUDDER - UPPER	192.000	168.100	.000	-17.400	32275.2	.0	-3340.8
FIN AND RUDDER - LOWER	180.600	167.300	.000	16.300	30214.4	.0	2943.8
FIN AND ELEVATOR - PORT	193.000	168.100	17.400	.000	32443.3	3358.2	.0
FIN AND ELEVATOR - STB.	192.000	168.100	-17.400	.000	32275.2	-3340.8	.0
TAIL ASSY TOTAL	757.600	167.909	.023	-.524	127208.1	17.4	-397.0
CAR ASSY	856.700	57.800	.000	27.500	49517.3	.0	23559.2
LANDING GEAR ASSYS							
LANDING GEAR-NO.1	104.500	68.000	-22.000	32.000	7106.0	-2299.0	3344.0
LANDING GEAR-NO.2	104.500	96.000	-22.000	32.000	10032.0	-2299.0	3344.0
LANDING GEAR-NO.3	104.500	96.000	22.000	32.000	10032.0	2299.0	3344.0
LANDING GEAR-NO.4	104.500	68.000	22.000	32.000	7106.0	2299.0	3344.0
LANDING GEAR ASSYS TOTAL	418.000	82.000	.000	32.000	34276.0	.0	13376.0
SUPPORT FRAME=2(527% CU FT	2888.600	82.000	.000	23.500	236865.2	.0	67882.1
ENGINES FWD THRUST							
ENGINE NO.1 FWD THRUST	195.000	94.000	-29.000	24.500	18330.0	-5655.0	4777.5
PROPELLER NO.1 FWD THRUST	75.000	92.500	-29.000	24.500	6937.5	-2175.0	1837.5
FUEL SYSTEM NO.1 FWD THRUST	37.500	99.800	-29.000	23.500	3742.5	-1087.5	881.3
CONTROLS NO.1 FWD THRUST	17.500	94.000	-29.000	24.500	1645.0	-507.5	428.8
ENGINE SECTION NO.1 FWD THRUST	50.000	94.000	.000	24.500	4700.0	.0	1225.0
ENGINE NO.2 FWD THRUST	195.000	94.000	29.000	24.500	18330.0	5655.0	4777.5
PROPELLER NO.2 FWD THRUST	75.000	92.500	29.000	24.500	6937.5	2175.0	1837.5
FUEL SYSTEM NO.2 FWD THRUST	37.500	99.800	29.000	23.500	3742.5	1087.5	881.3
CONTROLS NO.2 FWD THRUST	17.500	94.000	29.000	24.500	1645.0	507.5	428.8
ENGINE SECTION NO.2 FWD THRUST	50.000	94.000	.000	24.500	4700.0	.0	1225.0
ENGINES FWD THRUST TOTAL	750.000	94.280	.000	24.400	70710.0	.0	18300.0
ENGINES SIDE THRUST							
ENGINE NO.1 SIDE THRUST	195.000	83.000	-22.500	24.500	16185.0	-4387.5	4777.5
PROPELLER NO.1 SIDE THRUST	75.000	83.000	-24.000	24.500	6225.0	-1800.0	1837.5
FUEL SYSTEM NO.1 SIDE THRUST	37.500	83.000	-19.300	22.000	3112.5	-723.8	825.0
CONTROLS NO.1 SIDE THRUST	17.500	83.000	-22.500	24.500	1452.5	-393.8	428.8
ENGINE SECTION NO.1 SIDE THRUST	50.000	83.000	.000	24.500	4150.0	.0	1225.0
ENGINE NO.2 SIDE THRUST	195.000	83.000	22.500	24.500	16185.0	4387.5	4777.5
PROPELLER NO.2 SIDE THRUST	75.000	83.000	24.000	24.500	6225.0	1800.0	1837.5
FUEL SYSTEM NO.2 SIDE THRUST	37.500	83.000	19.300	22.000	3112.5	723.8	825.0
CONTROLS NO.2 SIDE THRUST	17.500	83.000	22.500	24.500	1452.5	393.8	428.8
ENGINE SECTION NO.2 SIDE THRUST	50.000	83.000	.000	24.500	4150.0	.0	1225.0
ENGINES SIDE THRUST TOTAL	750.000	83.000	.000	24.250	62250.0	.0	18187.5
HELICOPTER LESS ROTOR INSTALL.							
HELICOPTER - NO.1	868.200	65.200	-37.000	20.200	56606.6	-32123.4	17537.6
HELICOPTER - NO.2	868.200	110.200	-37.000	20.200	95675.6	-32123.4	17537.6
HELICOPTER - NO.3	868.200	110.200	37.000	20.200	95675.6	32123.4	17537.6
HELICOPTER - NO.4	868.200	65.200	37.000	20.200	56606.6	32123.4	17537.6
HELICOPTER LESS ROTOR TOTAL	3472.800	87.700	.000	20.200	304564.5	.0	70150.5
ROTOR INSTALL.							

	WT.	X	Y	Z	WX	WY	WZ
ROTOR - NO.1	108.600	64.500	-37.000	15.500	7004.7	-4018.2	1683.3
ROTOR - NO.2	108.600	109.500	-37.000	15.500	11891.7	-4018.2	1683.3
ROTOR - NO.3	108.600	109.500	37.000	15.500	11891.7	4018.2	1683.3
ROTOR - NO.4	108.600	64.500	37.000	15.500	7004.7	4018.2	1683.3
ROTOR INSTALL. TOTAL	434.400	87.000	.000	15.500	37792.8	.0	6733.2
WEIGHT EMPTY	14426.477	87.260	.001	16.367	1258861.0	17.4	236115.9
USEFUL LOAD LESS PAYLOAD							
PILOT	170.000	59.000	2.500	27.700	10030.0	425.0	4709.0
FLIGHT ENGINEER	170.000	59.000	-2.500	27.700	10030.0	-425.0	4709.0
FUEL							
ENGINE NO.1-FWD THRUST	400.000	99.800	-29.000	23.500	39920.0	-11600.0	9400.0
ENGINE NO.2-FWD THRUST	400.000	99.800	29.000	23.500	39920.0	11600.0	9400.0
ENGINE NO.1-SIDE THRUST	400.000	83.000	-19.300	22.000	33200.0	-7720.0	8800.0
ENGINE NO.2-SIDE THRUST	400.000	83.000	19.300	22.000	33200.0	7720.0	8800.0
HELICOPTER-NO.1	400.000	64.500	-37.000	25.400	25800.0	-14800.0	10160.0
HELICOPTER-NO.2	400.000	109.500	-37.000	25.400	43800.0	-14800.0	10160.0
HELICOPTER-NO.3	400.000	109.500	37.000	25.400	43800.0	14800.0	10160.0
HELICOPTER-NO.4	400.000	64.500	37.000	25.400	25800.0	14800.0	10160.0
FUEL TOTAL	3200.000	89.200	.000	24.075	285440.0	.0	77039.9
OIL							
ENGINE NO.1-FWD THRUST	6.400	94.000	-29.000	24.500	601.6	-185.6	156.8
ENGINE NO.2-FWD THRUST	6.400	94.000	29.000	24.500	601.6	185.6	156.8
ENGINE NO.1-SIDE THRUST	6.400	83.000	-22.500	24.500	531.2	-144.0	156.8
ENGINE NO.2-SIDE THRUST	6.400	83.000	22.500	24.500	531.2	144.0	156.8
HELICOPTER-NO.1	6.400	67.700	-37.000	23.300	433.3	-236.8	149.1
HELICOPTER-NO.2	6.400	112.700	-37.000	23.300	721.3	-236.8	149.1
HELICOPTER-NO.3	6.400	112.700	37.000	23.300	721.3	236.8	149.1
HELICOPTER-NO.4	6.400	67.700	37.000	23.300	433.3	236.8	149.1
OIL TOTAL	51.200	89.350	.000	23.900	4574.7	.0	1223.7
USEFUL LOAD LESS PAYLOAD TOTAL	3591.199	86.343	.000	24.416	310074.5	.0	87681.1
GROSS WEIGHT - LESS PAYLOAD	18017.664	87.077	.001	17.971	1568933.0	17.4	323796.8
PAYLOAD	5074.301	86.950	.000	26.000	441210.4	.0	131931.8
GROSS WEIGHT WITH PAYLOAD	23091.965	87.049	.001	19.735	2010143.0	17.4	455728.6
TOTALS	23091.965	87.049	.001	19.735	2010143.0	17.4	455728.6

	IXX	IYY	IZZ	IOX	IOY	IOZ	IXY	IXZ	IYZ
ENVELOPE - FWD SECTION	2061526.0	.0	378.4	315771.9	572022.0	572022.0	.0	27930.0	.0
ENVELOPE - AFT SECTION	2051750a.0	.0	558.3	464735.3	1588028.0	1588028.0	.0	106997.6	.0
BALLONET - FWD	256078.1	.0	34679.1	19711.1	19711.1	39391.8	.0	94236.8	.0
BALLONET - AFT	327M183.0	.0	36516.7	20458.0	20458.0	40864.5	.0	385989.0	.0
AIR LINES	408417.2	.0	22315.3	482.5	15040.1	15482.6	.0	95465.8	.0
CATENARY CURTAIN-PORT	365440.0	5710.0	19122.2	119.0	33215.8	33096.9	-45680.0	-83594.4	10449.3
CATENARY CURTAIN-STB.	365440.0	5710.0	19122.2	119.0	33215.8	33096.9	45680.0	-83594.4	-10449.3
SUSPENSION CABLES - PORT	233717.0	1647.5	3342.3	5292.6	12938.5	7645.8	-19622.0	28115.1	-2360.5
SUSPENSION CABLES - STB.	233707.0	1647.5	3342.3	5292.6	12938.5	7645.8	19622.0	28115.1	2360.5
OUTSIDE SUSPENSION	268927.2	.0	22906.4	373.3	2333.3	2706.7	.0	78486.6	.0
EXTERNAL SUPPORT CURTAINS(LH)	336200.0	12800.0	16200.0	46.2	5446.2	5400.0	-65600.0	73800.0	-14400.0
EXTERNAL SUPPORT CURTAINS(RH)	336200.0	12800.0	16200.0	46.2	5446.2	5400.0	65600.0	73800.0	14400.0
MOORING CONE	17.3	.0	6.2	376.0	213.4	213.4	.0	-10.4	.0
BATTENS AND ATTACH.	19104.6	.0	.0	2627M.1	18509.7	18509.7	.0	.0	.0
UNDER NOSE MOORING STIFFENING	13823.3	.0	7123.1	269.1	269.1	534.2	.0	9922.9	.0
FIN CATENARIES	1704245.0	.0	.0	11073.3	7793.6	7793.6	.0	.0	.0
CAR COVER	259469.9	.0	21870.0	560.0	2250.0	2610.0	.0	75329.9	.0
CAR FAIRING	46570.8	.0	3898.8	.0	.0	.0	.0	13474.8	.0
AIR VALVE - NO.1	29917.7	.0	12115.4	14.9	14.9	24.8	.0	19038.6	.0
AIR VALVE - NO.2	66893.4	.0	12115.4	14.9	14.9	24.8	.0	28468.3	.0
AIR VALVE - NO.3	378138.0	.0	12115.4	14.9	14.9	24.8	.0	67739.1	.0
AIR VALVE - NO.4	559358.0	.0	12156.7	14.9	14.9	24.9	.0	82461.6	.0
GAS VALVE - NO.1	159461.7	13320.0	320.0	16.8	28.1	16.8	-46087.2	7143.5	-2064.6
GAS VALVE - NO.2	159461.7	13320.0	320.0	16.8	28.1	16.8	46087.2	7143.5	2064.6
BLOWER - NO.1	622257.5	1850.0	42980.0	37.4	37.4	62.5	-33929.0	163537.7	-8917.0
BLOWER - NO.2	622257.5	1850.0	42940.0	37.4	-37.4	62.5	33929.0	163537.7	8917.0
STERN HANDLING LINES	547448.3	.0	1900.5	.0	.0	.0	.0	32255.8	.0
GROUND HANDLING BRIDLE	639555.8	.0	5513.9	.0	.0	.0	.0	59384.1	.0
NOSE LINES	156.8	.0	20250.0	.0	.0	.0	.0	-1792.0	.0
FIN AND RUDDER - UPPER	5425461.0	.0	58129.9	2500.0	10034.2	7534.2	.0	-561588.3	.0
FIN AND RUDDER - LOWER	5054865.0	.0	47983.6	1505.0	8591.9	7086.9	.0	492494.4	.0
FIN AND ELEVATOR - PORT	5453719.0	58432.6	.0	2513.0	7573.5	10086.5	564513.2	.0	.0
FIN AND ELEVATOR - STB.	5425461.0	58129.9	.0	2500.0	7534.2	10034.2	-561588.3	.0	.0
CAR ASSY	2862097.0	.0	647879.3	6728.7	10351.8	7942.3	.0	1361724.0	.0
LANDING GEAR-NO.1	483208.0	50578.0	107008.0	219.1	220.8	4.5	-156332.0	227392.0	-73568.0
LANDING GEAR-NO.2	963072.0	50578.0	107008.0	219.1	220.8	4.5	-220704.0	321028.0	-73568.0
LANDING GEAR-NO.3	963072.0	50578.0	107008.0	219.1	220.8	4.5	220704.0	321028.0	73568.0
LANDING GEAR-NO.4	483208.0	50578.0	107008.0	219.1	220.8	4.5	156332.0	227392.0	73568.0
SUPPORT FRAME-205270 CU FT	19422944.0	.0	1595228.0	1342236.0	511522.9	1805615.0	.0	5566331.0	.0
ENGINE NO.1 FWD THRUST	1723020.0	163995.0	117048.8	130.0	325.0	325.0	-531570.0	449085.0	-138547.5
PROPELLER NO.1 FWD THRUST	64171R.8	63075.0	45018.8	600.0	300.0	300.0	-201187.5	169968.8	-53287.5
FUEL SYSTEM NO.1 FWD THRUST	373501.5	31537.5	20709.4	18.8	37.5	37.5	-108532.5	87948.8	-25556.3
CONTROLS NO.1 FWD THRUST	154630.0	14717.5	10504.4	.0	.0	.0	-47705.0	40302.5	-12433.8
ENGINE SECTION NO.1 FWD THRUST	441890.0	.0	50012.5	95.3	151.8	151.8	.0	115150.0	.0

	MXX	MYY	MZZ	IOX	IOY	IOZ	MXY	MXZ	MYZ
ENGINE NO.2 FWD THRUST	1723020.0	-163995.0	117048.8	130.0	325.0	325.0	531570.0	449085.0	138547.5
PROPELLER NO.2 FWD THRUST	641718.8	63075.0	45018.8	600.0	300.0	300.0	201187.5	169968.8	53287.5
FUEL SYSTEM NO.2 FWD THRUST	373501.5	31537.5	20709.4	18.8	37.5	37.5	108532.5	87948.8	25556.3
CONTROLS NO.2 FWD THRUST	154630.0	14717.5	10504.4	.0	.0	.0	47705.0	40302.5	12433.8
ENGINE SECTION NO.2 FWD THRUST	441600.0	.0	30012.5	95.3	151.8	151.8	.0	115150.0	.0
ENGINE NO.1 SIDE THRUST	1343355.0	98718.8	117048.8	325.0	130.0	325.0	-364162.5	396532.5	-107493.8
PROPELLER NO.1 SIDE THRUST	516675.0	43200.0	45018.8	300.1	600.0	300.1	-149400.0	152512.5	-44100.0
FUEL SYSTEM NO.1 SIDE THRUST	258337.5	13968.4	18150.0	37.5	18.8	37.5	-60071.3	68475.0	-15922.5
CONTROLS NO.1 SIDE THRUST	120557.5	8859.4	10504.4	.0	.0	.0	-32681.3	35586.3	-9646.9
ENGINE SECTION NO.1 SIDE THRUST	344450.0	.0	30012.5	151.8	95.3	151.8	.0	101675.0	.0
ENGINE NO.2 SIDE THRUST	1343355.0	98718.8	117048.8	325.0	130.0	325.0	364162.5	396532.5	107493.8
PROPELLER NO.2 SIDE THRUST	516675.0	43200.0	45018.8	300.1	600.0	300.1	149400.0	152512.5	44100.0
FUEL SYSTEM NO.2 SIDE THRUST	258337.5	13968.4	18150.0	37.5	18.8	37.5	60071.3	68475.0	15922.5
CONTROLS NO.2 SIDE THRUST	120557.5	8859.4	10504.4	.0	.0	.0	32681.3	35586.3	9646.9
ENGINE SECTION NO.2 SIDE THRUST	344450.0	.0	30012.5	151.8	95.3	151.8	.0	101675.0	.0
HELICOPTER - NO.1	3690752.0	1188565.0	354260.1	2713.1	10110.9	10110.9	-2094445.0	1143453.0	-648892.4
HELICOPTER - NO.2	10543453.0	1188565.0	354260.1	2713.1	10110.9	10110.9	-3539998.0	1932647.0	-648892.4
HELICOPTER - NO.3	10543453.0	1188565.0	354260.1	2713.1	10110.9	10110.9	3539998.0	1932647.0	648892.4
HELICOPTER - NO.4	3690752.0	1188565.0	354260.1	2713.1	10110.9	10110.9	2094445.0	1143453.0	648892.4
ROTOR - NO.1	451803.1	148673.4	26091.1	9411.1	4707.8	4707.8	-259173.8	108572.8	-62282.1
ROTOR - NO.2	1302141.0	148673.4	26091.1	9411.1	4707.8	4707.8	-439992.8	184321.3	-62282.1
ROTOR - NO.3	1302141.0	148673.4	26091.1	9411.1	4707.8	4707.8	439992.8	184321.3	62282.1
ROTOR - NO.4	451803.1	148673.4	26091.1	9411.1	4707.8	4707.8	259173.8	108572.8	62282.1
WEIGHT EMPTY	124829104.0	6614622.0	5577130.0	2285598.0	2969073.0	4291536.0	2925.0	19441584.0	.9

	IXB	IYB	IZB	IXBYB	IXBZB	IYBZB
POUND FT SQ	10612883.0	19662144.0	25886560.0	1406.3	-1161968.0	-284.0
SLUG FT SQ	329859.0	611119.0	804580.1	43.7	-36115.1	-8.8

PILOT	591770.0	1062.5	130439.1	258.5	354.2	159.4	25075.0	277830.9	11772.5
FLIGHT ENGINEER	591770.0	1062.5	130439.1	258.5	354.2	159.4	-25075.0	277830.9	-11772.5
ENGINE NO.1-FWD THRUST	3984016.0	336400.0	220900.0	200.0	400.0	400.0	-1157680.0	938120.0	-272600.0
ENGINE NO.2-FWD THRUST	3984016.0	336400.0	220900.0	200.0	400.0	400.0	1157680.0	938120.0	272600.0
ENGINE NO.1-SIDE THRUST	2755600.0	148996.0	193600.0	400.0	200.0	400.0	-640760.1	730400.0	-169840.0
ENGINE NO.2-SIDE THRUST	2755600.0	148996.0	193600.0	400.0	200.0	400.0	640760.1	730400.0	169840.0
HELICOPTER-NO.1	1664100.0	547600.0	258063.8	333.3	514.7	781.3	-954600.0	655319.8	-375919.9
HELICOPTER-NO.2	4796100.0	547600.0	258063.8	300.0	300.0	.0	-1620600.0	1112519.0	-375919.9
HELICOPTER-NO.3	4796100.0	547600.0	258063.8	333.3	514.7	781.3	1620600.0	1112519.0	375919.9
HELICOPTER-NO.4	1664100.0	547600.0	258063.8	333.3	514.7	781.3	954600.0	655319.8	375919.9
ENGINE NO.1-FWD THRUST	56550.4	5382.4	3841.6	.0	.0	.0	-17446.4	14739.2	-4547.2
ENGINE NO.2-FWD THRUST	56550.4	5382.4	3841.6	.0	.0	.0	17446.4	14739.2	4547.2
ENGINE NO.1-SIDE THRUST	44089.6	3240.0	3841.6	.0	.0	.0	-11952.0	13014.4	-3528.0
ENGINE NO.2-SIDE THRUST	44089.6	3240.0	3841.6	.0	.0	.0	11952.0	13014.4	3528.0
HELICOPTER-NO.1	29333.0	8761.6	3474.5	.0	.0	.0	-16031.4	10095.4	-5517.4
HELICOPTER-NO.2	81288.2	8761.6	3474.5	.0	.0	.0	-26687.4	16805.8	-5517.4
HELICOPTER-NO.3	81288.2	8761.6	3474.5	.0	.0	.0	26687.4	16805.8	5517.4

	WXX	WYY	WZZ	IOX	IOY	IOZ	WXY	WXZ	WYZ
HELICOPTER-NO.4	24535.0	8761.6	3474.5	.0	.0	.0	16031.4	10095.4	5517.4
GROSS WEIGHT - LESS PAYLOAD	15243474.1	9830221.0	7724520.0	2288612.0	2972822.0	4295797.0	2925.026979152.0		.9

		IXH	IYB	IZH	IXHYB	IXBZH	IYBZH
	POUND FT SQ	14028384.0	21098416.0	30342080.0	1409.3	-1216224.0	-311.9
	SLUG FT SQ	436016 2	655759 8	943062 1	43 8	-37801 5	- 9.7

| PAYLOAD | 38563252.0 | .0 | 3430227.0 | 21142.9 | 179714.8 | 179714.8 | .011471469.0 | | .0 |
| GROSS WEIGHT WITH PAYLOAD | 191197936.0 | 9830224.0 | 11158747.0 | 2309754.0 | 3152536.0 | 4475511.0 | 2925.038450608.0 | | .9 |

		IXH	IYB	IZH	IXHYB	IXHZH	IYBZB
	POUND FT SQ	14304754.0	21533472.0	30521904.0	1409.8	-1220272.0	-342.6
	SLUG FT SQ	444606 2	669201.8	948651.2	43 8	-37927 3	- 10 6

| TOTALS | 191197936.0 | 9830224.0 | 11158747.0 | 2309754.0 | 3152536.0 | 4475511.0 | 2925.038450608.0 | | .9 |

		IXH	IYB	IZB	IXHYB	IXHZH	IYBZB
	POUND FT SQ	14304754.0	21533472.0	30521904.0	1409.8	-1220272.0	-342.6
	SLUG FT SQ	444606 2	669201 8	948651 2	43 8	-37927 3	- 10 6

	\T.	X	Y	Z	WX	WY	WZ
TOTALS	25091.965	87.049	.001	19.735	2010143.0	17.4	455728.6

	WXX	YY	WZZ	IOX	IOY	IOZ	WXY	WXZ	WYZ
TOTALS	191197936.0	9830224.0	11158747.0	2309754.0	3152536.0	4475511.0	2925.0	38450608.0	.9

	IXB	IYB	IZB	IXBYB	IXBZB	IYBZB
POUND FT SU	14304759.0	21533472.0	30521904.0	1409.8	-1220272.0	-342.6
SLUG FT SU	444606.2	669281.8	948651.2	43.8	-37927.3	-10.6

LOCATION OF PRINCIPAL AXES

THETA XY (DEG)	THETA XZ (DEG)	THETA YZ (DEG)
.01	-4.28	-.00

ROTATION OF AXES - MOMENT OF INERTIA

XY AXES (LB FT SU)	XZ AXES (LB FT SU)	YZ AXES (LB FT SU)
IXB 14304759.0	IXB 14304759.0	IYB 21533472.0
IYB 21533472.0	IZB 30521904.0	IZB 30521904.0
SUM 35838224.0	SUM 44826656.0	SUM 52055376.0
IXBP 14304759.0	IXBP 14576644.0	IYBP 21533472.0
IYBP 21533472.0	IZBP 30250000.0	IZBP 30521904.0
SUM 35838224.0	SUM 44826640.0	SUM 52055376.0

ROTATION OF AXES - PRODUCT OF INERTIA

XY AXES	XZ AXES	YZ AXES
IXBYBP .00	IXBZBP -2.00	IYBZBP -.00

RADIUS OF GYRATION

KX (FT)	KY (FT)	KZ (FT)
24.89	30.54	36.36

```
MASS - LBS                               23091.96
CENTER OF GRAVITY - FT
   X                                        87.05
   Y                                          .00
   Z                                        19.74
MOMENT OF INERTIA - SLUG FT SQ
   IX                                     444606 17
   IY                                     669201 78
   IZ                                     998651.21
PRODUCT OF INERTIA - SLUG FT SQ
   IXY                                        93.82
   IXZ                                    -37927.27
   IYZ                                       -10.65
LOCATION OF PRINCIPAL AXES - DEGREES
   THETA XY                                    .01
   THETA XZ                                  -4.28
   THETA YZ                                   -.00
RADIUS OF GYRATION - FT
   KX                                        24.89
   KY                                        30.54
   KZ                                        36.36
*EXIT*
```

APPENDIX B

GROUP WEIGHT STATEMENT

NAME _C. Belnap_

DATE _6-5-81_

PAGE _1_

MODEL _Flight Research_

REPORT _____

GROUP WEIGHT STATEMENT

ESTIMATED · ~~CALCULATED~~ · ~~ACTUAL~~

(Cross out those not applic ble)

Flight Research   _rship_

CONTRACT NO. _____

AIRSHIP, GOVERNMENT NO _____

AIRSHIP, CONTRACTOR NO. _____

MANUFACTURED BY · _____

		MAIN	AUXILIARY
ENGINE	MANUFACTURED BY		
	MODEL		
	NO.		
PROPELLER	MANUFACTURED BY		
	DESIGN NO.		
	NO.		

NAME _____
DATE _____

GROUP WEIGHT STATEMENT
WEIGHT EMPTY

PAGE ___2___
MODEL _____
REPORT _____

1	ENVELOPE GROUP						3635.1
2	ENVELOPE					2177.7	
3	BALLONETS					371.1	
4	FORWARD				182.1		
5	CENTER				—		
6	AFT				189.0		
7	AIR LINES					53.1	
8	*FRAME AND HELICOPTER SUSPENSION*					332.4	
9	INSIDE				187.6		
10	OUTSIDE				144.8		
11	BOW STIFFENING AND MOORING					315.6	
12	MOORING CONE, SPINDLE, NOSE CONE, TAPES				69.0		
13	BATTENS				} 178.9		
14	BATTEN ATTACHMENT				}		
15	NOSE STIFFENING *PROVISIONS*				67.7		
16	FIN CATENARIES OR SUSPENSION PROVISIONS					62.6	
17	*FRAME FAIRING*					50.7	
18	MISCELLANEOUS					271.9	
19							
20							
21	TAIL GROUP						757.6
22	FINS - UPPER					180.0	
23	FINS - LOWER					168.6	
24	FINS - HORIZONTAL (2)					361.0	
25	RUDDER OR RUDDEVATORS					—	
26	ELEVATORS					—	
27	FIN SUSPENSION					48.0	
28							
29	*CAR, HELICOPTER, SUPPORT FRAME*						7130.4
30	*CAR* STRUCTURE					334.6	
31	*HELICOPTER (MODIFIED OH-6A) (4 REQ)*					3907.2	
32	*SUPPORT FRAME*					2888.6	
33							
34	ALIGHTING GEAR GROUP (TYPE ____) *(4 REQ)*						418.0
35		LOCATION	WHEELS, BRAKES,	STRUCTURE	CONTROLS		
36			IT RES, TUBES, AIR				
37							
38							
39							
40							
41	PRESSURE GROUP						332.3
42	PRESSURE SYSTEM (LESS CONTROLS)					316.8	
43	CONTROLS					15.5	
44							
45	BALLAST GROUP						—
46	TANKS AND SUPPORTS						
47	PIPING, VALVES, PUMPS, ETC						
48	WATER RECOVERY SYSTEM						
49							
50	SURFACE CONTROL GROUP						87.7
51	COCKPIT CONTROLS					69.7	
52	AUTOMATIC PILOT					—	
53	SYSTEM CONTROLS (INCL POWER AND FUEL CONTROLS)					18.0	
54							
55	OUTRIGGER GROUP						—
56							
57	TOTAL TO BE BROUGHT FORWARD						12361.1

NAME _____ GROUP WEIGHT STATEMENT MODEL _____
DATE _____ WEIGHT EMPTY REPORT _____

#	Item		SIDE THRUST (2)		FORWARD THRUST (2)		
1	ENGINE SECTION AND NACELLE GROUP						200.0
2	ENGINE SECTION						
3	NACELLES						
4	DOORS, PANELS, MISCELLANEOUS						
5		I					
6	PROPULSION GROUP		650.0		650.0		1300.0
7	ENGINE INSTALLATION		390.0		390.0		
8	ACCESSORY DRIVES						
9	AIR INDUCTION SYSTEM						
10	EXHAUST SYSTEM						
11	COOLING SYSTEM						
12	LUBRICATING SYSTEM						
13	TANKS						
14	COOLING INSTALLATION						
15	PLUMBING, ETC						
16	FUEL SYSTEM		75.0		75.0		
17	TANKS						
18	PLUMBING, ETC						
19	TRANSMISSION SYSTEM						
20	ENGINE CONTROLS		35.0		35.0		
21	STARTING SYSTEM						
22	PROPELLER INSTALLATION		150.0		150.0		
23							
24	AUXILIARY POWER PLANT GROUP						—
25							
26	INSTRUMENTS AND NAVIGATIONAL EQUIPMENT GROUP						54.7
27							
28	HYDRAULIC AND PNEUMATIC GROUP						—
29							
30	ELECTRICAL GROUP						144.2
31							
32	ELECTRONICS GROUP						203.7
33	GOVERNMENT FURNISHED EQUIPMENT				—		
34	CONTRACTOR INSTALLATIONS				53.7		
35	FLY BY WIRE INSTALL.				150.0		
36	ARMAMENT GROUP						—
37							
38	FURNISHINGS AND EQUIPMENT GROUP						83.0
39	ACCOMMODATIONS FOR PERSONNEL				58.0		
40	MISCELLANEOUS EQUIPMENT				10.0		
41	FURNISHINGS				—		
42	EMERGENCY EQUIPMENT				15.0		
43							
44	AIR CONDITIONING AND ANTI-ICING EQUIPMENT GROUP						—
45	AIR CONDITIONING						
46	ANTI-ICING						
47							
48	AUXILIARY GEAR GROUP						79.8
49	WINCH AND CONTROLS				—		
50	HANDLING LINES				79.8		
51							
52							
53							
54							
55							
56	TOTAL FROM PAGE						1236.1
57	WEIGHT EMPTY						14426.5

NAME _____ GROUP WEIGHT STATEMENT MODEL _____
DATE _____ USEFUL LOAD AND GROSS WEIGHT REPORT _____

			LESS PAYLOAD	WITH PAYLOAD
1 / 2 LOAD CONDITION				
3 CREW (NO 2)			340.0	340.0
4				
5 PASSENGERS (NO)				
6				
7 FUEL			3200.0	3200.0
8 INTERNAL				
9 EXTERNAL				
10 SLIP TANKS				
11 UNUSABLE				
12				
13 OIL			51.2	51.2
14 ENGINE				
15 TRAPPED IN SYSTEM				
16				
17 FUEL TANKS (EXTERNAL)				
18				
19				
20				
21 BAGGAGE				
22				
23				
24				
25 CARGO			—	5074.3
26				
27				
28				
29 ARMAMENT				
30 MISSILES				
31 BOMBS				
32 TORPEDO				
33				
34 BOMB RACKS AND SWAY BRACING				
35				
36				
37				
38 EQUIPMENT				
39 PYROTECHNICS				
40 PHOTOGRAPHIC				
41				
42 MISCELLANEOUS				
43				
44				
45				
46 ELECTRONICS				
47				
48				
49				
50 BALLAST (WATER)				
51				
52				
53 USEFUL LOAD			3591.2	8665.7
54				
55 WEIGHT EMPTY			14426.5	14426.5
56				
57 GROSS WEIGHT			18017.7	23092.0

452-53 (R-55)M

B-5

NAME _____
DATE _____

GROUP WEIGHT STATEMENT
DIMENSIONAL AND STRUCTURAL DATA

PAGE _____5_____
MODEL _____
REPORT _____

		ENVELOPE	CAR	OUTRIGGERS	NACELLES
1	LENGTH · OVERALL (FT) 192.47	HEIGHT OVERALL STATIC (FT) 59.54			
2		ENVELOPE	CAR	OUTRIGGERS	NACELLES
3	VOLUME · DESIGN (CU. FT.)	202700			
4	VOLUME · STRETCHED (CU. FT.)	205270			
5	LENGTH · MAXIMUM (FT)	190.28			
6	DEPTH · MAXIMUM (FT)		13.78		
7	WIDTH · MAXIMUM (FT)	45.92	7.00		
8	WETTED AREA (SO. FT)				
9					
10	THEORETICAL ENVELOPE DATA				
11	SURFACE AREA			2400	SO,YDS.
12	FINENESS RATIO			4.14	
13	DISTANCE OF MAXIMUM SECTION FROM BOW			76.11	FEET
14	DISTANCE OF CENTER OF BUOYANCY FROM BOW			86.95	FEET
15	DISTANCE OF CENTER OF VOLUME OF BALLONETS FROM BOW			86.77	FEET
16					
17					
18	BALLONET VOLUMES				
19	FWD BALLONET			27400	CU.FT.
20	CTR BALLONET				CU.FT.
21	AFT BALLONET			31300	CU.FT.
22	TOTAL VOLUME			58700	CU.FT.
23	% ENVELOPE · STRETCHED			28.6	%
24					
25					
26	EMPENNAGE SURFACE AREA				
27	FINS			714	SO.FT.
28	RUDDEVATORS OR RUDDER			157	SO.FT.
29	ELEVATORS			134	SO.FT.
30	TOTAL AREA			1005	SO FT.
31					
32					
33	ALIGHTING GEAR			MAIN	AUXILIARY
34	LENGTH · OLEO EXTENDED ₵ AXLE TO ₵ TRUNNION (INCHES)				
35	OLEO TRAVEL · FULL EXTENDED TO FULL COLLAPSED (INCHES)				
36					
37					
38	FUEL AND LUBE SYSTEM	LOCATION	NO. TANKS	GALLONS	
39	FUEL · INTERNAL				
40		HELICOPTER	4	246	
41	· EXTERNAL	FRAME	4	246	
42	OIL				
43					
44					
45	HYDRAULIC SYSTEM CAPACITY (GALS.)				
46					
47	GENERAL DATA				
48	STATIC LIFT			12292	LBS.
49	HELICOPTER LIFT			10800	LBS.
50	GROSS LIFT			23092	LBS.
51	USEFUL LOAD · LESS PAYLOAD			3591.2	LBS.
52	USEFUL LOAD · WITH PAYLOAD			8665.7	LBS.
53					
54					
55					
56					
57					

APPENDIX C

OH-6A WEIGHT ESTIMATE

Weight Estimate of OH-6A Helicopter Pod
For Flight Research Airship

Item	OH-6A	POD
Helicopter and pod weight empty	1232.4	(976.8)
Rotor group-main	(173.7)	(173.7)
main rotor blades	108.6	108.6
hub and hinge	50.7	50.7
pitch housing and retension	14.4	14.4
Tail group	(23.0)	(-)
blades	4.0	-
hub	2.7	-
horizontal stabilizer	9.2	-
upper vertical stabilizer	5.7	-
lower vertical stabilizer	1.4	-
Body group	(249.7)	(236.3)
basic structure, lower	87.7	87.7
aft upper section	28.7	28.7
rotor support	21.0	21.0
transition structure	15.3	15.3
tailboom	13.4	-
windshield	19.3	19.3
windows, upper	2.7	2.7
secondary structure	61.6	61.6
Alighting gear group	(66.6)	(-)
skids	18.4	-
abrasion shoes	3.2	-
drag struts	4.3	-
side struts	19.7	-
dampers	6.4	-
fittings	7.8	-
fairings	4.4	-
fasteners	1.4	-
tail skid	1.0	-
Flight controls group	(65.0)	(65.0)
pilot's cyclic stick assy	2.6	2.6
copilot's cyclic stick assy	2.6	2.6
connecting members	3.3	3.3
supports	2.8	2.8
trim control	4.4	4.4
pilot's collective stick assy	1.4	1.4
copilot's collective stick assy	1.7	1.7
connecting members	1.9	1.9
pilot's t/r pedals	2.1	2.1
copilot's t/r pedals	2.1	2.1
connecting members	1.6	1.6
supports	2.9	2.9

Item	OH-6A	POD
Flight controls group (cont)		
friction adjust	.7	.7
load damper	1.4	1.4
supports and brackets	1.2	1.2
fasteners	3.0	3.0
longitudinal non-rotating controls	4.4	4.4
lateral non-rotating controls	4.1	4.1
directional non-rotating controls	6.9	6.9
collective non-rotating controls	3.7	3.7
rotating controls	10.2	10.2
Nacelle group	(8.2)	(8.2)
engine mount and fittings	2.4	2.4
firewall blanket and seals.	5.8	5.8
Propulsion group	(347.8)	(347.8)
engine install	145.8	145.8
air induction system	11.3	11.3
exhaust system	9.1	9.1
cooling system	1.6	1.6
lubricating system	19.9	19.9
fuel system	36.9	36.9
engine controls	7.9	7.9
starting system	1.9	1.9
drive system	113.4	113.4
Instruments and navigation group	(31.3)	(31.3)
indicators	14.5	14.5
transmitters and amplifiers	4.1	4.1
instruments	10.1	10.1
power system	2.6	2.6
Electrical group	(72.8)	(72.8)
d.c. system	72.8	72.8
Electronics group	(114.1)	(-)
G.F.E., electronics	71.4	-
C.F.E., electronics	42.7	-
Armament group	(12.3)	(4.5)
gun system circuitry and supports	4.5	4.5
armor installation	7.8	-
Furnishings and equipment group	(58.5)	(-)
crew accommodations	15.9	-
passenger accommodations	8.3	-
miscellaneous	34.3	-
Air conditioning group	(9.4)	(9.4)
vent system	.8	.8
heating system	7.9	7.9

Item	OH-6A	POD
Air conditioning group (cont)		
controls	.7	.7
Attaching structure	-	(27.8)

APPENDIX D

INTERCONNECTING STRUCTURE

MEMBER LOADINGS AND SIZES

Member No. (see Fig. 5-1)	Length (inches)	Ultimate axial Load (lb) Lift/Land	Combined bending moment (in-lb)	Selected size (in. x in.)	Critical loading condition	Stress (psi)
1	56.2	-5140./5006.	13290./11517.	3 x 058	buckling	43947
2	91.3	-5805./5146.	19707./17535.	3 x 058	combined	61777
3	77.7	11667./-10835.	36862./34322.	4 x .065	combined	61907
4	219.2	-5635./5301.	9000./8381.	4 x .065	buckling	18583
5	145.5	-4056./3815.	33168./31210.	3-3/1 x 065	combined	54066
6	196.	10347./-9734.	36833./34644.	4 x .065	combined	60226
7	146.	1062./-3081.	1026./3453.	2-3/8 x .049	buckling	25530
8	97.	-2713./1118.	251./820.	2 x .049	buckling	10789
9	69.	-2708./2048.	78./180.	2 x .049	buckling	9563
10	146.	2081./-968.	4317./3982.	2 x .049	buckling	37119
11	113.6	1166./1089.	10625./10128.	2-3/8 x 049	combined	55339
12	73.	2242./-1979.	3400./2921.	1-1/2 x .049	buckling	53348
13	69.	3188./-639.	319./247.	1-1/2 x .049	buckling	18334
14	97.	1736/1222.	73./50.	1-1/2 x .049	comb. (sym.)	8701
15	77.	1002./1337.	111./272.	1-1/2 x .049	comb. (sym.)	9450
16	111.	-1112./1822.	1030./2907	1-1/2 x 049	buckling	45188
17	116.2	-2648./-416.	453./1845.	2 x 049	buckling	14287
18	87.	604./-97.	170./1150.	1 x 049	combined	35302
19	94.5	-955./134.	69./265.	1-1/2 x 049	buckling	
20	77.8	317./-103.	300./1101.	1 x .049	secondary	33866
21	36.1	-429./336.	187./179.	1 x .049	minimum	8563
22	64.6	-401./-605.	63./249.	1 x .049	buckling	11633
23	64.6	844./987.	178./241.	1 x .049	secondary	14001
24	36.1	-420./-1036.	230./295.	1 x .049	minimum	15962

Member No. (see Fig. 5-1)	Length (inches)	Ultimate axial Load (lb) Lift/Land	Combined bending moment (in-lb)	Selected size (in. x in.)	Critical loading condition	Stress (psi)
25	52.4	1157./1198.	167./162.	1 x .049	minimum	12933
26	75.0	-1596./-2216.	634./315.	1-1/2 x .049	buckling	15221
27	87.0	1244./1781.	1316./1620.	1 x .049	secondary	60960
28	113.6	-2421./-1131.	3752./3493.	2 x .049	buckling	34300
29	70.	-2715./4571.	312./3453	1-1/2 x .049	buckling	64448
30	151.9	-1715./2059.	1270./3526.	2 x .049	buckling	31514
31	60.4	-1311./2814.	348./1889.	1-1/4 x .049	buckling	50594
32	114.1	-2045./5039.	2310./8266	2 x .049	buckling	74584
33	60.1	4./-15.	709./1703.	1 x .049	minimum	51398
34	91.5	-3386./2369.	1872./1462.	2 x .049	buckling	25066
35	69.3	-1609./3307.	273./349.	1-1/4 x .049	buckling	24421
36	126.7	-1335./54.	851./813.	2 x .049	buckling	10397
37	60.6	-3378./3751.	1405./1140.	1-1/2 x .049	buckling	33019
38	126.2	-1973./25.	2333./2380.	2 x .049	buckling	22885
39	64.3	3992./-4324.	4442./4228.	2 x .049	buckling	44356
40	71.3	6245./-4475.	5755./5255.	2 x .049	buckling	61041
41	69.2	58./37.	170./243.	1 x .049	minimum	13725
42	119.6	-1419./548.	90./89.	2 x .049	buckling	5355
43	60	348./144.	154./423.	1 x .049	minimum	-
44	124.4	780./-910.	83./112.	1-1/2 x .049	buckling	5500
45	61.2	-1./-25.	113./519.	1 x .049	minimum	-
46	88.5	8390./-14140.	1078./998.	3-1/4 x .065	buckling	23706
47	113.1	-261./-522.	396./1222.	1-1/4 x .049	buckling	25707
48	129.1	168./1497.	870./4381.	1-1/2 x .049	combined	62510
49	143.5	-536./-1878.	2054./.9936.	2-3/8 x .049	buckling	53950

Member No. (see Fig. 5-1)	Length (inches)	Ultimate axial Load (lb) Lift/Land	Combined bending moment (in-lb)	Selected size (in. x in.)	Critical loading condition	Stress (psi)
50	126.2	-392./-1755.	1616./4032.	2 x .049	buckling	34043
51	114.8	-383./798.	5647./5377.	2 x .049	combined	40259
52	61.5	232./2.	1871./1715.	1 x .049	combined	57940
53	99.3	335./214.	372./573.	1-1/4 x .049	secondary	18721
54	54.2	-2355./4161.	336./773.	1-1/4 x .049	buckling	33103
55	108.8	-1084./1309.	49./89.	1-1/2 x .049	buckling	6993
56	84.8	-58./-133.	8./34.	1 x .049	minimum	–
57	96.8	-528./464.	26./35.	1-1/4 x .049	buckling	–
58	96.8	-647./371.	18./19.	1-1/4 x .049	buckling	–
59	49.8	-3148./2278.	882./667.	1-1/4 x .049	buckling	33542
60	137.2	119./-598.	203./177.	1-1/2 x .049	buckling	–
61	103.5	4582./-3521.	771./879.	2 x .049	buckling	17872
62	109.0	3456./-3820.	266./66.	2-3/8 x .049	buckling	10958
63	133.0	-155./1741.	31./173.	1-1/4 x .049	secondary	–
64	103.5	582./-1134.	76./174.	1-1/2 x .049	buckling	7293
65	103.5	-369./-731.	62./168.	1-1/4 x .049	buckling	–
66	103.5	343./-421.	163./192.	1-1/4 x 049	buckling	–
67	103.5	788./160.	207./165.	1-1/4 x 049	secondary	–
68	90.0	45./687.	301./430.	1 x .049	secondary	17656
69	137.2	268./-52.	746./483.	1-1/4 x .049	secondary	15419
70	90.0	-1260./3835.	480./779.	1-1/2 x .049	buckling	27090
71	141.4	594./-2842	566./849.	2-3/8 x .049	buckling	12101
72	90.2	-45./944.	562./830.	1 x .049	minimum	31436
73	139.8	313./-793.	20./73.	1-1/2 x .049	buckling	–
74	56.5	94./3425.	280./285.	1 x .049	minimum	31979

Moment No. (see Fig. 5-1)	Length (inches)	Ultimate axial Load (lb) Lift/Land	Combined bending moment (in-lb)	Selected size (in. x in.)	Critical loading condition	Stress (psi)
75	90.9	914./1405.	129./69.	1 x .049	minimum	–
76	50.2	268./2946.	369./349.	1 x .049	minimum	30635
77	116.3	316./474.	81./113.	1-1/4 x 049	comb. (sym.)	–
78	49.5	-379./2000.	281./215.	1 x 049	minimum	–
79	113.2	166./194.	64./30.	1-1/4 x 049	secondary	–
80	59.3	305./847.	103./128.	1 x 049	minimum	–
81	98.4	596./-1089.	37./13.	1-1/2 x .049	buckling	7604
82	53.6	1646./-903.	71./133.	1 x .049	buckling	–
83	108.7	453./406.	47./31.	1-1/4 x 049	comb. (sym.)	–
84	54.2	2796./-563.	210./52.	1 x .049	buckling	25424
85	101.8	628./-611.	41./28.	1-1/4 x .049	buckling	–
86	53.3	2259./-427.	61./159.	1 x .049	minimum	–
87	105.2	814./-110.	33./26.	1-1/4 x 049	secondary	–
88	53.6	2959./-1257.	153./90.	1 x .049	buckling	24820
89	80.1	4879./-3464.	142./149.	2 x .049	buckling	–
90	133.8	-2542./548.	409./604.	2-3/8 x .049	buckling	–
91	82.1	64./-1362.	101./111.	1-1/2 x .049	buckling	7511
92	106.5	-525./674.	873./797.	1-1/4 x .049	buckling	19188
93	88.9	3260./-5339	917./1132.	2-3/8 x .049	buckling	20458
94	80.0	3131./-5238.	1030./1420.	2 x .049	buckling	27373
95	155.3	-1678./2453.	28./72.	2-3/8 x .049	buckling	–
96	106.5	483./-120.	71./94.	1-1/4 x .049	secondary	
97	88.8	-112./291.	24./34.	1 x .049	secondary	
98	88.8	-92./-436.	33./24.	1 x .049	buckling	
99	88.8	-18./677.	41./67.	1 x .049	secondary	

Moment No. (see Fig. 5-1)	Length (inches)	Ultimate axial Load (lb) Lift/Land	Combined bending moment (in-lb)	Selected size (in. x in.)	Critical loading condition	Stress (psi)
100	88.8	-222./-867.	13./10.	1-1/4 x .049	buckling	
101	94	1660./-867.	30./58.	1-1/4 x .049	buckling	
102	88.8	-1550./1756.	65./33.	1-1/2 x .049	buckling	
103	88.8	-148./549.	85./58.	1 x .049	secondary	
104	88.8	596./-468.	222./514.	1 x .049	buckling	18679
105	38.8	-1122./1864.	320./444.	1 x .049	buckling	26106
106	101.7	795./-1010.	59./92.	1-1/2 x .049	buckling	
107	94.0	191./96.	76./103.	1-1/4 x .049	secondary	
108	129.3	-38./298.	19./32.	1-1/4 x .049	secondary	
109	94.0	-587./774.	34./12.	1-1/4 x .049	buckling	
110	129.3	1044./-1173.	168./151.	2 x .049	buckling	
111	94.0	159./123.	60./75.	1 x .049	secondary	vert memb.
112	129.3	251./405.	478./531.	1-1/4 x .049	secondary	
113	98.5	-261./807.	59./76.	1-1/4 x .049	secondary	
114	93.3	200./-66.	35./59.	1-1/4 x .049	secondary	
115	137.6	162./546.	14./18.	1-1/4 x .049	secondary	
116	87.1	114./170.	42./9.	1 x .049	secondary	
117	109.6	-12./51.	28./23.	1-1/4 x .049	secondary	
118	115.1	1151./773.	35./8.	1-1/4 x 049	secondary	
119	85.6	1202./254.	71./38.	1 x .049	secondary	
120	109.7	-1170./-1385.	67./55.	2 x .049	buckling	
121	82.7	3367./-1525.	93./89.	1-1/2 x .049	buckling	
122	113.0	1861./-2745.	318./173.	2 x .049	buckling	
123	107.3	2617./-1480.	45./49.	2 x .049	buckling	

Moment No. (see Fig. 5-1)	Length (inches)	Ultimate axial Load (lb) Lift/Land	Combined bending moment (in-lb)	Selected size (in. x in.)	Critical loading condition	Stress (psi)
124	84.3	71./-1371.	45./29.	1-1/2 x .049	buckling	
125	135.8	1144./-2290.	304./385.	2-3/8 x .049	buckling	
126	90.7	2029./-3230.	417./379.	2 x .049	buckling	
127	82.0	2294./-3634.	547./543.	2 x .049	buckling	15898
128	109.1	-45./-428.	43./51.	1-1/4 x .049	buckling	
129	72.0	190./189.	73./66.	1 x .049	minimum	
130	147.0	175./-256.	8./8.	1-1/2 x .049	secondary	
131	147.0	288./353.	12./9.	1-1/2 x .049	secondary	
132	72.0	198./178.	85./27.	1 x .049	minimum	
133	147.0	-1477./1010.	53./65.	2 x .049	buckling	
134	147.0	-857./1361.	41./21.	2 x .049	buckling	
135	163.7	-383./578.	15./9.	1-1/2 x .049	buckling	
136	72.0	54./139.	41./31.	1 x .049	minimum	
137	163.7	-428./-455.	84./113.	1-1/2 x .049	buckling	3476
138	48.9	-89./342.	20./47.	1 x .049	minimum	–
139	87.0	-1./1.	45./40.	1 x .049	minimum	–
140	42.0	4132./-6560.	256./457.	1-1/2 x .049	buckling	35186
141	129.0	-10./142.	9./14.	1-1/4 x .049	secondary	–
142	42.0	186./489.	20./15.	1 x .049	minimum	–
143	152.9	39./-40.	11./16.	1-1/2 x .049	secondary	–
144	42.0	1093./-242.	56./18.	1 x .049	minimum	–
145	83.4	-1./1.	44./22	1 x .049	minimum	–
146	42.0	4692./-3505.	66./39.	1-1/4 x 049	buckling	28063
147	83.4	-1./0.	22./24.	1 x .049	minimum	–
148	42.0	3203./-3863	0./0.	2 x .049	buckling	base on ℓ = 84"!

Moment No. (see Fig. 5-1)	Length (inches)	Ultimate axial Load (lb) Lift/Land	Combined bending moment (in-lb)	Selected size (in. x in.)	Critical loading condition	Stress (psi)
149	152.9	-7./12.	19./33.	1-1/2 x .049	secondary	–
150	152.9	-2./1.	28./20.	1-1/2 x 049	secondary	–
151	126.3	674./-12.	17./13.	1-1/4 x 049	secondary	–
152	93.4	-128./-246.	72./154.	1 x 049	buckling	–
153	97.4	-736./908.	125./64.	1-1/4 x .049	buckling	6321
154	86.7	-1172./1100.	182./215.	1-1/4 x .049	buckling	9975
155	145.9	-474./642.	52./137.	1-1/2 x .049	buckling	3867
156	82.2	-3285./1300.	132./231.	2 x .049	buckling	11862
157	116.8	-756./267.	106./98.	1-1/2 x .049	buckling	4734
158	80.2	-1062./953.	48./90.	1-1/4 x .049	buckling	6840
159	122.4	-624./1151.	146./106.	1-1/4 x .049	buckling	6109
160	80.9	-1223./575.	125./111.	1-1/4 x .049	buckling	8955
161	120.9	-1237./2154.	187./192.	1-1/4 x .049	buckling	15245
162	85.8	3969./-4302.	352./266.	2 x .049	buckling	15678
163	122.3	-643./59.	462./630.	1-1/2 x .049	buckling	–
164	124.8	2808./-1697.	250./733.	2 x .049	buckling	12722
165	108.2	2043./-1698.	2259./3035.	2 x .049	buckling	26878
166	53.0	881./1689.	2889./10969	2-3/8 x .049	combined	58486
167	88.6	-1234./-2782.	2614./3701	2 x .049	buckling	35145
168	128.6	-1241./3417.	2264./3548.	2 x .049	buckling	36190
169	56.2	-5401./5337.	3538./5586.	2 x .049	buckling	comb 56835
170	91.3	-7113./5884.	6819./18348	3-1/4 x .065	combined	45179
171	77.7	12182./-11613.	6161./9877.	3 x .058	buckling	53464
172	56.2	-4303./5457.	7894./22787.	3-1/4 x 065	combined	53264
173	91.4	-7134./4839.	16107./48381.	4-1/2 x .065	combined	54223

Moment No. (see Fig. 5-1)	Length (inches)	Ultimate axial Load (lb) Lift/Land	Combined bending moment (in-lb)	Selected size (in. x in.)	Critical loading condition	Stress (psi)
174	77.7	9223./-14506.	6705./13294.	3 x .058	buckling	48483
175	48.7	784./-728.	4290./5535.	2 x .049	combined	41131
176	38.7	185./-76.	10760./4847.	2-3/8 x .049	combined	53262
177	37.0	-578./530.	5926./3889.	2 x .049	combined	43365
178	97.3	1315./1140.	1950./11229.	2-3/8 x .049	combined	58228
179	77.5	-1090./-453	4345./6060.	2 x 049	combined	43886
180	74.0	-2081./-1251.	1826./1851.	1-1/2 x .049	buckling	32576
181	54.9	1309./158.	8213./7420.	2 x 049	combined	61793
182	116.9	-548./-1898.	3794./4224.	2 x .049	buckling	35859
183	75.0	831./-568.	1365./11256.	2-3/8 x .049	combined	56763
184	148.2	2873./3989.	1360./3505.	2 x .049	combined	37794
185	17.0	0./0.	74161./69766	5 x .065	combined	60421
186	17.0	0./0.	74161./69766.	5 x .065	combined	60421

APPENDIX E

PILOTED HYBRID AIRSHIP FLIGHT SIMULATION

FLIGHT SIMULATION

1. GENERAL

The real-time hybrid airship flight simulation existing at Goodyear Aerospace was adapted to determine the flight research vehicle control and maneuverability characteristics on a preliminary basis. A brief description of the simulating hardware, mathematical model, and control system used in this application are given below.

2. SIMULATION HARDWARE

The simulation was set up on a hybrid system consisting of a Sigma 9 digital computer, an EAI 7800 analog computer, and the interface equipment. Figure E-1 shows the complete simulation set up including pilot controls, visual display, flight instruments, and analog computer.

The bulk of the computation was done on the digital computer. The analog computer was used to set up autopilots, pilot inputs, instrumentation and display circuitry. it also provided the means to record 16 real-time variables on the strip chart recorders (not shown in the figure).

The visual display consisted of a top view (Figure E-2) which gave the pilot cues on horizontal plane motion of the vehicle. Each grid in the display represents a square with 100-foot side dimension. An X-Y plotter was also used in hovering tasks to give the pilot visual cues which were accurate to a foot.

Motion of the vehicle, with or without a sling load, in the longitudinal and lateral vertical planes was displayed as combined elevation. The roll attitude of the vehicle was displayed as a change in inclination of a horizontal line aligned with the vehicle horizontal plane.

The flight instruments used (Figure E-2) were: airspeed indicator, turn indicator, angle-of-attack and sideslip angle indicators, vertical speed indicator (not shown in figure) and digital read-out of any desired variable, on the analog panel.

In addition, the strip chart recorders were located adjacent to the visual display for easy reference and 16 real-time variables were recorded on these charts. A particular selection of input and output variables recorded depended on the task to be executed.

3. MATHEMATICAL MODEL

Six degree-of-freedom motion of the vehicle was simulated by using general non-linear motion equations of the FRV represented as a rigid body. The external forces and moments acting on the vehicle due to gravity, buoyancy, aerodynamics, and control inputs were represented in the simulation.

a. Aerodynamics Representation

The static aerodynamic characteristics of the airship support frame described previously in Section IV were used to represent the lateral/directional aerodynamics of the vehicle.
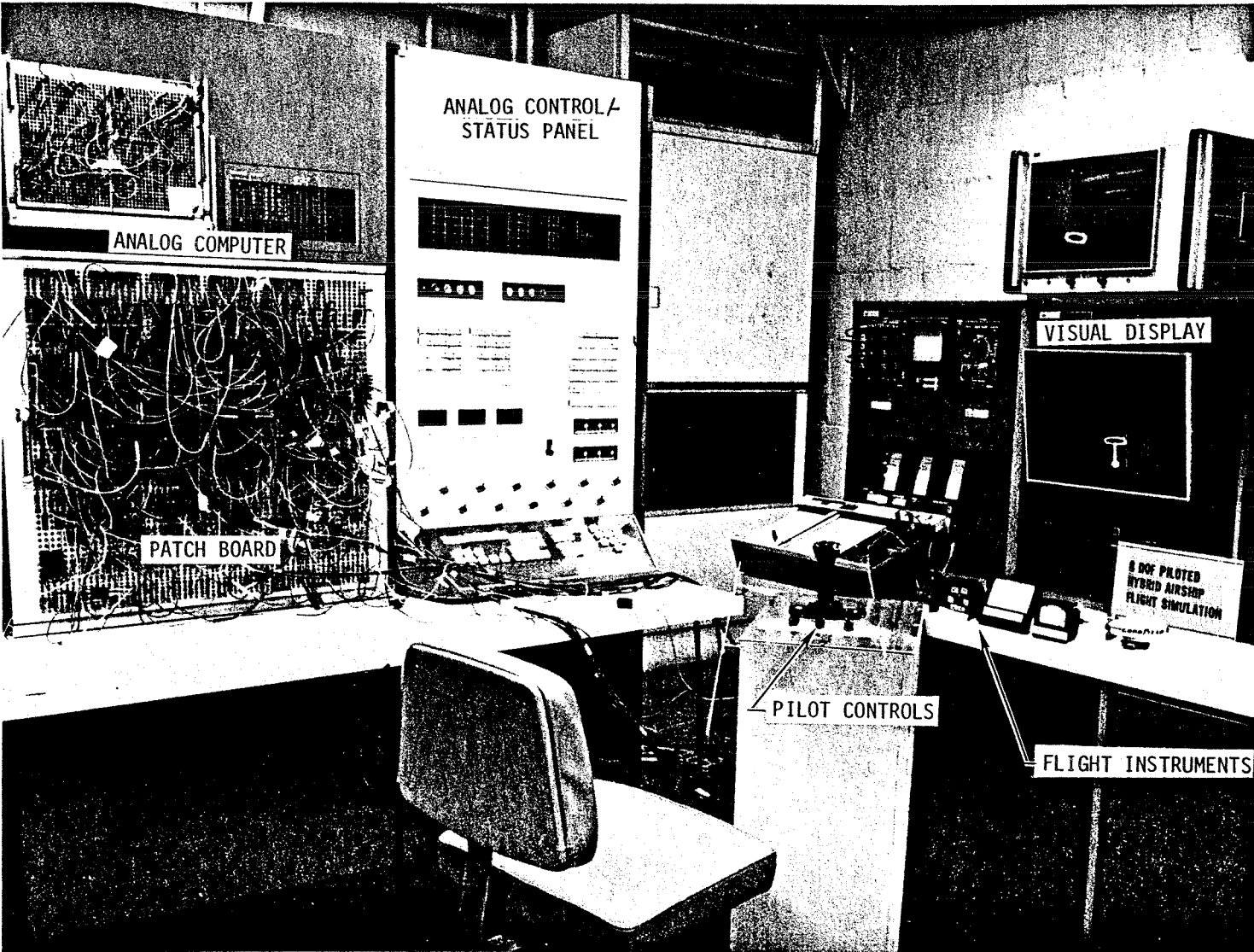
E-2

Figure E-1 - Hybrid Airship Flight Simulation Facility

ANALOG COMPUTER

ANALOG CONTROL/
STATUS PANEL

VISUAL DISPLAY

PATCH BOARD

6 DOF PILOTED
HYBRID AIRSHIP
FLIGHT SIMULATION

PILOT CONTROLS

FLIGHT INSTRUMENTS

Figure E-2 - Hardware Components Used for Piloted Flight Simulation
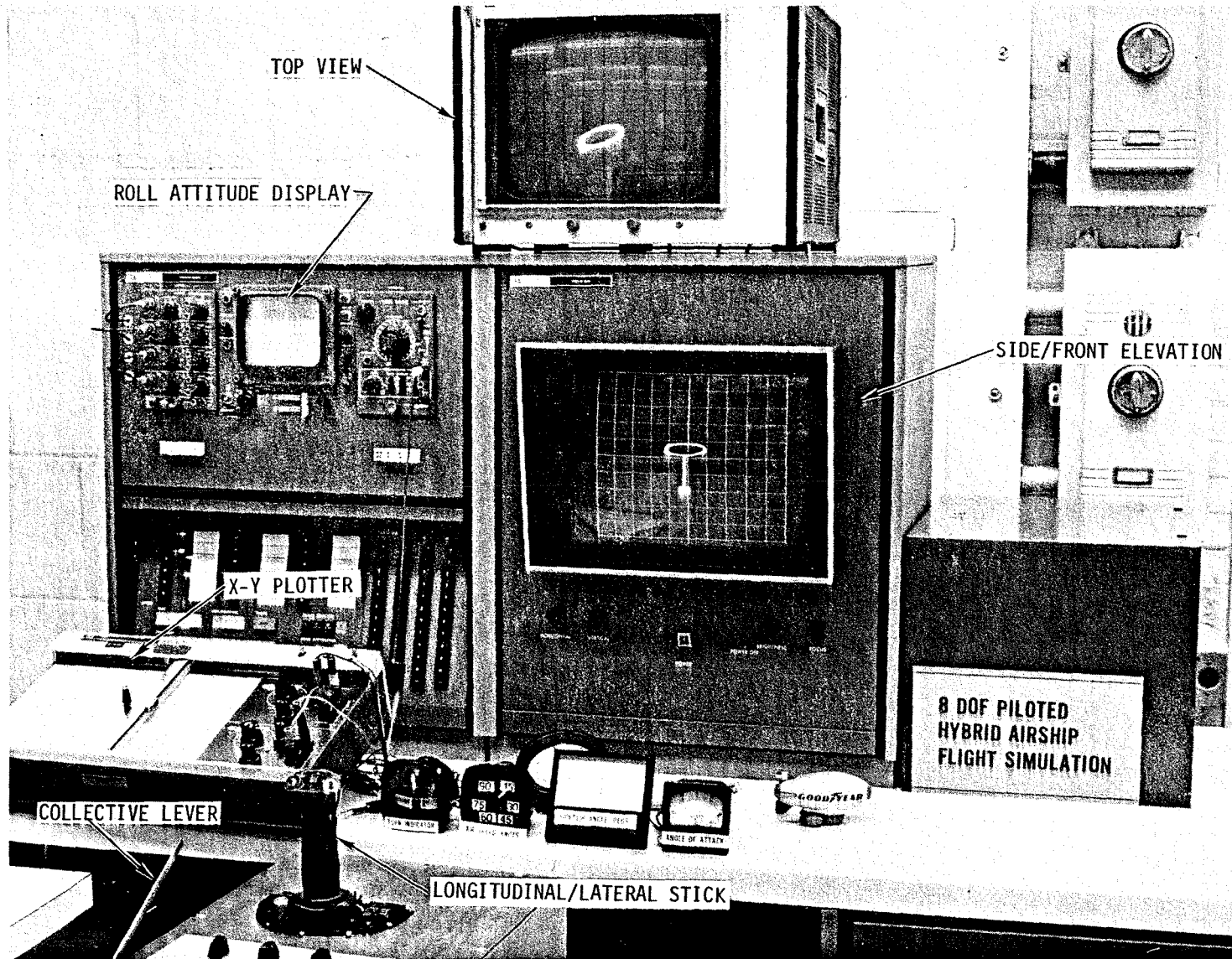
As a first approximation, the normal force and pitching moment characteristics of the vehicle were assumed to be equal to its side force and yawing moment characteristics, respectively. The axial force on the vehicle due to the envelope as well as support frame has also been included as discussed previously. The damping moments due to pitching and yawing of the airship component were estimated from the corresponding derivative data. (See Table 8-3.)

Similarly, acceleration dependent aerodynamic forces and moments of the airship component are included in terms of their derivatives. (See Table 8-5.)

b. Helicopter Model

Basically, the helicopter rotor is represented by a thrust vector which can be tilted in pitch and roll. The magnitude of the thrust is assumed to be linearly proportioned to collective pitch input.

Longitudinal and lateral cyclic pitch inputs were limited to four degrees each on a steady-state basis. This would permit the life of the main rotor strap pack to approximate 3333 flight hours. The cyclic pitch inputs were assumed to tilt the rotor thrust vectors through the corresponding angles in pitch and roll, instantaneously.

Stability derivatives of the quad-helicopter configuration, described earlier, are used to represent pitch and roll damping moments contribution from the helicopters in the corresponding flight condition. Aerodynamics of the helicopter fuselages are incorporated in the overall airship support frame aerodynamics.

c. Auxiliary Thruster Model

Each of the four auxiliary propulsion units are modeled as pure force generators with 100 percent reversible thrust capability. The collective pitch input to each unit is assumed to be linearly proportional to the thrust generated by it.

d. Payload Model

The payload was modeled as a single unit which is held snugly to the bottom of the airship envelope, behind the car. Consequently, sling load dynamics was not included in this application.

Aerodynamic drag of the payload can be represented in this simulation, given appropriate data. However, in the present case, the payload was treated as a concentrated mass, for simplicity.

4. CONTROL SYSTEM

The control system represented in the simulation consists of control system logic, autopilot and closed loop systems, and pilot controls. The simulation was set up so that it could be run purely open loop through the individual control inputs or via the pilot controls and autopilot systems.

No specific studies were conducted with pilots in the control loop. However, vehicle response to pilot control inputs was determined.
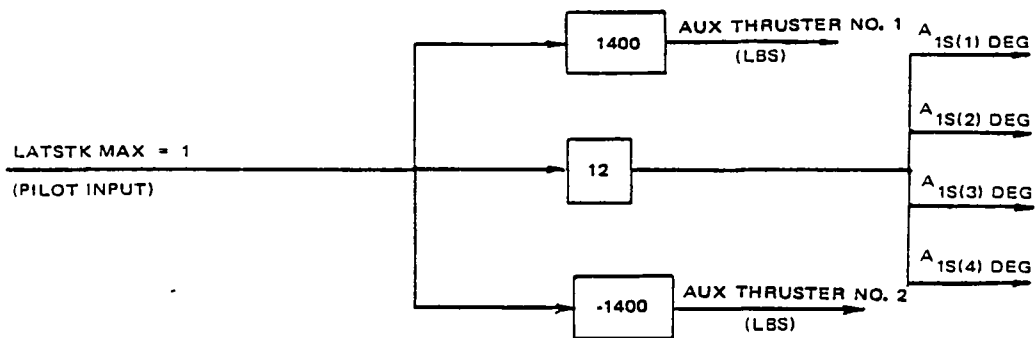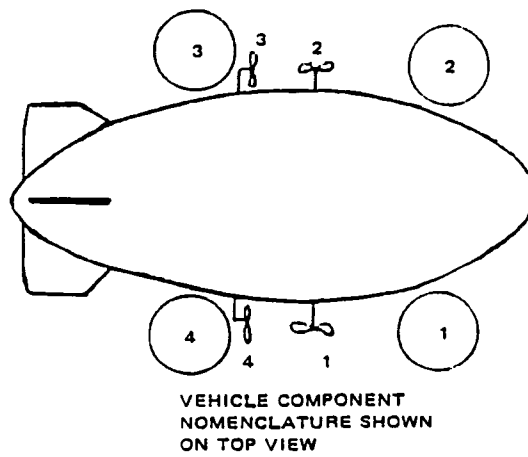
VEHICLE COMPONENT
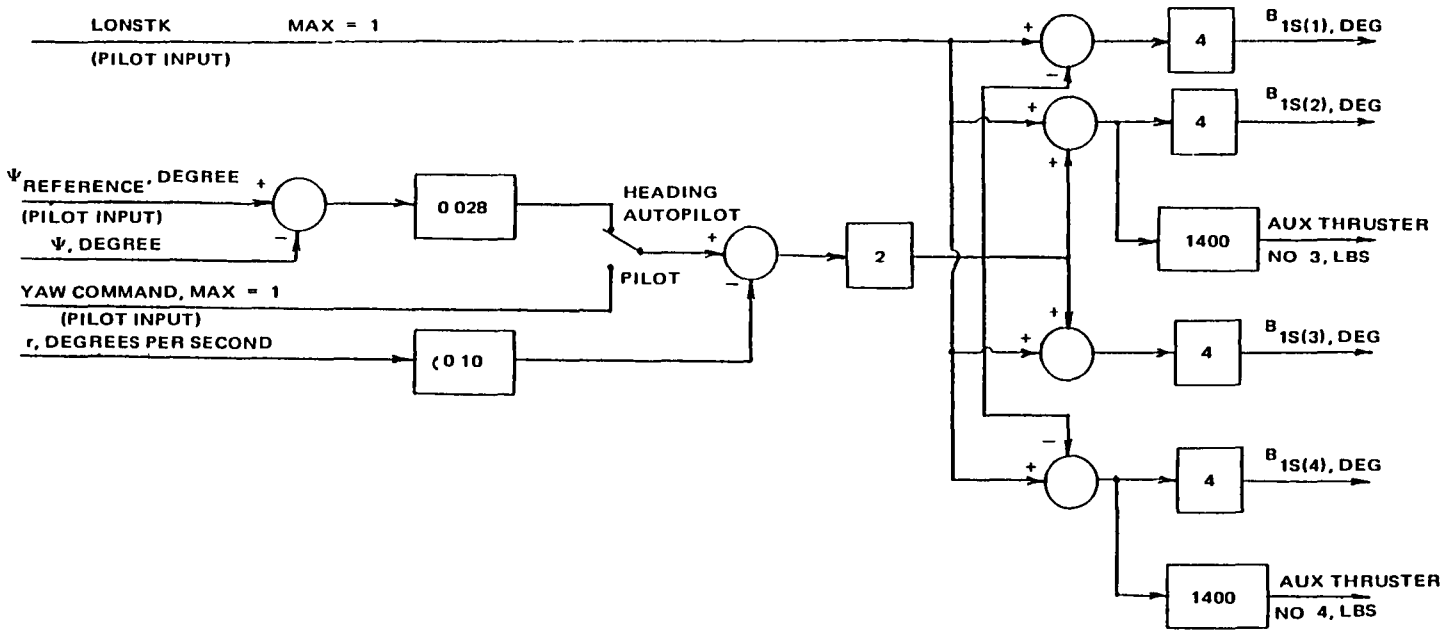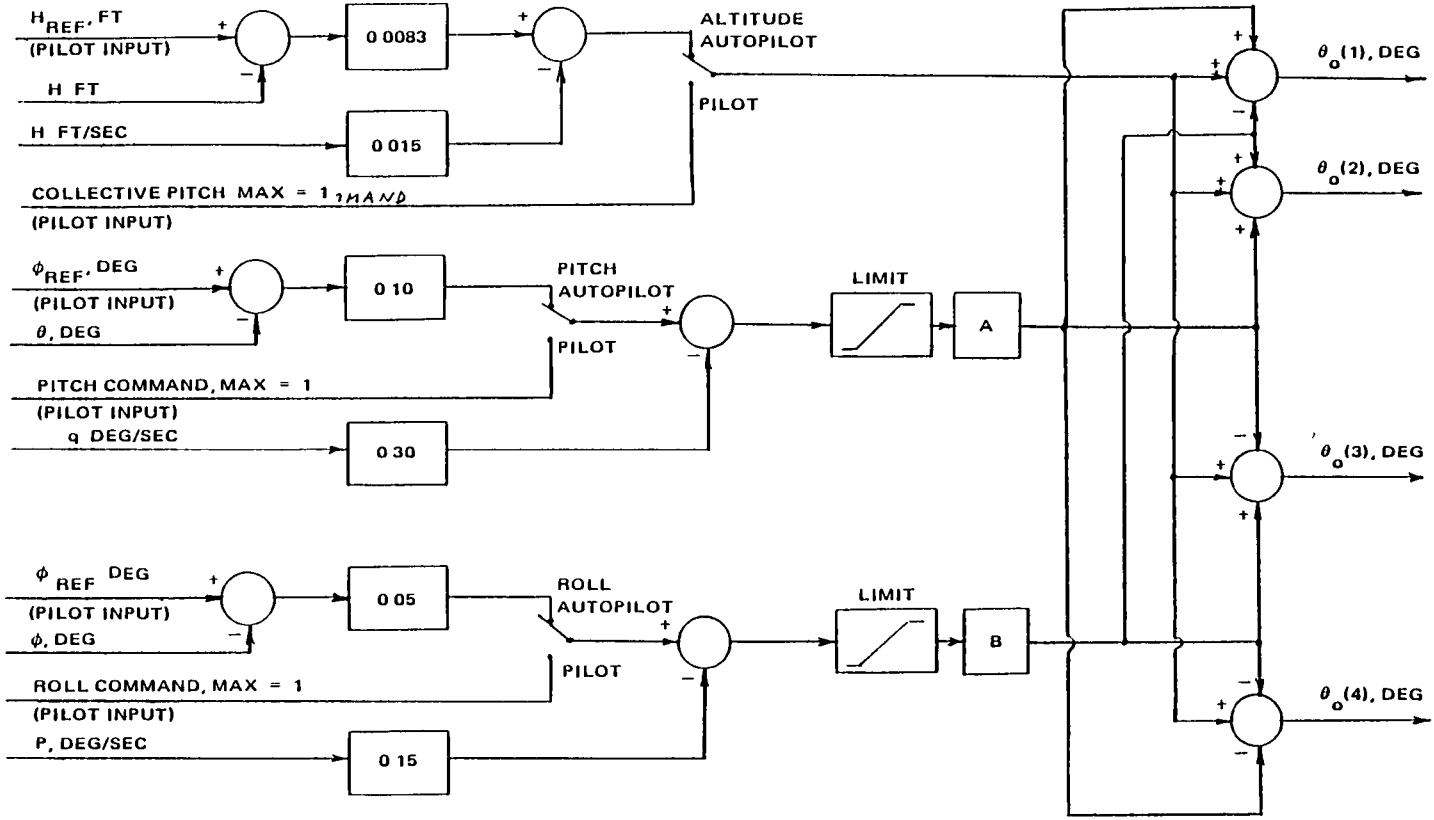NOMENCLATURE SHOWN
ON TOP VIEW

Figure E-3 – Logic for Lateral Control System

Figure E-4 — Logic for Longitudinal and Yaw Control System

Figure E-5 – Logic for Vertical Pitch and Roll Control System

H_{REF}, FT
(PILOT INPUT)

H FT

H FT/SEC

0 0083

0 015

ALTITUDE
AUTOPILOT

PILOT

COLLECTIVE PITCH MAX = 1 $_{MAND}$
(PILOT INPUT)

ϕ_{REF}, DEG
(PILOT INPUT)

θ, DEG

0 10

PITCH
AUTOPILOT

PILOT

PITCH COMMAND, MAX = 1
(PILOT INPUT)

q DEG/SEC

0 30

LIMIT

A

ϕ_{REF} DEG
(PILOT INPUT)

ϕ, DEG

0 05

ROLL
AUTOPILOT

PILOT

ROLL COMMAND, MAX = 1
(PILOT INPUT)

P, DEG/SEC

0 15

LIMIT

B

$\theta_o(1)$, DEG

$\theta_o(2)$, DEG

$\theta_o(3)$, DEG

$\theta_o(4)$, DEG

<u>a</u>. <u>Control System Logic</u>

Concepts for controlling the vehicle during hover and forward flight have been previously discussed. In the simulation, a baseline control logic (Figures E-3 to E-5) was used to fly the vehicle. In this logic it has been assumed that the helicopters on the hinges (roll only) would provide thrust vectors capable of a 12 degree tilt in roll and a 4 degree tilt in pitch with respect to a reference frame on the outrigger structure.

The control authority of pitch and roll command inputs is limited to ±10 percent over the corresponding trim value of the collective pitch of individual rotors. However, provisions have been made to change these authority limits via the authority parameters A and B for pitch and roll, respectively. (See Figure E-5).

<u>b</u>. <u>Autopilots</u>

Several autopilots were designed and used during simulation of the FRV to examine vehicle control characteristics and maneuverability. They included X and Y autopilots to maintain position over ground (Figure E-6), altitude autopilot (Figure E-5), heading autopilot (Figure E-4), pitch attitude autopilot (Figure E-5), and roll attitude autopilot (Figure E-5). The autopilots were set up on the analog computer because of the convenience of connecting and disconnecting them during simulation.

These autopilots consisted of proportional and rate feedback only. Consequently, in some cases, constant errors were observed, during the simulation.
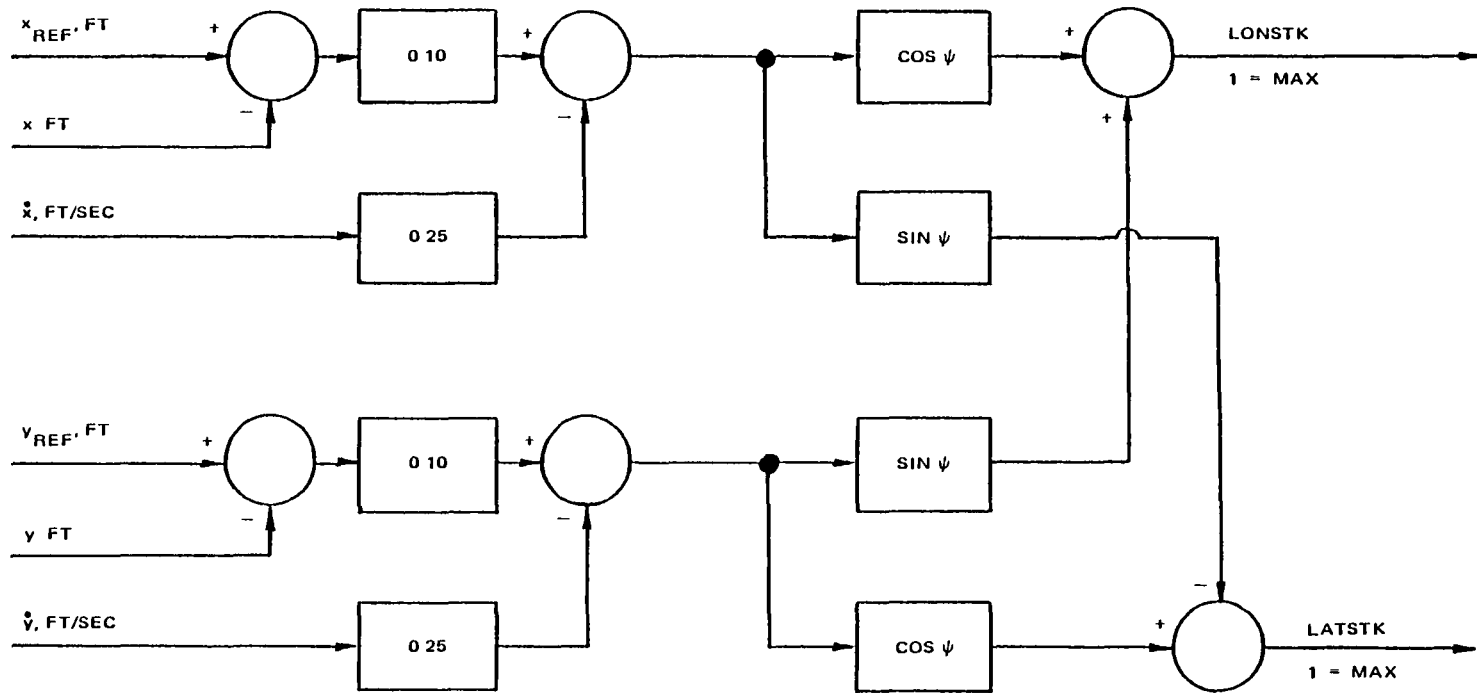
<u>c</u>. <u>Pilot Controls</u>

Pilot controls (Figure E-2) consisted of an airplane stick which was used for longitudinal stick and lateral stick inputs. It was similar in function to the cyclic stick of a conventional helicopter. A lever attached to a potentiometer was used as the collective stick. Pitch, roll, and yaw command controls were potentiometers with calibrated dials. They were located behind the longitudinal/lateral stick on the same panel.
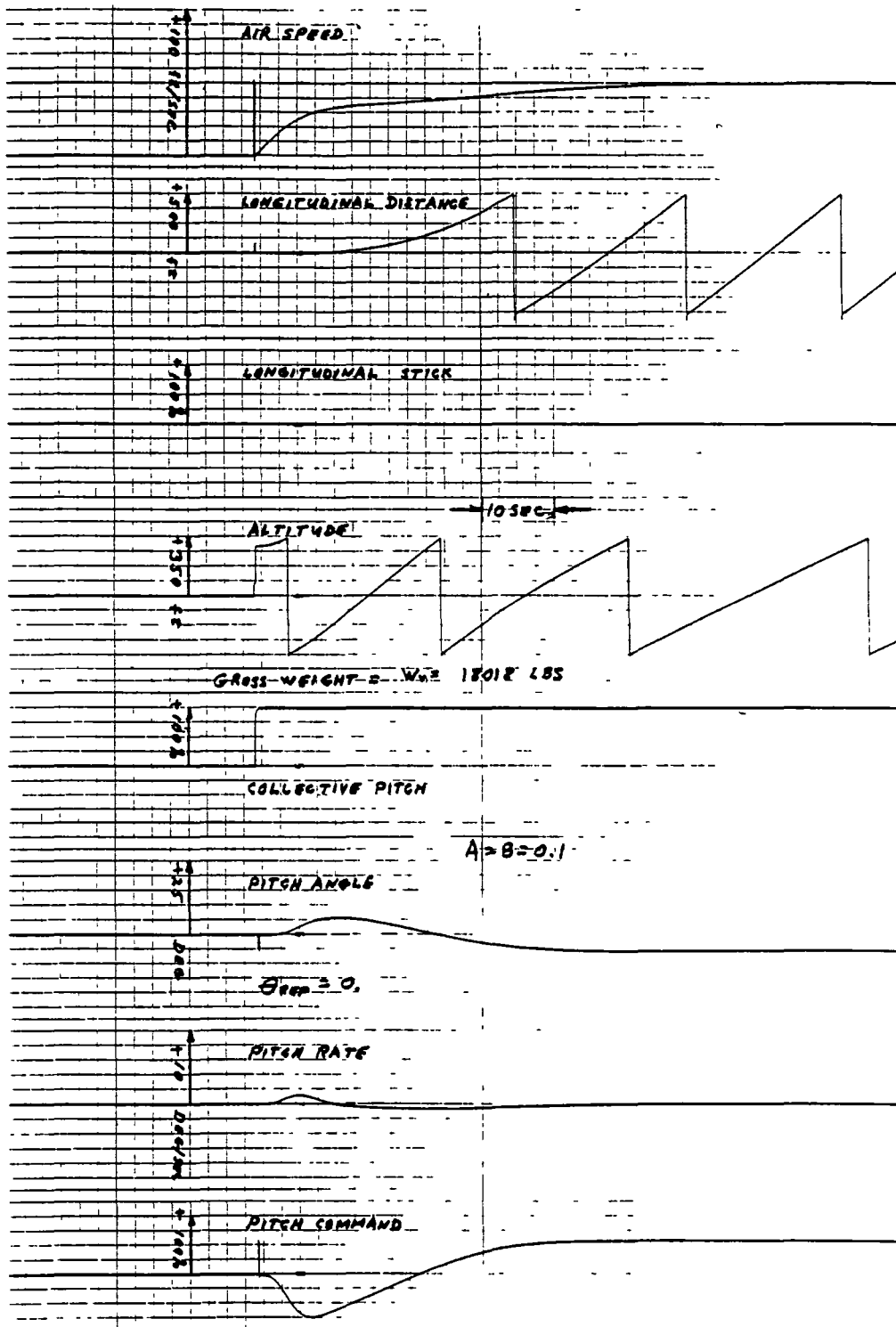
These control inputs supplied proportional voltages to the analog computer which were amplified and then converted to digital signals by the A-D converter.

During the piloted simulation in the unaugmented mode, the rate feedbacks in pitch, roll, and yaw were disconnected to give the pilot direct access to control moments in these axes in an open loop fashion.
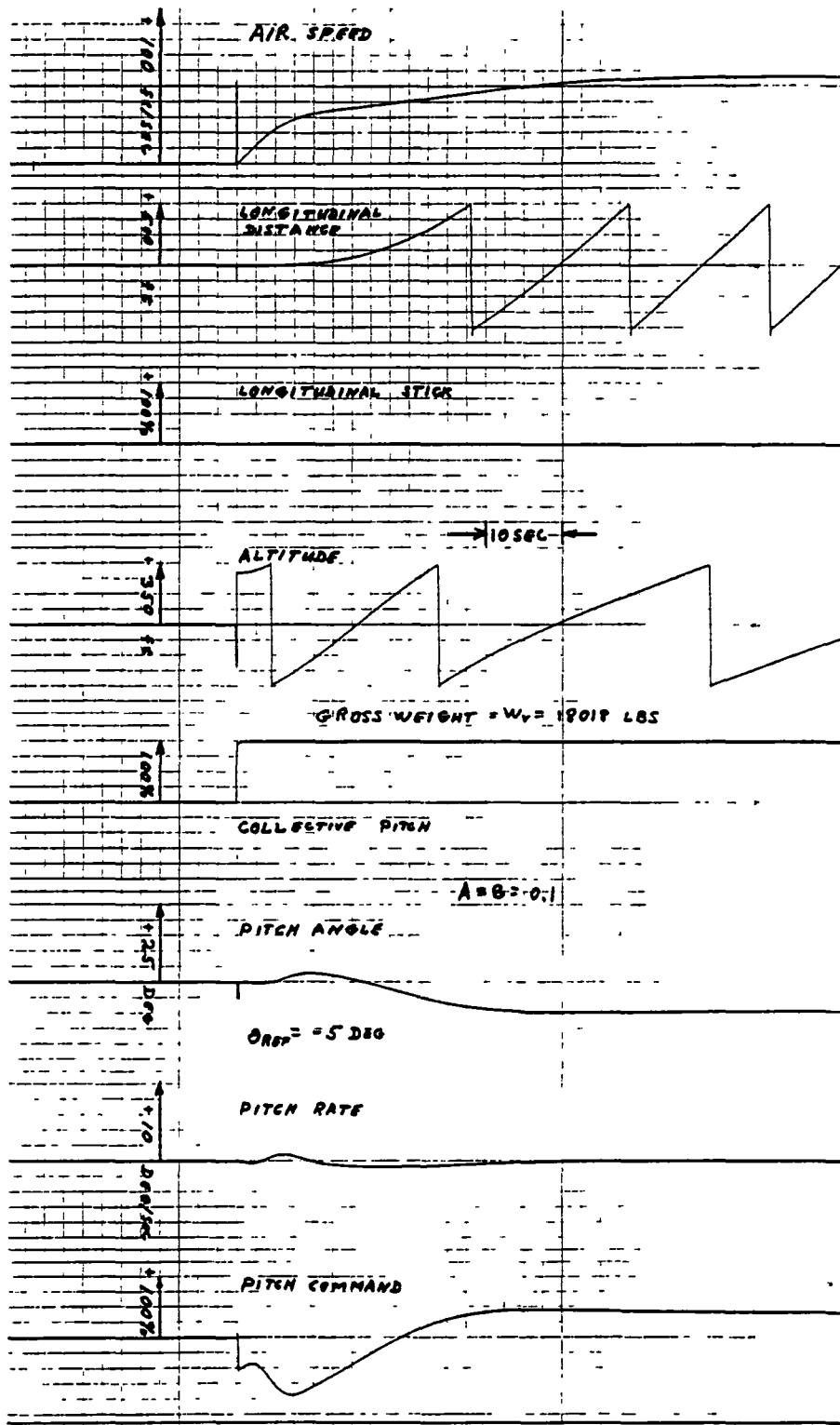
Figure E-6 – X and Y Autopilots

APPENDIX F

FRV CLOSED LOOP RESPONSE

AIR SPEED

LONGITUDINAL DISTANCE

LONGITUDINAL STICK

10 SEC

ALTITUDE

GROSS WEIGHT = W_n = 18018 LBS

COLLECTIVE PITCH

A = B = 0.1

PITCH ANGLE

θ_{REF} = 0.

PITCH RATE

PITCH COMMAND
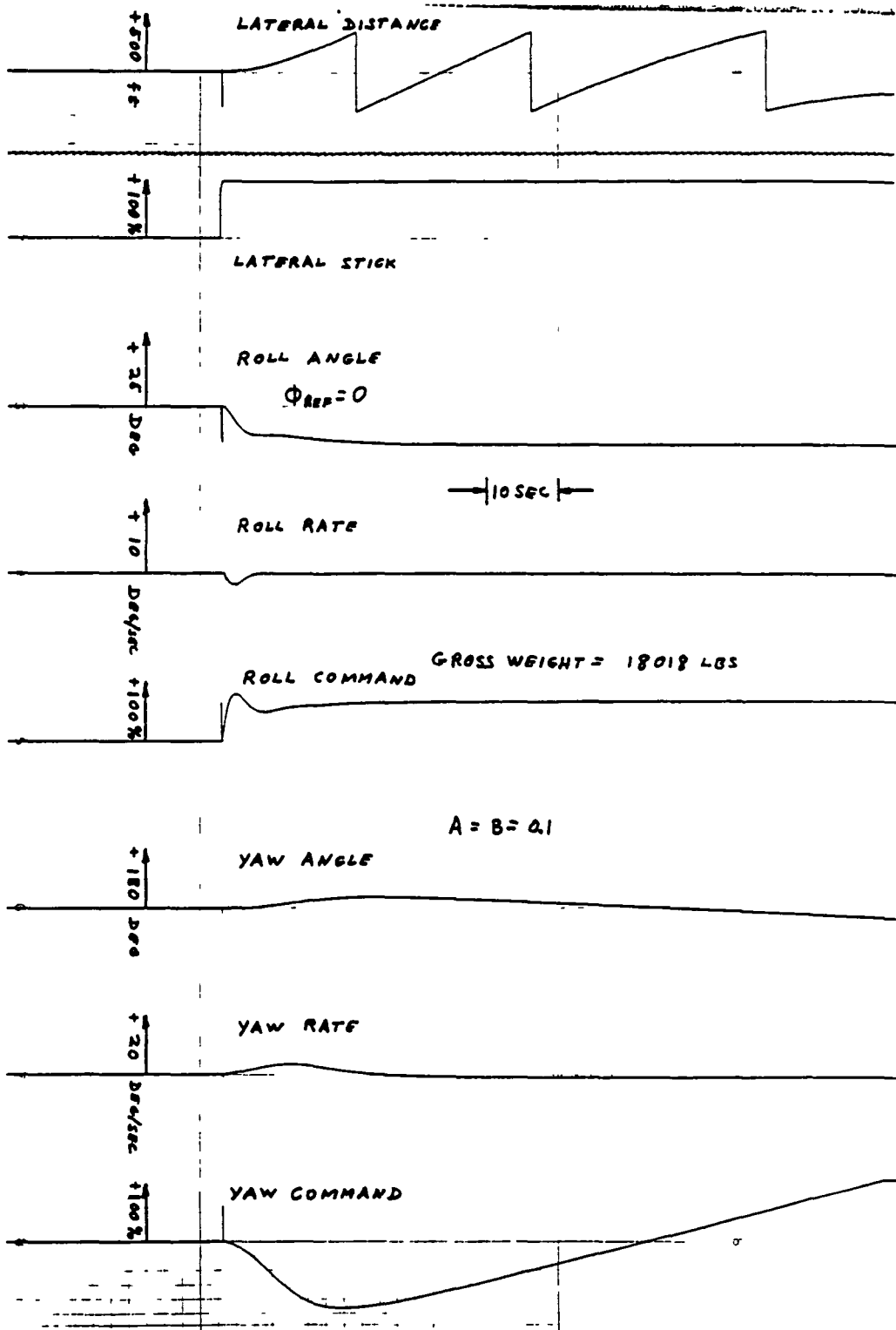
Closed Loop Response of The Vehicle - Run No. 1

Run No. 2

AIR SPEED

LONGITUDINAL DISTANCE

LONGITUDINAL STICK

|← 10-SEC ←|

ALTITUDE

GROSS WEIGHT = 18018 lbs

COLLECTIVE PITCH

.477

$A = B = 0.1$

PITCH ANGLE

$\theta_{REF} = 0$

PITCH RATE

PITCH COMMAND

Run No. 3

LATERAL DISTANCE

+500 ft

LATERAL STICK

+100 %

ROLL ANGLE

$\Phi_{REF} = 0$

+25 DEG

$\rightarrow$|10 SEC|$\leftarrow$

ROLL RATE

+10 DEG/SEC

ROLL COMMAND   GROSS WEIGHT = 18018 LBS

+100 %

A = B = 0.1

YAW ANGLE

+180 DEG

YAW RATE

+20 DEG/SEC

YAW COMMAND

+100 %

σ

Run No. 4

AIR SPEED

LONGITUDINAL DISTANCE

LONGITUDINAL STICK

⊢·10 SEC⊢

ALTITUDE

GROSS WEIGHT = 18018 LBS

COLLECTIVE PITCH

.477

A = B = 0.1

PITCH ANGLE

$\Theta_{REF} = 0$
LATSTK = 1

PITCH RATE

PITCH COMMAND

Run No. 4

AIR SPEED

LONGITUDINAL DISTANCE

LONGITUDINAL STICK

⟶|10 sec|⟵

ALTITUDE

GROSS WEIGHT ≈ 18018 LBS

COLLECTIVE PITCH

.477

$A = \theta = 0.1$

PITCH ANGLE

$\theta_R = 5$ DEG

PITCH RATE

PITCH COMMAND

Run No. 5

AIR SPEED

LONGITUDINAL DISTANCE

LONGITUDINAL STICK

$\longmapsto$ 10 SEC $\longmapsto$

ALTITUDE

GROSS WEIGHT = 18018 LBS

COLLECTIVE PITCH

.477

$A = \theta \geq 0.1$

PITCH ANGLE

$\theta_R = -10$ DEG

PITCH RATE

PITCH COMMAND

Run No. 6

AIR SPEED

+100 Ft/sec

LONGITUDINAL
DISTANCE

+500 Ft

LONGITUDINAL STICK

+100%

ALTITUDE

+50 Ft

←|10 SEC|→

GROSS WEIGHT = 18018

+100%

COLLECTIVE PITCH

+A > B = -0.4

PITCH ANGLE

+5 DEG

$\Theta_{REF} = 0$

PITCH RATE

+10 DEG/SEC

PITCH COMMAND

+100%
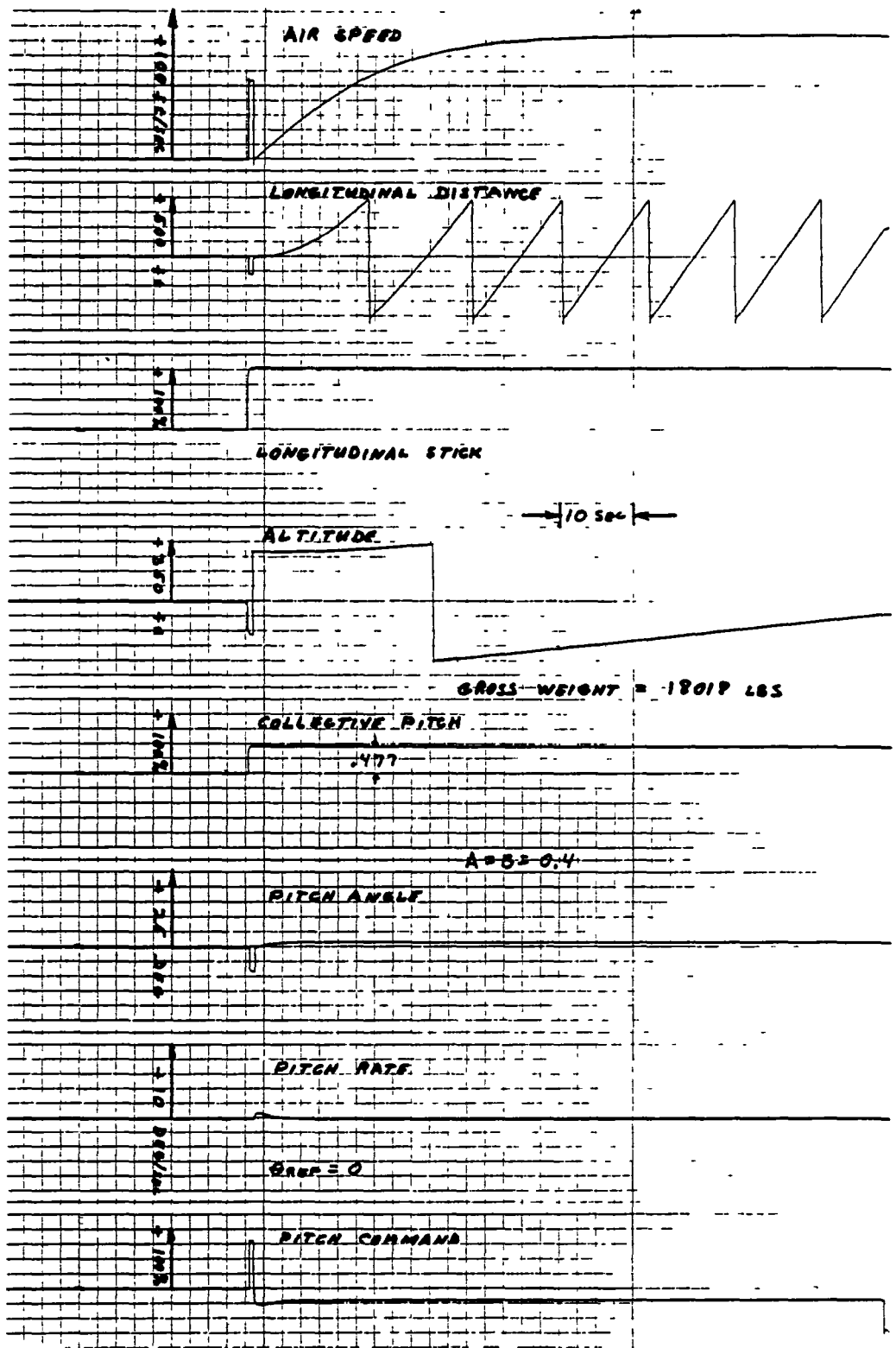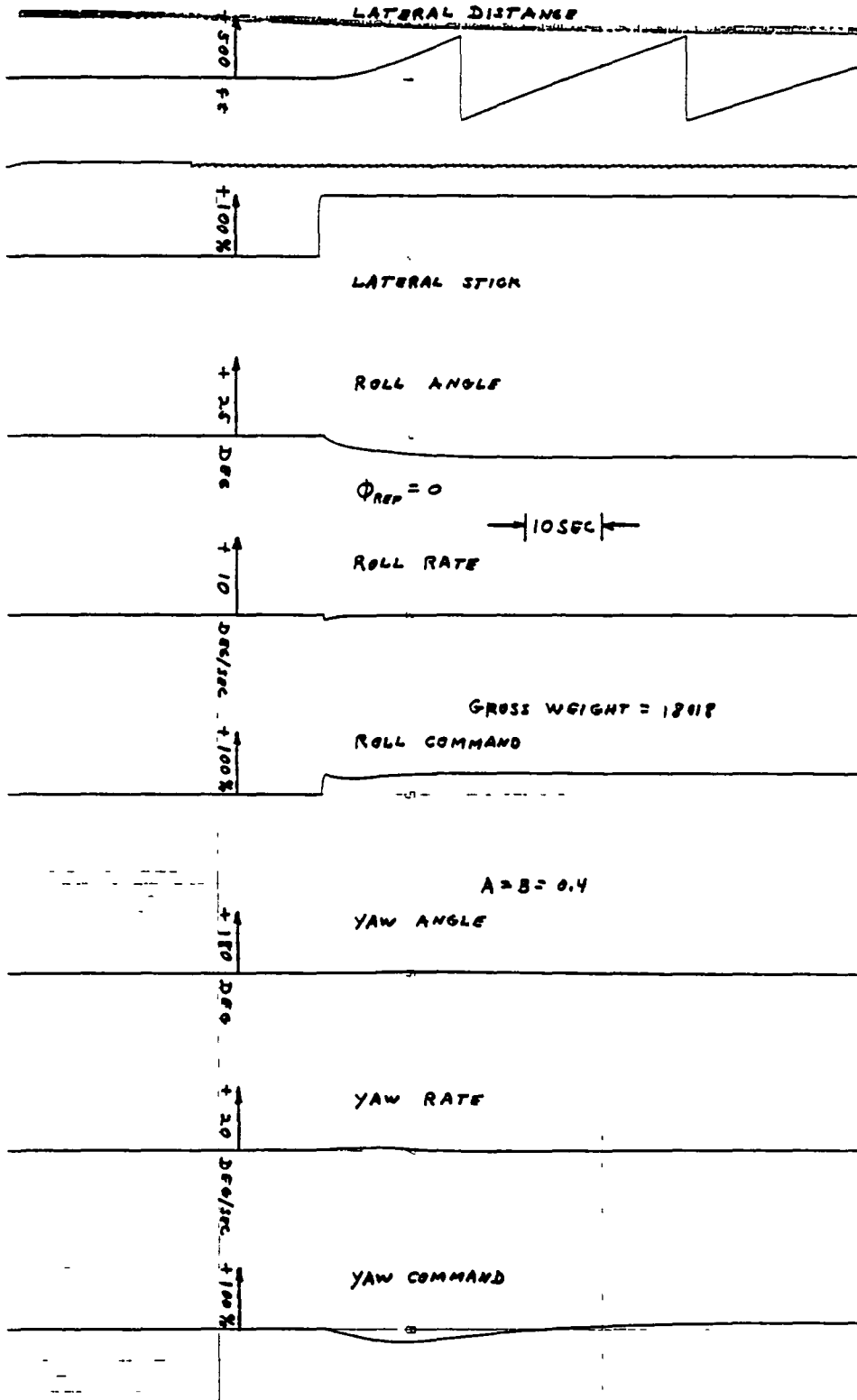
Run No. 7

Run No. 8

Run No. 9

LATERAL DISTANCE

500 ft

+100%

LATERAL STICK

+ 25 Deg

ROLL ANGLE

$\phi_{REP} = 0$

$\rightarrow$|10 SEC|$\leftarrow$

+ 10 Deg/sec

ROLL RATE

GROSS WEIGHT = 18018

+100%

ROLL COMMAND

A = B = 0.4

+ 180 Deg

YAW ANGLE

+ 20 Deg/sec

YAW RATE

+100%

YAW COMMAND

Run No. 10

F-12

AIR SPEED

LONGITUDINAL DISTANCE

LONGITUDINAL STICK

|← 10 SEC →|

ALTITUDE

GROSS WEIGHT = 18018 LBS

COLLECTIVE PITCH

.477

A = B = 0.4

PITCH ANGLE

$\theta_{REF} = 0$

PITCH RATE

PITCH CONTROL

Run No. 10

AIR SPEED

LONGITUDINAL DISTANCE

LONGITUDINAL STICK

|← 10 SEC →|

ALTITUDE

GROSS WEIGHT = 18018

COLLECTIVE PITCH

.477

A = θ = 0.4

PITCH ANGLE

$\theta_{REF} = -10$ DEG

PITCH RATE

PITCH CONTROL

Run No. 11

Run No. 11

AIR SPEED

100 ft/sec

LONGITUDINAL DISTANCE

500 ft

LONGITUDINAL STICK

100 %

← 10 sec →

ALTITUDE

250 ft

GROSS WEIGHT = 22292 LBS

COLLECTIVE PITCH

100 %

A = B = 0.1

PITCH ANGLE

5 Deg

$\theta_{REF} = 0$

PITCH RATE

10 Deg/sec

PITCH COMMAND

100 %

Run No. 12

F-16

AIR SPEED

LONGITUDINAL
DISTANCE

LONGITUDINAL STICK

←—10 SEC—→

ALTITUDE

GROSS WEIGHT = 22292

COLLECTIVE PITCH

$A = B = 0.1$

PITCH ANGLE

$\theta_R = -5$ DEG

PITCH RATE

PITCH COMMAND
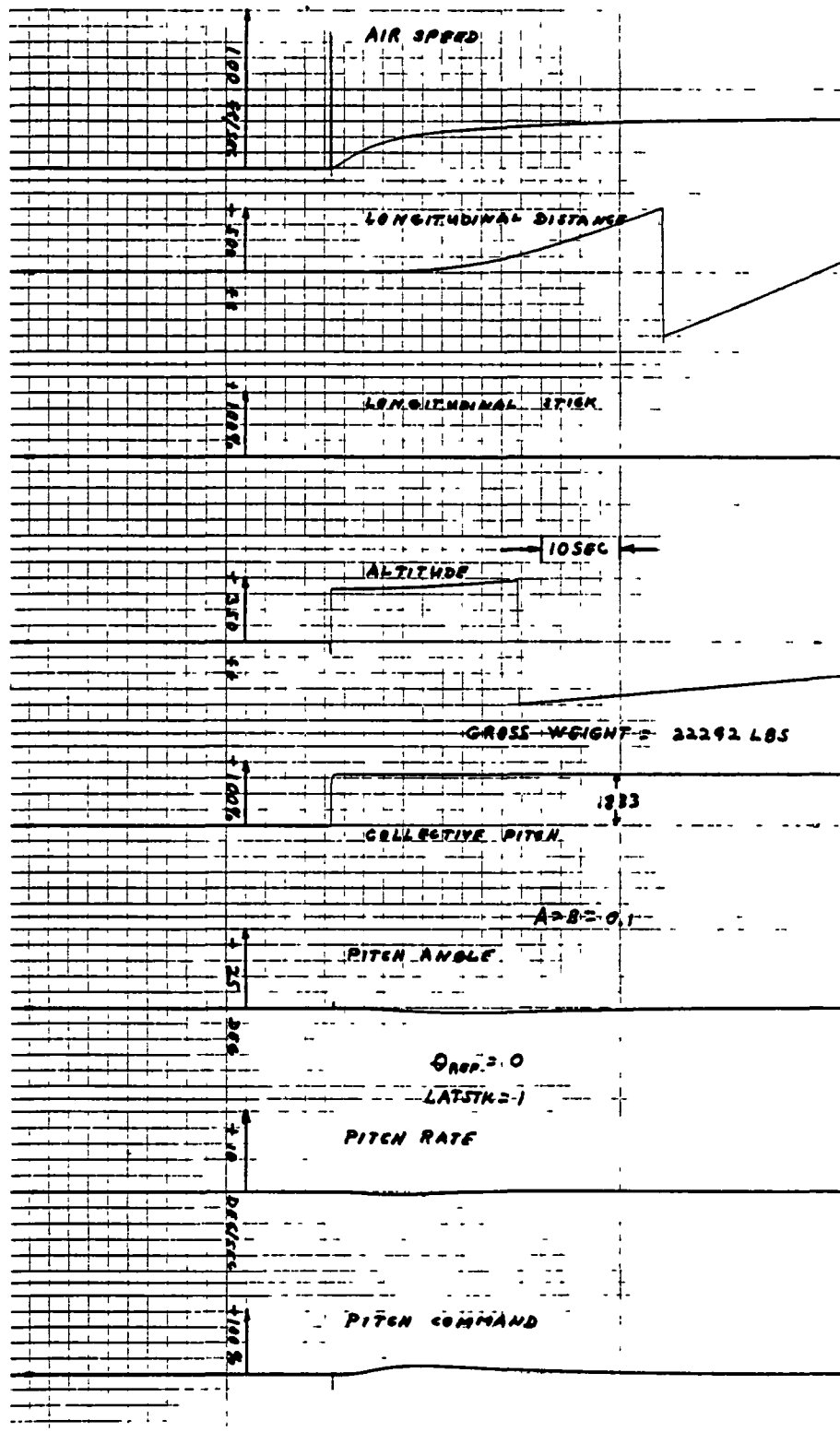
Run No. 13

Run No. 14

Run No. 15

LATERAL DISTANCE

+500

ft

LATERAL STICK

+100%

ROLL ANGLE

+25

DEG

|10SEC|

ROLL RATE

+10

DEG/SEC

GROSS WEIGHT = 22292

ROLL COMMAND

+100%

A = B = 0.1

YAW ANGLE

+130

DEG

YAW RATE

+20

DEG/SEC

YAW COMMAND

+100%

Run No. 15

Run No. 16

Run No. 17

AIR SPEED

LONGITUDINAL DISTANCE

LONGITUDINAL STICK

|← 10 SEC →|

ALTITUDE

GROSS WEIGHT = 22292

COLLECTIVE PITCH

A = B = 0.4

PITCH ANGLE

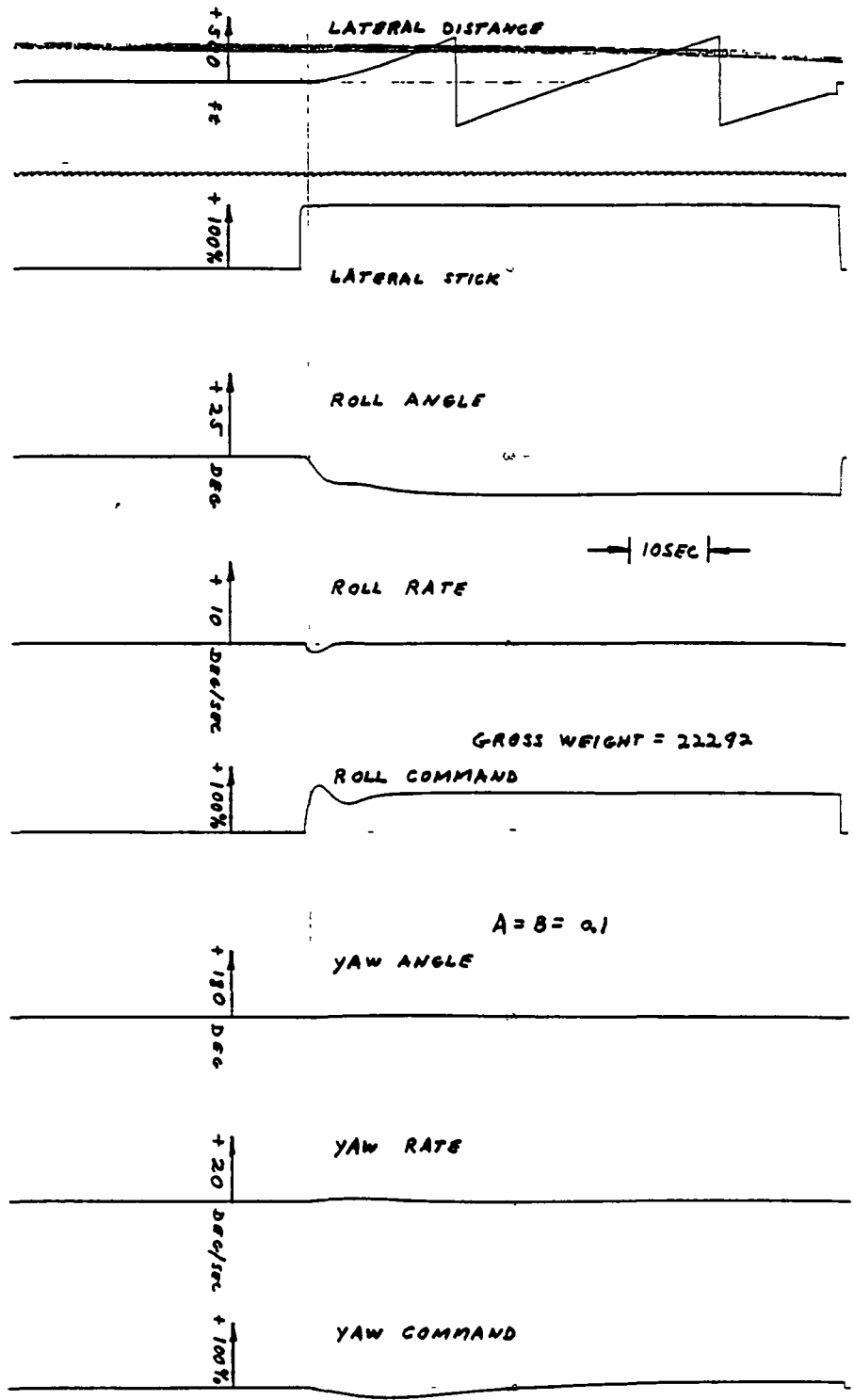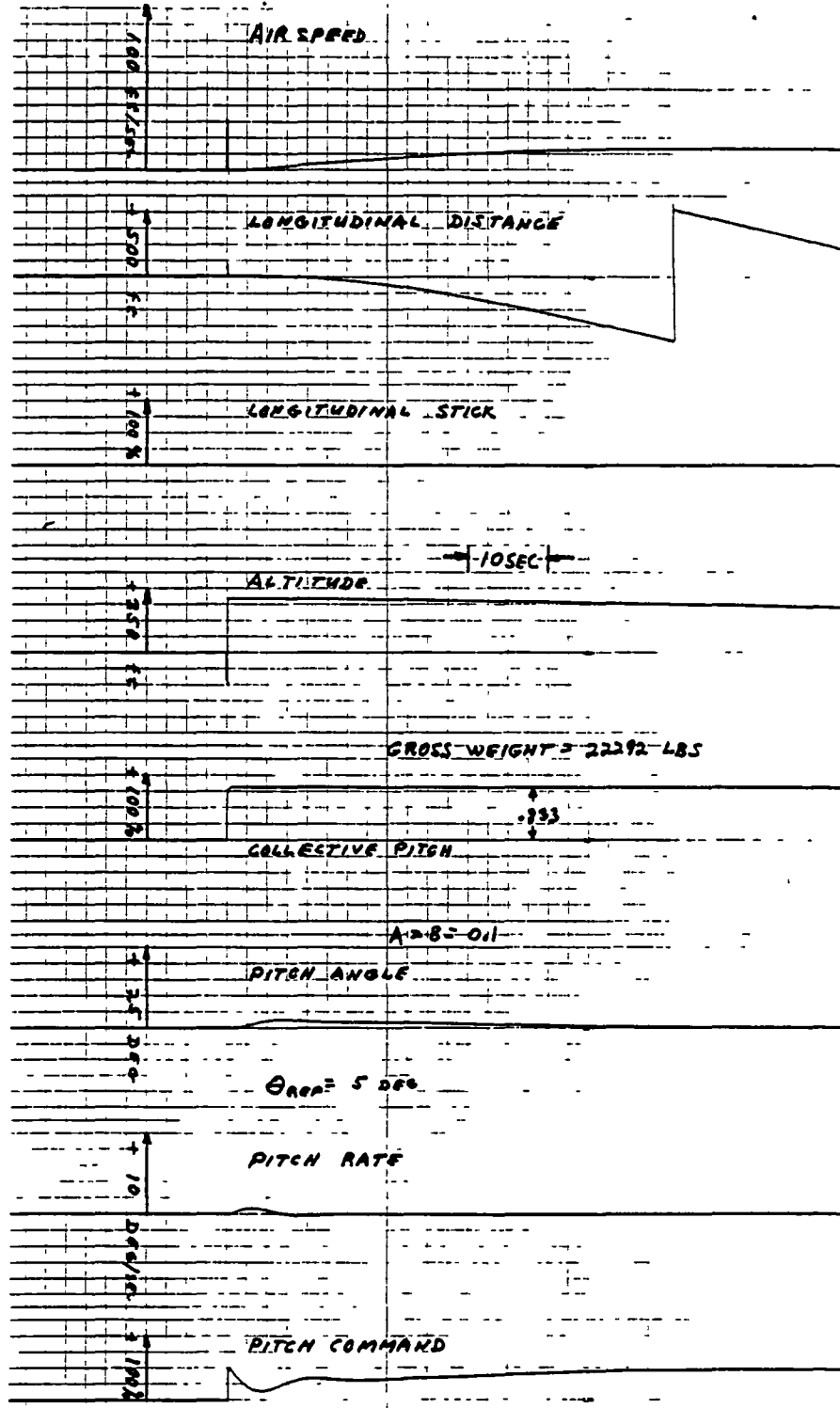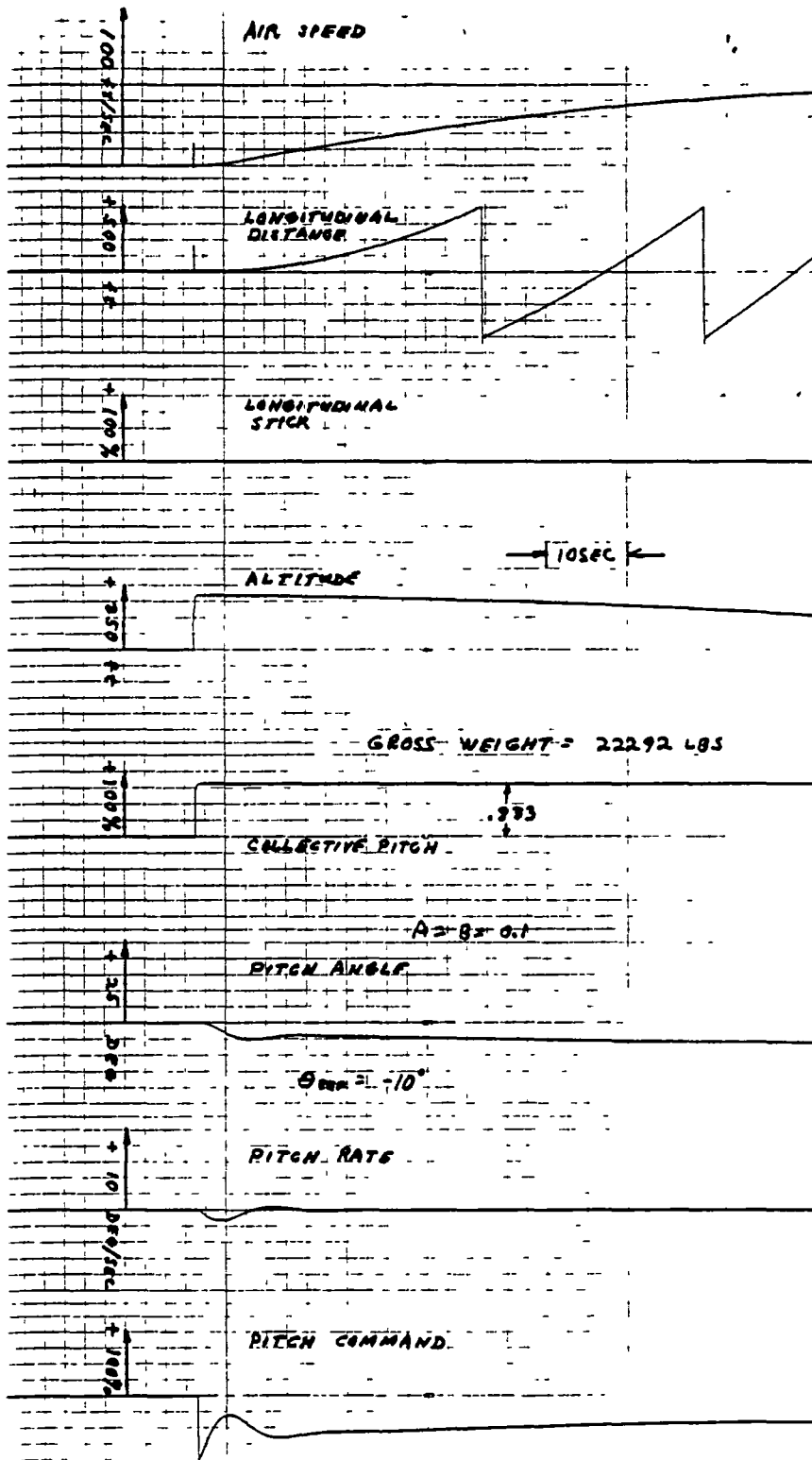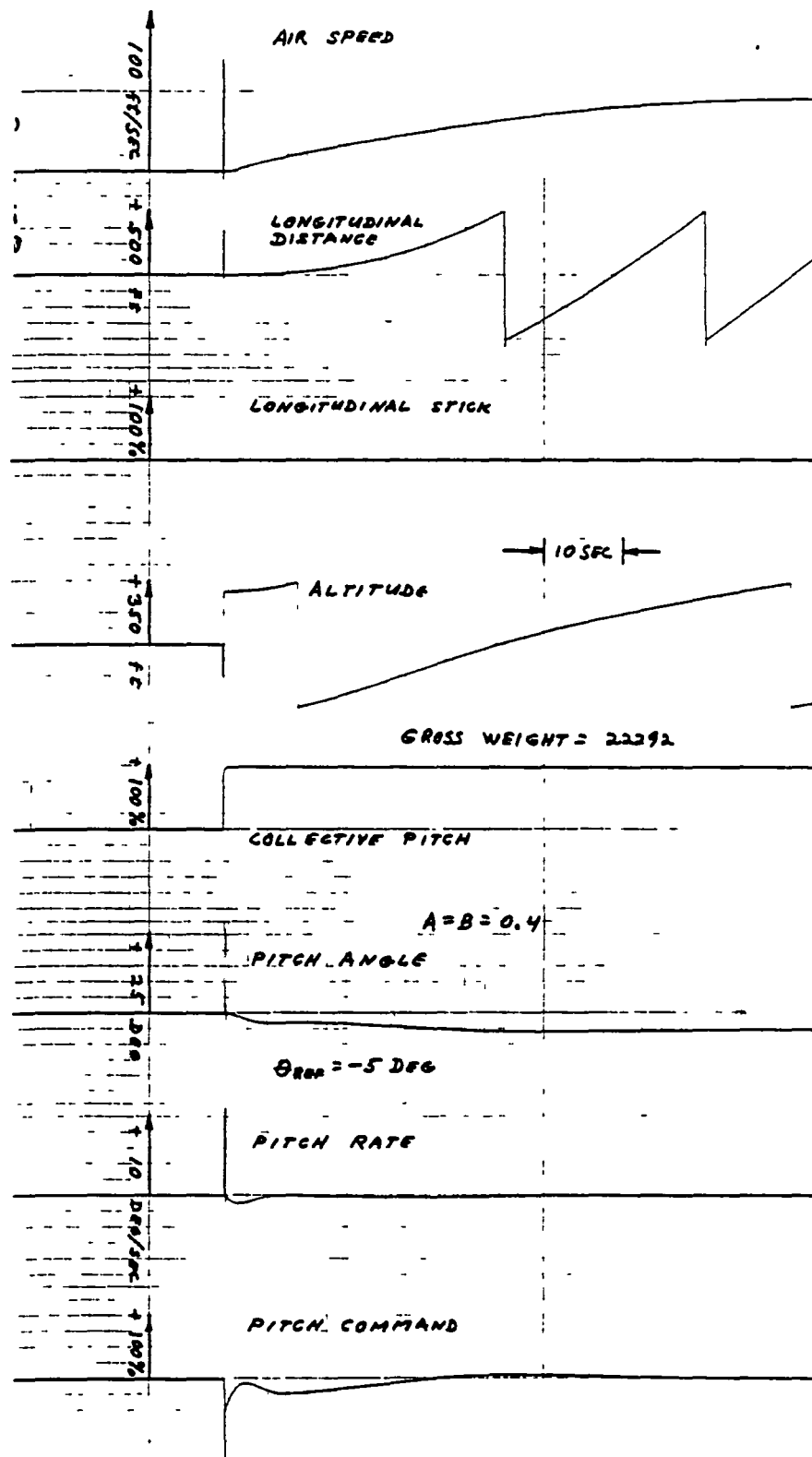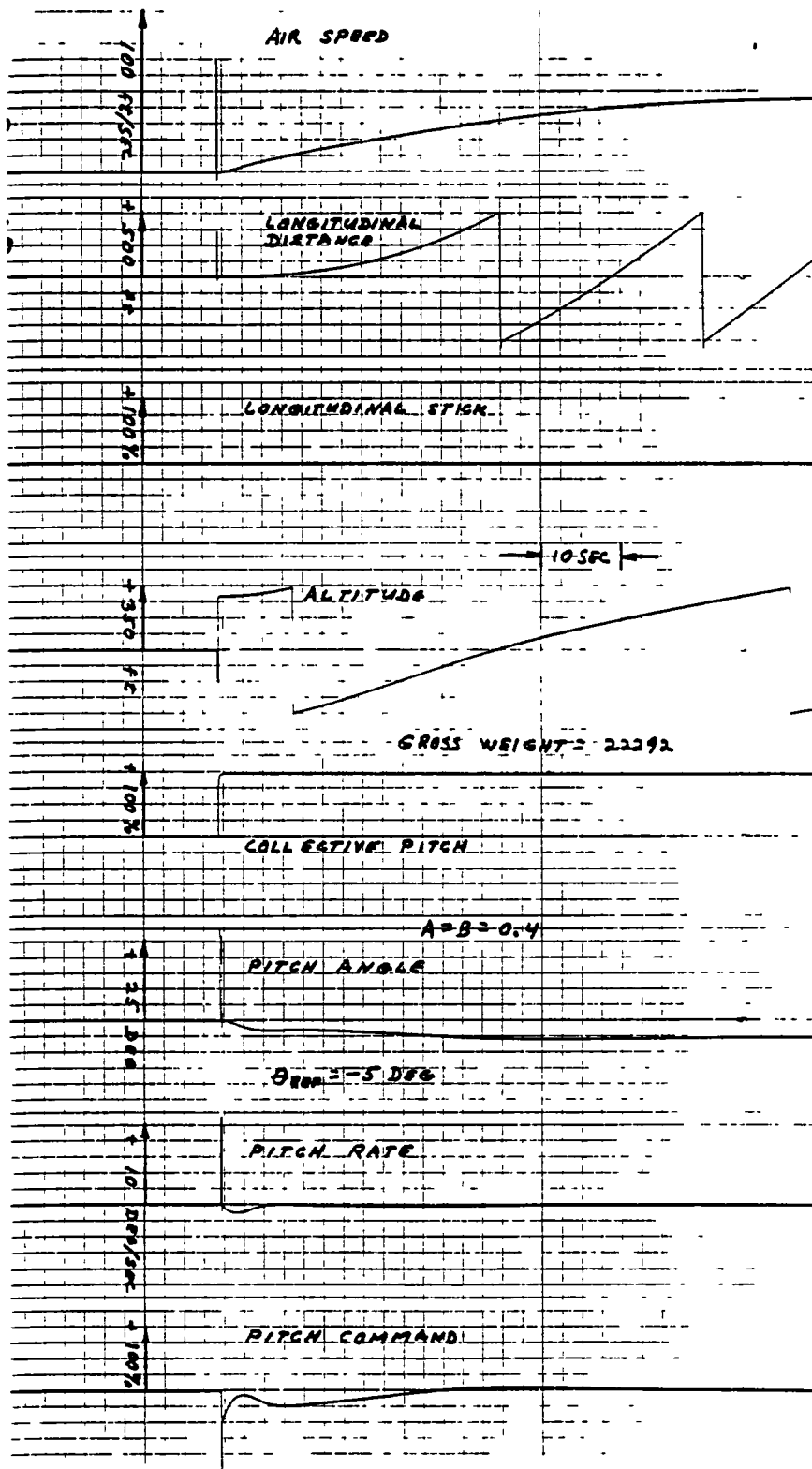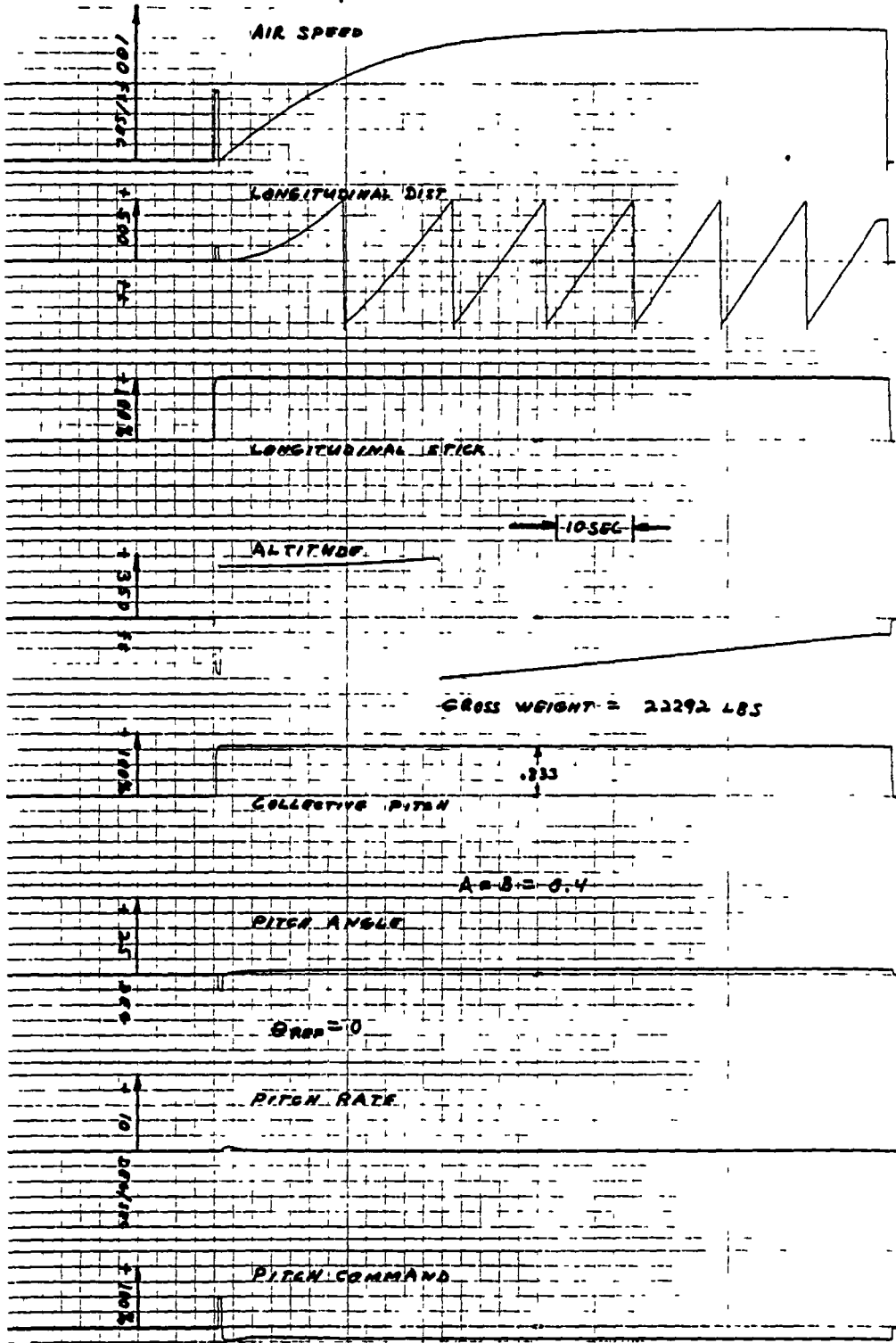$\theta_{REF} = -5$ DEG

PITCH RATE

PITCH COMMAND

Run No. 18

Run No. 19

Run No. 20

Run No. 21

LATERAL DISTANCE

+50

45

+100%

LATERAL STICK

+ ROLL ANGLE

25

DEG

|10SEC|

+ ROLL RATE

10

DEG/SEC

GROSS WEIGHT = 22292 LBS

+100%

ROLL COMMAND

A = B = 0.4

+ YAW ANGLE

180

DEG

+ YAW RATE

120

DEG/SEC

+100%

YAW COMMAND

Run No. 21

AIR SPEED

LONGITUDINAL
DISTANCE

LONGITUDINAL STICK

|← 10 SEC →|

ALTITUDE

GROSS WEIGHT = 22592 LBS

.833

COLLECTIVE PITCH

A - B = 0.4

PITCH ANGLE

θ_{REF} = -10 DEG

PITCH RATE

PITCH COMMAND
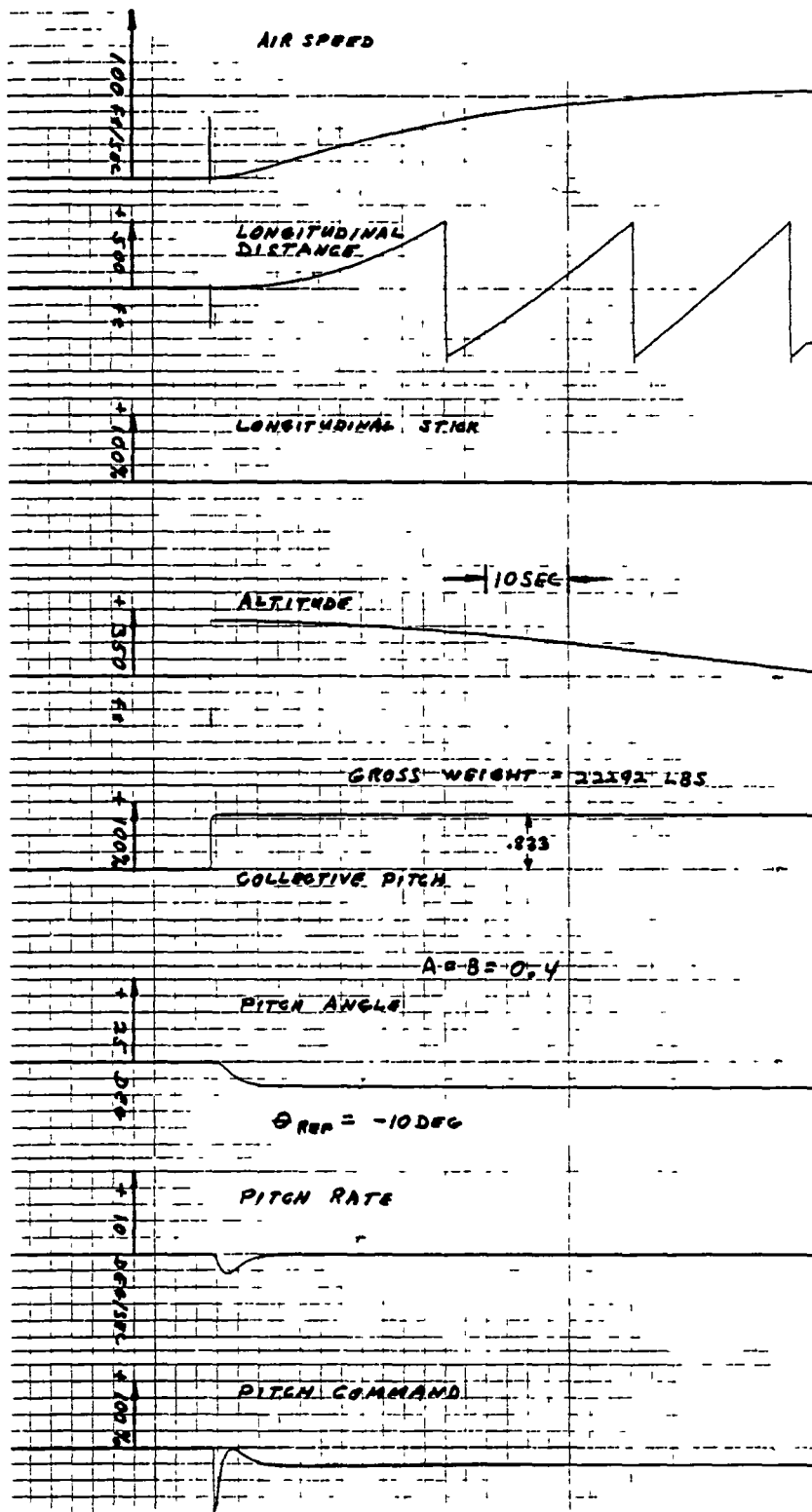
Run No. 22

F-28

LIST OF REFERENCES

1. Carter, E.S.; Cooper, D.E.; and Knapp, L.G.: Single Rotor Options for Heavy Lift and Potential of Multi-Lift. SAE Technical Paper Series No. 791087, Society of Automotive Engineers, Inc., Warrendale, Pa., December 1979.

2. Pope, A. and Harper, J.J.: Low Speed Wind Tunnel Testing. Wiley and Sons, Inc., New York., 1966.

3. Problems in Wind Tunnel Testing Techniques. AGARD Report No. 601, NATO, June 1974.

4. Summary of Meteorological Observations, Surface. Naval Weather Service Detachment, Asheville, N.C., Station 23244, July 1978.

5. Silverstein, A.; and Gulick, B.G.: Ground Handling Forces on a 1/40-Scale Model of the U.S. Airship "Akron". NACA Report No. 566, Langley Memorial Aeronautical Laboratory, Langley Field, Va., April 8, 1936.

6. Black, S.: A Short Method for Estimating the Lift and Drag of Infinitely Long Inclined Cylinders. GER-2859, Akron, Ohio, September 12, 1951.

7. Boldt, T.R.: Towed Model Tests of 1/75 Scale ZPN Airship During Undocking. GDC Report R50-8-1, General Development Corporation, Elkton, Maryland, December 31, 1953.

8. Boldt, T.R.: Towed Model Tests of 1/75th Scale ZPN Airships. GDC Report R50-8-2, General Development Corporation, Elkton, Maryland, March 22, 1954.

9. Operator's Manual, Helicopter Observation OH-6A. TM 55-1520-214-10. Headquarters, Dept of the Army, 17 December 1976.

10. Logher, R.D.: et al: ICES STRUDL-II, The Structural Design Language Engineering User's Manual. Volume 1, Frame Analysis, MIT, Cambridge, Mass., November 1968.

11. Aircraft Tubing Data. Summerill Tubing Company, Bridgeport, Pa., June 1943.

12. Talbot, Peter D., Miura, Hirokazu and Tucker, George E., Piloted Simulation of a Buoyant Quad Rotor Aircraft, AIAA Paper No. 81-1345, preented at AIAA LTA Systems Technology Conference, Annapolis, Maryland July 1981.

13. Nagabhushan, B.L.: Linear System Definition of Heavy Lift Airship/Payload Configuration. GER-16498, Goodyear Aerospace Corp., Akron, Ohio,. December 1977.

14. Bezbatchenko, J.W.; Davis, R.J.; and Sowa, W.W.: GZ20(G/L) Airship Stability and Control. GER-13844, Goodyear Aerospace Corp., Akron, Ohio, May 1968.

15. Nagabhushan, B.L.: Empennage Contribution to Aerodynamic and Control Characteristics of Airship Configurations. GER-16906, Goodyear Aerospace Corp., Akron, Ohio, October 1980.

16. Nagabhushan, B.L.: Contribution of Gimballed Helicopters/Rotor Modules to Force and Moment Derivatives of the Heavy Lift Airship. GER-16578, Goodyear Aerospace Corp., Akron, Ohio, May 1978.

17. Heffley, Robert K.; et al: A Compilation and Analysis of Helicopter Handling Qualities-Data. NASA CR-3144, August 1979.

18. Lamb, Sir Horace: Hydrodynamics., Dover, New York, 1945.

19. Nagabhushan, B.L., and Tomlinson, N.P.: Flight Dynamics Simulation of a Heavy Lift Airship. Journal of Aircraft, VoL 18, No. 2, February 1981.

20. Tischler, Mark B.; Jex, Henry R.; and Ringland, Robert F.: Simulation of Heavy Lift Airship Dynamics Over Large Ranges of Incidence and Speed. AIAA Paper No. 81-1335, July 1981.

21. Nagabhushan, B.L., and Tomlinson, N.P.: Piloted Simulation of a Heavy Lift Airship with a Sling Load. (GER-17010, to be published by Goodyear Aerospace Corp., Akron, Ohio, December 1981.)

22. Nagabhushan, B.L.; Lichty, D.W.; and Tomlinson, N.P.: Control Characteristics of a Buoyant Quad-Rotor Research Aircraft. (paper presented at AIAA Guidance and Control Conference, Albequerque, N.M., August 19-21, 1981). Paper No. 81-1838.

1. Report No	2. Government Accession No.	3. Recipient's Catalog No.
NASA CR-166246		

4. Title and Subtitle	5. Report Date
Preliminary Design Study of a Hybrid Airship for Flight Research	July 1981
	6. Performing Organization Code

7. Author(s)	8. Performing Organization Report No.
Ronald G.E. Browning	GER-17016

9. Performing Organization Name and Address	10. Work Unit No.
Goodyear Aerospace Corporation	T3701Y
1210 Massillon Road	11. Contract or Grant No.
Akron, Ohio 44315	NAS2-10777

12. Sponsoring Agency Name and Address	13. Type of Report and Period Covered
National Aeronautics and Space Administration	Contractor Final Report 10/80-7/81
Washington, D.C. 20546	14. Sponsoring Agency Code
	505-42-51

15. Supplementary Notes

Mr. Peter D. Talbot, Technical Monitor, Mail Stop 237-11,
NASA Ames Research Center, Moffett Field, CA 94035
(415) 965-5887 FTS 448-5887

16. Abstract

The feasibility of using components from four small helicopters and an airship envelope as the basis for a quad-rotor research aircraft was studied. Preliminary investigations included a review of candidate hardware and various combinations of rotor craft/airship configurations. A selected vehicle was analyzed to assess its structural and performance characteristics.

17. Key Words (Suggested by Author(s))	18. Distribution Statement
Hybrid Airship	Unclassified - Unlimited
Lighter-than-air	
Quad-Rotor Aircraft	STAR Category 05

19. Security Classif. (of this report)	20. Security Classif. (of this page)	21. No. of Pages	22. Price*
Unclassified	Unclassified	285	

End of Document